Investigating the role of *Leucine Rich Repeat Kinase 2 (LRRK2)* in human induced pluripotent stem cell derived macrophages

Heyne "Cecilia" Lee

Sir William Dunn School of Pathology

Lincoln College

University of Oxford

A thesis submitted for the degree of

Doctor of Philosophy

Michaelmas 2017

Abstract

Mutations in *Leucine Rich Repeat Kinase 2* (*LRRK2*) are the most prevalent cause of familial PD. Genome Wide Association Studies (GWAS) have linked its variants with increased risk of developing sporadic PD, inflammatory bowel disease, and leprosy, diseases commonly associated with inflammation and immune dysfunction. LRRK2 is predominantly expressed in a subset of immune cells, notably macrophages and microglia and has been implicated in innate immunity. Yet, most studies report conflicting results, and data are based on mouse models or in immortalised cell lines which do not faithfully recapitulate all aspects of tissue macrophages. In this thesis, macrophages and microglia differentiated from human induced pluripotent stem cells (hiPSCs) have been used as a genetically tractable tool that expresses *LRRK2* at physiological levels from its endogenous promoter in its normal human chromosomal location. Using this physiologically relevant cell model, the aim of this thesis was to investigate the expression, subcellular localisation and role of LRRK2 protein in macrophages and microglia. This thesis maps the cleavage region of an N-terminal proteolytically cleaved form of LRRK2 in macrophages and shows that LRRK2 can form heterodimers of full-length and cleaved forms. My results demonstrate that LRRK2 is recruited to late phagosomes and that treatment of LRRK2 kinase inhibitors leads to the formation of LRRK2 super-coated phagosomes. However, I demonstrate that LRRK2 is not required for the acidification of phagosomes, and its role at the phagolysosome remains unresolved. Lastly, using hiPSC-microglia in co-culture with iPSC-cortical neurons, I demonstrate that in human cells, LRRK2 is robustly expressed in microglia and is undetectable in cortical neurons. In this co-culture model,

under the conditions tested, inflammatory cytokine release was broadly unaffected by LRRK2 mutation or KO, although two different TNFα assay approaches gave conflicting results. This thesis provides novel insights into the role of LRRK2 in macrophages and microglia, and shows that hiPSC-macrophages and microglia can serve as a valuable platform to examine LRRK2 biology.

Acknowledgements

First of all, I would like to thank my supervisors, Dr. Sally Cowley and Professor William James, for their support, guidance and mentorship. I have learnt tremendously under their supervision and I was fortunate enough to have them throughout my DPhil training. I would like to also thank the members of James Lab, specially Jane Vowles and Cathy Browne whose excellent expertise in human iPSCs has been extremely helpful and valuable learning experience. I am also grateful for the current and past members of the lab, particularly Dr. Walther Haenesler for his expertise in microglia, Dr. Rowan Flynn, Dr. Kenny Moore, Olga Perestenko, Dr. Julian Buchrieser, Ben Dodsworth, Dr. Hazel Roberts, Damien Warner, and Dr. Federica Rinaldi. I would like to also thank Professor Yoland Smith, who drew me into the exciting research field of Parkinson's Disease. Finally, I would like to thank and express my endless love to my family and Theo for their support and encouragements.

Table of Contents

1. **Introduction** 1
  1.1 Parkinson's disease 1
    1.1.1. Introduction 1
    1.1.2. Clinical and neuropathological features of PD 2
    1.1.3. Selective vulnerability of nigral dopaminergic neurons 2
    1.1.4. Environmental factor 4
    1.1.5. Genetics of PD 5
    1.1.6. Microglia-mediated neurotoxicity 10
    1.1.7. The role of PD genes in the immune system 12
  1.2 Leucine Rich Repeat Kinase 2 15
    1.2.1. LRRK2 mutations, epidemiology, and penetrance 15
    1.2.2. Clinical and neuropathological features of LRRK2 PD patients 17
    1.2.3. LRRK2 is a multi-domain, multi-functional enzyme 18
    1.2.4. Cellular functions of LRRK2 - what we know so far 20
    1.2.5. LRRK2 kinase inhibitors 25
  1.3 Modelling Parkinson's disease 28
    1.3.1. Criteria for an ideal model 28
    1.3.2. Animal models of PD 28
    1.3.3. Modelling PD using human induced pluripotent stem cells 31
    1.3.4. Gene-editing technologies 33
  1.4 Aim of the thesis 36
2. **Materials and Methods** 37
  2.1 Cell culture 37
    2.1.1. List of materials and media 37
    2.1.2. hiPSC cultures 38
    2.1.3. Differentiation of MΦ from hiPSCs 39
    2.1.4. hiPSC-microglia, cortical neuron co-culture 40
  2.2 Protein analysis 42
    2.2.1. List of buffers and materials 42
    2.2.2. Preparation of cell lysates 44
    2.2.3. Western blot 44
    2.2.4. Immunoprecipitation 45

2.2.5. Immunocytochemistry 46
2.2.6. Automated image analysis for quantification of phagosomes 46
2.2.7. Automated image analysis for quantification of hiPSC-microglia 48
2.3 Functional assays 50
2.3.1. List of materials 50
2.3.2. Phagocytosis 51
2.3.3. TNFα ELISA 51
2.3.4. Luminex 34plex cytokine and chemokine assay 52
2.4 Generation of CRISPR/Cas9-edited hiPSCs 53
3. **Regulation of LRRK2 protein expression in hiPSC-MΦs** 55
3.1 Introduction 55
3.1.1. LRRK2 protein expression in precisely regulated in myeloid cells 55
3.1.2. Phosphoregulation of ANK-LRR interdomain region 56
3.1.3. Functional implications of phosphorylated S910, S935 residues 58
3.1.4. Aims 59
3.2 Results 59
3.2.1. Validation of CRISPR/Cas-9 edited LRRK2 hiPSC lines. 59
3.2.2. IFNγ upregulates endogenous LRRK2 protein expression in hiPSC-MΦs 63
3.2.3. LRRK2 kinase inhibitors reduce phosphorylation of LRRK2 at S935 65
3.2.4. LRRK2 kinase inhibitors reduce the stability of LRRK2 protein 67
3.2.5. LRRK2 forms a cleaved product in hiPSC-MΦs 69
3.3 Summary and Discussion 73
4. **Dissecting the physiological role of LRRK2 in phagocytosis** 77
4.1 Introduction 77
4.1.1. Phagocytosis 77
4.1.2. Neurodegeneration and phagocytosis 81
4.1.3. Aims 82
4.2 Results 83
4.2.1. LRRK2 is recruited to the phagosomes during late stages of phagocytosis 83
4.2.2. LRRK2 kinase inhibitors enhance the formation of LRRK2 super-coated phagosomes 87
4.2.3. LRRK2 is not involved in the acidification of the phagosomes 89
4.2.4. Investigating the molecular interactors of LRRK2 97
4.3 Summary and discussion 101
5. **LRRK2 in hiPSC-derived microglia and cortical neuron co-culture** 105
5.1 Introduction 105

5.1.1. hiPSC-microglia and cortical neuron co-culture 106
5.1.2. LRRK2 in the regulation of cytokine release 107
5.1.3. Aim 107
5.2 Results 107
5.2.1. LRRK2 is expressed in hiPSC-microglia but not detectable in hiPSC-cortical neurons 107
5.2.2. IFNγ upregulates LRRK2 protein expression in hiPSC-microglia 110
5.2.3. TNFα release by hiPSC-microglia with LRRK2 G2019S mutation 112
5.2.4. Multiplex cytokine and chemokine profiling in hiPSC-MΦs and hiPSC-microglia 115
5.3 Summary and Discussion 120
6. **General discussion** 125
6.1 General discussion and future perspectives 125
6.1.1. LRRK2 has diverse regulatory mechanisms 125
6.1.2. LRRK2 is recruited to phagosomes during late stages of phagocytosis 130
6.1.3. LRRK2 is highly expressed in microglia but not in neurons 133
6.2 Concluding remarks 135
A. **Appendix** 137
A.1. Proteasome activity 137
A.2. List of LRRK2 peptide sequences analysed by mass spectrometry 138
A.3. SNP analysis results 144
A.4. Quantification of LRRK2(+) phagosomes 146

Bibliography 147

List of figures

Chapter 1

Figure 1.1 PD associated genes in microglial function 13

Figure 1.2 Schematic representation of full-length LRRK2 with PD-associated variants. 15

Figure 1.3 Schematic view of LRRK2-associated cellular pathways in association with Rab GTPases. 24

Figure 1.4 LRRK2 kinase inhibitors. 26

Figure 1.5 A diagram showing three major programmable nucleases. 33

Chapter 2

Figure 2.1 Differentiation of MΦs from hiPSCs 39

Figure 2.2 Workflow of automated imaging analysis for quantification of LRRK2(+) phagosomes. 47

Figure 2.3 Workflow of automated imaging analysis for quantification of LRRK2(+) microglia. 48

Chapter 3

Figure 3.1 LRRK2 phosphorylation sites. 55

Figure 3.2 Generation of CRISPR/Cas-9 edited hiPSC lines 60

Figure 3.3 Myeloid differentiation of all four hiPSC lines used in this study 61

Figure 3.4 IFNγ upregulates endogenous LRRK2 expression in hiPSC-MΦs 63

Figure 3.5 LRRK2 kinase inhibitors reduce phosphorylation of LRRK2 at S935 65

Figure 3.6 G2019S mutation does not affect the stability of LRRK2 protein upon long-term treatment with LRRK2 kinase inhibitors. 67

Figure 3.7 Inhibition of proteasome subunit blocks the formation of cleaved LRRK2 69

Figure 3.8 Identifying the putative cleavage site of LRRK2 using proteomics 71

Chapter 4

Figure 4.1 Phagosome maturation 78
Figure 4.2 LRRK2 is recruited to the phagosomes 84
Figure 4.3 LRRK2 is recruited to the late phagosomes. 85
Figure 4.4 LRRK2 kinase inhibitors enhance the formation of super-coated LRRK2 phagosomes. 87
Figure 4.5 Application of LRRK2 kinase inhibitors does not affect the internalisation of zymosan bioparticles in hiPSC-MΦs 89
Figure 4.6 Complete absence of LRRK2 protein does not affect the internalisation of zymosan bioparticles in hiPSC-MΦs 90
Figure 4.7 The presence of G2019S mutation does not affect the internalisation of zymosan bioparticles in hiPSC-MΦs. 91
Figure 4.8 Application of LRRK2 kinase inhibitors does not affect the acidification of phagosomes in hiPSC-MΦs. 93
Figure 4.9 Complete absence of LRRK2 protein does not affect the acidification of phagosomes in hiPSC-MΦs. 94
Figure 4.10 The presence of G2019S mutation does not affect the acidification of phagosomes in hiPSC-MΦs. 95
Figure 4.11 LRRK2 does not colocalise with Rab GTPases, ER, or peroxisomes 98
Figure 4.12 Interactome of LRRK2 in hiPSC-MΦs 99

Chapter 5

Figure 5.1 Differentiation of hiPSC-microglia 105
Figure 5.2 LRRK2 protein is expressed in hiPSC-microglia but not in hiPSC-cortical neurons. 108
Figure 5.3 IFNγ upregulates LRRK2 protein expression in hiPSC-microglia. 110
Figure 5.4 *LRRK2* G2019S mutation in co-hiPSC-microglia enhances TNFα release upon IFNγ priming and LPS stimulation 113
Figure 5.5 *LRRK2* KO co-hiPSC-microglia display low levels of CCL2 and CCL4 116
Figure 5.6 LPS stimulation decreases the level of CCL4 in *LRRK2* KO hiPSC-MΦs 117
Figure 5.7 *LRRK2* KO and *LRRK2* G2019S hiPSC-MΦs display an elevated level of CCL4 118

List of tables

Chapter 1

Table 1.1 List of PD-associated loci and genes 12

Table 1.2 Expression of PD-related genes in the brain and immune cells in periphery 26

Chapter 2

Table 2.1 List of reagents used for differentiation 36

Table 2.2 List of media used for differentiation 37

Table 2.3 List of hiPSC lines used in this thesis 38

Table 2.4 List of reagents used for protein analysis 41

Table 2.5 List of buffers used for protein analysis 41

Table 2.6 List of primary antibodies 42

Table 2.7 List of secondary antibodies 42

Chapter 5

Table 5.1 Summary of the results from multiplex cytokine and chemokine profiling 115

Abbreviations

2-ME	2-mercaptoethanol2
aa	Amino acids
AD	Alzhiemer's Disease
AIMP2	Aminoacyl-tRNA synthetase-interacting multifunctional protein type 2
Aβ	Amyloid β
ANOVA	Analysis of variance
αsyn	α-synuclein
αTUB	α-tubulin
ATG5	Autophagy protein 5
BAC	Bacterial artificial chromosomes
BAI1	Brain-specific angiogenesis inhibitor 1
BBB	Blood brain barrier
BMDM	Bone marrow drived macrophages
BMP-4	Bone Morphogenetic Protein 4
BSA	Bovine serum albumin
CK1α	Casein kinase 1α

CMA	Chaperone-mediated autophagy
CORVET	C core vacuole/endosome tether
CRISPR	Clustered Regularly Interspaced Short Palindromic Repeats
DAPI	4',6-Diamidino-2-Phenylindole
DAT	Dopamine transporter
DBS	Double strand break
DC	Dendritic cells
DMP	Dimethylpimelimidate dihydrochloride
DMSO	Dimethyl sulfoxide
e.g.	Example
EB	Embryoid Body
EEA1	Endosomal antigen 1
ELISA	Enzyme-Linked Immunosorbent Assay
ER	Endoplasmic Reticulum
ERK5	Extracellular signal-regulated kinase 5
FACS	Fluorescence Activated Cell Sorting
FBS	Fetal bovine serum
FGF	Fibroblast growth factor
GD	Gaucher Disease
G-MCSF	Granulocyte macrophage stimulating factor

GWAS	Genome wide association studies
h	hour
HD	Huntington’s Disease
HDR	Homology directed repair
HOPS	Homotypic fusion and vacuole-sorting
Hsp	Heat shock protein
IBA1	Ionized calcium binding adaptor molecule 1
IFN	Interferon
IKKs	IκB kinases
IL	Interleukin
IP	Immunoprecipitation
iPSC	Induced pluripotent stem cell
IRF	Interferon-regulatory factor
IRS	IRF recognition sequence
JAK	Janus kinase
KD	Knock down
KI	Knock in
KO	Knock out
LAMP-1, -2	Lysosome-associated membrane protein 1 and 2
LB	Lewy Bodies

LC3	Microtubule-associated protein 1A/1B-light chain 3
L-DOPA	L-3,4-dihydroxyphenylanine
LN	Lewy Neurites
LPS	Lipopolysaccharide
M6PR	Mannose 6-phosphate receptors
MAP2	Microtubule associated protein 2
MAPK	Mitogen-activated protein kinase
M-CSF	Macrophage colony stimulating factor
MEF	Mouse embryo fibroblasts
MPTP	n-methyl-4-phenyl-1,2,3,6-tetrahydropyridine
mRNA	messenger RNA
MΦs	Macrophages
NDS	Normal donkey serum
NFκB	Nuclear factor κ-light-chain-enhancer of activated B
NHEJ	Non homologous end joining
NO	Nitric oxide
ns	Non significant
NSF	N-ethylmaleimide-sensitive factor
PAM	Protospacer adjacent motif
PAMP	Pathogen associated molecular patterns

PBMC	Peripheral blood mononuclear cell
PD	Parkinson's Disease
PI(3)P	Phosphatidylinositol 3-phosphate
PINK1	PTEN-induced putative kinase 1
PKA	Protein Kinase A
PP1	Protein phosphatase 1
PPR	Pattern recognition receptors
PS	Phosphatidylserine
PVDF	Polyvinylidene difluoride
ROS	Reactive oxygen species
RT	Room temperature
SCF	Stem cell factor
SNAP	Synaptosomal associated protein
SNARE	NSF attachment protein receptor
SNP	Single nucleotide polymorphisms
SNpc	*Substantia nigra pars compacta*
STAT	Signal transducers and activators of transcription
SV	Synaptic vesicle
TALEN	Transcription activator-like effector nucleases
TBK1	Transforming growth factor β-activated kinase 1

TGF-β	Transforming growth factor β
TGN	Trans-golgi network
TIM	T cell immunoglobulin mucin
TNF	Tumor necrotic factor
TX-100	Triton X-100
UNTR	Untreated
UPS	Ubiquitin proteasome system
v-ATPase	vacuolar-type H+ -ATPase
VEGF	Vascular endothelial growth factor
VMAT2	Vesicular monoamine transporter type 2
Vps34	Vacuolar protein-sorting 34
VTA	Ventral tegmental area
WT	Wild-Type
ZFN	Zinc finger nuclease

1 Introduction

1.1 Parkinson's disease

1.1.1 Introduction

This year marks exactly 200 years since a British surgeon, James Parkinson, published "An Essay on the Shaking Palsy" in 1817, which accounts for the first official medical record recognising Parkinsonism as a neurological condition (Parkinson 2002). While his text is the most well-known medical description of classical symptoms of PD, there is an earlier account of it in 1690 published by Ferenc Pápai Páriz (Bereczki 2010). The name Parkinson's disease (PD) was given decades later by a French neurologist, Jean-Martin Charcot, who greatly contributed to the comprehensive description of clinical symptoms of PD (Goetz 1986, 2011).

Today, PD is the second most common neurodegenerative disease after Alzheimer's disease (AD), accounting for 1% of the population over the age of 60 in North America (de Lau et al. 2006). The prevalence of PD ranges from 1 to 2 per 1,000 in unselected populations (von Campenhausen et al. 2005) and the number of affected individuals in Western Europe has been projected to increase from 4.6 million in 2005 to 9.3 million in 2030 (Dorsey et al. 2007). As the life expectancy continues to increase, PD imposes a growing financial and social burden (Christensen et al. 2009).

1.1.2 Clinical and neuropathological features of PD

PD patients manifest motor symptoms characterized by resting tremor, bradykinesia, rigidity, and postural instability. Symptoms are progressive, with an average age at onset of 62 years (Pagano et al. 2016). Patients also display non-motor symptoms, which can be present up to 10 years prior to the onset of the motor symptoms (Schrag et al. 2015; Kalia and Lang 2015). The non-motor symptoms include autonomic and gastrointestinal dysfunction (constipation, hypotension, urinary dysfunctions), psychiatric dysfunction (anxiety, depression and cognitive impairment), sleep dysfunction (Rapid Eye Movement [REM] sleep behavioral disorder), and olfactory dysfunction (Pagano et al. 2016).

Neuropathologically, PD is defined by the slow and progressive loss of dopaminergic neurons in the *Substantia Nigra pars compacta* (SNpc) of the midbrain. The remaining nigral dopaminergic neurons display accumulation of α-synuclein (αsyn) protein aggregates called Lewy Bodies (LBs) if present in perikarya (cell body of neurons) or Lewy Neurites (LNs) if present in the axons (Gelb, Oliver, and Gilman 1999; Hughes et al. 1992). By the onset of clinical motor symptoms, there is a loss of about 50 – 60% of the nigral dopaminergic neurons, making the early diagnosis as well as preventative treatments challenging (Cheng, Ulane, and Burke 2010). Currently, only symptomatic treatments are available, notably dopamine replacement therapy with L-3,4-dihydroxyphenylalanine (L-DOPA) or deep brain stimulation for patients who are not responsive to L-DOPA. However, these treatments have limited effect with undesirable side effects, particularly L-DOPA induced dyskinesia (Thanvi, Lo, and Robinson 2007).

1.1.3 Selective vulnerability of nigral dopaminergic neurons

In PD, dopaminergic neurons in the SNpc, but not in the Ventral Tegmental Area (VTA), are disproportionately lesioned (Greenfield and Bosanquet 1953; Hirsch, Graybiel, and Agid 1988). Dopaminergic neurons in SNpc project to the striatum and form an integral

part of basal ganglia-thalamo-cortical circuit, which controls voluntary movement. Motor symptoms manifested in PD are as a result of the imbalance of basal ganglia-thalamo-cortical circuit, caused by a severe reduction in the dopamine level in the striatum (Smith and Kieval 2000).

The etiological factors which trigger the onset of degeneration of nigral dopaminergic neurons remain incompletely understood. The current notion is that PD is a complex, multifactorial disease involving both genetic and environmental factors, which have been implicated to disrupt various cellular pathways, namely vesicular trafficking pathway, autophagy/lysosomal pathway, accumulation of misfolded proteins, oxidative stress, and mitochondrial dysfunction (Dauer and Przedborski 2003).

Dopaminergic neurons in the SNpc are intrinsically vulnerable to any of these insults. The autonomous tonic firing of dopaminergic neurons in the SNpc are dependent on constant Ca^{2+} flux via L-type Ca^{2+} channels, unlike mesolimbic dopaminergic neurons in the VTA (Surmeier et al. 2011). The high consequential Ca^{2+} flux in nigral dopaminergic neurons requires a greater supply of ATP by mitochondria as well as higher activity of the endoplasmic reticulum (ER)–mitochondrial system to sequester excess Ca^{2+}. Furthermore, nigral dopaminergic neurons have an extensive axonal and dendritic arborisation, demanding much high maintenance energy to transport cargoes (Tepper, Sawyer, and Groves 1987; W. Matsuda et al. 2009). Because of this, dopaminergic neurons in the SNpc exhibit higher basal rate of mitochondrial metabolism than dopaminergic neurons in the VTA (Guzman et al. 2010; Puopolo, Raviola, and Bean 2007; Chan et al. 2007). Certain neurotoxins (e.g. rotenone) that inhibit mitochondrial function selectively affect nigral dopaminergic neurons but not dopaminergic neurons in VTA (Blesa and Przedborski 2014). Therefore, nigral dopaminergic neurons are particularly susceptible to mitochondrial dysfunction.

Dopamine metabolites (e.g. 6-hydroxydopamine) are toxic to neurons, therefore, the cytosolic level of dopamine is strictly regulated. Dopamine transporter (DAT) mediates the uptake of extracellular dopamine while vesicular monoamine transporter type 2 (VMAT2) sequesters intracellular dopamine into storage vesicles. It has been suggested that the functional balance between the two transporters is differentially regulated in nigral and mesolimbic dopaminergic neurons, making nigral dopaminergic neurons more susceptible to dopamine-mediated toxicity (N. Takahashi et al. 1997; González-Hernández 2010).

Ageing is the main risk factor for PD and dopaminergic neurons in the SNpc are more affected by ageing than those in the VTA. Normal aged brain displays preferential loss of nigral dopaminergic neurons in the midbrain, which corresponds to the age-related decline in motor function often seen in aged animals and human (Rodriguez et al. 2015; Collier, Kanaan, and Kordower 2011). The major difference between normal aged brain versus PD brain is the extent of nigral dopaminergic neuronal loss (Buchman et al. 2012; Fearnley and Lees 1991; Damier et al. 1999; Collier, Kanaan, and Kordower 2011; Rodriguez et al. 2015). Age-associated decline of physiological function of survived nigral dopaminergic neurons, together with other PD associated pathological factors, could drive the ultimate collapse of any compensatory mechanisms that have kept the dopamine system functional. The next sections discuss possible PD-associated pathological factors.

1.1.4 Environmental factors

The discovery of the neurotoxin, n-methyl-4-phenyl-1,2,3,6-tetrahydropyridine (MPTP), and its mechanisms of action have suggested that environmental toxins cause degeneration of nigral dopaminergic neurons via mitochondrial dysfunction. In the late 1970s, MPTP was inadvertently discovered by a group of young people who attempted to

synthesize an opioid analogue. After intravenous self-injection, all of them developed Parkinsonism, which strongly resembled that of late-onset PD patients. Later, post-mortem studies confirmed the loss of nigral dopaminergic neurons in these patients (Davis et al. 1979; Langston et al. 1999). The selective loss of dopaminergic neurons results from the inhibition of complex I of the electron transport chain in the mitochondrial matrix by an MPTP metabolite, and results in a build-up of damaging free radicals (Langston et al. 1983; Sherer et al. 2007).

Rural livings, use of well water, and agricultural professions have been suggested as risk factors for PD (Zorzon et al. 2002; Lai et al. 2002). These observations can be explained by individuals having higher incidences of being exposed to groups of pesticides or herbicides, notably paraquat and rotenone (Tanner et al. 2011; McCormack et al. 2002). These toxins mediate selective degeneration of dopaminergic neurons by impairing mitochondrial function (Bus, Aust, and Gibson 1976; Day et al. 1999; Xiong, Dawson, and Dawson 2012; Marey-Semper, Gelman, and Lévi-Strauss 1995).

1.1.5 Genetics of PD

The majority of PD cases is sporadic with about 10% of them accounting for familial PD (B. Thomas and Beal 2007). The past twenty years, genetic research has identified 17 distinctive chromosomal loci, termed *PARK* to signify their link to PD and numbered in chronological order of their identification (Table 1.1). It should be noted that this *PARK* nomenclature does not comprehensively reflect genetics of PD because some of the chromosomal loci (*PARK3, PARK10, PARK12, PARK16*) require further identification of causative genes while other chromosomal loci (*PARK5, PARK9, PARK11, PARK13, PARK14, PARK15, PARK18*) require further validation of their association with PD.

Locus	Chromosome loci	Gene	Protein name
PARK1/4	4q21	*SNCA*	α-synuclein
PARK2	6q25-q27	*Parkin*	E3 ubiquitin ligase
PARK3	2p13	*Unknown*	
PARK5	4p14	*UCHL1*	Ubiquitin carboxyl-terminal hydrolase isozyme L1
PARK6	1p35-p36	*PINK1*	PTEN-induced putative kinase 1
PARK7	1p36	*DJ-1*	Protein deglycase DJ-1
PARK8	12q12	*LRRK2*	Leucine rich repeat kinase 2
PARK9	1p36	*ATP13A2*	ATPase 13A2
PARK10	1p32	*Unknown*	
PARK11	2q36	*GIGYF2*	GRB10-interacting GYF protein 2
PARK12	Xq21-q25	*Unknown*	
PARK13	2p12	*HTRA2*	Mitochondrial, Serine protease HTRA2
PARK14	22q13	*PLA2G6*	calcium-independent phospholipase A2
PARK15	22q12-q13	*FBXO7*	F-box only protein 7
PARK16	1q32	*Unknown*	
PARK17	16q11.2	*VPS35*	Vacuolar protein sorting-associated protein 35
PARK18	3q27	*EIF4G1*	Eukaryotic translation initiation factor 4 gamma 1
-	1q21	*GBA*	Glucosylceramidase
-	17q21	*MAPT*	Microtubule-associated protein tau
-	15q22.2	*VPS13C*	Vacuolar protein sorting-associated protein 13C

Table 1.1 List of PD-associated loci and genes

PD-associated genes manifest PD in various forms. Mutations within *Parkin, PINK1, DJ-1, ATP13A2* cause monogenic forms of PD, *GBA, MAPT* alleles are genetic risk factors, accountable for increasing risk of developing PD. Lastly, *SNCA,* and *LRRK2* alleles have been implicated in both monogenic PD and genetic risk factors. I summarise the current

knowledge of the best-characterised PD-associated genes below, particularly *SNCA, GBA, Parkin, PINK1, and DJ-1*. I will review *LRRK2*, which is the subject of my thesis, in Section 1.2.

1.1.5.1 *SNCA*

SNCA is the first gene to be identified in familial PD (Polymeropoulos et al. 1996). *SNCA* is an autosomal dominant PD allele and three pathogenic point mutations, A53T, A30P, and E46K (Polymeropoulos et al. 1997; Krüger et al. 1998; Zarranz et al. 2004) as well as duplications (Chartier-Harlin et al. 2004; Ibáñez et al. 2004) and triplications (Singleton et al. 2003) have been identified in association with PD. Recent Genome Wide Association Studies (GWAS) also have also identified single nucleotide polymorphisms (SNPs) within the *SNCA* in sporadic PD cases (Simón-Sánchez et al. 2009a; Satake et al. 2009; M Farrer et al. 2001; Maraganore et al. 2006). Patients with *SNCA* mutations or multiplications often show dementia as an additional key clinical feature and display early-onset PD <50 years (Polymeropoulos et al. 1996). Penetrance of the missense mutations appears is suggested to be as high as 85% for the A53T mutation (Polymeropoulos et al. 1996).

SNCA encodes for α-synuclein (αsyn) protein, which is expressed widely in the brain and localises mostly to presynaptic nerve terminals (P J Kahle et al. 2000). Natively unfolded, αsyn can oligomerize and form fibrils (Rosenbloom et al. 2011), which are the main components of LBs and LNs found within the nigral neurons of PD patients (Spillantini et al. 1997). Multiplications of *SNCA* increase the overall αsyn protein level up to twofold (Matt Farrer et al. 2004). A30P and A53T αsyn mutants have tendency for self-aggregation (Conway, Harper, and Lansbury 1998).

The physiological function of αsyn or the exact pathology of αsyn is partly understood. Monomeric αsyn normally localizes to the presynaptic terminal and associates with synaptic vesicles (Iwai et al. 1995; P J Kahle et al. 2000), therefore, it has been suggested that αsyn potentially regulates synaptic vesicle trafficking (Cabin et al. 2002; Murphy et al. 2000; Scott and Roy 2012). Once in the form of aggregates or oligomers, αsyn localizes to the cell body and neurites, disrupting various cellular function, notably inhibiting dopamine release by impairing synaptic exocytosis (Nemani et al. 2010; K. E. Larsen et al. 2006), blocking protein degradation by the 26S proteasome (Snyder et al. 2003), or inducing mitochondrial dysfunction (Reeve et al. 2012; Di Maio et al. 2016).

1.1.5.2 *GBA*

Mutations in the *GBA* gene cause Gaucher Disease (GD), which is a recessively inherited lysosomal storage disorder (Hruska et al. 2008). Interestingly, GD patients and heterozygous *GBA* mutation carriers have increased risk of developing PD (E. Sidransky et al. 2009). The frequency of heterozygous *GBA* mutations range from 10 to 30% among Ashkenazi Jewish population and 2 – 10% in other ethnic groups (Ellen Sidransky and Lopez 2012; Toft et al. 2006; Aharon-Peretz, Rosenbaum, and Gershoni-Baruch 2004). To date *GBA* mutations are the most common genetic risk factor for PD (Rosenbloom et al. 2011; Schapira and Gegg 2013).

GBA encodes glucosylceramidase, a lysosomal enzyme, which cleaves glucosylceramide to ceramide and glucose. How the mutations contribute to the PD pathogenesis is becoming clearer. Most of PD-causing *GBA* mutations are missense, leading to a misfolded protein (Ellen Sidransky and Lopez 2012). Mutant forms of glucocerebrosidase has been found within the LBs of PD patients (Goker-Alpan et al. 2010). In dopaminergic neurons derived from human induced pluripotent stem cells (hiPSCs), *GBA* N370S mutation causes an increase in extracellular level of αsyn. Misfolded N370S mutants

were found within the ER, inducing an activation of ER stress and caused an abnormal enlargement of lysosomal compartments, a sign for autophagy disturbance (Fernandes et al. 2016).

1.1.5.3 *Parkin*

Parkin is an autosomal recessive PD allele causing early onset PD with mean age of onset around 32 years (Lücking et al. 2000). Numerous mutations ranging from point mutations to multiplications have been identified, notably more than 30 exon rearrangements, 30 missense mutations, 8 nonsense mutations, and 20 indels (Abbas et al. 1999). The encoded protein, Parkin, is a ubiquitin E3 ligase. Together with ubiquitin-conjugating enzyme (E2), Parkin catalyses ubiquitin attachment to protein targets, signalling proteasome degradation (Tanaka et al. 2000). Several Parkin substrates have been reported, particularly CDCrel-1 (a septin GTPase which is associated with synaptic vesicles), synphilin-1 (αsyn interacting protein), or AIMP2 (Aminoacyl-tRNA synthetase-interacting multifunctional protein type 2, which are found in LBs) (Tanaka et al. 2000; Y. Zhang et al. 2000; Corti et al. 2003; K. K. K. Chung et al. 2001). Parkin is predominantly localized in the cytosol, ER, Golgi complex, and the outer mitochondrial membrane (Mouatt-Prigent et al. 2004). Together with PINK1 it has been shown to regulate mitochondrial quality control (Pickrell and Youle 2015).

1.1.5.4 *Pink1*

Pink1 is another autosomal recessive PD allele, causing early-onset PD (Valente et al. 2001). Most of mutations are missense and nonsense mutations, notably P196L, G309D, G440E, and structural deletions are rare (Lill 2016). *Pink1* encodes phosphatase and tensin homolog (PTEN)-induced kinase 1 (PINK1) which consists of 8 exons and 581 amino acids. The protein sequence of PINK1 contains a mitochondrial targeting sequence at the N terminus and it has been shown that PINK1 is imported into the mitochondrion

(Valente et al. 2001). PINK1 selectively accumulates on the outer membrane of damaged or dysfunctional mitochondria (Jin et al. 2010; Meissner et al. 2011) and recruits Parkin to initiate mitophagy by ubiquitinating damaged mitochondria (Narendra et al. 2008; Geisler et al. 2010; N. Matsuda et al. 2010; Vives-Bauza et al. 2010).

1.1.5.5 *DJ-1*

Mutations in *DJ-1* cause an early onset PD age onset around 20 – 40 years (Bonifati et al. 2003). *DJ-1* encodes for 189 amino acids protein, DJ-1, which exists as a dimer and is expressed in both neurons and glial cells (Bonifati et al. 2003; Rizzu et al. 2004; Yanagida et al. 2006). Although the full understanding of its function is required, DJ-1 functions as a cellular sensor of oxidative stress (Bonifati et al. 2003). Under oxidative stress, its expression is upregulated, particularly in reactive astrocytes (Yanagida et al. 2006). L166P mutation reduces stability of DJ-1 protein, leading to subsequent degradation by the proteasome. Lack of functional DJ-1 protein has been reported to reduce antioxidant activity (Anderson and Daggett 2008; Malgieri and Eliezer 2008). Similarly, knock out (KO) or knock down (KD) of *DJ-1* inhibits astrocyte-mediated neuroprotection against oxidative stress (Mullett and Hinkle 2011; Waak et al. 2009; N. J. Larsen et al. 2011).

1.1.6 Microglia-mediated neurotoxicity

Signs of chronic inflammation are commonly displayed in various neurodegenerative diseases (Amor et al. 2014). Meta-analysis studies report that blocking inflammation can reduce the risk of the onset or progression of the diseases. Individuals with extended exposure to nonaspirin nonsteroidal anti-inflammatory drugs (NSAIDs) are protective from the onset or progression of developing PD (Gagne and Power 2010) and Alzheimer's disease (AD) (Etminan, Gill, and Samii 2003). Exactly how inflammation

leads to the onset and/or exacerbate the progression of disease is an active area of research.

Microglia, the resident macrophages (MΦs) in the central nervous system (CNS), perform a set of homoeostatic functions to maintain a healthy environment for neurons. They phagocytose cell debris, extracellular protein aggregates and incompetent synapses. Microglia are also responsible for responding to inflammation by secreting inflammatory mediators, notably TNFα, and a myriad of cytotoxic factors, especially reactive oxygen species (ROS) and nitric oxide (NO), which are all harmful to neurons. Potentially damaging side-effects of microglia activation can instigate a feedforward cycle of chronic inflammation and neurodegeneration. Therefore, microglia play a vital role as they are not only involved in preventing the disease by phagocytosing potentially harmful materials but also can contribute to disease progression by initiating exaggerated inflammatory responses.

In this section, I review the evidence for the involvement of inflammation in PD, and how some of key PD-associated genes are implicated in this process (Figure 1.1).

1.1.6.1 Inflammation and PD

In PD brains, patients and animal models display more activated microglia compared to controls (Barcia et al. 2013; McGeer et al. 1988). Elevated levels of inflammatory cytokines, especially tumour necrotic factor-α (TNFα), interleukin-1β (IL-1β), IL-2, IL-6, IL-8, and Interferonγ (IFNγ) have been detected in the brain, cerebrospinal fluid, and blood of PD patients (Mogi et al. 2000; Dobbs et al. 1999; Koziorowski et al. 2012; Dzamko, Rowe, and Halliday 2016). Infiltration of peripheral immune cells, particularly CD4(+) and CD8(+) T cells, have been shown in a mouse model of PD, possibly as a result of leakage of the blood brain barrier (BBB) (Brochard et al. 2009; Kurkowska-

Jastrzębska et al. 1999). Involvement of humoral immunity has also been implicated, as LBs and dopaminergic neurons in the SNpc of PD patients showed strong immunolabelling for immunoglobulin G (C. F. Orr et al. 2005). Collectively, all of these on-going inflammatory processes involve chronic activation of microglia, supporting the hypothesis that neuroinflammation in association with dysregulated microglial function contribute to the progression of neurodegeneration.

1.1.6.2 The role of PD genes in the immune system

Several PD-associated genes *LRRK2*, *SNCA*, *GBA*, *VPS35*, *Parkin*, *PINK1*, and *DJ-1* are expressed in immune cells (Table 1.2) and are implicated in various aspects of innate immune responses, suggesting an intriguing link between genetic mutations and inflammation-driven neurotoxicity (Moehle et al. 2012; Thévenet et al. 2011; Gardai et al. 2013; Bader et al. 2005; Tran et al. 2011; S. Kim et al. 2004; H. Lee, James, and Cowley 2017; Waragai et al. 2007; Wilhelmus et al. 2011). For example, overexpression of αsyn or the presence of A30P or E46K variants elicits pro-inflammatory responses in mouse microglia (Su, Federoff, and Maguire-Zeiss 2009; Hoenen et al. 2016) and impairs phagocytosis in mouse microglia (Park et al. 2008; Gardai et al. 2013) and in hiPSC-derived MΦs (Haenseler, W; Zambon, F; Lee, H; Vowles, Jane; Rinaldi, F; Duggal, G; Houlden, H; Gwinn, K; Wray, S; Luk, K; Wade-Martins, R; James, W; Cowley 2017). N370S *GBA* mutant in hiPSC-derived MΦs displays no defect in the uptake of erythrocytes while impairing subsequent digestion of them (Aflaki et al. 2014; Panicker et al. 2012).

Deficiency in *DJ-1* in both LPS activated astrocytes and microglia induces elevation of IL-6, iNOS, NO and intracellular ROS in mice (Waak et al. 2009; Trudler et al. 2014). Parkin has been reported to suppress inflammation and cytokine-induced cell death by

promoting degradation of TNFα receptor-associated factor 2/6 (TRAF2/6) (J.-Y. Chung et al. 2013).

Cell types	Relative expression level					
	LRRK2 *PARK8*	αsyn *PARK1/4*	DJ-1 *PARK7*	PINK1 *PARK6*	Parkin *PARK2*	GBA
Brain						
Neurons	+	+++	+++	++	+++	+
Microglia	+++	++	+	+	+	++
Astrocytes	+	+	++	+++	+	+++
Oligodendrocytes	+	++	++	++	+	+
Periphery						
B Cells	+++	++	Expression in PBMC	N/D	N/D	+
T Cells	N/D	++		N/D	N/D	+
Macrophages	*+++	N/D		N/D	+	+
Monocytes	*+++	+++		N/D	N/D	+
Dendritic Cells	+	N/D		N/D	N/D	+

Table 1.2. Expression of PD-related genes in the brain and immune cells in periphery. Relative expression was scored by +++ being the highest and + being the lowest in comparison with listed cell types. * denotes upregulation by interferon-γ (IFNγ). N/D, not determined; PBMC, peripheral blood mononuclear cells.

Parkin has also been implicated in the removal of intracellular pathogens in a similar ubiquitin-mediated mechanism involved in mitophagy (Manzanillo et al. 2013). *PINK1* deficiency has been shown to elevate inflammatory cytokine levels in mice (J. Kim et al. 2013) while another study has suggested that PINK1 interacts with TRAF6 and transforming growth factor β-activated kinase 1 (TAK1), positively regulating IL-1β-mediated signalling pathways (H. J. Lee et al. 2012).

Lastly, numerous evidence supports the functional implication of LRRK2 in cells of myeloid lineage, notably MΦs and microglia. Certain inflammatory cytokines (e.g. IFNγ) upregulates LRRK2 protein expression in these cells and LRRK2 has been implicated in

both phagocytosis and inflammatory cytokine release. Variants of *LRRK2* are linked to be risk factors for other immune-related disorders, particularly Crohn's disease and leprosy (Barrett et al. 2008; Franke et al. 2010; Umeno et al. 2011; F.-R. Zhang et al. 2009). The role of *LRRK2* in the immune system will be more extensively discussed in the next chapters.

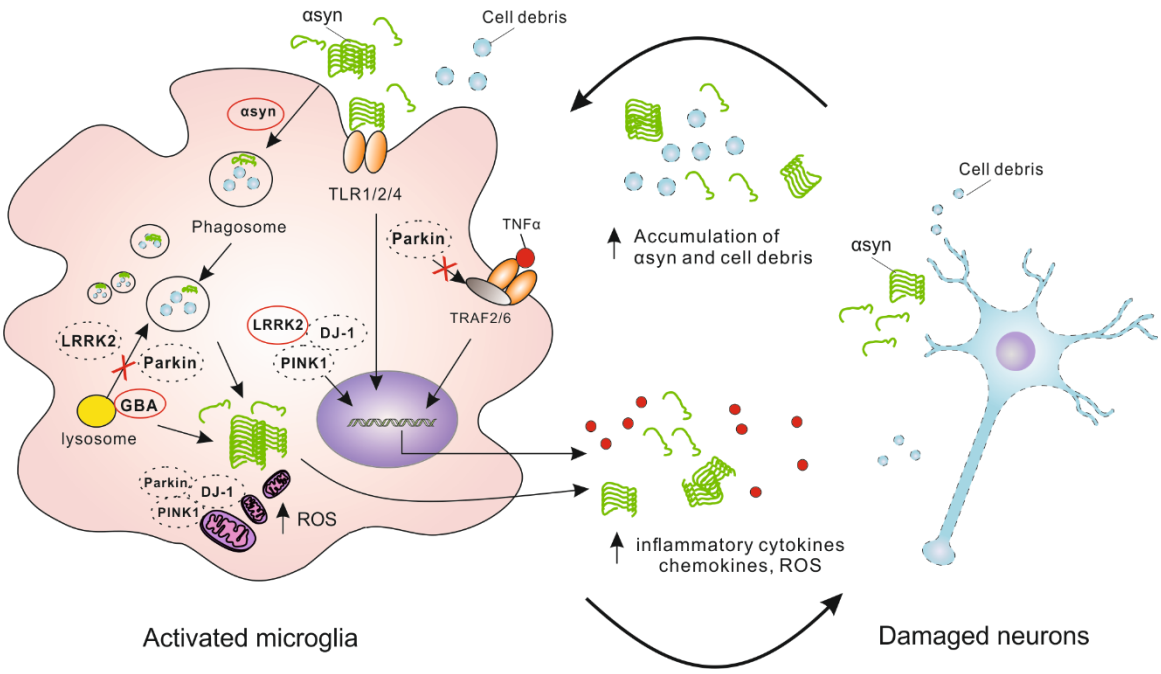

Figure 1.1 PD-associated genes in microglial functions. Disease causing mutation is represented in red circle and KO or KD of expression is shown in dotted circle. In brief, accumulation of αsyn (both monomers and aggregates), lack of expression in *LRRK2*, *Parkin*, and the presence of PD-causing *GBA* mutant impair phagocytosis. This leads to the accumulation of cell debris and protein aggregates which are harmful to neurons. PD-causing mutations in *LRRK2*, αsyn, and lack of expression in *DJ-1*, *PINK1*, and *Parkin* may generate dysregulated pro-inflammatory cytokine release and ROS, causing neuronal damage. Damaged neurons will then instigate further activation of microglia, generating a feedforward cycle of neuroinflammation and neurodegeneration. TLR, toll-like receptors; TRAF2/6, transforming growth factor β-activated kinase 1; ROS, reactive oxygen species.

1.2 Leucine Rich Repeat Kinase 2

1.2.1 *LRRK2* mutations, epidemiology, and penetrance

In 2002, genome-wide linkage analysis of a Japanese family with PD has identified a new *PARK8* chromosome locus on 12p11.2 (Funayama et al. 2002). Two years later, two independent groups identified *LRRK2* as the causative gene for PD (Paisán-Ruíz et al. 2004; Zimprich et al. 2004). Analysis of 24 populations worldwide revealed that *LRRK2* mutations are found in 4% of familial PD patients and 1% of idiopathic PD patients (Healy et al. 2008), accounting for one of the most common genetic causes for PD.

Over 45 PD-associated mutations in *LRRK2* have been identified, and six mutations have been confirmed to be pathogenic by segregation studies with multiple families. These mutations consist of the most common mutation, G2019S (Healy et al. 2008; Lesage et al. 2005; Marongiu et al. 2006; Papapetropoulos et al. 2006; Ishihara et al. 2007; Latourelle et al. 2008a; Munhoz et al. 2008; Bras et al. 2008; Gorostidi et al. 2009; Alcalay et al. 2013), R1441G (Paisán-Ruíz et al. 2004; Mata et al. 2005; Ferreira et al. 2007; Bras et al. 2008; Gorostidi et al. 2009), R1441C (Zimprich et al. 2004), R1441H (Zabetian et al. 2005; Spanaki, Latsoudis, and Plaitakis 2006), Y1699C (Paisán-Ruíz et al. 2004; Zimprich et al. 2004) and I2020T (Funayama et al. 2005). Apart from these monogenic-disease associated mutations, GWAS have identified several polymorphisms within *LRRK2* to be associated with sporadic PD (Simón-Sánchez et al. 2009b; Satake et al. 2009) (Figure 1.2).

The frequency of monogenic *LRRK2* mutation varies depending on ethnicity and region. Among Ashkenazi Jews, Moroccans, Algerians and Tunisians, carriers of G2019S mutations account for 20 – 40% of familial PD and 10 – 30% of sporadic cases (Lesage et al. 2005; Hulihan et al. 2008; Bouhouche et al. 2017; Ishihara et al. 2007; Alcalay et al.

2013). Among North Americans of European origins, close to 2% of familial PD patients are G2019S carriers, while 0 – 9% of sporadic cases have the allele (Ferreira et al. 2007; Sierra et al. 2011; Cilia et al. 2014; Yescas et al. 2010; Johnson et al. 2007; Saunders-Pullman et al. 2011).

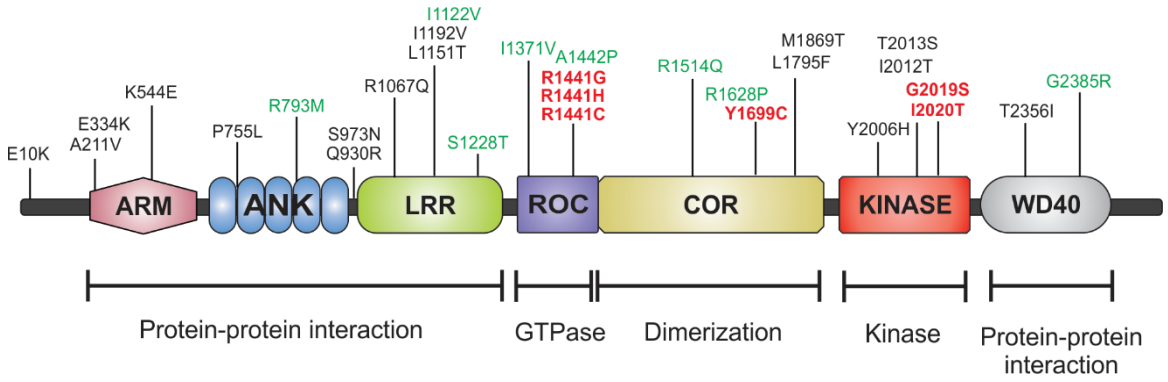

Figure 1.2 Schematic representation of full-length LRRK2 with PD-associated variants. Mutations that are pathogenic are shown in red. Amino acid substitutions that increase a risk of developing PD and/or are putatively pathogenic are shown in green. *LRRK2* variants that have been identified in PD patients with uncertain pathogenicity are shown in black. Predicted functions of LRRK2 domains are listed. Abbreviations: ARM, armadillo repeats; ANK, ankyrin repeats; LRRs, leucine-rich repeats, ROC, Ras of complex protein GTPase domain; COR, C-terminal of Roc; WD40, WD40 repeats.

Recent GWAS results have also identified variants of *LRRK2* as risk factor for idiopathic PD. Most of single nucleotide polymorphisms (SNPs) are found within the promoter region of *LRRK2* (Nalls et al. 2014). While more in-depth analysis of these SNPs is required, it is conceivable that these variants may contribute to the overall expression level of LRRK2 protein.

LRRK2 mutations display an incomplete, age-dependent penetrance. Healy et al., have analysed 133 families worldwide and have reported that for an individual with *LRRK2* G2019S mutation, the risk of developing PD is 28% at age 59 years, 51% at 69 years, and

74% at 79 years (Healy et al. 2008). Similarly, other research groups have reported age-dependent partial penetrance of *LRRK2* G2019S among Ashkenazi Jewish PD patients (Marder et al. 2015), Arab-Berber PD patients from Tunisia (Hulihan et al. 2008), and worldwide screening of 509 families (Latourelle et al. 2008b). *LRRK2* R1441G mutation also shows age-dependent penetrance of 12.5% at 65 years and of 83.4% at 80 years among PD patients in the Basque Country (Ruiz-Martínez et al. 2010).

1.2.2 Clinical and neuropathological features of *LRRK2* PD patients

LRRK2 mutations display clinical features that are indistinguishable from idiopathic PD. The mean age of onset is around 60 years, similar to typical late-onset sporadic PD, ranging from 28 to 82 years. *LRRK2* PD patients develop slow and progressive resting tremor, bradykinesia, rigidity, postural instability, and freezing. They respond to dopamine replacement therapy, sometimes with accompanying L-DOPA dyskinesia, mirroring key symptoms of sporadic PD (Ishihara et al. 2006; Kay et al. 2006; Trinh, Guella, and Farrer 2014).

Although clinical symptoms resemble that of idiopathic PD cases, the neuropathological features of *LRRK2* PD are pleomorphic. The majority of *LRRK2* PD brain autopsies have reported a loss of nigral neurons and the formation of LBs in the brain stem (Giasson et al. 2006a; Ross et al. 2006). However, atypical neuropathological features have also been observed, notably nigral neuronal loss without LB formation (Giasson et al. 2006a; Gaig et al. 2007; Funayama et al. 2005), diffused LBs throughout the brain (Zimprich et al. 2004; Ross et al. 2006), or the presence of Tau pathology (Rajput et al. 2006; Khan et al. 2005; Ujiie et al. 2012).

1.2.3 LRRK2 is a multi-domain, multi-functional enzyme

LRRK2 has 51 exons and encodes 2527 amino acids protein, consisting of four protein-protein interaction domains and two enzymatic domains (Figure1.2). LRRK2 is a member of the Roco protein family, also known as Ras-related GTPase family, in which the structure of the enzymatic core is characterised by a Ras of complex proteins (Roc) G-domain in tandem with the C-terminal of Roc (COR) domain (Bosgraaf and Van Haastert 2003). The Roc domain has the GTP binding site and is adjacent to the COR domain, which acts as a dimerization device (Marín, van Egmond, and van Haastert 2008; Gotthardt et al. 2008; Gasper et al. 2009; Rudi et al. 2015). Four protein-protein interaction domains surround this enzymatic core; N-terminal armadillo repeats (ARM), ankyrin (ANK), and leucine rich repeat (LRR) domains along with the C-terminal WD40 domain.

Pathological mutations of are clustered within the enzymatic core of GTPase (R1441C/H/G, Y1966C) and kinase (G2019S, I2020T) domains. Since the *bona fide* cellular substrates of LRRK2 are not completely clarified, LRRK2 kinase activity has been examined in cell-free systems using purified recombinant proteins. Studies have consistently reported that the *LRRK2* G2019S mutation enhances kinase activity *in vitro* by two to eight-fold (West et al. 2005; Greggio et al. 2006; MacLeod et al. 2006; Guo et al. 2007; Luzon-Toro et al. 2007; Imai et al. 2008; Anand et al. 2009). The effect of I2020T mutation is less consistent: some studies have reported an increase in kinase activity (Gloeckner et al. 2005; West et al. 2007; Imai et al. 2008) while others have observed no difference compared to WT (Luzon-Toro et al. 2007). Mutations within Roc-COR domain, R1441C/H/G, and Y1966C, have been reported to reduce GTPase activity (Guo et al. 2007; Lewis et al. 2007; Stafa et al. 2012; Liao et al. 2014; Xianting Li et al. 2007; Rudi et al. 2015).

Whether there are any inter-regulatory mechanisms between the two enzymatic domains has been an active area of research. Understanding this link would help to answer why mutations in either GTPase or kinase domain equally lead to the same disease phenotype. So far, *in vitro* assays have shown no link between the two activities, for mutants within the Roc-COR domain do not alter LRRK2 kinase activity (Anand et al. 2009; Jaleel et al. 2007; Lewis et al. 2007). Also, providing non-hydrolysable GTP homologues, thereby generating a constitutive GTP-bound LRRK2, does not change the kinase activity of LRRK2 (Taymans et al. 2011; M. Liu et al. 2011).

It is possible that cell-free systems lack crucial factors that influence LRRK2 enzymatic activity. Recent studies have reported that LRRK2 forms a dimer in intact cells by various biochemical approaches, notably by co-immunoprecipitation of two differentially tagged LRRK2 (Greggio et al. 2009), and by size-exclusion chromatography followed by Native PAGE of LRRK2 protein extracts from LRRK2-overexpressing HEK 293T cells (Sen, Webber, and West 2009). In both overexpression system and endogenous LRRK2, it has been reported that LRRK2 predominantly exists as a monomer in the cytosol and as a dimer at the cellular membrane (Berger, Smith, and Lavoie 2010; James et al. 2012; Schapansky et al. 2014). Berger et al., have reported that isolated membrane-bound dimeric LRRK2 displayed higher kinase activity *in vitro* by demonstrating higher autophosphorylation level compared to cytosolic monomeric form (Berger, Smith, and Lavoie 2010). Therefore, diverse factors may control LRRK2 enzymatic activity, notably LRRK2 dimerization, cellular localisation, and interaction with yet to be identified interactors. Thus, more biochemical understanding of LRRK2 activation mechanism in a physiologically relevant setting (e.g. endogenous expression in a relevant cell type), is merited to fully understand how GTPase and kinase activities are inter-regulated.

1.2.4 Cellular functions of LRRK2 - what we know so far

LRRK2 has been implicated in almost every cellular pathway: endosome vesicle trafficking; cytoskeleton reorganization; mitochondrial function; regulation of ER/Golgi retromer complex; autophagy/lysosomal pathway and in various signalling pathways; particularly wingless/int (wnt); TNF-α/Fas ligand (FasL)/Fas-associated protein with death domain; mitogen-activated protein kinase (MAPK); and nuclear factor κ-light-chain-enhancer of activated B (NFκB) pathways (Loukia Parisiadou and Cai 2010; Häbig et al. 2013; Wang et al. 2012; Saha et al. 2009; Cho et al. 2014; Gómez-Suaga et al. 2012; López de Maturana et al. 2016; Gardet et al. 2010; Chen et al. 2012). The long list of potential cellular functions of LRRK2 makes it difficult to discern which of these pathways reflect true functions of LRRK2.

Studies have also implicated the interaction of LRRK2 with various Rab GTPases (Berger, Smith, and Lavoie 2010; James et al. 2012; Schapansky et al. 2014). Rab GTPases regulate a variety of cellular processes by recruiting specific enzymes, coordinating vesicle transport via interactions with cytoskeletal networks (Villarroel-Campos, Bronfman, and Gonzalez-Billault 2016). Interestingly, LRRK2 has been implicated in equally diverse roles, suggesting that LRRK2 may work in rapport with Rab GTPases. Studies using yeast two-hybrid screening followed by GST pull down/co-immunoprecipitation assays has suggested Rab5b as an interacting protein of LRRK2 (Shin et al. 2008). The same research group later reported that recombinant LRRK2 protein directly phosphorylates Rab5b at Thr7 residue *in vitro* (Yun et al. 2015a). Additional interacting partners have been reported; Rab32 and Rab38 (Waschbüsch et al. 2014) by yeast two-hybrid screening, Rab7L1 (also known as Rab29) by high-throughput protein-protein interaction arrays (Beilina et al. 2014). In *Drosophila melanogaster*, the LRRK2 homolog has been reported to co-localise with Rab7 (Dodson et al. 2012).

Recently, phosphoproteomic screens have identified endogenous LRRK2 phosphorylates Rab10 at its Thr73 residue in mouse fibroblasts. In follow-up studies, a selection of Rabs, Rab3, Rab8 and Rab12, were shown to be phosphorylated by LRRK2 at their Thr86, Thr72, Thr73 residues, respectively *in vitro* and in HEK 293T cells (Steger et al. 2016).

In the next section, I will discuss our current understanding of possible cellular functions of LRRK2 in its association with Rab GTPases (Figure 1.3). However, it should be noted that, most of these observations have been made in LRRK2-overexpresison system. As LRRK2 is a multidomain, dual-enzymatic protein, likely to have multiple interacting partners, therefore, some of the reported functions/interactors require further validation at the endogenous level.

1.2.4.1 Synaptic endocytosis

A set of Rab GTPases has been identified to regulate synaptic vesicle (SV) trafficking. In general, Rab3a/b/c and Rab27b are involved in exocytosis (Fischer von Mollard et al. 1994) while Rab4, Rab5, Rab10, Rab11b and Rab14 are involved in the recycling of SVs (Fischer von Mollard et al. 1994; Khvotchev et al. 2003; Schlüter et al. 2002).

LRRK2 has been described to localise on SVs in mouse cortical neurons (Piccoli et al. 2011) and hippocampal neurons (Shin et al. 2008). KD or overexpression of *LRRK2* harbouring G2019S mutation has been reported to impair SV endocytosis in LRRK2 overexpressing PC12 cells (Shin et al. 2008), in *Drosophila melanogaster* neuromuscular junctions (Matta et al. 2012), and in mouse hippocampal neurons (Shin et al. 2008; Arranz et al. 2015). Transfecting human *LRRK2* R1441C mutant in *Drosophila* dopaminergic neurons also has been reported to impair SV endocytosis (Islam et al. 2016).

Although exactly how LRRK2 mediates SV endocytosis is not clear, several studies have suggested that LRRK2 interacts with numerous SV proteins, notably synaptojanin-1 and

EndophilinA, which modify the SV membrane lipid content (Islam et al. 2016; Matta et al. 2012; Arranz et al. 2015) or N-ethylmaleimide sensitive factor (NSF), which is involved in the fusion of SV with plasma membrane by SNARE (Soluble NSF-Attachment protein REceptor) proteins (Belluzzi et al. 2016). Co-expression of pathogenic *LRRK2* (R1441C and G2019S) and a constitutively active form of Rab5 in rat primary hippocampal neurons has been reported to rescue LRRK2 mutation-mediated impair of SV endocytosis (Shin et al. 2008). Rab5 regulates the SV retrieval and transport by endocytosis (Fischer von Mollard et al. 1994; de Hoop et al. 1994). Although this observation suggests a link between LRRK2 and Rab5, more evidence is merited to clearly understand how LRRK2 regulate synaptic endocytosis in relation to Rab GTPases.

1.2.4.2 Neuronal outgrowth

During development of the nervous system, post-mitotic symmetric neuronal precursors acquire highly asymmetric morphologies, forming a long axon with multiple short dendrites. This process of elongation and specification of neurites involves dynamic signalling pathways, cytoskeletal reorganization, and distribution of various membrane organelles. Several Rab GTPases contribute to the neurite development by orchestrating multiple cellular events: Trans-Golgi Network (TGN)-derived vesicles are transported to newly growing axons (Rab6, 8, 10, 13, 33), early and late endosomes distribute membrane receptors and adhesion molecules (Rab5, 7, 12, 22), and finally recycling endosomes deliver a membrane supply and proteins (Rab4, 11, 35) (Villarroel-Campos, Bronfman, and Gonzalez-Billault 2016).

Pathogenic mutations of *LRRK2* have been reported to impair neurite outgrowth by various cell and animal models, notably hiPSC-derived dopaminergic neurons, SH-SY5Y, PC12 cells, primary rat neurons, primary mouse neurons (Reinhardt et al. 2013; Heo et al. 2010; MacLeod et al. 2006; L. Parisiadou et al. 2009; Dächsel et al. 2010; Winner et al.

2011). The fact that a constitutively active form of Rab5 inhibits neuronal outgrowth (J. Liu et al. 2007) and Rab5 has been suggested as an interacting partner of LRRK2 (Shin et al. 2008; Yun et al. 2015b), led Heo et al., to propose an interplay between LRRK2 and Rab5 in neuronal shortening. However, they observed that co-expressing pathogenic LRRK2 with constitutively inactive Rab5 did not rescue LRRK2-mediated impair of neurite outgrowth (Heo et al. 2010). If Rab5 were a true substrate of LRRK2, this observation does not fully explain why *LRRK2* G2019S mutation, with higher kinase activity therefore generating an inactive form of Rab5, leads to a shortening of neurite outgrowth. However, Heo et al., have also reported that KD of LRRK2 together with expressing an active form of Rab5 rescued shortening of neurite caused by LRRK2 mutations (Heo et al. 2010). Since LRRK2 and its likely target Rab GTPases (Rab5, 7, 8, 10), are implicated in various cellular processes leading to neurite outgrowth pathogenic LRRK2-mediated impairment of neuronal outgrowth probably occurs in combination of several or all above events.

1.2.4.3 LRRK2 in autophagy/lysosomal pathways

Autophagy is a well conserved mechanism in which a cell degrades a range of materials from protein aggregates to damaged organelles via the lysosomal pathway. Since many neurodegenerative diseases, notably PD, AD, and Huntington's Disease (HD), feature accumulation of abnormal proteins (Banerjee, Beal, and Thomas 2010), how dysregulation of autophagy contributes to a disease course has been actively investigated.

The basic mechanism of autophagy starts by sequestering the target inside an ER/trans-golgi network (TGN)-derived lipid bilayer, forming a double-membrane autophagosome. Microtubule-associated protein light chain 3 (LC3) is a crucial player of autophagy. Cytosolic LC3-I is lipidated to LC3-II which bind to the autophagosomal membrane. Therefore LC3 has become a popular marker to observe autophagy activity (Kabeya et al.

2000; Loos, du Toit, and Hofmeyr 2014). The final step involves the fusion of lysosome with autophagosome, leading to a complete destruction of the target.

Various Rab GTPases are involved in the processing of autophagosomes. In brief, Rab4, 5, 7 are involved in maturation of autophagosomes by delivering necessary accessory proteins, notably Beclin-1 complex (Ravikumar et al. 2008; Talaber et al. 2014; Bains et al. 2011). Rab1, 9, 11 are involved in recycling and transporting cargo proteins to and from TGN (Longatti et al. 2012; Nozawa et al. 2012). Rab32 is involved in biogenesis of lysosome-related organelles (Hirota and Tanaka 2009). Rab24 delivers LC3 to autophagosomes (Munafó and Colombo 2002). Rab8 takes a part in the unconventional export pathway of the proinflammatory cytokine, IL-1β, together with autophagy protein 5 (ATG5), inflammasome (Dupont et al. 2011).

LRRK2 has been reported to colocalise with LC3 and have been found within autophagic organelles including multivesicular bodies (MVBs) and autophgolysosomes (Alegre-Abarrategui et al. 2009). Ectopic overexpression of these pathogenic mutants in HEK 293T cells or in SH-SY5Y cells has also resulted in decreased LC3 turnover, leading to accumulation of autophagic vacuoles (Alegre-Abarrategui et al. 2009; Plowey et al. 2008; Bravo-San Pedro et al. 2013). This was also observed in iPSC-derived dopaminergic neurons from *LRRK2* G2019S PD patients (Reinhardt et al. 2013) and in R1441C and G2019S *LRRK2* transgenic mice (Ramonet et al. 2011).

1.2.4.4 Regulation of immune responses

Endogenous LRRK2 is highly expressed in subsets of immune cells in the presence of IFNγ (Gardet et al. 2010; Gillardon, Schmid, and Draheim 2012; Kuss, Adamopoulou, and Kahle 2014; Thévenet et al. 2011). Rab GTPases also play an important role in the immune system. For example, phagocytosis is highly coordinated by various Rab

GTPases, notably Rab1,4 5,7,10,11 (Gutierrez 2013; Pei, Bronietzki, and Gutierrez 2012). As the role of LRRK2 in the immune system is the main theme of the thesis, the current literature will be reviewed and experimental evidence of potential LRRK2 function in the immune system will be discussed throughout the results chapters.

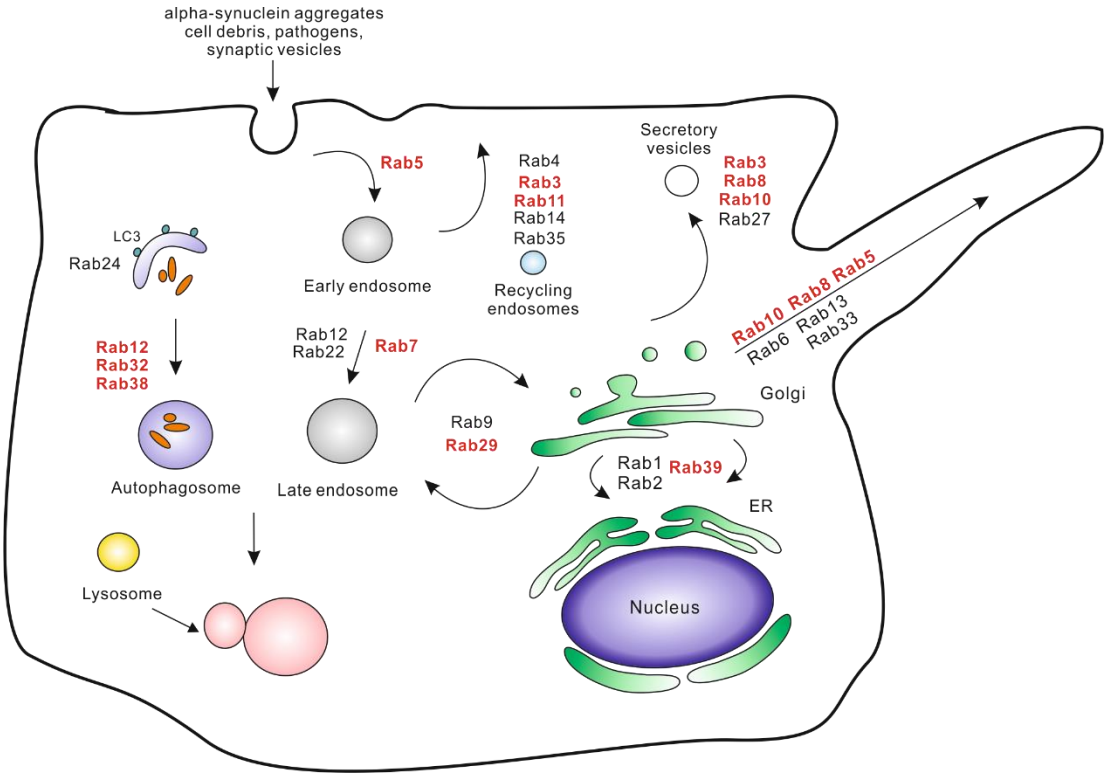

Figure 1.3 Schematic view of LRRK2-associated cellular pathways in association with Rab GTPases. Rab GTPases that have been reported to interact with LRRK2 are shown in red. LC3, Microtubule-associated protein 1A/1B-light chain 3; ER, endoplasmic reticulum.

1.2.5 LRRK2 kinase inhibitors

Developing LRRK2 kinase inhibitors has been the focus of the development of potential treatment of PD (Figure 1.4). LRRK2-IN-1 was the first generation of selective LRRK2 kinase inhibitor, which was characterised by a high-throughput kinase screening of 442 kinases (Deng et al. 2011). This compound had an IC_{50} of 13.0 nM for WT and 6.0 nM

for G2019S LRRK2 protein, therefore, was widely used in the early studies. However, a few years later, LRRK2-IN-1 was shown to have multiple off-targets, particularly ERK5, which is involved in JAK/STAT pathway-mediated LRRK2 expression in immune cells (Kuss, Adamopoulou, and Kahle 2014; Luerman et al. 2014). CZC-54252 and CZC-25146 compounds are potent against LRRK2, with IC_{50} of 1.28 nM for WT and 1.85 nM for G2019S LRRK2 protein. These compounds only inhibited five to ten of 185 other kinases screened (Ramsden et al. 2011) Unfortunately, both CZC compounds and LRRK2-IN-1 cannot cross the BBB, therefore, were less favourable for clinical applications.

Second generation LRRK2 kinase inhibitors involve small compounds with high BBB permeability and potency against LRRK2. HG-10-102-1 was the first compound reported to penetrate the BBB and inhibit LRRK2 activity in mouse brain (Choi et al. 2012). However, its potency against LRRK2 was about 10 times lower than the first-generation inhibitors (IC_{50} of 20.3 nM for WT and 3.2 nM for G2019S LRRK2 protein). GSK2578215A and GNE-7915 are potent, BBB-permeable drugs. They have IC_{50} of 10.9 nM and 9 nM for WT LRRK2, respectively, and their efficiency was tested in rats (Reith et al. 2012; Hatcher et al. 2017; Estrada et al. 2012). The most recent LRRK2 inhibitor is MLi-2. It is highly potent (IC_{50} of 0.8 nM for WT and 0.76 nM for G2019S LRRK2 protein) and is able to cross the BBB (Fell et al. 2015).

Unfortunately, currently available LRRK2 kinase inhibitors have been developed by high-throughput screening rather than structure-based drug design. This is because the high-resolution structure of full-length LRRK2 protein by X-ray crystallography, NMR, or Cryo-EM is currently unobtainable due to the technical challenges of purifying sufficient amount of full-length LRRK2 protein. Because ATP binding sites are highly conserved across kinases, LRRK2 kinase inhibitors face a risk of unknown kinases being

inhibited in the cell. Furthermore, without knowing the true physiological substrates of LRRK2, the direct evidence that any of these LRRK2 kinase inhibitors do inhibit LRRK2 kinase activity in physiological circumstances is questionable.

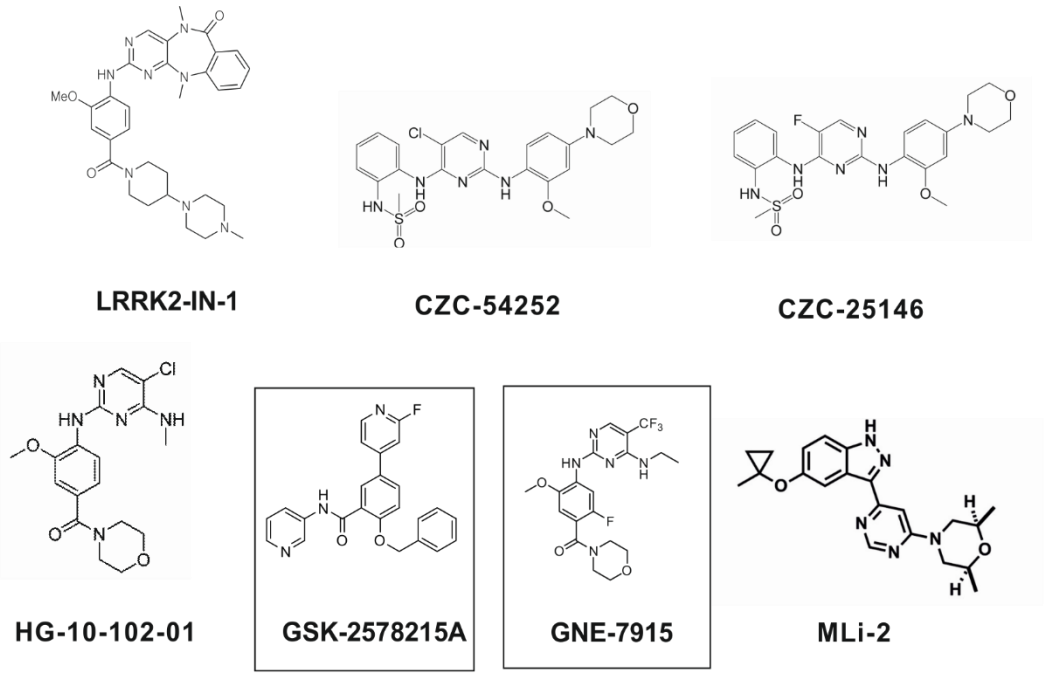

Compound	IC_{50}, nM		Brain penetrance	Off-target kinases/Total tested
	WT	G2019S		
LRRK2-IN-1	13.0	6.0	No	12/442
CZC-54252	1.28	1.85	No	10/185
CZC-25146	4.76	6.87	No	5/185
HG-10-102-01	20.3	3.2	Yes	2/451
GSK-2578215A	10.9	8.9	Yes	2/451
GNE-7915	9.0	3.0	Yes	2/451
MLi-2	0.8	0.8	Yes	5/308

Figure 1.4 LRRK2 kinase inhibitors. LRRK2 kinase inhibitors used in this thesis were highlighted in box.

1.3 Modelling Parkinson's disease

1.3.1 Criteria for an ideal model

The ideal model of PD should reflect key pathological and clinical features of PD. These includes the selective degeneration of nigral dopaminergic neurons, the formation of LBs and LNs containing αsyn, and motor deficits that are responsive to L-DOPA treatment. Furthermore, age-dependent onset and progressive debilitation of pathology should be reflected to capture any compensatory changes occurring over the course of PD progression. Unfortunately, there is no single model which meets all of above criteria. In this section, I review most of the commonly used strategies to model PD, and discuss their advantages and disadvantages.

1.3.2 Animal models of PD

1.3.2.1 Toxin-based animal models

The standard toxin-based animal models are generated by using neurotoxins that selectively cause lesions in the SNpc. The most commonly used neurotoxins are 6-hydroxydopamine (6-OHDA), MPTP, paraquat, and rotenone. 6-OHDA is a hydroxylated analogue of dopamine and can be taken up by both noradrenergic and dopamine transporters, inducing degeneration in both systems (Ungerstedt 1968). Because of this, and its inability to cross the BBB, 6-OHDA is injected stereotactically into the midbrain region. 6-OHDA is oxidized in the cytosol, generating reactive oxygen species, which ultimately cause oxidative stress-mediated cytotoxicity although the exact molecular mechanisms have not been elucidated (Van Kampen, McGeer, and Stoessl 2000; Saner and Thoenen 1971).

MPTP, on the other hand, is lipophilic, therefore, can readily cross the BBB and induce nigral dopaminergic neurodegeneration. Once in the brain, MPTP is taken up by

astrocytes, metabolized by monoamine oxidase-B (MAO-B), and converted to the active toxic form, MPP+. MPP+ is then selectively taken up by dopaminergic neurons through dopamine transporters (DATs). MPP+ induces neurotoxicity by inhibiting complex I of the mitochondrial electron transport chain, leading to ATP depletion and accumulation of free radicals (Nicklas, Vyas, and Heikkila 1985; Mizuno, Sone, and Saitoh 1987; Dauer and Przedborski 2003).

Paraquat is one of the most widely used herbicides and has structural similarity to MPP+. While MPP+ cannot cross the BBB, paraquat can, potentially through the neutral amino acid transporters (Shimizu et al. 2001; McCormack and Di Monte 2003). As the BBB becomes more permeable with age (Kleine, Hackler, and Zöfel n.d.; Wu et al. 2016), accumulation of paraquat in the brain has been reported to be age-dependent (Widdowson et al. 1996). Paraquat is not taken up by DAT therefore it is still not clear how paraquat causes degeneration of nigral dopaminergic neurons. Once inside the cell, cytotoxicity is induced by accumulation of superoxide radicals generated by cyclic reduction and oxidation of paraquat by NADPH and nitric oxide synthase (Bus, Aust, and Gibson 1976; Day et al. 1999).

Lastly, rotenone is a lipophilic pesticide, which is able to cross the BBB. Once in the cell, it inhibits complex I of the electron transport chain, inducing oxidative stress. Rotenone can enter any cells without using specific transporters, yet systemic injections of rotenone selectively affect nigral dopaminergic neurons, consistent with the notion that nigral dopaminergic neurons are intrinsically vulnerable to oxidative stress (Marey-Semper, Gelman, and Lévi-Strauss 1995; Huang et al. 2009).

The major advantage of using neurotoxin-models is that they all display motor deficits accompanied by degeneration of nigral dopaminergic neurons. Therefore, they have been

used extensively as preclinical models to assess the anti-parkinsonian effect of newly developed therapeutic treatments. However, neurotoxins cause acute damage to neurons, failing to recapitulate the progressive nature of PD pathology. Additionally, none of these neurotoxin-based animal models display αsyn containing LBs, which is another key neuropathological component of PD (Huang et al. 2009; Kleine, Hackler, and Zöfel n.d.; Wu et al. 2016; Mizuno, Sone, and Saitoh 1987; Dauer and Przedborski 2003).

1.3.2.2 Genetic animal models

Genetic animal models are generated by manipulating PD-causing genes mostly in rodents but also in *Drosophila melanogaster*, or *Caenorhabditis elegans*. Unlike neurotoxin models, genetic models better recapitulate the progressive nature of PD. However, most transgenic rat or mouse models have failed to display key pathological and clinical features of PD, namely dopaminergic neurodegeneration, presence of LBs, and motor deficits are lacking (Dawson, Ko, and Dawson 2010). For example, it has been consistently reported that *LRRK2* KO mice or rats do not display any motor-symptoms, dopaminergic neurodegeneration or αsyn accumulation (Lin et al. 2009; Y. Tong et al. 2010; Youren Tong et al. 2012; Bichler et al. 2013). Instead, kidney abnormalities have been consistently reported in *LRRK2* KO rodents (Youren Tong et al. 2012; Baptista et al. 2013; Ness et al. 2013). On the other hand, *LRRK2* G2019S transgenic mice show selective degeneration of nigral dopaminergic neurons but do not display any motor symptoms or formation of LBs (Ramonet et al. 2011; Chen et al. 2012; Zhou et al. 2011). However, the generation of transgenic mice often leads to the promiscuous expression of the transgene, resulting from the random insertion of multiple copies of transgene (Matthaei 2007). To overcome this problem, bacterial artificial chromosomes (BAC) can be used as BAC constructs are larger and contain all the regulatory elements to drive gene expression. BAC transgenic constructs generally integrate within the genome at lower

copy number (1 – 10 copies). Using this approach, two groups have observed any dopaminergic neurodegeneration, accumulation of αsyn, or motor deficits in BAC mice expressing human *LRRK2* G2019S mutant (Melrose et al. 2010; X. Li et al. 2010). However, BAC R1441C mutant rats and mice have been reported to exhibit motor deficits that are L-DOPA responsive (Sloan et al. 2016).

1.3.3 Modelling PD using human induced pluripotent stem cells

The idea that fully differentiated cells can regain their pluripotency was first shown experimentally by John Gurdon using *Xenopus* in 1958 (Gurdon, Elsdale, and Fischberg 1958). In 2006, Shinya Yamanaka discovered that four transcription factors, *Oct4*, *Sox2*, *Klf4* and *c-Myc*, collectively known as Yamanaka factors, can "reprogram" mouse somatic cells back to pluripotent stem cells, which display similar gene expression profile and development potential to embryonic stem cells (K. Takahashi and Yamanaka 2006). These cells are termed induced pluripotent stem cells (iPSCs). The successful generation of iPSC from human fibroblasts followed within a year (K. Takahashi et al. 2007).

Since then, iPSC technology has become widely used for modelling various diseases in a dish, testing efficacy of potential therapeutic drugs, and developing clinical applications for cell-replacement therapy. Although the human neuroblastoma cell line, SH-SY5Y, immortalized rat dopamine cell line, N27, murine microglia-like BV-2, or MΦ-like RAW264.7 cells (Henn et al. 2009; Westerink and Ewing 2008; Clarkson et al. 1998; M. G. Thomas et al. 2013; Lopes et al. 2010) have been used to dissect molecular functions of PD-associated proteins *in vitro*, these immortalized or transformed cell lines do not faithfully reflect the physiology of human cells. Human iPSCs can overcome this problem, allowing one to investigate the molecular functions of PD-associated proteins using authentic human cells that reflect normal physiology.

Human iPSCs also can be an attractive alternative to primary cells from human donors. The major drawback of using primary cell lines is the limited accessibility and availability of disease-relevant cell types, notably dopaminergic neurons or microglia. Patient fibroblasts-drerived iPSCs, on the other hand, can be expanded indefinitely and differentiated into any cell types. Currently, various protocols are available to differentiate these iPSCs into PD-relevant cell types - dopaminergic neurons (Kriks et al. 2011), cortical neurons (Shi, Kirwan, and Livesey 2012), MΦs (van Wilgenburg et al. 2013), astrocytes (TCW et al. 2017), and microglia (Haenseler et al. 2017). Differentiated cells can be used for subsequent molecular, biochemical *in vitro* experiments as well as for patient-matched cell-replacement therapy.

One of the major drawbacks of human iPSCs is that the differentiation potential of iPSC lines can be influenced by residual epigenetic memory of the parental fibroblasts as a result of incomplete reprogramming (K. Kim et al. 2011; Ohi et al. 2011; Bar-Nur et al. 2011). Additionally, during the generation of iPSCs, cellular age is erased and most of the differentiated cells display immature, fetal-like phenotypes (Robertson, Tran, and George 2013; Studer, Vera, and Cornacchia 2015), which throws their applicability in modelling age-associated, late-onset disease like PD into question. This can be partly overcome by direct differentiation from fibroblasts. It has been reported that direct differentiation of neurons (Mertens et al. 2015) and astrocytes (Tian et al. 2016) from fibroblasts retains cellular age. However, only limited starting materials can be obtained using this approach compare to hiPSCs which are expandable. Also, a recent study has reported that after the extended culture (about six months) of hiPSC-differentiated dopaminergic neurons displayed spliced tau isoforms which are normally found in the adult brain (Beevers et al. 2017).

Lastly, culturing one cell type fails to fully reflect the complex cell-to-cell interaction present *in vivo*. To address this problem, co-culture models can be helpful. For example, by co-culturing microglia and neurons differentiated from the same iPSC source can serve as an ideal platform to investigate the involvement of microglia in neuroinflammation-mediate pathology of PD (Haenseler et al. 2017).

1.3.4 Gene-editing technologies

Gene-editing technologies have greatly enhanced the applicability of iPSCs. Notably, the problem of iPSC line-to-line variations can be minimised by either correcting PD-causing mutations in patient-derived iPSC lines or by introducing mutations in control iPSC lines (Liang and Zhang 2013). Genetically matched, isogenic iPSC lines faithfully capture the impact of pathogenic alleles. Furthermore, primary cells that are resistant to genetic manipulations (e.g. MΦs or microglia), can be genetically engineered at the stem cell level. Finally, by tagging a reporter protein or KO of a gene, iPSC combined with editing technology offers sophisticated ways to investigate molecular function of PD-implicated proteins in these cell types.

Precise genome editing can be achieved by programmable nucleases that introduce DNA double strand breaks (DSBs) at specific loci. Subsequently, recruitment of endogenous repair machinery either results in non-homologous end-joining (NHEJ) or homology directed repair (HDR) to restore DSB lesion site. NHEJ generates error-prone small indels, resulting in the production of non-functional truncated proteins or mRNA degradation by nonsense-mediated decay (Hentze and Kulozik 1999). HDR machinery uses a DNA template to repair the lesion site, therefore, a specific change of DNA sequence is possible. For example, HDR can be used to repair PD-causing mutations, restoring the gene function (Choulika et al. 1995; Krejci et al. 2012; Bibikova et al. 2003; Plessis et al. 1992).

Using this principle, three major reprogrammable nucleases – zinc finger nucleases (ZFNs), transcription activator like effector nucleases (TALENs), and CRISPR-associated nuclease Cas9 - have been employed to specifically modify gene of interest (Figure 1.5). Both ZFNs and TALENs contain a DNA-binding domain and bacterial FokI nuclease domain which cleaves DNA upon dimerization. The sequence specificity is determined by the DNA binding domain. ZFNs consist 3 – 6 zinc finger proteins, each recognizes DNA sequence in triplet while TALENs consists of 33 – 35 transcription activator like effectors (TALEs), each recognizing a single nucleotide (Y. G. Kim, Cha, and Chandrasegaran 1996; Bibikova et al. 2003; Miller et al. 2007; Boch et al. 2009; Christian et al. 2010). Although both systems have proven their efficiency in various models, the use of ZFNs and TALENs has been greatly hampered by the painstaking process of engineering DNA-binding modules.

Clustered regularly interspaced short palindromic repeats (CRISPR)/Cas (CRISPR-associated)-9 system consists of a Cas9 endonuclease that is directed to cleave a target sequence by a guide RNA (gRNA) (Bolotin et al. 2005; Barrangou et al. 2007; Garneau et al. 2010; Jinek et al. 2012; Cong et al. 2013). By using a simple gRNA, CRISPR/Cas-9 system circumvents the problem of using bulky protein modules. Target specificity is simply determined by approximately 20 nucleotide sequence adjacent to the protospacer adjacent motif (PAM), 5'-NGG, allowing to an easy way to target any genomic location of choice. Additionally, use of short gRNAs enables multiplexed targeting by applying a library of gRNAs (Kabadi et al. 2014). Since the method offers a much simpler, efficient, and cost-effective way to introduce DSB, CRISPR/Cas9 system has rapidly replaced ZFNs and TALENs.

However, along with ZFNs and TALENs, CRISPR/Cas-9 system confers potential off-targets. It has been shown that Cas9 tolerates mismatches within the seed region of

gRNAs, depending on the number, position, and distribution of mismatches (Fu et al. 2013; Mali et al. 2013; Pattanayak et al. 2013). To minimize the off-targets and to improve fidelity of target recognition, Cas9 nickase (D10A mutant) has been engineered to generate a single-stranded break, requiring a pair of gRNAs to recognise the target site of interest (Ran et al. 2013).

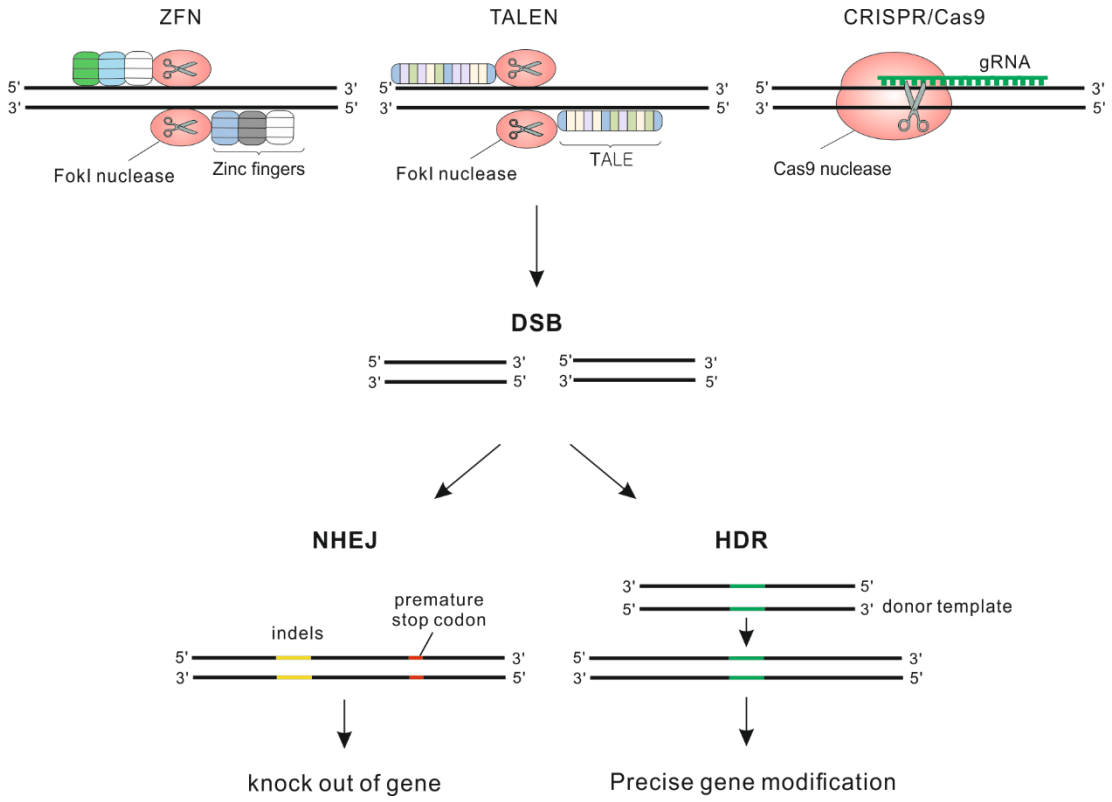

Figure 1.5 A diagram showing three major programmable nucleases. ZFN, TALEN, and CRISPR/Cas9 all collectively lead to DBS, which can be repaired by either NHEJ, which generally result in KO of gene expression by indels, or HDR, which can be used to precisely modify gene of interest - by correcting disease-causing mutation or by tagging a reporter protein to gene of interest. DBS, double strand break; NHEJ, non-homologous end joining; HDR, homology directed repair.

1.4 Aims of the thesis

The overarching aim of this thesis is to investigate the role of LRRK2 in MΦs and microglia and to interrogate whether LRRK2 contributes to PD progression by impairing their functions. To examine functions of LRRK2 in the most physiologically-relevant cell model, this thesis uses genetically-tractable, authentic human MΦs and microglia differentiated from iPSCs. Chapter 3 explores various regulatory mechanisms of LRRK2 protein in hiPSC-MΦs. Chapter 4 investigates the involvement of LRRK2 in phagocytosis. Lastly, chapter 5 uses hiPSC-microglia, cortical neuron co-culture to examine the role of LRRK2 in inflammatory cytokine release.

2

Materials and Methods

1.1 Cell culture

1.1.1 List of materials and media

	Supplier	**Catalogue number**
2-mercaptoethanol (2-ME)	Life Technologies	31350
Advanced DMEM F12	Thermo Fisher	12634-010
AggreWell™	Stem Cell Technologies	27865
B27 supplement	Thermo Fisher	17504044
BD Matrigel	BD Biosciences	354277
Costar™ Cell Culture Plates	Fisher Scientific	3524
Dispase	Thermo Fisher	17105041
Dorsomorphin	Tocris	3093
Fibroblast growth factor 2	Invitrogen	PHG0024
GlutaMax	Thermo Fisher	35050-038
GM-CSF	Invitrogen	PHC2015
IL-3	Life Technologies	PHC0033
IL-34	PeproTech	200-34
Insulin	Sigma	16634
KO DMEM	Invitrogen	10829018
KO serum replacement	Invitrogen	10828028
M-CSF	Life Technologies	PHC9501
N2 supplement	Life Technologies	17502048
Neurobasal medium	Thermo Fisher	21103-049
Non essential amino acid	Life Technologies	11140
Penicillin/Streptomycin (P/S)	Life Technologies	15140
Rock inhibitor Y-27632	Tocris	1254
SB431542	Tocris	1614
StemPro Accutase	Thermo Fisher	A1110501

TrypLE	Gibco by Life Technologies	12604013
X-Vivo-15	Scientific Laboratory Supplies	LZBE02-060F

Table 2.1 List of reagents used for differentiation

Media	Composition
MΦ differentiation	
EB differentiation medium	mTeSR, 50 ng/mL BMP4, 50 ng/mL VEGF, 20 ng/mL SCF
Factory medium	X-VIVO-15, 100 ng/mL M-CSF, 25 ng/mL IL-3, 2 mM Glutamax, 100U/mL P/S, 0.055 mM 2-ME
MΦ differentiation medium	X-VIVO-15, 100 ng/mL M-CSF, 2 mM Glutamax, 100 U/mL P/S, 0.055 mM 2-ME
Microglia-cortical neuron co-culture	
Neural induction medium	10 mL Neural maintenance medium, 10 µL SB431542, 10 µL Dorsomorphin
Neural maintenance medium	500 mL Advanced DMEM F12 + N2 supplement, 0.25 mL Insulin, 1mL 2-ME, 2.5 mL P/S, 10 mL B27, 5 mL GlutaMax, 500 mL Neurobasal medium
Microglia-neuron co-culture medium	Advanced DMEM F12 + N2 supplement, 100 ng/mL IL-34, 10 ng/mL GM-CSF

Table 2.2 List of media used for differentiation

1.1.2 hiPSC cultures

Fibroblasts were derived from skin biopsies collected from PD patients and healthy controls recruited through the Oxford Parkinson's Disease Centre and StemBANCC projects (participants were recruited to the study having given signed informed consent, which included mutation screening and derivation of hiPSC lines from skin biopsies (Ethics committee: National Health Service, Health Research Authority, NRES Committee South Central – Berkshire, UK, who specifically approved this part of the study - REC 10/H0505/71). All hiPSC lines were generated by Jane Vowles or Cathy Browne in the James Martin Stem Cell Facility, using the commercial kit Cytotune (Life Technologies), comprising four human reprogramming factors, Oct3/4, Sox2, Klf4, and

cMyc delivered using Sendai virus. Bulk stocks of each line were generated and banked in nitrogen vapour, and quality-control checked for mycoplasma, sterility, viability, Tra-1-60 and Nanog expression by FACs. Additionally, Illumina human SNP karyotyping and transcriptome analysis followed by PluriTest (Müller et al. 2011) were applied to screen for genome integrity and pluripotency respectively. During derivation and for specific applications, iPSCs were cultured as discrete colonies on feeder layers of MEF in KO-DMEM medium supplemented with 2 mM GlutaMax, 1% non-essential amino acids, 10% KO-serum replacement and 10 ng/mL fibroblast growth factor 2 (FGF2) (all from Invitrogen). For routine culture, using feeder free cell culture, hiPSC colonies were grown in Matrigel-coated tissue culture plates in mTeSR medium (StemCell Technologies) and passaging was routinely carried out as small cell clusters using PBS with 0.5 M EDTA (Gibco) or for specific applications by TrypLE (Gibco) and 10 µM Rock inhibitor Y27632 (Tocris). The list of hiPSC lines used in this thesis is listed in Table 2.3 and their SNP analysis results are attached in the Appendix.

Label		ID of fibroblast	ID of iPSC clone	Diagnosis	Genotype	Gender	Age of Biopsy (years)	Reprogramming method
Ctrl-1	●	SFC840	SFC840-03-03	Healthy	WT/WT	F	67	Cytotune1
Ctrl-1.1$^{-/-}$	○	SFC840	SFC840-03-03 D10	CRISPR/Cas-9 edited	-/-			
Ctrl-1.2$^{-/-}$	○	SFC840	SFC840-03-03 C11	CRISPR/Cas-9 edited	-/-			
Ctrl-2	●	SFC856	SFC856-03-04	Healthy	WT/WT	M	78	Cytotune1
Ctrl-3	●	SBAD	SBAD-02-01	Healthy	WT/WT	F	36	Cytotune1
Pat$^{G2019S/WT}$	▲	SFC832	SFC832-03-06	PD	G2019S/WT	F	77	Cytotune1
Pat$^{WT/WT}$	●	SFC832	SFC832-03-06	CRISPR/Cas-9 edited	WT/WT			

Table 2.3 List of hiPSC lines used in this thesis. Published worked with SFC840-03-03 can be found in (Fernandes et al. 2016), SFC856-03-04 (Haenseler et al., 2017b).

1.1.3 Differentiation of MΦ from hiPSCs

MΦ differentiation protocol was developed in our lab (Figure 2.1) (van Wilgenburg et al. 2013). Feeder-free hiPSC were lifted in single cell suspension with TrypLE and approximately 4 x 10^6 cells were transferred onto each well of Aggrewell plate in EB differentiation medium containing 50 ng/mL BMP4, 50 ng/mL VEGF, and 20 ng/mL

SCF to induce mesoderm, hemogenic endothelium and hematopoietic precursors. Alternatively, hiPSC colonies grown on MEFs were scraped manually with a cell scraper and transferred into low attachment plates (Corning Costar; CLS3471) where cultures were matured in embryoid body (EB) differentiation medium. After 4 days, EBs were redistributed into T175 flasks (Corning, CLS431080) with factory medium. After about three weeks, MΦ precursors emerging into the supernatant were harvested, passed through a 40 µM strainer, centrifuged 5 minutes at 400 *g* and were further differentiated into MΦs in MΦ differentiation medium on Greiner tissue culture plates or 10 cm^2 tissue culture dishes. Cells were given a 50% medium change at day 4 and used for experiments after 1 week of differentiation.

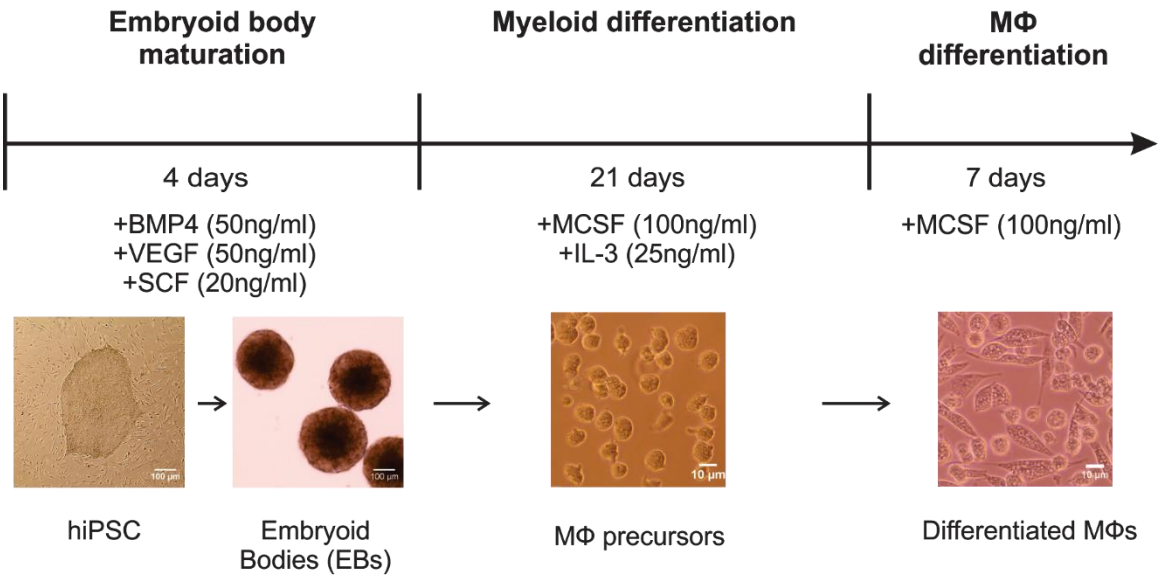

Figure 2.1 Differentiation of MΦs from hiPSCs. BMP4, Bone Morphogenetic Protein 4; VEGF, Vascular Endothelial Growth Factor; SCF, Stem Cell Growth Factor; M-CSF, Macrophage Colony Stimulating Factor; IL-3, Interleukin-3.

1.1.4 hiPSC-microglia, cortical neuron co-culture

Differentiation of cortical neurons from hiPSCs was performed based on the protocol (Shi, Kirwan, and Livesey 2012). Once the hiPSC culture approached 100% confluence, cells

were incubated in neural induction media and were fed every 2 days with fresh medium. On day 12 after induction, neural stem cells (NSCs) were lifted and plated onto laminin-coated wells. For laminin-coating, 1 mL of 10 µg/mL laminin in PBS were applied and coated at 37ºC at least for 4 h. 200 µL of dispase was added directly to the cell culture in the well. After 3 – 30 min incubation at 37ºC, NSCs should start detaching, and they were removed by pipetting carefully two or three times from the edge. The cells were then cultured overnight in neural induction medium overnight at 37ºC. The next day, medium was changed to neural maintenance medium containing 20 ng/mL of FGF2 and NSCs were further cultured for four days. After 4 days of FGF2 treatment, FGF2 was withdrawn and cells were passaged 1:2 with dispase when rosettes start to meet. On day 25 after induction, cells were dissociated with accutase at a ratio of 1:1 and kept in neural maintenance medium with a fresh media change every other day. On Day 29, cells were either frozen in neural freezing medium (10 % DMSO in neural maintenance medium with 20 ng/mL of FGF2) or continued to be cultured until Day 35 for co-culture experiment. To thaw the neurons, they were first partially thawed in 37ºC water bath and then were transferred into 10 volumes of RT neural maintenance medium. Cells were centrifuged once at 400 *g* for 3 min and were resuspended in 2 mL of neural maintenance medium containing 20 ng/mL of FGF2. The following day, FGF2 was withdrawn and neurons were cultured in neural maintenance medium.

The hiPSC-differentiated microglia, cortical neuron co-culture model was developed by Dr. Haenseler in our laboratory (Haenseler et al. 2017). Prior to the addition of MΦ precursors, Day 29 cortical neurons were first plated at a density of 50, 000 cells per cm^2 and were matured for another 14 days. 100, 000 cells per cm^2 of MΦ precursors in microglia differentiation medium were added to the cortical neurons. Experiments were performed after 14 days of differentiation in co-culture.

1.2 Protein analysis

1.2.1 List of buffers and materials

Name	Supplier	Catalogue number
Bovine Serum Albumin (BSA)	Sigma	A7906
cOmplete, Mini, EDTA-free protease inhibitor	Roche	4693159001
Dimethyl pimelimidate dihydrochloride (DMP)	Sigma	D8388
DMSO	Sigma	D2650
G Sepharose beads	Sigma	P3296
iBind Flex Cards	Thermo Fisher	SLF2010
iBind Flex Fluorescent Detection (FD) solution kit	Thermo Fisher	SLF2019
iBind Flex Western Device	Thermo Fisher	SLF2000
Normal donkey serum	Sigma	D9663
NuPAGE 3 - 8% Tris-Acetate gel	Invitrogen	EA0375
NuPAGE Antioxidant	Invitrogen	NP0005
NuPAGE LDS sample buffer (4X)	Invitrogen	NP0007
NuPAGE Sample Reducing Agent (10X)	Invitrogen	NP0004
NuPAGE Transfer buffer (10X)	Invitrogen	NP0006
NuPAGE Tris-Acetate SDS Running Buffer (20X)	Invitrogen	LA0041
Odyssey Blocking buffer (PBS)	Li-Cor	927-40000
PBS	Lonza	BE17-516F
Phophatase inhibitor cocktail 2	sigma	P5726-1ML
Pierce 1-Step Transfer Buffer	Thermo Fisher	84731
Pierce Power Blotter	Thermo Fisher	22834
PVDF membrane	Thermo Fisher	22860

Table 2.4 List of reagents used for protein analysis

Buffers	Composition
Base buffer	50 mM Tris-HCl (pH 8.0), 150 mM NaCl, 0.5 mM EDTA
Lysis buffer	10 mL base buffer, 1 tablet of protease inhibitor, 100 µL of phosphatase inhibitor, 1% Maltoside
Wash buffer (IP)	10 mL base buffer, 1 tablet of protease inhibitor, 100µL of phosphatase inhibitor
Elution buffer (IP)	50 mM Tris-HCl (pH 8.0), 1mM EDTA, 1% SDS, 100 nM DTT
Blocking buffer (IF)	5% BSA, 10% Normal Donkey Serum (NDS), 0.05% NaN_3 in PBS
FACS buffer	PBS, 10 µg/mL human serum IgG + 1% FBS

Table 2.5 List of buffers used for protein analysis

	Supplier	Cat No.	Species	WB	IF
Calnexin	Abcam	ab22595	Rabbit	1:5000	1:200
Catalase	Cell Signaling	D4P7B	Rabbit		1:800
CDC37	Abcam	ab166723	Rabbit		1:100
IBA1	Abcam	ab5076	Goat		1:200
LAMP-1	Cell Signaling	D2D11	Rabbit	1:1000	1:200
LRRK2 N-Term (N138/6)	NeuroMAB	73-188	Mouse	1:1000	1:1000
LRRK2 C-Term (N241A/34)	NeuroMAB	75-266	Mouse	1:1000	1:1000
LRRK2 phospho S935	Abcam	ab133450	Rabbit	1:500	
MAP2	Abcam	ab32454	Rabbit		1:1000
pan-14-3-3	Thermo Fisher	51-0700	Rabbit	1:500	1:100
Rab4	Cell Signaling	D36C4	Rabbit	1:1000	1:100
Rab5	Cell Signaling	3347	Rabbit		1:200
Rab7	Cell Signaling	9367	Rabbit		1:200
Rab8	Cell Signaling	D22D8	Rabbit		1:200
Rab9	Cell Signaling	5118	Rabbit		1:200
Rab10	Cell Signaling	D36C4	Rabbit	1:1000	1:200
Rab11	Cell Signaling	5589	Rabbit		1:200
Tsg101	Abcam	ab30871	Rabbit	1:5000	1:200
α-Tubulin	Sigma	T5168	Mouse	1:5000	

Table 2.6 List of primary antibodies

	Supplier	Cat No.	Species	WB	IF
Rabbit IgG (IRDye 680RD)	Li-Cor	926-68071	Goat	1:10,000	
Mouse IgG (IRDye 800CW)	Li-Cor	926-32210	Goat	1:10,000	
Mouse IgG (Alexa 647 conjugated)	Life Technologies	A31571	Donkey		1:500
Rabbit IgG (Alexa 568 conjugated)	Life Technologies	A10042	Donkey		1:500
Goat IgG (Alexa 488 conjugated)	Life Technologies	A11055	Donkey		1:500

Table 2.7 List of secondary antibodies

1.2.2 Preparation of cell lysates

For western blot analysis, adherent MΦs were washed with ice-cold PBS and then lysed directly by adding lysis buffer to a final concentration of $1x10^5$ cells/μL. Using cell scrapers, cells were transferred into Eppendorf tubes and further lysed for 10 min in ice. For immunoprecipitation, MΦs were first detached from 10 cm^2 dish by incubating them with warm TrypLE for 5 min and harvested using cell scrapers. Cells were washed in PBS, spun down at 400 *g* for 5 min and then lysed in lysis buffer to a final concentration of 20 – 24 x 10^6 cells/mL in ice for 30 min. Cell lysates were then centrifuged at 17,000 rpm for 20 min at 4ºC. Pellets were discarded and supernatants were used for subsequent protein analysis.

1.2.3 Western blot

The cleared lysate was mixed with 4x NuPAGE LDS (lithium dodecyl sulphate) sample buffer and 10x NuPAGE sample reducing agent and heated for 10 min at 70 ºC. Each sample containing 25 – 30 μg of protein was loaded into either 3-8% Tris-Acetate or 4-12% Bis-Tris NuPAGE pre-cast gels. Electrophoresis was performed for 60 min at 120 V using NuPAGE SDS running buffer. Proteins were transferred onto polyvinylidene difluoride (PVDF) membrane using Pierce Powerblotter system. Gels were sandwiched with filter papers, PVDF membrane that were pre-soaked with Pierce 1-Step Transfer Buffer. Pre-Programmed Methods for high MW (>150kDa) (18 V, 1.3A, 10 min) was used to transfer LRRK2. Membrane was blocked with 5% (w/v), BSA (Sigma) in TBS-T or commercially available blocking buffer (Li-Cor) and blotted overnight at 4ºC with the relevant primary antibodies. Following incubation with relevant secondary antibodies, the membrane was scanned with Odyssey Sa Infrared Imaging System (Li-Cor) and fluorescent intensity was quantified using MyImage analysis software (Thermo Sicentific, USA). Alternatively, iBind Flex system (Life Technologies) was used to blot membranes

with antibodies. First, using iBind Fluorescent Detection (FD) solution kit, FD solution was first prepared according to the manufacturer's instructions. Primary antibodies and secondary antibodies were diluted in FD solution. Membrane was placed on to the iBind card that was pre-soaked with FD solution, protein side down. 2 mL of diluted primary antibody, 2 mL FD solution, 2 mL of diluted secondary antibody, and 6 mL of FD solution was added to each well of iBind Device Well. Once the last well is empty, the membrane was washed with distilled water and scanned with Odyssey Sa Infrared Imaging System (Li-Cor) and fluorescent intensity was quantified using MyImage analsysis software (Thermo Sicentific, USA).

1.2.4 Immunoprecipitation

For crosslinking antibodies to beads, Protein G Sepharose beads were washed with PBS and were incubated with antibody against LRRK2 (NeuroMAB) overnight at 4ºC on a rotating wheel. For each prep, 40 µg of antibodies and 60 µL of Protein G Sepharose beads were mixed in 1 mL PBS. Any unbound antibodies were washed off with 1 mL of 0.2 M sodium borate buffer (pH 9.0). Crosslinking was carried out by incubating antibody-bead complexes with 20 mM dimethyl pimelimidate dihydrochloride (DMP) in 0.2 M sodium borate buffer (pH 9.0) for 40 min at RT. Antibody-bead complexes were washed once with 0.2 M ethanolamine (pH 8.0) and were incubated in 0.2 M ethanolamine buffer for 2 h at RT. Beads were quenched with 0.58% v/v acetic acid and 150 mM NaCl. Crosslinked beads were washed three times with PBS and stored in 4ºC until used.

Nonspecific proteins were cleared by incubating whole cell lysates with G Sepharose beads on a rotating wheel in 4ºC for 30 min. About 20 x 10^6 to 30 x 10^6 cells were incubated in 30 µL of G sepharose beads. Pre-cleared cell lysates were then incubated with G Sepharose beads cross-linked with LRRK2 antibody (NeuroMAB) overnight on

rotating wheel in 4ºC. Unbound proteins were washed off three times using wash buffer (lysis buffer without detergents). Finally, LRRK2 interactors were eluted by boiling protein-bead complexes at 70ºC for 10 min in SDS elution buffer.

1.2.5 Immunocytochemistry

Cells were washed in PBS three times then fixed with 4% PFA in PBS in RT for 10 min. Cells were then blocked and permeabilised at the same time in blocking buffer containing 0.1% Triton-X overnight at 4 ºC. Primary antibody was diluted in blocking buffer containing 0.05% Triton-X and cells were stained for 1 h at RT. Any unbound antibodies were washed in PBS with 0.3% Triton-X for three times, 15 min each. Secondary antibodies were diluted 1:500 in blocking buffer containing 0.05% Triton-X and incubated for 1 h at RT. Unbound antibodies were again washed in PBS with 0.3% Triton-X for 15 min, three times. Finally, cells were stained with DAPI in PBS with 0.3% Triton-X for 10 min, and then cells were washed three times with PBS. Confocal images were taken by Olympus Fluoview FV1200 (Olympus) or The Opera Phenix High Content Screening System (PerkinElmer).

1.2.6 Automated image analysis for quantification of phagosomes

For each experiment, MΦ precursors collected from three independent differentiation batches and 50,000 cells were seeded into separate wells of Ibidi treated 96 well microplate (Ibidi, 89626) and stained according to above protocol. Z-stacked confocal images were acquired using Opera Phenix High Content Screening System (PerkinElmer) with a 63x objective. At least five images per well were acquired from randomised fields. Once all the images were acquired, quantification of phagosomes was carried out by Columbus Image Data Storage and Analysis System (CambridgeSoft). First, a workflow for automated imaging analysis was generated as following, and screen shots are listed in (Figure 2.2). Input image command processed confocal images by stacking with

maximum projection. Find Nuclei command with Method B was used to identify the population of nuclei in DAPI channel. Next command was “Find Surrounding Region” and using Alexa 647 channel (used for LRRK2 staining), which was used to define approximate cell boundaries. This command ensures that only internalised zymosan bioparticles are quantified. “Find Spots” command was used to identify zymosan bioparticles using Alexa 488 Channel. “Find Surrounding Region” command finds regional spots surrounding each identified zymosan bioparticle. Next, “Calculate Intensity Properties” command was used to calculate intensity of LRRK2 signal (in Alexa 647 channel) in the surrounding zymosan bioparticles. “Select Population” command was used to quantify either the number of LRRK2(+) phagosomes by setting the threshold of signal intensity above 400 or the number of LRRK2 super-coated phagosomes above 1000. These parameters were determined by first deciding which of them are LRRK2(+) and super-coated phagosomes. The same workflow of commands was used to quantify the number of LRRK2(+) phagosomes that display positivity for Rab5, Rab9, and LAMP-1 (collectively referred to as markers). But in this case, “Calculate Intensity Properties” command was used twice, once to measure the intensity of LRRK2 signal (Alexa 647) and the other for the intensity of marker signal (Alexa 568). “Select Population” command first defined marker(+) phagosomes by setting the threshold based on the Alexa 568 signal intensity in the zymosan population. The second filter was applied so that LRRK2(+) phagosomes were defined by setting the threshold based on the Alexa 647 signal intensity in the marker(+) phagosomes population.

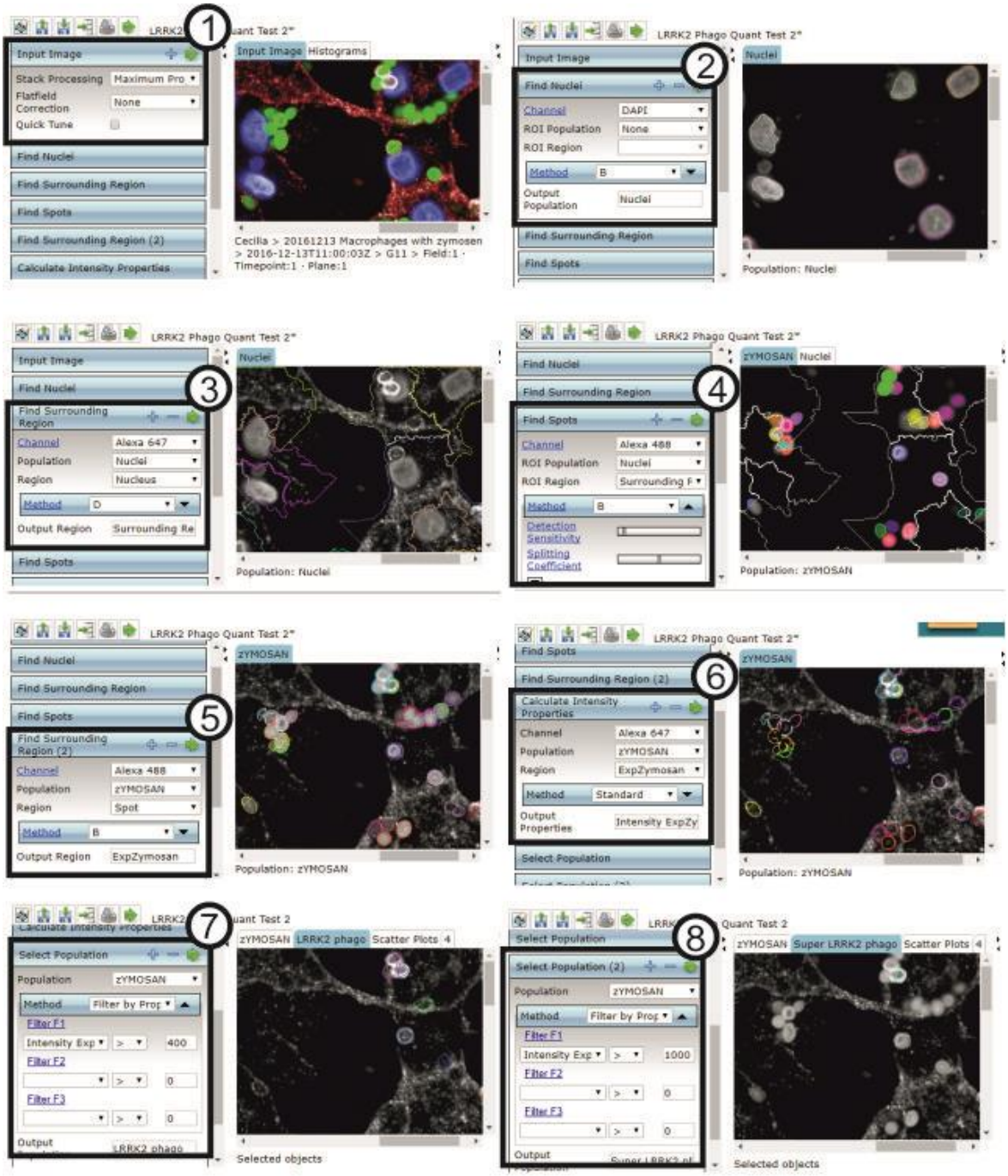

Figure 2.2 Workflow of automated imaging analysis for quantification of LRRK2(+) phagosomes.

1.2.7 Automated image analysis for quantification of hiPSC-microglia

Z-stacked confocal images were acquired using Opera Phenix High Content Screening System (PerkinElmer) with a 20x objective. At least five images were acquired per well

from randomized fields. Columbus Image Data Storage and Analysis System (CambridgeSoft) was used to automatically quantify the number of hiPSC-microglia (defined by IBA1 positivity). Images were first processed by acquiring maximal projection of Z-staked confocal images. “Find Cells” command was used in Alexa 488 channel where IBA1 signal could be detected. This command identified the cells that showed positivity for IBA1. The next command, “Calculate Intensity Properties” calculated the intensity of Alexa 647 signal (LRRK2) among the cells positive for IBA1. The next command “Select Population” quantified the number of IBA1 positive cells that have LRRK2 signal intensity above 400.

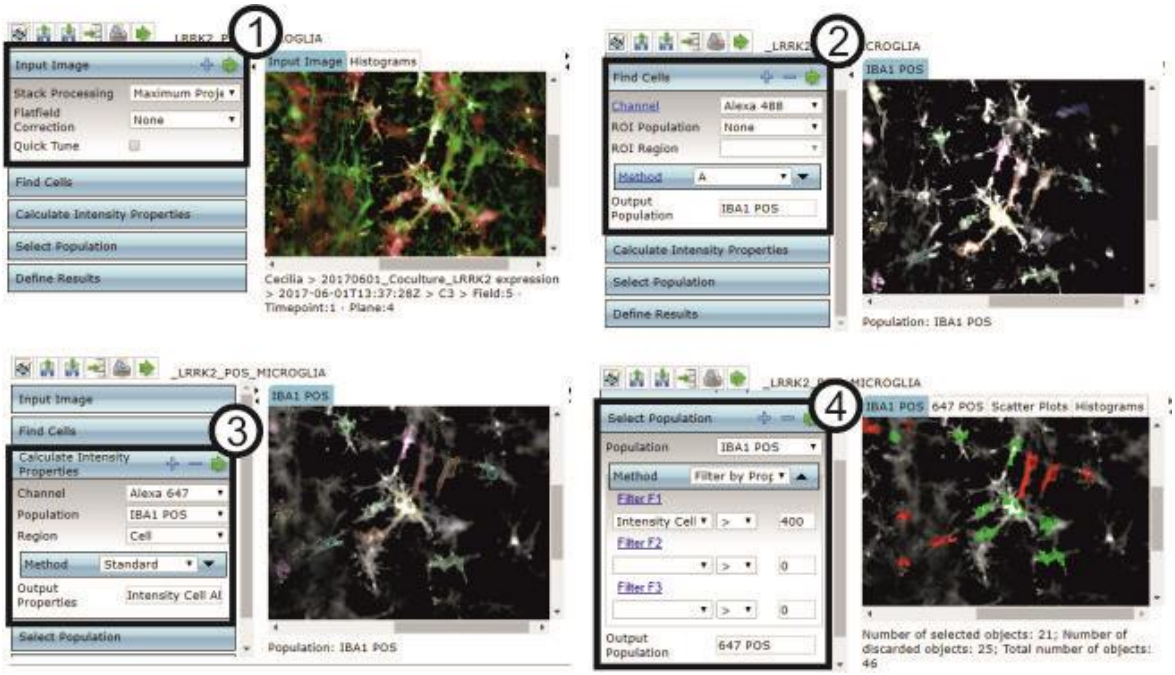

Figure 2.3 Workflow of automated imaging analysis for quantification of LRRK2(+) microglia.

1.3 Functional assays

1.3.1 List of materials

Name	Supplier	Catalogue number
Zymosan bioparticles Alexa 488	Life Technologies	Z23373
pHrodo Green *E.coli* Bioparticles	Life Technologies	P35366
pHrodo Green Zymosan Bioparticles	Life Technologies	P35365
Salmonella typhimurium NCTC 12023	Tocris	MM11-25
αsyn-fibril	(Haenseler et al. 2017b)	
Fluoresbrite YG Microspheres	Polysciences	18338-5
Live Cell Imaging Solution	Sigma	A14291DJ
Trypan Blue solution	Sigma	T8154
TNFα ELISA kit	Thermo Fisher	88-7346-22
Luminex Cytokine & Chemokine Convenience 34-Plex Human ProcartaPlex kit	Thermo Fisher	EPXR340-12167-901

Table 2.8 List of materials used for phagocytosis assay and cytokine/chemokine release assay

	Concentration	Supplier	Cat No.	Function
LPS	100 ng/mL	Sigma	L4391	TLR4 agonist
IFNγ	100 ng/mL	Invitrogen	PHC4031	cytokine
IFNα	1000 units/mL	Calbiochem	407291	cytokine
IFNβ	100 ng/mL	PeproTech	300-02BC	cytokine
TNFα	10 ng/mL	Peprotech	AF-300-01A	cytokine
GSK 2578215A	1 µM	Tocris	4629	LRRK2 kinase inhibitor
GNE-7915	1 µM	Chemie Tek	135176-44-8	LRRK2 kinase inhibitor
Cytochalasin D	10 µM	Sigma	C8273	Inhibit actin polymerization
Cycloheximide	20 µg/mL	Sigma	C7698	Inhibit protein synthesis
Leupeptin	100 µM	Sigma	L8511	Inhibit serine, cysteine proteases; plasmin, trypsin, papain, calpain, and cathepsin B
Lactacystin	5 µM	Sigma	L6785	Inhibit proteome subunit β5
MG-132	25 µM	Sigma	C2211	Inhibit proteome subunit β5

Table 2.9 List of cytokines, TLR4 agonist, and inhibitors

1.3.2 Phagocytosis

1.3.2.1 Uptake of bioparticles using FACS

Uptake of bioparticles was quantitatively assessed by applying zymosan bioparticles (Alexa Fluor 488 conjugated) to hiPSC-MΦs. 2 bioparticles per cell were added and phagocytosis was allowed to occur for 30 min at 37 ºC in MΦ differentiation medium followed by wash steps with PBS and trypan blue (250 μg/mL in PBS) to quench any bioparticles that are not internalised. Cells were detached by using TrypLE and cell scrapers, subsequently centrifuged at 400 *g* for 5 min, and were fixed with 4% formaldehyde in PBS. Internalised zymosan particles were quantified using a Becton-Dickinson FACS Calibur flow cytometer (BD biosciences) and data were analysed using FlowJo software.

1.3.2.2 Acidification of phagosomes

Quantification of acidified phagosomes was evaluated using pHrodo Green zymosan bioparticles or pHrodo Green *E. coli* bioparticles, which fluoresce in an acidic environment (pH 4.5 - 5.5). pHrodo bioparticles were resuspended in live imaging solution according to manufacturer's instruction and were sonicated for 10 min (Bioruptor) prior to each experiment. During the assay, 70,000 hiPSC-MΦs in each well in a 96-well clear bottom black plate (Corning, CLS3603) were kept in live imaging solution along with 0.2 mg/mL pHrodo bioparticles. The number of fluorescent bioparticles were monitored every 10 or 15 min in InCucyte Live Cell Analysis System (Essen Bioscience) for 2 h (Kapellos et al. 2016).

1.3.3 TNFα ELISA

TNFα ELISA was performed with collected supernatants according to the manufacturer's instructions. Briefly, 100 μL capture antibody diluted in the coating buffer were added to each well of a 96 well plate (Corning Costar, 9018) and were incubated overnight in 4 ºC.

The next day, plates were washed with Tween 0.05% in PBS (PBS-T) and 250 µL of assay diluent were added to each well for blocking. One hour later plates were washed and 100 µL diluted samples (1:100) or standards diluted in assay diluent were added. Samples were incubated for 2 h at RT after which they were washed with PBS-T and detection antibody was added to all samples. Plates were washed and 100 µL conjugated streptavidin-horseradish peroxidase (HRP) used to amplify the positive signal from the detection antibody. After an incubation of 20 min at RT and further wash step, 50 µL of TMB-H_2SO_4 substrate were added to each well. The reaction was stopped with 50 µL of 2M H_2SO_4 once standards formed a colour gradient.

1.3.4 Luminex 34plex cytokine and chemokine assay

The Magnetic Luminex Screening Assay (Thermo Fisher, Cytokine and Chemokine 34-Plex Human ProcartaPlex Panel 1A) was used to measure the levels of 34 cytokines and chemokines. In brief, 50 µL of Magnetic Beads solution was added to the 96-well plate and washed with Wash Buffer using a Hand-Held Magnetic Plate Washer. 50 µL of Universal Assay Buffer was added to each well followed by 50 µL of prepared standard samples and collected supernatants. After covering the plate with the Black Microplate Lid, the plate was placed on shaker (500 rpm) for 2 h at RT. Plate was washed three times and Detection Antibody Mixture was added to each well. Plate was placed on a shaker (500 rpm) for 30 min at RT and subsequently washed three times before the addition of 50 µL of streptavidin-R-phycoerythrin (SAPE) solution. After another 30 min of incubation on the shaker at RT, 120 µL of Reading Buffer was added to each well. After 5 min incubation on the shaker at RT, the plate was analysed on a Bio-Plex 200 system (Bio-Rad).

1.4 Generation of CRISPR/Cas9-edited hiPSCs

In this thesis, two CRIPSR/Cas9 generated hiPSCs lines were used. Exon3 targeted homozygous *LRRK2* KO hiPSCs and *LRRK2* G2019S mutation corrected hiPSCs (Table 2.3). All of these lines were generated by Dr. Sally Cowley (*LRRK2* KO) and Dr. Rowan Flynn (correction of *LRRK2* G2019S mutation), who designed gRNAs, transfected hiPSCs, and identified clones that had correct genomic sequence. I took over from this point, expanded the genetically-corrected/KO hiPSC clones, and differentiated them to MΦs to validate their genotypes at the protein level.

In brief, the process of CRISPR/Cas9-mediated gene editing is described as following. A double nickase strategy was employed to generate homozygous *LRRK2* KO hiPSC lines. First, gRNAs were cloned into Cas9 nickase plasmid with puromycin section (PX462; Addgene, #48141). hiPSCs were transfected by Cells were transfected by neon-transfection system (Life Technologies) and were seeded onto 10cm^2 tissue-culture treated dish (Fisher) at low density to ensure selection of each individual colony. To screen possible KO clones, genomic DNA was extracted and concentration was measured using picogreen (Life Technologies). PCR amplicons were produced by Phusion Hot start DNA polymerase (NEB) on PT-200 PCR machine (MJ Research) and quantitative reverse transcript polymerase chain reaction (qRT-PCR) was carried out with LC Green Plus+ (BioChem) and AmpliTaq master mix (Applied Biosystems) on StepOne plus (Applied Biosystems). Continuous melting step was allowed to screen for aberrant melt curve by using High Resolution Melting Software (Applied Biosystems), and the presence of out-of-frame deletion/insertion was confirmed by sequencing analysis. Similarly, for the repair of heterozygous *LRRK2* G2019S mutation, a donor template was designed with silent mutations in the PAM site to maximize the efficiency of gene-editing and *PstI* site for screening clones.

1.5 Statistical analysis

Statistical analysis was carried out with GraphPad Prism 7.0 software. All data are represented as mean ± SEM of at least three independent experiments carried out by using cells collected from at least three independent differentiation batches. When comparing the means from multiple groups against one control group, one-way analysis of variance (ANOVA) with Dunnett's *post hoc* comparison or for the data that do not display normal distribution, the non-parametrical Kruskal-Wallis with Dunn's *post hoc* comparison was used. For assessing data collected from experiments with two independent categorical variables and one continuous dependent variable, a two-way ANOVA with Sidak's *post hoc* multiple comparisons test was used. Statistical significance was defined as ns, $P > 0.05$; *$P < 0.05$; **$P < 0.01$; ***$P < 0.001$; ****$P < 0.0001$.

3

Regulation of LRRK2 protein expression in hiPSC-MΦs

3.1. Introduction

3.1.1. LRRK2 protein expression in precisely regulated in myeloid cells

LRRK2 protein is expressed in most brain regions that are affected in PD, notably the striatum and the SNpc, and is also expressed in other organs, particularly in the kidney and immune-related peripheral tissues; the spleen, thymus, and lymph nodes (Hakimi et al. 2011). Although LRRK2 protein expression has been observed across various cell types, notably neurons, CD19(+) B cells, MΦs, or dendritic cells (DCs), a subset of immune cells show upregulation of LRRK2 protein in the presence of inflammatory stimuli. For example, IFNγ upregulates LRRK2 in human PBMC-derived CD11b(+) monocytes, CD3(+) T lymphocytes, CD19(+) B lymphocytes (Gardet et al. 2010), human blood monocyte-derived MΦs, mouse primary microglia (Gillardon, Schmid, and Draheim 2012), and in transformed cell lines, including human THP-1 monocytic leukaemia cells (Gardet et al. 2010; Kuss, Adamopoulou, and Kahle 2014). TNFα, and IL-6 also moderately upregulate LRRK2 protein in human peripheral blood mononuclear cell (PBMCs) (Thévenet et al. 2011). The Toll-like receptor 4 (TLR4) agonist, LPS-mediated upregulation of LRRK2 was reported in primary mouse microglia and in THP-1 cells (Gillardon, Schmid, and Draheim 2012; Moehle et al. 2012). But the effect of LPS is inconsistent because LPS does not affect LRRK2 protein level in primary mouse

microglia, in mouse microglia-like cell-line BV-2 (Russo et al. 2015), or in mouse bone marrow derived MΦs (BMDMs) (Dzamko and Halliday 2012).

3.1.2. Phosphoregulation of ANK-LRR interdomain region

LRRK2 is a serine/threonine kinase which is phosphorylated on several serine and threonine residues: some residues are targeted by LRRK2 itself and others by several upstream kinases (Figure 3.1). Autophosphorylation occurs mainly within the GTP-binding ROC domain (S1403, T1404, and T1410) and the kinase domain (T1967 and T1491), while phosphorylation by upstream kinases occurs within the ANK-LRR interdomain region (S910, S935, S955, S973) (Gloeckner et al. 2010).

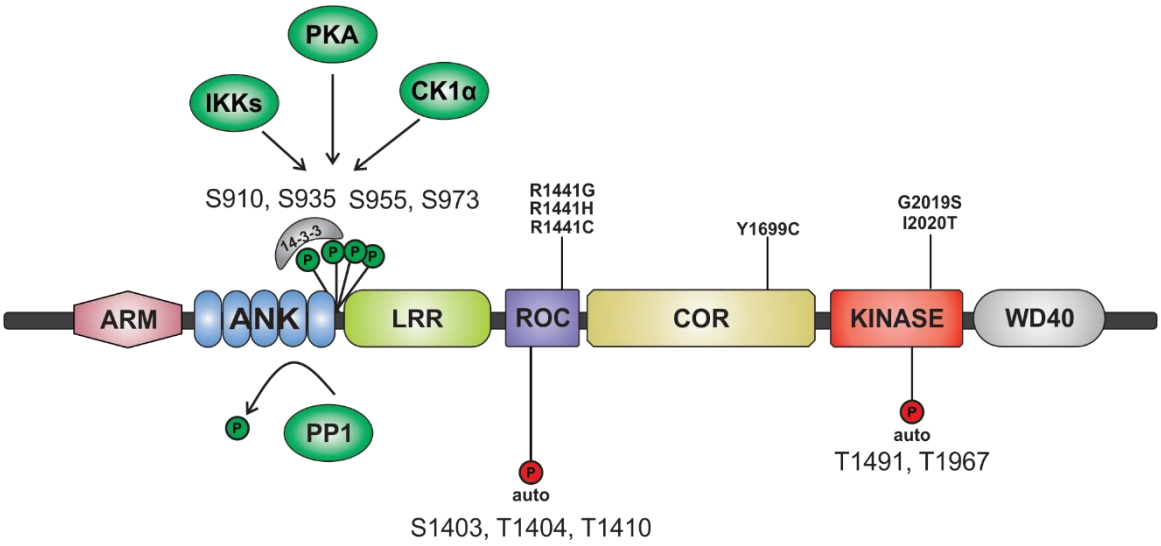

Figure 3.1 LRRK2 phosphorylation sites. Autophosphorylation sites are represented in red while phosphorylation sites by upstream kinases are represented in green. To date, IKKs, PKA, and CK1α have been reported to phosphorylate LRRK2 at S910, S935, S955, and S973 while PP1 dephosphorylate them. 14-3-3 protein has been reported to bind to phosphorylated S910, S935. Abbreviations: CK1α, casein kinase 1α; IKKs, IκB kinases; PP1, protein phosphatase 1; Protein Kinase A (PKA).

It is important to note that the autophosphorylation sites are mainly mapped *in vitro* by incubating ATP with purified LRRK2, and most of these autophosphorylation sites are not clearly detected in mammalian cells (Gloeckner et al. 2010; Greggio et al. 2009; Kamikawaji, Ito, and Iwatsubo 2009). On the other hand, S910, S935, S955, S973 phosphosites are more consistently detected in mammalian cells, including mouse primary neurons (E Lobbestael et al. 2016), mouse embryonic fibroblasts (Dzamko and Halliday 2012), mouse BMDMs (Dzamko and Halliday 2012), and human PBMC (Dzamko et al. 2013; Delbroek et al. 2013). Phosphorylated S910, S935, S955, and S973 were also confirmed on endogenous LRRK2 protein in Swiss 3T3 or in NIH3T3 cells (Nichols et al. 2010; Evy Lobbestael et al. 2013).

Identification of kinases that may be phosphorylating LRRK2 has been investigated in LRRK2-overexpressing HEK 293T cells. These studies have reported that cAMP-dependent protein kinase A (PKA) (Muda et al. 2014), casein kinase 1α (CK1α) (Chia et al. 2014) and IκB kinases (IKKs) (Dzamko and Halliday 2012) phosphorylate LRRK2 at S910, S935, S955, S973, while protein phosphatase 1 (PP1) dephosphorylates these serine sites (Evy Lobbestael et al. 2013).

Strangely, although S910, S935, S955, S973 are not phosphorylated by LRRK2 itself, inhibition of LRRK2 kinase activity by all small molecule LRRK2 kinase inhibitors result in dephosphorylation of these serine sites (Perera et al. 2016; Deng et al. 2011; Doggett et al. 2012; Nichols et al. 2010). This suggests that LRRK2 kinase activity is somehow indirectly regulating phosphorylation of LRRK2. However, several pieces of evidence strongly invalidate this inference. In HEK 293T and Swiss 3T3 cells over expressing LRRK2, LRRK2 kinase-dead mutants still display phosphorylation at S910, S935 and undergo inhibitor-induced dephosphorylation of the S910, S935 site (Kamikawaji, Ito, and Iwatsubo 2009; Doggett et al. 2012; Nichols et al. 2010; Ito et al.

2012). Additionally, LRRK2 G2019S mutation, which upregulates LRRK2 kinase activity by 2 – 8 fold, has no impact on the phosphorylation of S910, S935 (Doggett et al. 2012; Nichols et al. 2010; Li et al. 2011). For this reason, caution must be taken when interpreting data using LRRK2 kinase inhibitors, and one should be aware that LRRK2 kinase inhibitors, via an unknown mechanism, independently lead to the inactivation of LRRK2 kinase activity and dephosphorylation of S910, S935 residues.

3.1.3. Functional implications of phosphorylated S910, S935 residues

S910, S935, S955, S973 phosphosites within the ANK-LRR interdomain region have been implicated in regulation various aspects of LRRK2 function. Several groups have shown the binding of 14-3-3 protein to phosphorylated LRRK2 at S910 and S935. Overexpressed LRRK2 protein in HEK 293T cells interacts with all isoforms of 14-3-3, and phosphor-dead S910A or S935A LRRK2 mutants or application of LRRK2 kinase inhibitors prevent its interaction with 14-3-3 (Dzamko et al. 2010; Li et al. 2011; Nichols et al. 2010). Interestingly, alanine substitution of S955, S973 does not affect the binding of LRRK2 with 14-3-3, indicating that 14-3-3 protein binding is specific to phosphorylated S910, S935 but not S955, S973 (Doggett et al. 2012; Nichols et al. 2010).

PD-causing mutations, R1441C, R144G, R1441H, Y1699C and I2020T but not G2019S display low levels of phosphorylation of all S910, S935, S955, S973 compared to WT in LRRK2-overexpressing HEK 293T cells. And these mutants all displayed impaired interaction with 14-3-3 protein, and LRRK2 subcellular localisation was affected from uniform cytosolic distribution to punctate cytosolic inclusions (Doggett et al. 2012; Nichols et al. 2010). Therefore, phosphoregulation of ANK-LRR interdomain region may be an important regulatory site for LRRK2 function. However, these findings have been

shown in LRRK2-overexpression cell system, therefore, more critical evaluations are needed using a cell system expressing endogenous level of LRRK2 protein.

3.1.4. Aims

The aim for this chapter is to investigate the regulation of LRRK2 protein in human MΦs differentiated from iPSCs. This chapter explores the effect of inflammatory stimuli on the overall expression level of LRRK2 and the consequences of reduced phosphorylation at S935 by LRRK2 kinase inhibitors. Finally, this chapter provides a novel insight to another potential mechanism of LRRK2 regulation – formation of LRRK2 cleavage product.

3.2. Results

3.2.1. Validation of CRISPR/Cas-9 edited LRRK2 hiPSC lines.

To elucidate the role of LRRK2 in the immune system, my first aim was to have CRISPR/Cas-9 edited hiPSC lines with various genetic modification of *LRRK2*. In this thesis, a double allele *LRRK2* KO hiPSC line and a PD patient-derived line, in which the G2019S mutation (A) had been mutated to G (WT) were used. *LRRK2* KO in healthy control hiPSC line (Ctrl-$1^{WT/WT}$) was generated in by Dr Rowan Flynn, who designed gRNAs targeting exon 3, and Dr Sally Cowley who identified correct clones by high resolution melt analysis (HRMA) and then sequencing analysis. At the genomic level, two clones displayed out-of-frame homozygous deletion of *LRRK2* (Figure 3.2A). I took over from this point, did the expansion of these KO hiPSC clones, differentiated them into MΦs and validated them at the protein level by using western blot analysis. As shown by western blot (Figure 3.2B), hiPSC-MΦs differentiated from both clone Ctrl-$1.1^{-/-}$ and Ctrl-$1.2^{-/-}$ show complete absence of LRRK2 protein. CRISPR/Cas-9-corrected

G2019S hiPSC clone ($Pat^{WT/WT}$) was generated by Dr Rowan Flynn. I differentiated this clone to MΦs and validated it by western blot (Figure 3.2B).

To account for any technical variability between differentiation preps, I performed all experiments using MΦ precursors collected from at least three independent differentiation batches. CRISPR/Cas-9 edited hiPSC lines displayed no significant difference in the production of MΦ precursors compared to their parental lines (Figure 3.3A). Differentiated MΦs all display classic MΦ markers, CD45 and CD14 (Figure 3.3B).

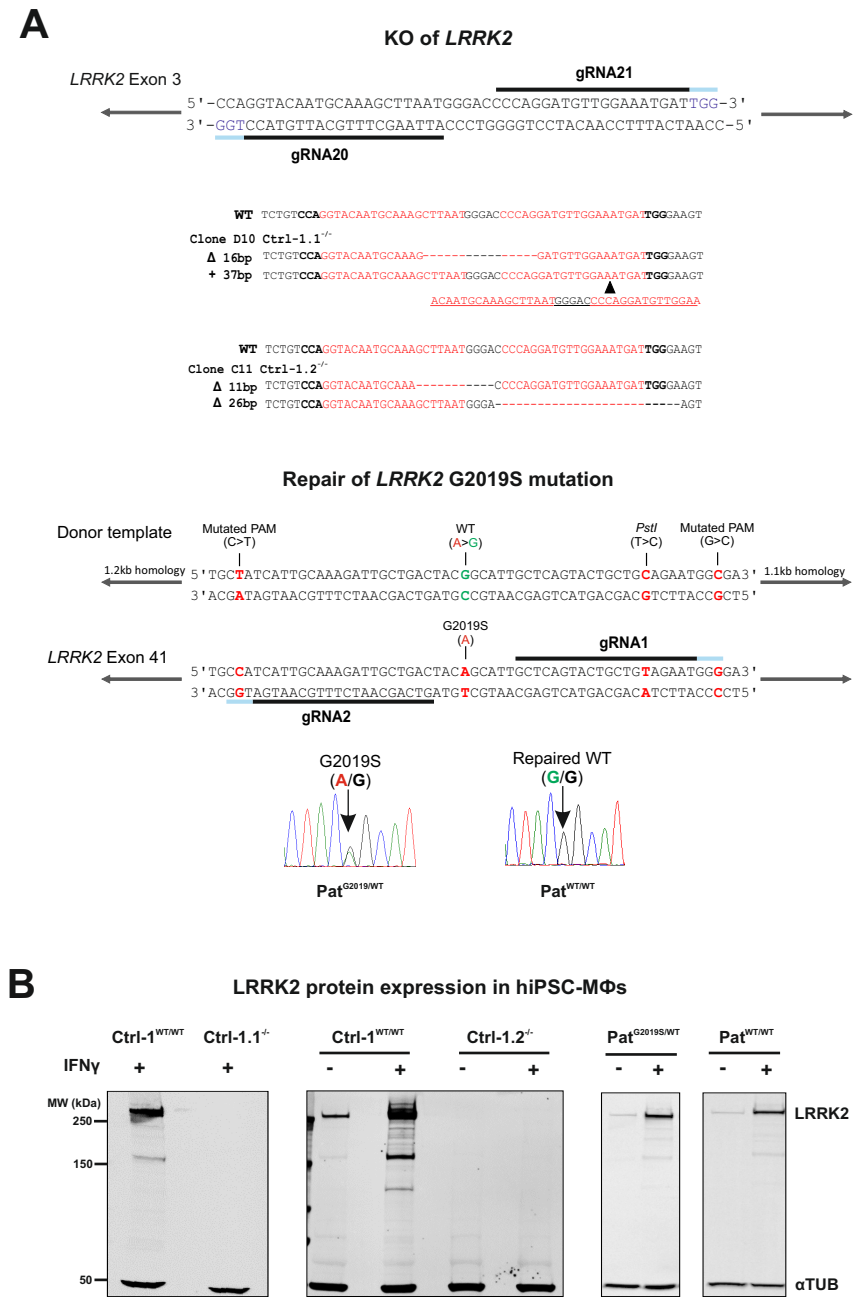

Figure 3.2 Generation of CRISPR/Cas-9 edited hiPSC lines. (A) CRISPR/Cas-9 mediated knock out (KO) of *LRRK2* was performed using a double nickase strategy. Guide RNAs (gRNA20 and gRNA21) were designed to target exon 3 of *LRRK2*. Sequencing analysis shows that clone D10 (Ctrl-1.1$^{-/-}$) has a 16 bp deletion in one allele and a 37 bp insertion in the other allele. Clone C11 (Ctrl-1.2$^{-/-}$) has a 11 bp deletion and a 26 bp deletion. These out-of-frame indel led to KO of a LRRK2 protein. For CRISPR/Cas-9 mediated repair of *LRRK2* G2019S mutation, a donor template was designed with silent mutations in the PAM site to maximize the efficiency of gene-editing and *PstI* site for screening clones. **(B)** Western blots show complete deletion of LRRK2 protein in MΦs differentiated from *LRRK2* KO clones (Ctrl-1.1$^{-/-}$ and Ctrl-1.2$^{-/-}$). Western blots also validate LRRK2 protein expression in MΦs differentiated from *LRRK2* G2019S patient iPSC line (Pat$^{G2019S/WT}$) and from the CRISPR/Cas-9 repaired isogenic control iPSC line (Pat$^{WT/WT}$). Differentiated MΦs were activated with IFNγ (100 ng/ml) for 72 h before cell lysates were collected. Alpha tubulin (αTUB) was used as endogenous control.

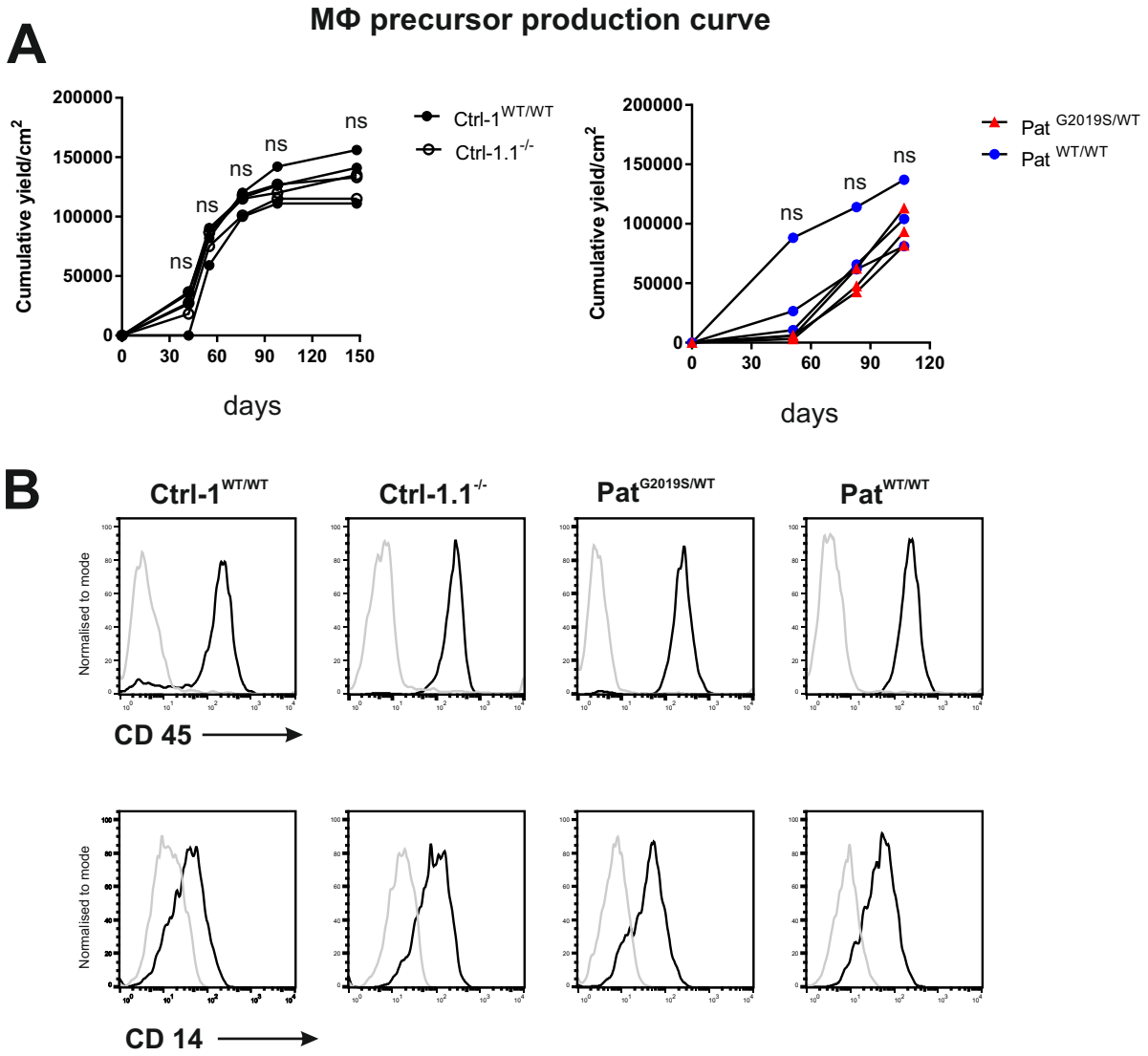

Figure 3.3 Myeloid differentiation of all four hiPSC lines used in this study. (A) MΦ precursor production curve showing cumulative yield of MΦ precursors over the differentiation period. There was no significant difference between genetically modified hiPSC lines compared to their parental hiPSC lines. Two-way ANOVA with Bonferroni multiple comparisons test was used for statistical analysis. ns denotes not significant. **(B)** FACS plots showing representative CD45 and CD14 staining of MΦs precursors from all four hiPSC lines used in this thesis.

3.2.2. IFNγ upregulates endogenous LRRK2 protein expression in hiPSC-MΦs

In agreement with previously published data in human blood-derived-MΦs (Thévenet et al. 2011; Gardet et al. 2010; Moehle et al. 2012) and other human myeloid cell-like cell lines (Gardet et al. 2010; Kuss, Adamopoulou, and Kahle 2014), IFNγ significantly enhanced endogenous LRRK2 protein expression in hiPSC-MΦs up to 10 fold and its expression level plateaued around 72 h treatment (Figure 3.4A).

To explore whether other stimuli are involved in regulating LRRK2 expression, hiPSC-MΦs were treated with TNFα, type 1 interferons (IFNα, β), and a toll-like receptor 4 (TLR4) agonist, LPS. IFNα, IFNβ and TNFα treatment had no significant effect on the expression level of LRRK2 (Figure 3.4B). LPS, on the other hand, showed a significant increase in endogenous LRRK2 expression by 3-fold (Figure 3.4B). Combined treatment of IFNγ with these stimuli all resulted in significant upregulation of LRRK2 protein expression, except for the combined treatment with IFNγ and IFNβ, which was not statistically significant (Figure 3.4B).

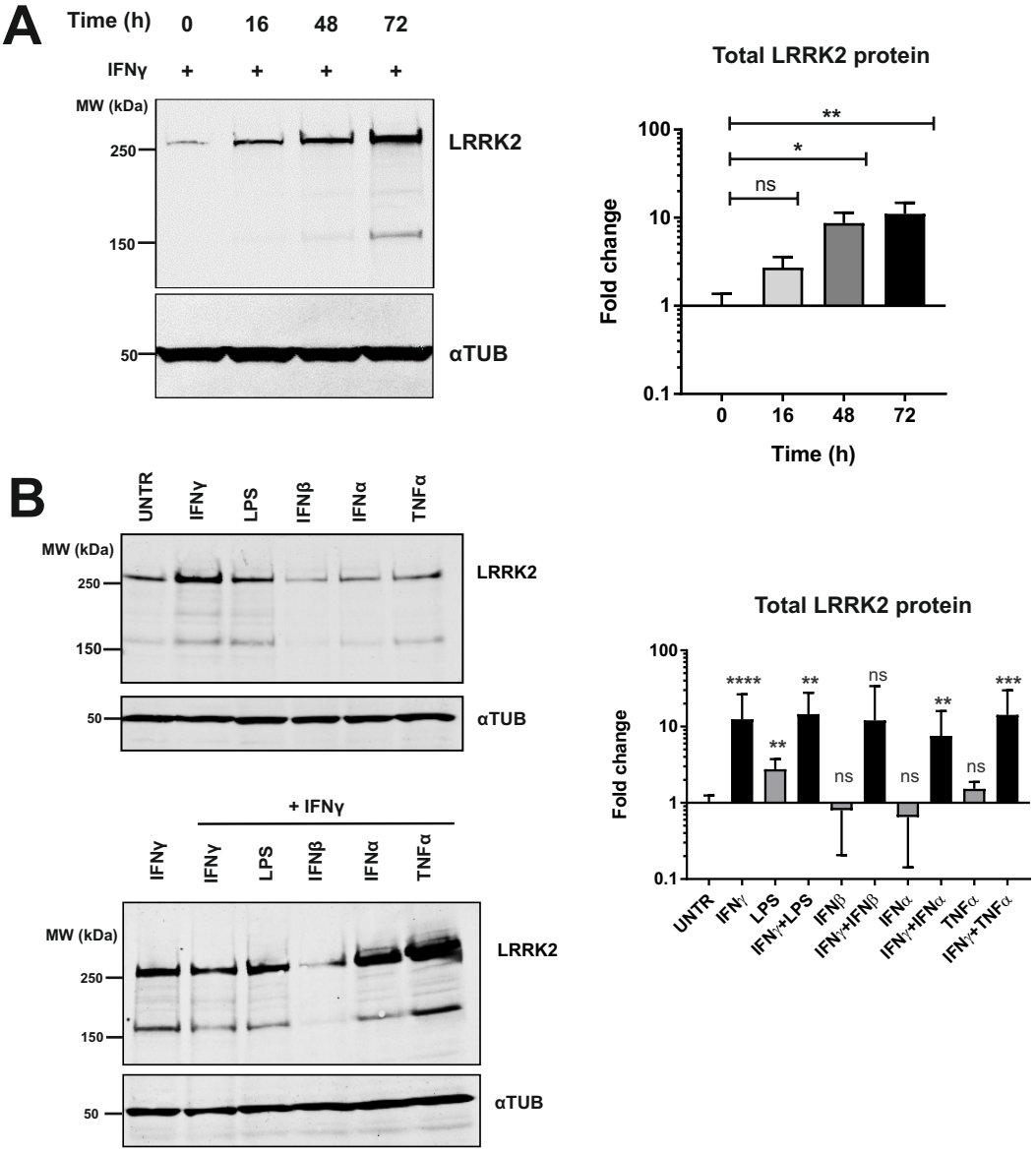

Figure 3.4 IFNγ upregulates endogenous LRRK2 expression in hiPSC-MΦs. Western blot showing cell lysates collected from MΦs treated **(A)** with IFNγ (100 ng/mL) at different time points and **(B)** with IFNγ (100 ng/mL), LPS (100 ng/mL), IFNβ (100 ng/mL), IFNα (1000 units/mL), or TNFα (10 ng/mL) alone or in combination with IFNγ (100 ng/mL) for 72 h. Western blots were quantified as total LRRK2 signal relative to loading control (αTUB) and normalized against untreated control (UNTR). Bar graphs show fold change in mean ± SEM of four independent experiments. Statistical significance was tested using one-way ANOVA against UNTR controls. *$P < 0.05$, **$P < 0.01$, ***$P < 0.001$, ns denotes not significant.

3.2.3. LRRK2 kinase inhibitors reduce phosphorylation of LRRK2 at S935

Several small LRRK2 kinase inhibitors consistently lead to dephosphorylation of LRRK2 at S910, S935 via an unknown mechanism. To confirm this observation in hiPSC-MΦs, two structurally distinct LRRK2 kinase inhibitors, GSK2578215A (GSK, 1 μM), or GNE-7915 (GNE, 1 μM), were used. These two inhibitors show high potency (IC_{50} 10.9 nM and 9.0 nM, respectively) with the least off-targets compared to other LRRK2 kinase inhibitors.

MΦs differentiated from healthy control iPSCs were treated with IFNγ for 72 h and LRRK2 kinase inhibitors were applied for 30, 60, or 120 min. Both GSK and GNE significant reduced phosphorylation of LRRK2 at S935 by 120 min (Figure 3.5B). hiPSC-MΦs with the heterozygous G2019S mutation ($Pat^{G2019S/WT}$) showed no significant difference in either the basal phosphorylation level at S935 or the degree of dephosphorylation upon treatment with LRRK2 kinase inhibitors compared to its isogenic pair ($Pat^{WT/WT}$) (Figure 3.5B).

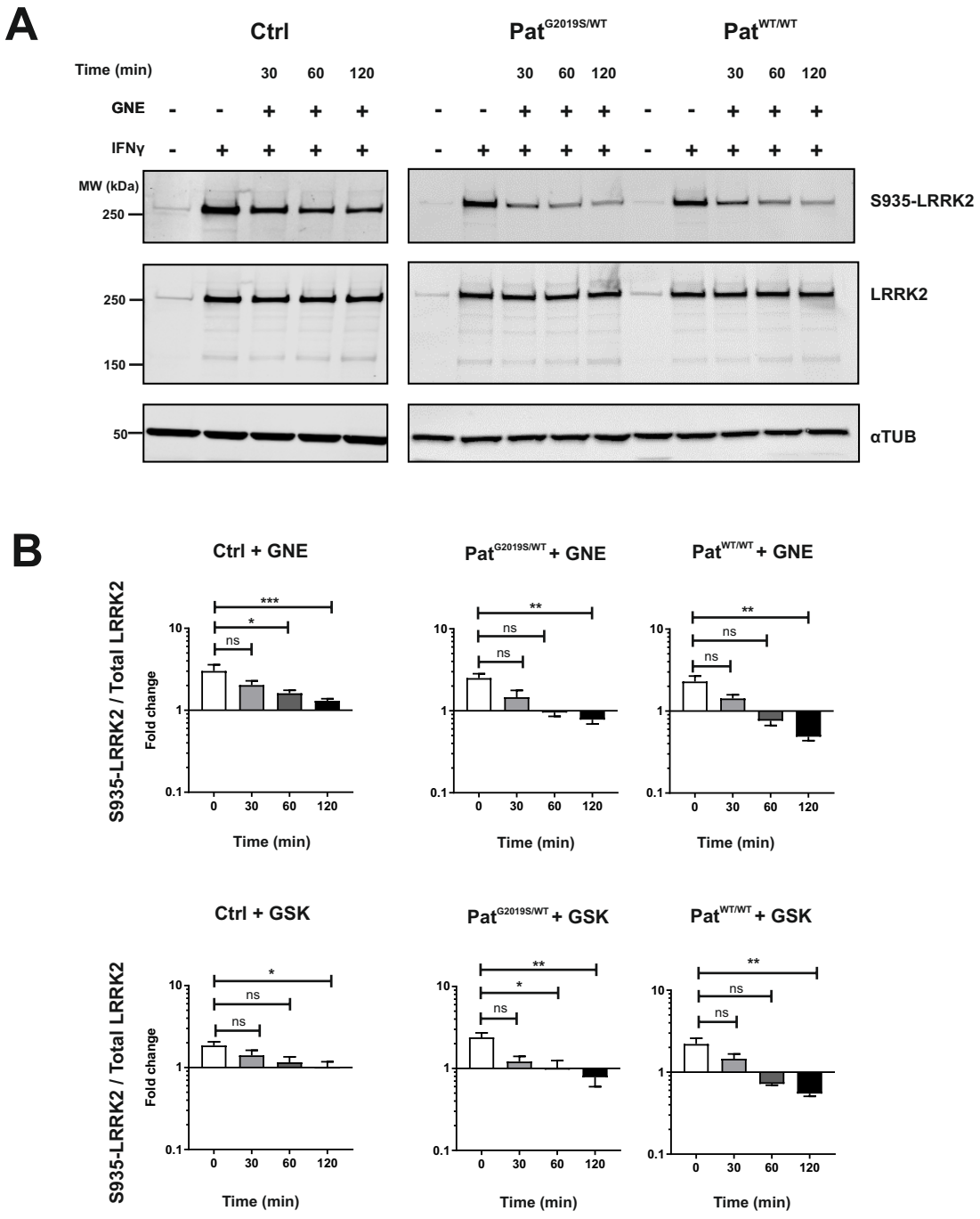

Figure 3.5 LRRK2 kinase inhibitors reduce phosphorylation of LRRK2 at S935. (A) MΦs differentiated from Ctrl$^{WT/WT}$, Pat$^{G2019S/WT}$, and Pat$^{WT/WT}$ hiPSC lines were activated with IFNγ (100 ng/mL) for 72 h and then LRRK2 kinase inhibitors, GNE-7915 (GNE; 1 μM) or GSK-2578215A (GSK; 1 μM), were applied for 30, 60, or 120 min. **(B)** Graphs show fold change in S935-LRRK2 signal over total LRRK2 relative to UNTR control. Error bars indicate SEM of at least three independent experiments. Statistical significance was tested using one-way ANOVA against UNTR controls. *$P < 0.05$, **$P < 0.01$, ***$P < 0.001$, ns denotes not significant.

3.2.4. LRRK2 kinase inhibitors reduce the stability of LRRK2 protein

It has been reported that LRRK2 kinase inhibitors lead to degradation of LRRK2 in LRRK2-overexpressing HEK 293T cells (Zhao et al. 2015) or SH-SY5Y cells (E Lobbestael et al. 2016). To test whether endogenous LRRK2 protein undergoes similar process, I examined the level of total LRRK2 protein in hiPSC-MΦs that were treated with GNE for 16, 24, or 48 h in the presence of cycloheximide (CX; 10 μM). CX inhibits protein synthesis by blocking translational elongation, therefore, was used here to prevent new synthesis of LRRK2 at the time of LRRK2 kinase inhibitor treatment, so that the degradation rate of LRRK2 protein could be assessed. Combined treatment of CX and GNE significantly reduced the total LRRK2 protein level to around 25% after 48 h treatment (Figure 3.6A).

Because pharmacological inhibition of LRRK2 kinase activity affected the stability of LRRK2 protein, I hypothesized that the presence of hyper-kinase activity by the G2019S mutation, would counteract the inhibitor-induced degradation of LRRK2 protein. To test this hypothesis, MΦs derived from a PD patient with G2019S mutation ($Pat^{G2019S/WT}$) were treated with GSK or GNE for 48 h in the presence of CX. GNE or GSK treatment for 48 h showed a reduction in total LRRK2 protein to 40% compared to DMSO-treated control. However, there was no significant difference in the level of total LRRK2 protein in $Pat^{G2019S/WT}$ MΦs and its isogenic control, $Pat^{WT/WT}$ MΦs (Figure 3.6B).

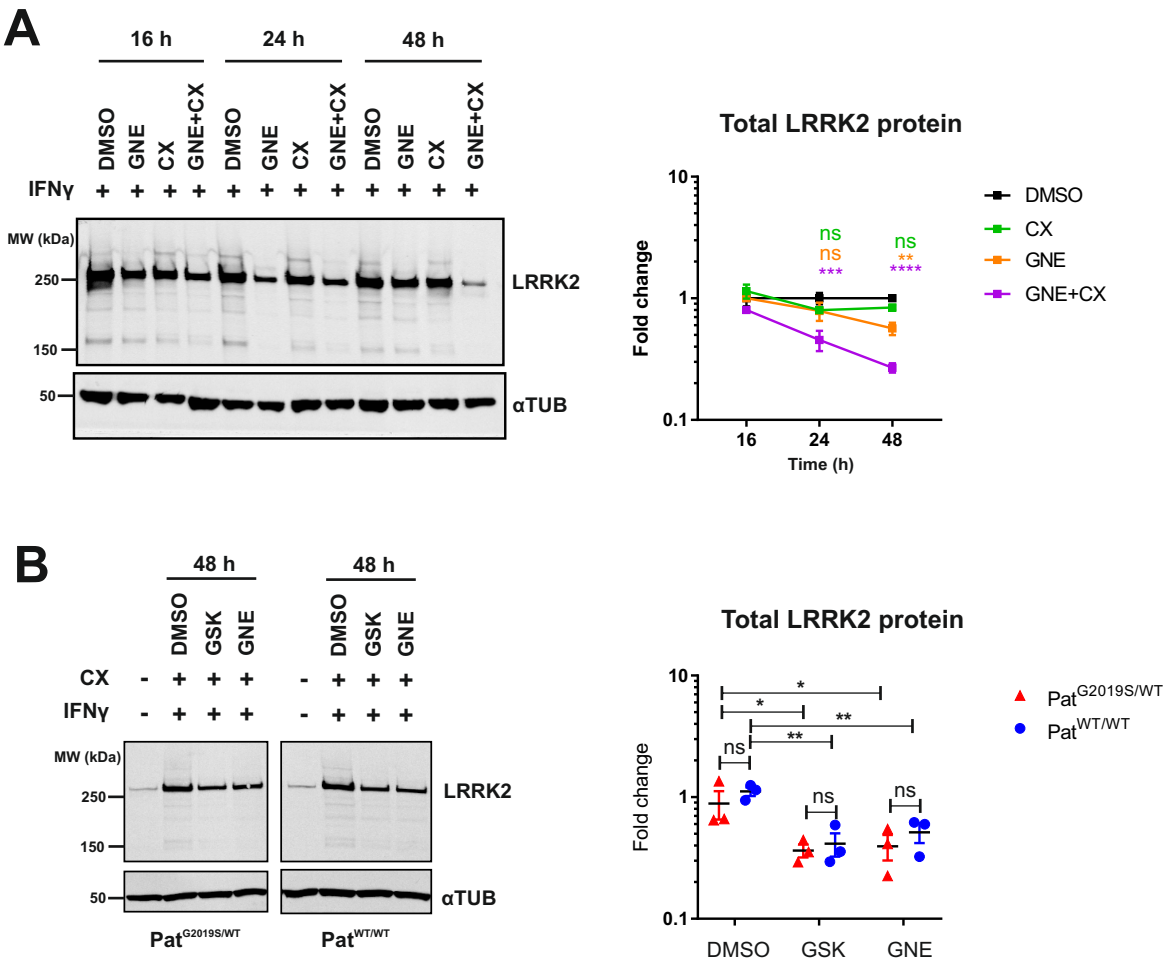

Figure 3.6 G2019S mutation does not affect the stability of LRRK2 protein upon long-term treatment with LRRK2 kinase inhibitors. (A) MΦs differentiated from Ctrl hiPSC lines were activated with IFNγ (100 ng/mL) for 48 h and then LRRK2 kinase inhibitor, GNE (1 μM), for 16, 24, 48 h with or without cycloheximide (CX; 20 μg/mL). CX inhibits translation therefore was used to measure half-life of LRRK2. Graph shows fold change in total LRRK2 protein signal over loading control (αTUB) relative to DMSO control. **(B)** MΦs differentiated from Pat$^{G2019S/WT}$ and Pat$^{WT/WT}$ hiPSC lines were activated with IFNγ (100 ng/mL) for 48 h and then LRRK2 kinase inhibitor, GNE (1 μM) or GSK (1 μM), for additional 48 h with CX (20 μg/mL). Graphs show fold change in total LRRK2 protein signal over loading control (αTUB) relative to DMSO control. Error bars represent SEM of at least three independent experiments. Statistical analysis was performed by two-way ANOVA with Bonferroni multiple test. *$P < 0.05$, **$P < 0.01$, ***$P < 0.001$, ns denotes not significant.

3.2.5. LRRK2 forms a cleaved product in hiPSC-MΦs

Western blot of IFNγ activated hiPSC-MΦs repeatedly showed a band that is approximately 170 kDa in size which is not present in the CRISPR/Cas-mediated *LRRK2* KO MΦs(Figure 3.7A). Additionally, this band does not correspond to any known LRRK2 transcripts (Figure 3.7B). This suggests that the 170 kDa band is a *LRRK2*-derived product and could be a post-translational cleavage product. To rule out any possibility that this cleaved product forms because of post-lysis proteolysis, I spiked *LRRK2* KO hiPSC-MΦs cell lysates with full-length recombinant LRRK2 protein. Recombinant protein did not form the cleaved product, suggesting that cleavage is happening inside the cells not during or post cell lysis (Figure 3.7A).

In cells, protein degradation is generally regulated by the ubiquitin-proteasome pathway and/or the autophagic-lysosomal systems (Figure 3.7C). To investigate which pathway is involved in the formation of the LRRK2 cleaved product, I used leupeptin, which inhibits serine and cysteine proteases in the lysosomal organelles, namely plasmin, trypsin, papain, calpain, and cathepsin B. The proteasome is a 26S enzyme complex, comprised of 20S core and two 19S regulatory complex. The 20S proteasome core has three distinct subunits, each has distinct protease activity, namely chymotrypsin-like (β5), trypsin-like (β2), and peptidyl glutamyl-like (β1) activities. Lactacystin and MG-132 inhibit β5 subunit of 20s proteasome chymotrypsin-like activity, which is also the rate-limiting step of proteolysis (Kisselev et al. 1999; Fenteany and Schreiber 1998; Rajkumar et al. 2005; Goldberg 2012). Interestingly, only MG-132 led to significant reduction of cleaved LRRK2 while leupeptin or lactacystin had no significant effect (Figure 3.7D). Although lactacystin is known to be as effective as MG-132, the lactacystin used in this experiment (5 µM, Sigma) had only a partial effect on inhibiting proteasome activity in hiPSC-MΦs.

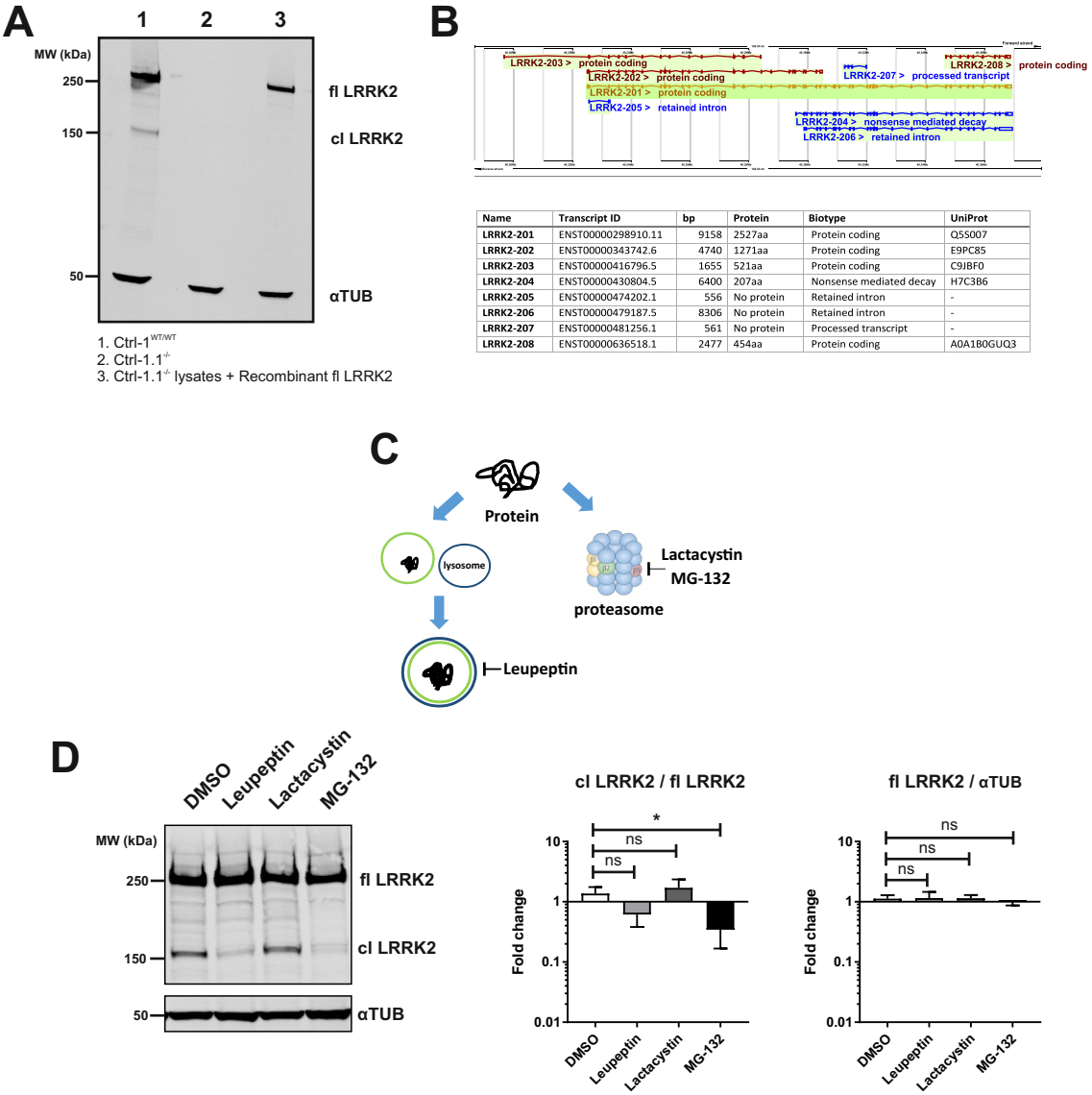

Figure 3.7 Inhibition of proteasome subunit blocks the formation of truncated LRRK2. (A) Western blot showing full-length LRRK2 (fl LRRK2) and cleaved LRRK2 (cl LRRK2) in MΦs differentiated from WT (Ctrl-1$^{WT/WT}$), KO (Ctrl-1.1$^{-/-}$), and KO (Ctrl-1.1$^{-/-}$) cell lysates spiked in with recombinant fl LRRK2 protein. Antibody recognizing C-terminus of LRRK2 (N241A/36) was used. **(B)** Data from Ensembl showing transcripts of *LRRK2* (ENSG00000188906) **(C)** Major protein degradation pathways. Leupeptin inhibits cysteine and serine proteases in the lysosome. Lactacystin and MG-132 inhibit β5 subunits of 20S proteasome, most effectively inhibiting chymotrypsin-like activity. **(C)** MΦs were treated with IFNγ (100 ng/mL) for 72 h then leupeptin (100 μM), lactacystin (5 μM), and MG-132 (25 μM) for 16 h before cell lysates were collected. Bar graph on the left shows fold change in cl LRRK2 signal over fl LRRK2 signal relative to DMSO control. Bar graph on the right shows fold change in full-length LRRK2 signal over αTUB relative to DMSO control. All statistical analysis was performed by one-way ANOVA and error bars represent SEM of three independent experiments. *$P < 0.05$, **$P < 0.01$, ***$P < 0.001$, ns denotes not significant.

This experiment was performed by Dr. Haenseler and the results can be found in the Appendix.

I next sought to identify the cleavage site. I isolated endogenous LRRK2 protein by immunoprecipitation (IP) and analysed the cleaved product by mass spectrometry. Results from mass spectrometry confirmed that the cleaved product indeed belongs to LRRK2, lacking the N-terminal part of LRRK2. Western blot also supports this result by showing that the cleavage product lacks phosphorylation at S935 site (Figure 3.8C).

By analysing the distribution of peptide fragments, it appears that the cleavage occurs within the ANK-LRR interdomain region (aa861 – aa983), particularly between aa901 – aa910, which contains one chymotrypsin cleavage site (aa902) (Figure 3.8A-C). However, more careful assessment must be carried out to identify the exact location of cleavage.

Interestingly when I pulled down endogenous LRRK2 with antibody against N-terminus of LRRK2 (N138/6) and then used antibody recognizing C-terminus LRRK2 (N241A/36) to identify the final immunoprecipitated product, the cleaved product was also detected (Figure 3.8E). This unexpected result suggests that LRRK2 may form a heterodimer complex comprising full-length and the cleaved product.

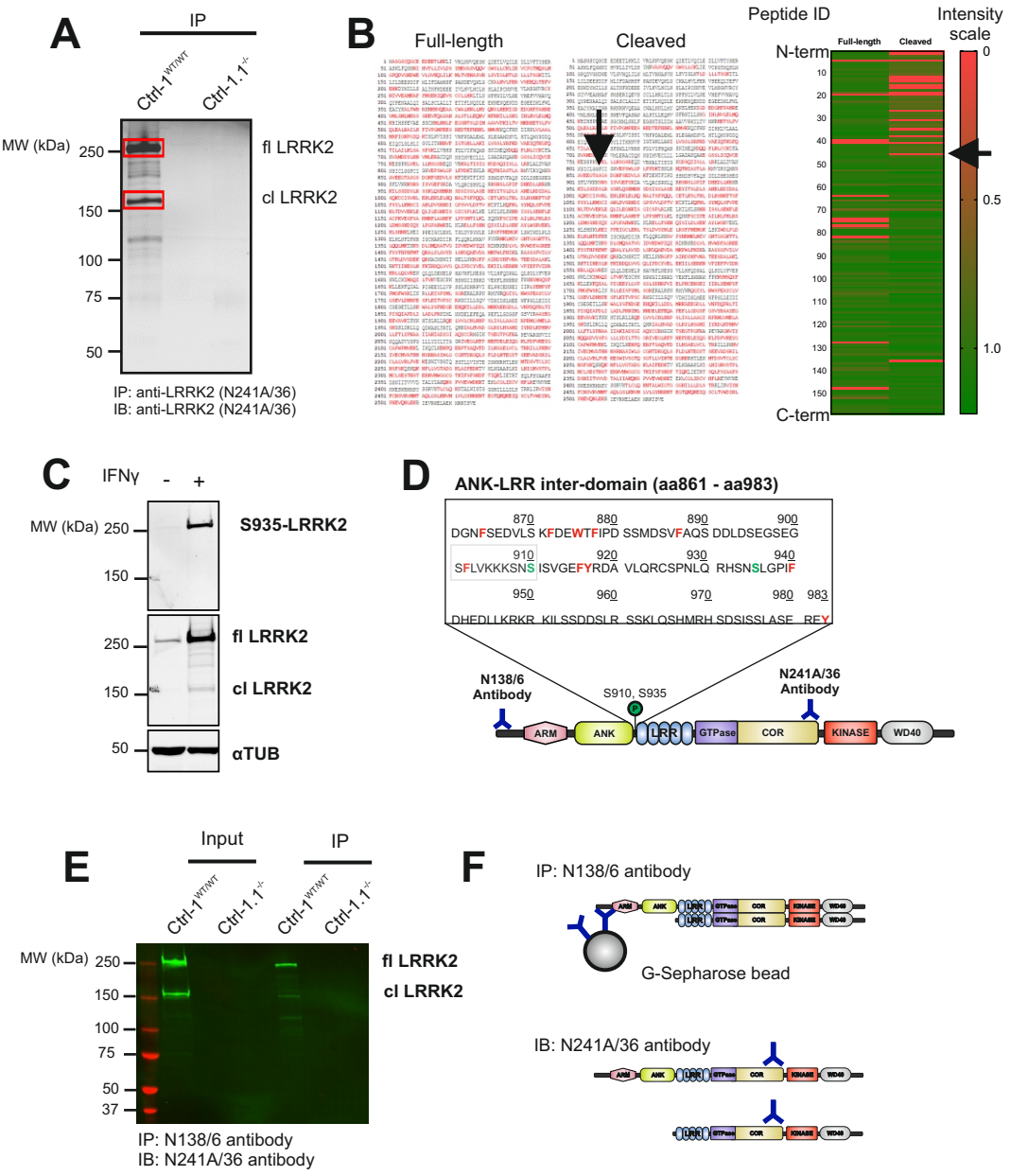

Figure 3.8 Identifying the putative cleavage site of LRRK2 using proteomics. (A) Western blot showing immunoprecipitated LRRK2 protein from Ctrl-1$^{WT/WT}$ and Ctrl-1.1$^{-/-}$ derived MΦs. Silver stained gel bands corresponding to fl LRRK2 and cl LRRK2 were cut and analyzed by mass spectrometry. **(B)** The amino acid sequence of LRRK2 with peptides identified by mass spectrometry presented in red. Heat map showing intensity of identified peptides (ordered from N-terminal to C-terminal) of fl LRRK2 and cl LRRK2 protein. The final analysis reveals that tr LRRK2 is largely missing N-terminal peptides up to around aa901 – aa910. **(C)** Western blot probed with antibody against phosphor S935-LRRK2 (above) and against C-terminus LRRK2 (below). Cl LRRK2 is missing phosphorylation at S935. **(D)** A schematic structure of LRRK2 showing the sequence of ANK-LRR interdomain region. Chymotrypsin cleavage sites are presented in red and phosphorylation sites in green. According to peptide analysis, the putative cleavage site is around aa901 – 910, which contains one chymotrypsin cleavage site (aa902) **(E)** LRRK2 protein was pulled down using antibody recognizing the N-terminus of LRRK2 (N138/6) and the immunoprecipitated eluates were blotted using antibody recognizing C-terminus of LRRK2 (N241A/36). Western blot confirms the presence of cl LRRK2 in the immunoprecipitated eluates, suggesting that fl LRRK2 and cl LRRK2 form a heterodimer complex. **(F)** A summary of immunoprecipitation experiment showing the formation of fl LRRK2, cl LRRK2 heterodimer complex.

3.3. Summary and Discussion

In this chapter, I have explored various ways how LRRK2 protein are regulated in hiPSC-MΦs. My results demonstrate that IFNγ and LPS significantly upregulate endogenous LRRK2 protein expression. LRRK2 becomes dephosphorylated at S935 in the presence of LRRK2 kinase inhibitors, which leads to degradation of LRRK2 protein. Lastly, LRRK2 is cleaved in hiPSC-MΦs and the putative cleavage site lies within the ANK-LRR interdomain region, where S935 phosphorylation site is located.

In hiPSC-MΦs, LRRK2 protein expression was significantly increased by IFNγ or LPS but not by other stimuli. IFNγ-driven upregulation of LRRK2 has been reported by several groups using mouse and human myeloid cells (Gardet et al. 2010; Gillardon, Schmid, and Draheim 2012; Kuss, Adamopoulou, and Kahle 2014; Thévenet et al. 2011; Moehle et al. 2012; Dzamko and Halliday 2012). LRRK2 promoter region contains multiple interferon-regulatory factor (IRF) recognition sequence (IRS) which the DNA binding domains of the IRF family binds to (Thévenet et al. 2011). IFNγ directly regulates LRRK2 expression via Janus kinase (JAK)/signal transducers and activators of transcription (STAT) and the extracellular signal-regulated kinase 5 (ERK5) pathway (Kuss, Adamopoulou, and Kahle 2014). TLR4 signalling by LPS activates various transcription factors, particularly NF-κB and IRF8 (Medzhitov and Horng 2009), therefore, it is conceivable that LPS may drive LRRK2 protein expression by activating IRF8.

Thevenet et al., have shown that LRRK2 expression is also significantly induced by IFNβ, TNFα, and IL-6 stimulation (Thévenet et al. 2011), however, my results show that IFNβ or TNFα do not affect the expression level of LRRK2 in hiPSC-MΦs (Figure 3.4B). This could be because Thevenet et al. used human PBMCs. Our hiPSC-MΦs are relatively

naïve as they have never been exposed to stimuli other than the ones that I applied in my experiments, whereas human PBMCs might been exposed to *in vivo* stimuli which prime them to be more responsive to stimuli other than IFNγ.

Consistent with the literature (Perera et al. 2016; Deng et al. 2011; Doggett et al. 2012; Dzamko et al. 2010; Nichols et al. 2010), small molecule kinase inhibitors, GNE and GSK, significantly reduced the level of phosphorylation at S935 in hiPSC-MΦs. The presence of the heterozygous *LRRK2* G2019S mutation did not alter either the basal phosphorylation level at S935 or the degree of dephosphorylation upon treatment with LRRK2 kinase inhibitors (Figure 3.5). This is in accordance with the observations made in LRRK2 overexpression systems (Li et al. 2011; Doggett et al. 2012; Nichols et al. 2010; E Lobbestael et al. 2016). Altogether, my results further confirm that phosphoregulation of S935 probably does not involve LRRK2 kinase activity itself.

Studies have reported that LRRK2 can be degraded by chaperone-mediated autophagy (CMA) and the presence of *LRRK2* G2019S mutation compromises its degradation in LRRK2-overexpressing HEK293T cells (Orenstein et al. 2013). LRRK2 can also be degraded by ubiquitin proteasome system (UPS) by interacting with E3 ubiquitin ligase CHIP (C-terminus of Hsp70-Interacting Protein) in LRRK2-overexpressing HEK 293T cells (Ding and Goldberg 2009) and SH-SY5Y cells (Ko et al. 2009). Treating cells with LRRK2 kinase inhibitors appear to enhance this process of LRRK2 degradation. A significant reduction of LRRK2 protein was observed in HEK 293T cells overexpressing LRRK2 treated with GNE-1023 (2 µM) (Zhao et al. 2015). Similarly, this was shown in SH-SY5Y cells overexpressing LRRK2 treated with six different LRRK2 kinase inhibitors, MLi-239 (10 nM), PF-0644747544 (150 nM), GSK2578215A (2 µM), LRRK2-IN-1 (1 µM), HG 10-102-01 (1 µM), and CZC-2514647 (200 nM) (E Lobbestael et al. 2016). My results also confirm this observation in hiPSC-MΦs expressing

endogenous level of LRRK2, treated with GSK (1 μM) or GNE (1 μM) (Figure 3.6). This inhibitor-induced degradation of LRRK2 has been suggested to be UPS-dependent. Proteasome inhibitors, MG-132 or Bortezomib, reversed inhibitor-induced degradation while inhibition of lysosomal pathway by Bafilomycin A1 did not rescue inhibitor-induced degradation in LRRK2-overexpressing SH-SY5Y cells (Zhao et al. 2015).

My results show that treating hiPSC-MΦs expressing physiological level of LRRK2 with lysosomal protease inhibitor, leupeptin, or proteasome inhibitors, MG-132 or lactacystin, did not change the level of total LRRK2 protein (Figure 3.7D). However, MG-132 treatment, which inhibits chymotrypsin-like activity of proteasome, significantly reduced the level of LRRK2 cleavage product. A similarly sized cleaved form of LRRK2 has been found by western blot analysis in mouse kidney but less extensively in lung and brain (E Lobbestael et al. 2016; Herzig et al. 2011; Dächsel et al. 2007). Using IP and mass spectrometry approach, I have identified that this cleavage product lacks N-terminus of LRRK2 and the cleavage site appears to be within ANK-LRR interdomain region (aa861 – aa983), where S910, S935, S955, S973 phosphosites and multiple chymotrypsin cleavage sites are located (Figure 3.8D). By analysing peptide distributions, the putative cleavage site is within aa901 and aa910, where one chymotrypsin cleavage site, aa902, is found (Figure 3.8C). Western blot shows that cleaved product does not contain phosphorylation at S935 (Figure 3.8D). This could be because of its proximal location to putative cleavage site, S935 may no longer be recognizable by upstream kinases, or as a result of cleaving, this site may become more accessible to phosphatases.

Whether the formation of cleaved LRRK2 is carefully regulated by unidentified chymotrypsin-like proteases or is simply an intermediate product of LRRK2 degradation via UPS requires further investigation. However, the existence of cleaved LRRK2 appears to be more than a by-product of LRRK2 degradation via UPS because my results

demonstrate that LRRK2 can exist as a heterodimer complex of full-length and the cleavage product (Figure 3.8). A recent study by Guaitoli et al., has provided a predicted 3D model of full-length LRRK2 structure using computational modelling and chemical cross-linking of LRRK2 followed by mass spectrometry (CL-MS) (Guaitoli et al. 2016). This model provides a moderate resolution of how each LRRK2 domain interacts. According to this model, LRRK2 dimer is oriented a head-to-head direction with COR domain placed in the middle docking the two monomers while the C-terminal (kinase and WD40) domains are folded backward so that they are in contact with N-terminal domains. This model suggests that N-terminal region of LRRK2 may have a significance in regulating enzymatic activity of LRRK2 by potentially exposing substrate binding site (Guaitoli et al. 2016). Therefore, the ANK-LRR interdomain region may act as an important regulatory switch for LRRK2 enzymatic activity. By phosphorylation or cleavage, it may regulate LRRK2 by affecting LRRK2 dimerization, cellular localisation, and/or interaction with other proteins. Understanding how LRRK2 activity orchestrates regulation of its own activity and how mutations of LRRK2 may disrupt this balance, could provide important clues to understand its pathological mechanisms.

4

Dissecting the physiological role of LRRK2 in phagocytosis

4.1 Introduction

4.1.1 Phagocytosis

Phagocytosis was first described in 1800s by a Russian zoologist, Ilya Ilyich Metchnikoff. He observed “mobile cells” within the larvae of starfishes, which engaged in “eating to defend” mechanism to protect the larvae against invading pathogens. He termed this process, phagocytosis, which derives from Ancient Greek φαγεῖν (phagein), which means 'to devour' and κύτος (kytos), which means 'cell’ (Tauber 2003). More than 100 years have passed and phagocytosis is still an active area of research.

Phagocytosis resembles endocytosis pathways, such as pinocytosis or receptor-mediated endocytosis, in that the target is ingested into a vesicle, which subsequently undergoes multiple fusion and fission events until it is destroyed. Phagocytosis, however, mainly differs from other endocytic pathways. There are specific pools of targets that are involved in phagocytosis, these are any particles lager than > 0.5 μm and those that display specific ligands, notably bacteria or yeast. Phagocytosis requires special machineries to process these particles, therefore, phagocytosis is predominantly performed by a subset of cells, namely professional phagocytes. Professional phagocytes include MΦs, neutrophils, monocytes, DCs, osteoclasts, and eosinophils (Rabinovitch

1995). These cells are equipped with a range of pattern recognition receptors (PRRs), which efficiently identify materials from foreign pathogens to apoptotic cells and allow appropriate downstream signals to initiate. Pathogen-associated molecular patterns (PAMPs) displayed by bacteria, fungi or parasites are recognised by certain receptors, particularly TLRs and Dectin-1, and induce the release of pro-inflammatory cytokines (Hayashi et al. 2001; Takeuchi et al. 2000). Conversely, binding of phosphatidylserine (PS) presented by apoptotic cells is mediated by T cell immunoglobulin mucin (TIM) family, brain-specific angiogenesis inhibitor 1 (BAI1) and Stabilin-2 (Kobayashi et al. 2007; Nakayama et al. 2009; J.-Y. Park et al. 2008; D. Park et al. 2007), and generally results in anti-inflammatory responses, notably promotion of transforming growth factor β (TGF-β) and prostaglandin E2 secretion (Fadok et al. 1998; M.-L. N. Huynh, Fadok, and Henson 2002), signalling the resolution of inflammation.

Once a phagocytic substrate is internalised, the newly formed nascent phagosome undergoes sequential steps of fission and fusion with endosomal vesicles until it finally matures to phagolysosome. These endosomal vesicles not only change the inner biochemical composition of phagosomes but also ensure these changes occur in step-wise fashion. Small GTPases Rab proteins are key regulators of phagosome maturation, and they are responsible for coordinating endocytic vesicular trafficking between the phagosome and cell organelles via the actin cytoskeleton network (Gutierrez 2013).

Transition from the nascent phagosome to early phagosome is marked by the recruitment of Rab5. Active Rab5 induces the membrane localisation of the class III phosphoinositide 3-kinase, vacuolar protein-sorting 34 (Vps34), which facilitates the synthesis of the lipid phosphatidylinositol 3-phosphate [PI(3)P] from phosphatidylinositol (Ellson et al. 2001). Accumulation of PI(3)P then recruits early endosomal antigen 1 (EEA1) and the class C core vacuole/endosome tether (CORVET) complex (Lawe et al. 2002; Peplowska et al.

2007), which acts as a bridge between the phagosome and other endosomal vesicles. During this stage, the phagosome starts to gradually acquire vacuolar-type H+ -ATPase (v-ATPase) which pumps H+ inward to initiate the acidification process (Yates et al. 2007).

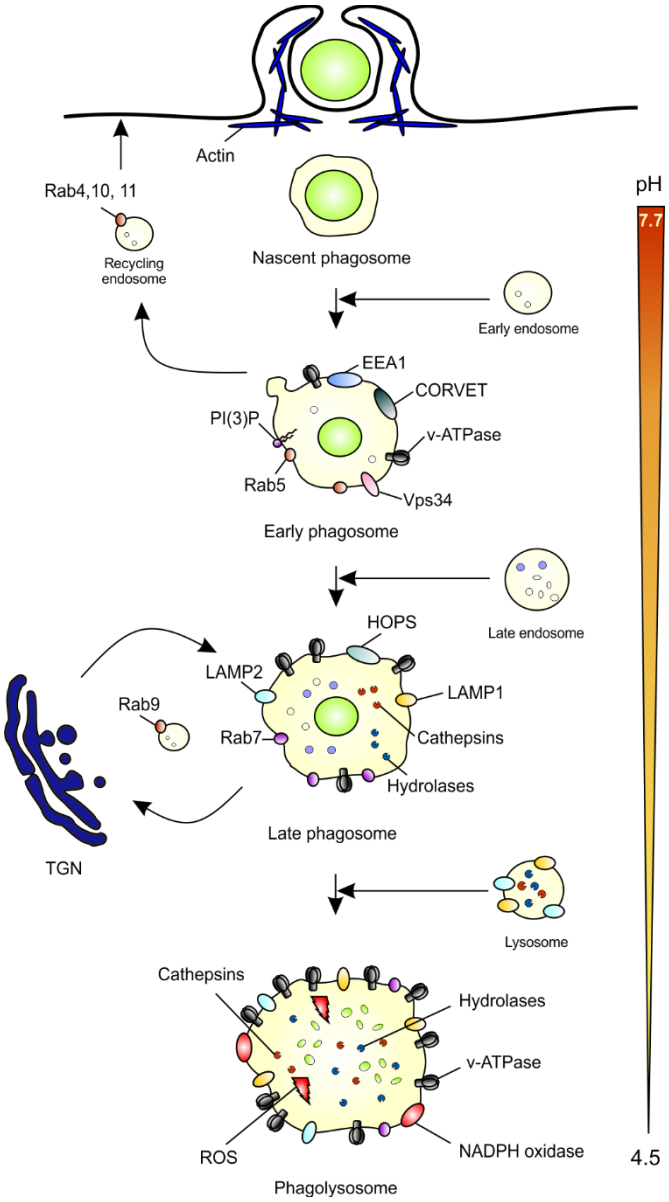

Figure 4.1 Phagosome maturation. Soon after the nascent phagosome is formed Rab5 is recruited and EEA1 further matures the phagosomes to Rab7 recruitment. Late phagosome finally fuses with lysosome forming phagolysosome. By this stage the inner environment of phagolysosome reaches pH = 4.0, which is optimal pH for many hydrolases and proteases. Recycling endosomes, Rab4,9,10, and 11 are constantly shuffled between phagosomes and other intracellular compartments, such as trans-Golgi network (TGN).

Transition from early to late phagosome is marked by the replacement of Rab5 and CORVET to Rab7 and late tethering complex, homotypic fusion and vacuole-sorting (HOPS) (Rink et al. 2005). Although the precise mechanisms of this transition remain to be determined, the acquisition of lysosome-associated membrane protein 1 and 2 (LAMP-1 and -2) is a prerequisite for the recruitment of Rab7. In mice that lack both LAMP-1 and LAMP-2 displayed phagosomes that are arrested at the Rab5(+), PI3P(+) stage (K. Huynh et al. 2007). HOPS complex acts downstream of Rab7 recruitment and is crucial in the maturation of phagosomes to phagolysosome. Worms lacking certain components of HOPS complex display phagosomes that are arrested at the Rab7(+) phagosome (Kinchen and Ravichandran 2008).

The final fusion of late phagosome and lysosome is mediated by SNARE complex composed of syntaxin7 and synaptosomal associated protein of 23 kDa (SNAP-23) (Sakurai et al. 2012). The phagolysosome is highly degradative, as it contains numerous hydrolytic enzymes, notably glycosidases, lipases, DNases, and proteases which become highly active in an acidic environment (pH = 4.5) (Yates, Hermetter, and Russell 2009). By this stage, the phagolyososome also contains NADPH oxidase complex, which generates oxygen radicals (Savina et al. 2006), further maximising its antimicrobial capacity.

Another critical component of phagosome maturation is the retrieval of cargo proteins via recycling pathways. During internalisation of phagocytic substrates, a considerable amount of plasma membrane is internalised, along with receptors such as TLRs. These elements must be retrieved back to their origins, and this is mediated by Rab4, 10, 11 and other members of the retromer complex (Damiani et al. 2004; Ullrich et al. 1996). Rab9 recycles mannose 6-phosphate receptors (M6PRs) from late phagosomes to Golgi

complex, which carry lysosomal enzymes (Lombardi et al. 1993; Barbero, Bittova, and Pfeffer 2002).

It should be noted that phagosome maturation steps described above are overly simplified and that phagosome maturation is a very dynamic and complex process, involving rapid and transient interactions occurring in parallel. The process of phagosome maturation also depends on the context of phagocytic substrates, types of phagocytes, and the microenvironment (such as presence of inflammatory signals) (Rettig et al. 2010; Beningo and Wang 2002). There is also extensive crosstalk between vesicular events because it is important to signal to coordinate the overall kinetics of phagosome maturation. For example, in DC, phagosome maturation is significantly delayed compared to other phagocytes as the antigens from pathogens must be spared for antigen presentation (Salao et al. 2016).

4.1.2 Neurodegeneration and phagocytosis

Microglia are the chief professional phagocytes in the CNS and their main function is to maintain a homeostatic environment for neurons. During development, microglia detect and phagocytose weak synapses (a process called synaptic pruning), shaping proper neuronal network (Schafer et al. 2012; Hong et al. 2016). Microglia can also actively phagocytose dead or damaged neurons (Fraser, Pisalyaput, and Tenner 2010), as well as potentially harmful extracellular protein aggregates, notably amyloid beta (Aβ) (Ard et al. 1996; Webster et al. 2000; Koenigsknecht and Landreth 2004), or αsyn (J.-Y. Park et al. 2008). Because microglial function is essential in overall well-being of neurons, it is conceivable that defects in its function could potentially be harmful for neurons. Consistent with this idea, variants in phagocytosis-related genes have been identified to be risk factors for neurodegenerative disease, including AD and PD. For example, *TREM2, CD33,* are associated with AD and its variants have been shown to impair

phagocytosis (Kleinberger et al. 2014; Griciuc et al. 2013). PD-causing mutations in *SNCA* also reduce phagocytic capacity of MΦs (Lee et al. 2008; Haenseler et al. 2017). N370S *GBA* mutant in human iPSC-derived MΦs displays no defect in the uptake of erythrocytes impairs complete digestion of them (Aflaki et al. 2014; Panicker et al. 2012).

LRRK2 is highly expressed in professional phagocytes – MΦs, microglia, DC – and has been reported to interact with key Rab GTPases of phagocytosis pathway, particularly Rab5, 7, 8, 10, and 32, suggesting its possible role in phagocytosis (Chapter1.2). However, interaction of LRRK2 with these Rab GTPases (Rab5, 7, and 32) must be critically evaluated as these interactions so far have been confirmed by *in vitro* studies in LRRK2-overexpressing HEK 293T cells (Yun et al. 2015; Dodson et al. 2012; Gómez-Suaga et al. 2014; Steger et al. 2016; Waschbüsch et al. 2014), or at a physiological level (Rab8 and 10) but in non-professional phagocytes, mouse fibroblasts (Steger et al. 2016). Furthermore, the direct evidence that LRRK2 is involved in phagocytosis is lacking as different research groups have reported conflicting results (Gardet et al. 2010; Marker et al. 2012; Schapansky et al. 2014; Moehle et al. 2015; Maekawa et al. 2016).

4.1.3 Aims

The overall aim of this chapter is to critically assess the involvement of LRRK2 in phagocytosis by using authentic human MΦs differentiated from hiPSCs. I have used immunofluorescent techniques to investigate subcellular localisation of LRRK2 during phagocytosis. I have explored the involvement of LRRK2 function in two different stages of phagocytosis; during the initial internalisation of phagocytic substrates and later during the acidification of phagosomes, and with different phagocytic substrates and opsonisation conditions. Lastly, I undertook a proteomics approach in an attempt to capture molecular interactors of LRRK2 during phagocytosis.

4.2 Results

4.2.1 LRRK2 is recruited to the phagosomes during late stages of phagocytosis

LRRK2 protein has been reported to localise to the phagosomes containing *S. typhimurium* in mouse MΦ-like RAW 264.7 cells (Gardet et al. 2010). However, no attempt was made to identify at which stage of phagocytosis LRRK2 is recruited to the phagosomes. Furthermore, more rigorous validation of immunostaining is required as the antibody used in this study (NB300-268, Novus Biologicals) was not validated using *LRRK2* KO cells (Gardet et al. 2010).

Based on this observation, I investigated whether LRRK2 is recruited to the phagosomes during different stages of phagocytosis. Phagocytosis of fluorescent zymosan bioparticles was allowed for 2 h and the hiPSC-MΦs were subsequently fixed and stained with antibody against LRRK2. Confocal imaging analysis clearly demonstrated the presence of LRRK2 on a subset of zymosan-containing phagosomes (Figure 4.2A). And the specificity of the immunostaining was validated by using *LRRK2* KO hiPSC-MΦs (Ctrl-1.1$^{-/-}$), which do not show any signal for LRRK2 (Figure 4.2A,B).

Zymosan activates dectin-1 and TLR2 receptors (Gantner et al. 2003). To examine whether recruitment of LRRK2 is dependent on certain receptors, *E.coli* bioparticles activating TLR4 and live *S.typhimurium* activating TLR2 and TLR4 were given to hiPSC-MΦs. Recruitment of LRRK2 protein was confirmed on these phagosomes (Figure 4.2A). To examine whether the size of target matters, I opsonized zymosan bioparticles (~3 μm) and *E.coli* bioparticles (0.1 μm) with IgG so that both particles are recognized by FcRs. LRRK2 recruitment was observed in both cases (Figure 4.2B). I extended this observation by feeding hiPSC-MΦs with latex beads (2.5 μm) of similar size as zymosan bioparticles but which are taken up by multiple scavenger receptors. This

time, LRRK2 was not observed on latex beads containing phagosomes (Figure 4.2D). Interestingly, LRRK2 protein was also absent on the phagosomes containing αsyn fibrils, which have been reported to activate TLR1, 2, and 4 (Kim et al. 2013; Fellner et al. 2013; Stefanova et al. 2011).

Since LRRK2 was not found in all phagosomes but only on a subset of phagosomes, whether this was zymosan, *E. coli* or *S. typhimurium*, I hypothesized that LRRK2 must be recruited during a specific stage of phagocytosis. I stained hiPSC-MΦs fed with fluorescent zymosan bioparticles with markers that represent early phagosome (Rab5) and late phagolysosome (Rab9 and LAMP-1). Zymosan bioparticles were chosen to investigate this hypothesis because of its relatively larger size, the presence of LRRK2 on phagosomes could be easily detected and closely examined, making quantification more reliable and reproducible. A significantly higher proportion of zymosan-containing phagosomes were LRRK2-positive when incubation was 120 min compared to 30 min (Figure 4.3). LRRK2 was detected significantly more on LAMP-1(+) phagosomes, which represent late–phagolysosomes, than Rab5(+) phagosomes, which represent early phagosomes (Figure 4.3). Interestingly, LRRK2 protein does not appear to co-localise with neither Rab5 nor LAMP-1 but rather co-exists on the same phagosome (Figure 4.3).

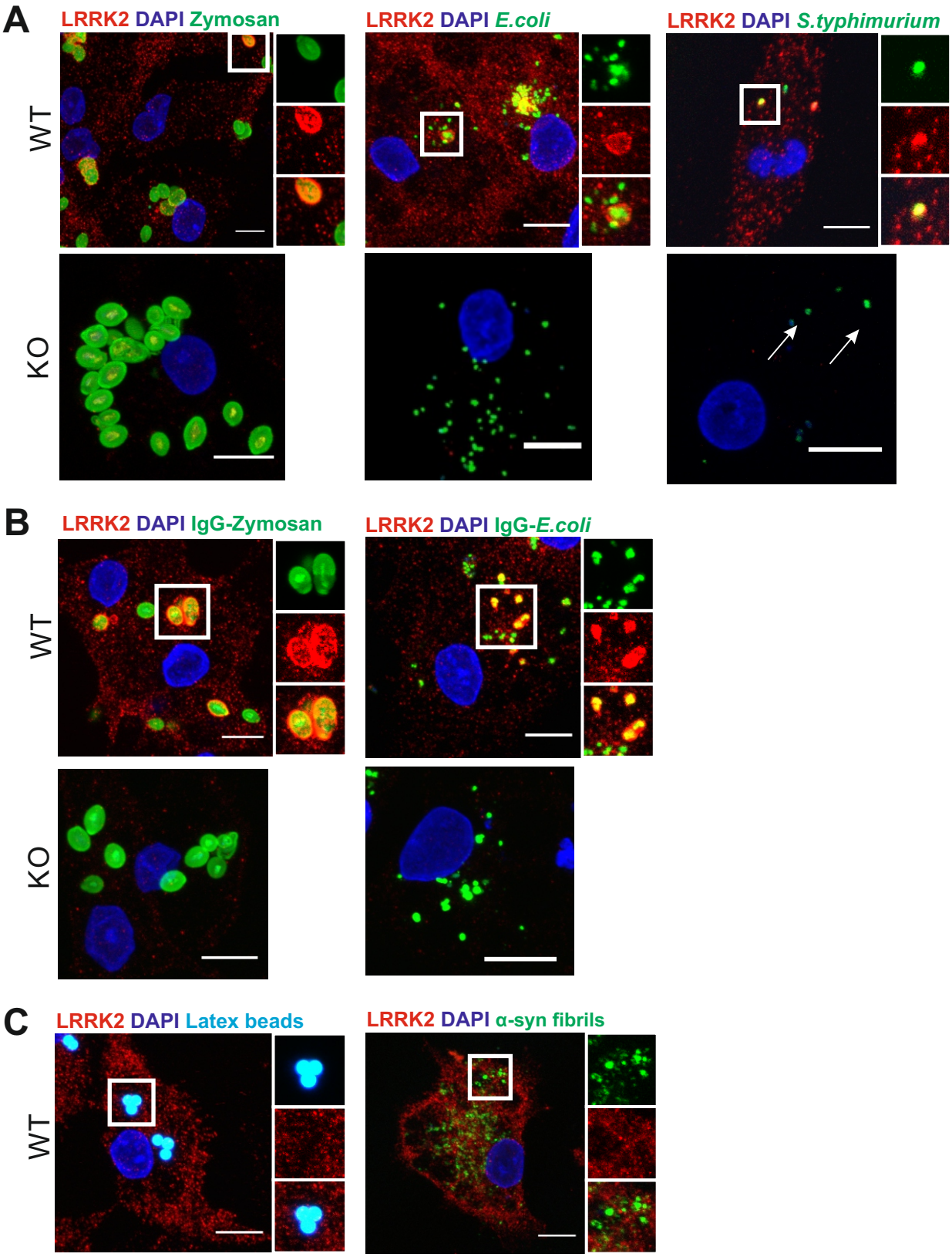

Figure 4.2 LRRK2 is recruited to the phagosomes. (A) Confocal images of *LRRK2* WT and *LRRK2* KO hiPSC-MΦs fed with fluorescent zymosan bioparticles, fluorescent *E. coli* bioparticles, live GFP-expressing *S.typhimurium*, **(B)** IgG-opsonised zymosan bioparticles, IgG-opsonised fluorescent *E. coli* bioparticles, and **(C)** fluorescent latex beads and Alexa-488 conjugated α-syn fibrils. Phagocytosis was allowed for 120 min then cells were fixed and stained with antibody against LRRK2. All scale bars represent 10 µm.

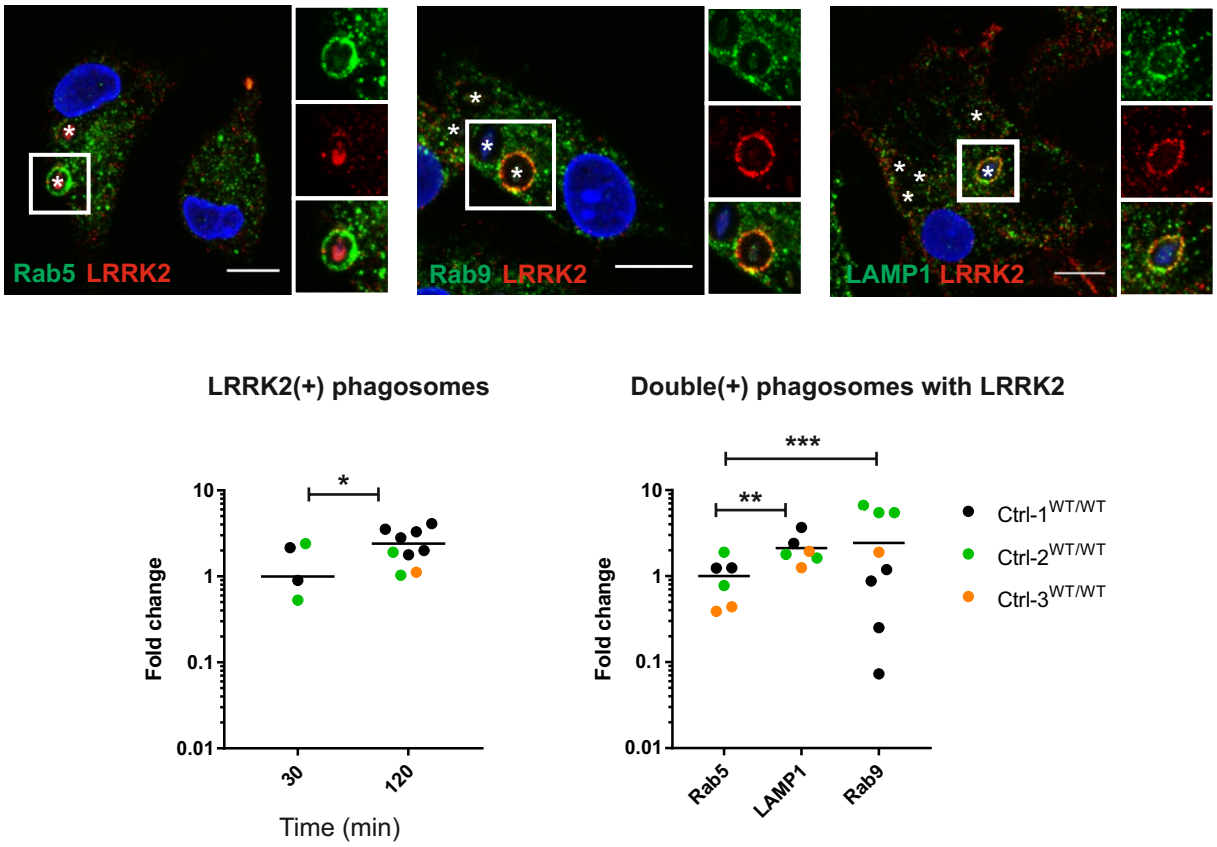

Figure 4.3 LRRK2 is recruited to the late phagosomes. hiPSC-MΦs were fixed and stained with Rab5, an early phagosome marker, and LAMP-1, a late phagosomes/phagolysosomes marker. All scale bars represent 10 µm. Bar graph on the left shows the quantification of LRRK2(+) phagosomes in MΦs that were fed with fluorescent zymosan bioparticles for 30 min and for 120 min. Internalized zymosan bioparticles are indicated in asterix. Data represent the fold change against time point 30 min in mean ± S.E.M. Student t-test was used for statistical analysis. Bar graph on the right shows the fold change in the number of LRRK2(+) phagosomes displaying late phagosomal markers (Rab9, LAMP-1) against early phagosomal marker (Rab5). Data are presented in mean ± S.E.M. Statistical analysis was performed by two-way ANOVA with Dunnett's multiple comparisons test. * $P < 0.05$, ** $P < 0.01$, *** $P < 0.001$

4.2.2 LRRK2 kinase inhibitors enhance the formation of LRRK2 super-coated phagosomes

At least in LRRK2-overexpressing HEK 293T cells, it has been reported that LRRK2 kinase inhibitors affect localisation of LRRK2 within the cell from diffused cytosolic distribution to more discrete cytosolic pools (Dzamko et al. 2010). Therefore, I investigated whether the application of LRRK2 kinase inhibitors would affect the localisation of LRRK2 to phagosomes during phagocytosis.

On average about 20% of zymosan containing phagosomes were positive for LRRK2 and about 10% of these LRRK2(+) phagosomes displayed strong positivity for LRRK2 (referred as LRRK2 super-coated phagosomes) (Figure 4.4B and Appendix A4). Pre-treating hiPSC-MΦs with two structurally distinct LRRK2 kinase inhibitors, GSK2578215A (GSK) or GNE-7915 (GNE), significantly increased the proportion of LRRK2 super-coated phagosomes (Figure 4.4C) while the overall number of LRRK2(+) zymosan containing phagosomes did not change (Figure 4.4C).

Since pharmacological inhibition of LRRK2 kinase activity enhanced the formation of LRRK2 super-coated phagosomes, I next investigated whether the presence of *LRRK2* G2019S heterozygous mutation, which displays hyper-kinase activity, would impact this observation. First, there was no difference in the total number of LRRK2(+) phagosomes or in the number of LRRK2 super-coated phagosomes between LRRK2 G2019S hiPSC-MΦs and its isogenic pair. Similarly, the formation of LRRK2 super-coated phagosomes was also detected in hiPSC-MΦs with *LRRK2* G2019S mutation in the presence of GNE, but not GSK, although no significant difference was detected compared to its isogenic pair (Figure 4.4D).

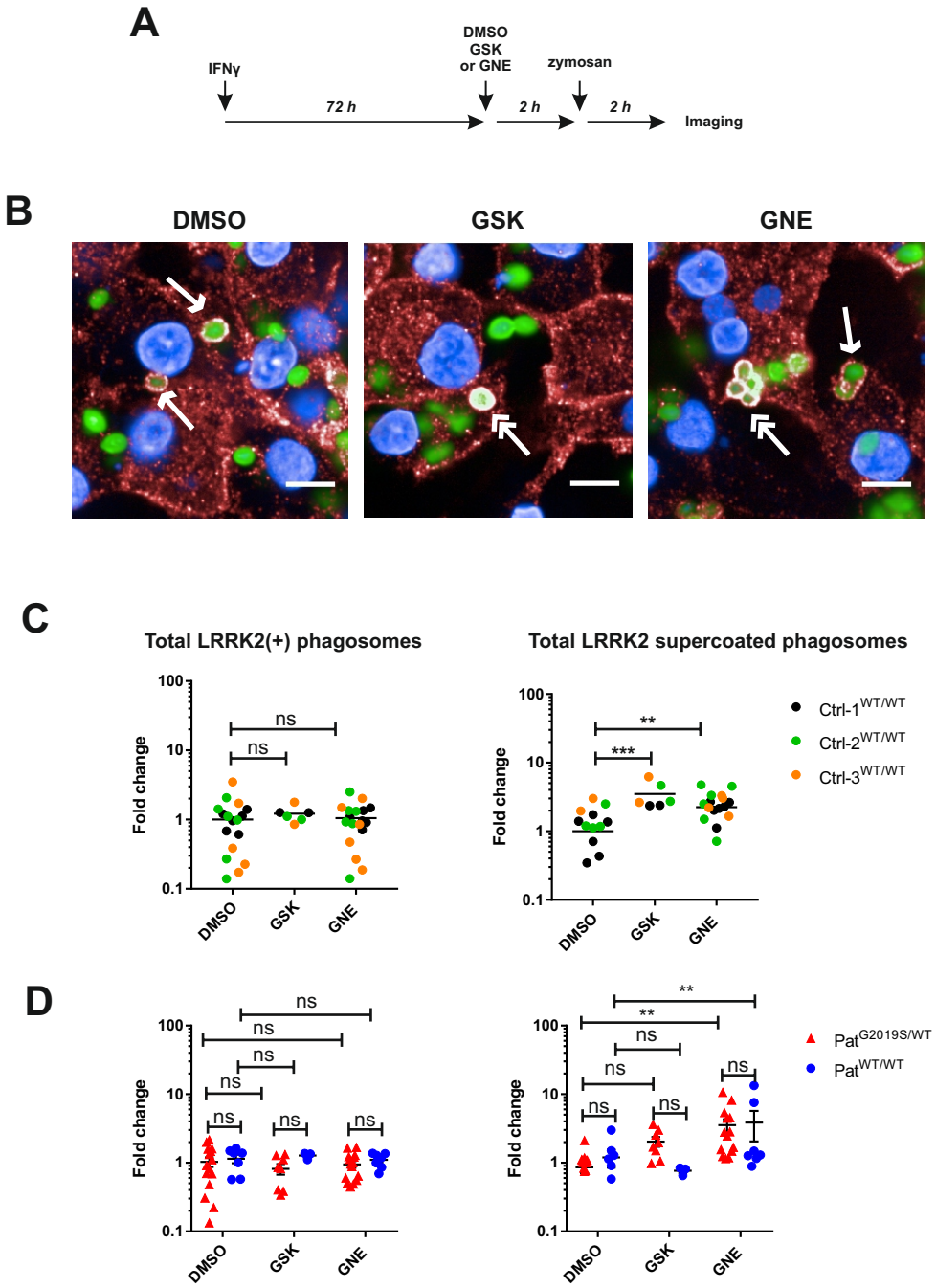

Figure 4.4 LRRK2 kinase inhibitors enhance the formation of super-coated LRRK2 phagosomes. (A) hiPSC-MΦs were pre-treated with GSK (1μM), GNE (1μM), or DMSO for 2 h before fluorescent zymosan bioparticles were added. Phagocytosis was allowed for 2 h and cells were fixed and stained with antibody against LRRK2. **(B)** Confocal images show an example of LRRK2(+) phagosomes (labelled with a single-headed arrow) and LRRK2 super-coated phagosomes (labelled with double-headed arrow). All scale bars represent 10 μm. **(C, D)** Each dot represents data (mean) collected from at least 300 cells based on images acquired from at least five randomised fields. Two-way ANOVA with Fisher's LSD test was used for statistical analysis. * $P < 0.05$, ** $P < 0.01$, *** $P < 0.001$, ns denotes not significant.

4.2.3 LRRK2 is not involved in the acidification of the phagosomes

Since LRRK2 is recruited during the late stages of phagocytosis, I hypothesised that LRRK2 has a functional role during the downstream phagosome maturation steps. The simplest way of testing this hypothesis is to quantify the number of acidified phagosomes using bioparticles conjugated to acid-sensitive dye. To ensure that the number of acidification events are not influenced by varied internalisation rate, I tested whether the internalisation of bioparticles are affected by LRRK2 kinase inhibitors, or across different LRRK2 hiPSC-MΦs.

MΦs differentiated from three healthy control iPSC lines (Ctrl-1.1$^{WT/WT}$, Ctrl-1.2$^{WT/WT}$, Ctrl-1.3$^{WT/WT}$) were pre-treated with GSK or GNE for 2 h before zymosan bioparticles were applied for 30 min. The number of zymosan containing cells were quantified using flow cytometry (Figure 4.5A). LRRK2 kinase inhibitors had no significant effect on the internalisation of zymosan bioparticles (Figure 4.5C). Similarly, neither *LRRK2* KO hiPSC-MΦs (Ctrl-1.2$^{-/-}$) nor *LRRK2* G2019S hiPSC-MΦs (Pat$^{G2019S/WT}$) showed any significant difference compare to their isogenic pairs (Figure 4.6-7).

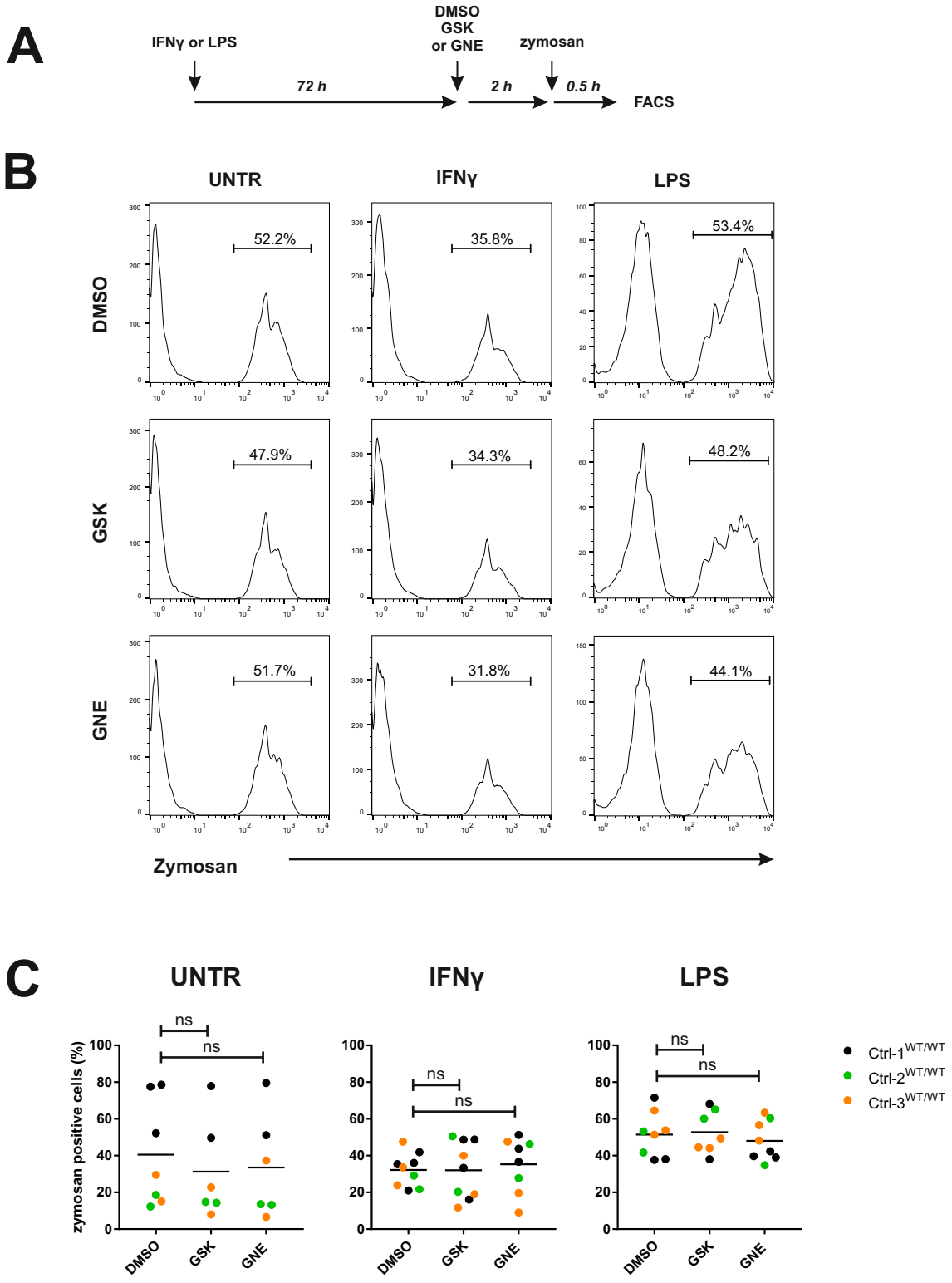

Figure 4.5 Application of LRRK2 kinase inhibitors does not affect the internalisation of zymosan bioparticles in hiPSC-MΦs. (A) Outline of the experimental design **(B)** FACS plots showing the percentage of zymosan(+) hiPSC-MΦs **(C)** Graphs represent mean ± SEM of the percentage of zymosan(+) hiPSC-MΦs from at least three independent experiments from three healthy control lines (Ctrl-1, -2, -3). Each dot represents data from each independent experiment. Two-way ANOVA with Dunnett multiple comparisons test against vehicle control (DMSO) was used for statistically analysis. ns denotes not significant.

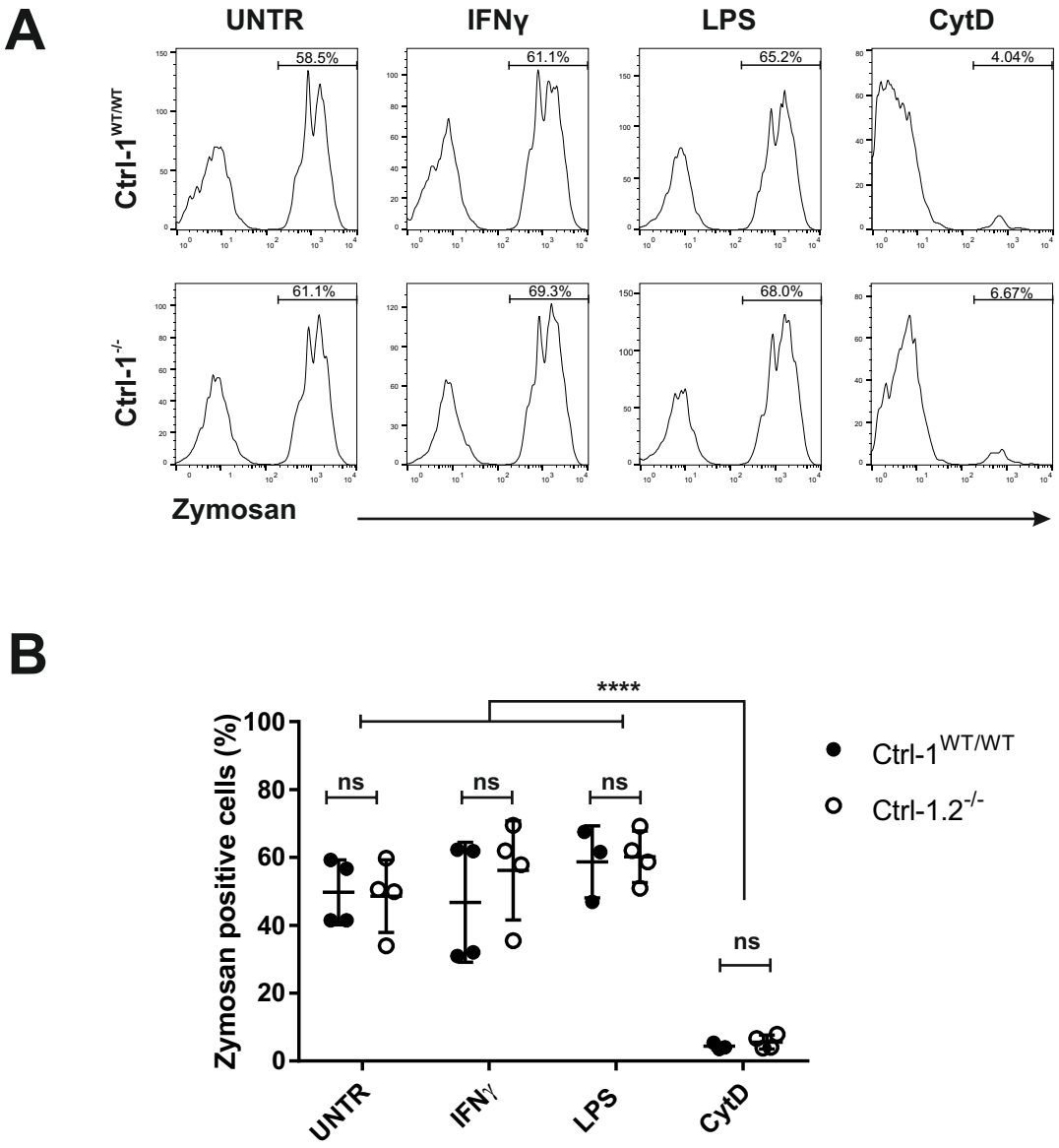

Figure 4.6 Complete absence of LRRK2 protein does not affect the internalisation of zymosan bioparticles in hiPSC-MΦs. (A) FACS plots showing the percentage of zymosan(+) hiPSC-MΦs from *LRRK2* KO (Ctril-1.2$^{-/-}$) and its parental control line (Ctrl-1$^{WT/WT}$) **(B)** Graph represents mean ± SEM of the percentage of zymosan(+) hiPSC-MΦs from at least three independent experiments. Each dot represents data from each independent experiment. Cytochalasin D (CytD; 10 μM) inhibits actin polymerisation therefore was used as a negative control. Two-way ANOVA with Dunnett multiple comparisons test was used for statistically analysis. * $P < 0.05$, ** $P < 0.01$, *** $P < 0.001$, ns denotes not significant.

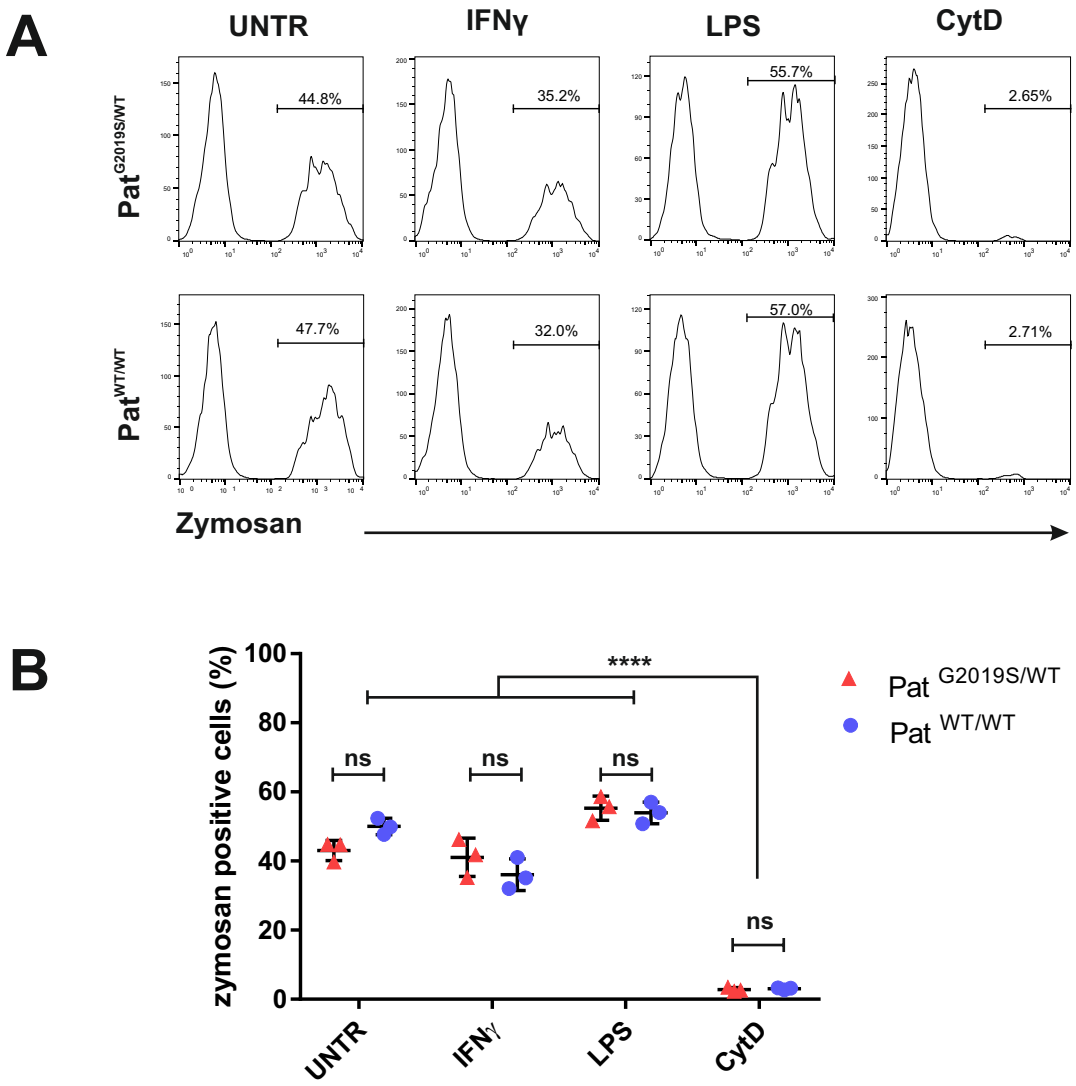

Figure 4.7 The presence of G2019S mutation does not affect the internalisation of zymosan bioparticles in hiPSC-MΦs. (A) FACS plots showing the percentage of zymosan(+) hiPSC-MΦs from LRRK2 G2019S patient line ($Pat^{G2019S/WT}$) and its CRISPR/Cas-9 edited isogenic control line ($Pat^{WT/WT}$) **(B)** Graph represents mean ± SEM of the percentage of zymosan(+) hiPSC-MΦs from at least three independent experiments. Each dot represents data from each independent experiment. Cytochalasin D (CytD; 10 µM) inhibits actin polymerisation therefore was used as a negative control. Two-way ANOVA with Dunnett multiple comparisons test was used for statistically analysis. * $P < 0.05$, ** $P < 0.01$, *** $P < 0.001$, ns denotes not significant.

Zymosan and *E. coli* bioparticles conjugated to pHrodo dye become fluorescent in the acidic environment (pH 5.5 – 4.5) of the phagolysosome. Acidification events were monitored live for 2 h and the number of acidified phagosomes were quantified using an incuCyte ZOOM system (Essen Bioscience) (Kapellos et al. 2016).

hiPSC-MΦs treated with LRRK2 kinase inhibitors did not show a significant difference in acidification of phagosomes compared to vehicle control (Figure 4.8). The kinetics of acidification events as well as the total number of acidified phagosomes at the end of the assay were not affected by LRRK2 kinase inhibitors. This was surprising because I have shown in the previous section that LRRK2 kinase inhibitors significantly increased the number of LRRK2 super-coated phagosomes (Figure 4.4C). Similarly, neither complete absence of LRRK2 protein nor the presence of G2019S mutation had a significant impact on the acidification of phagosomes (Figure 4.9-10). Together, these results imply that LRRK2 is dispensable for phagosome acidification.

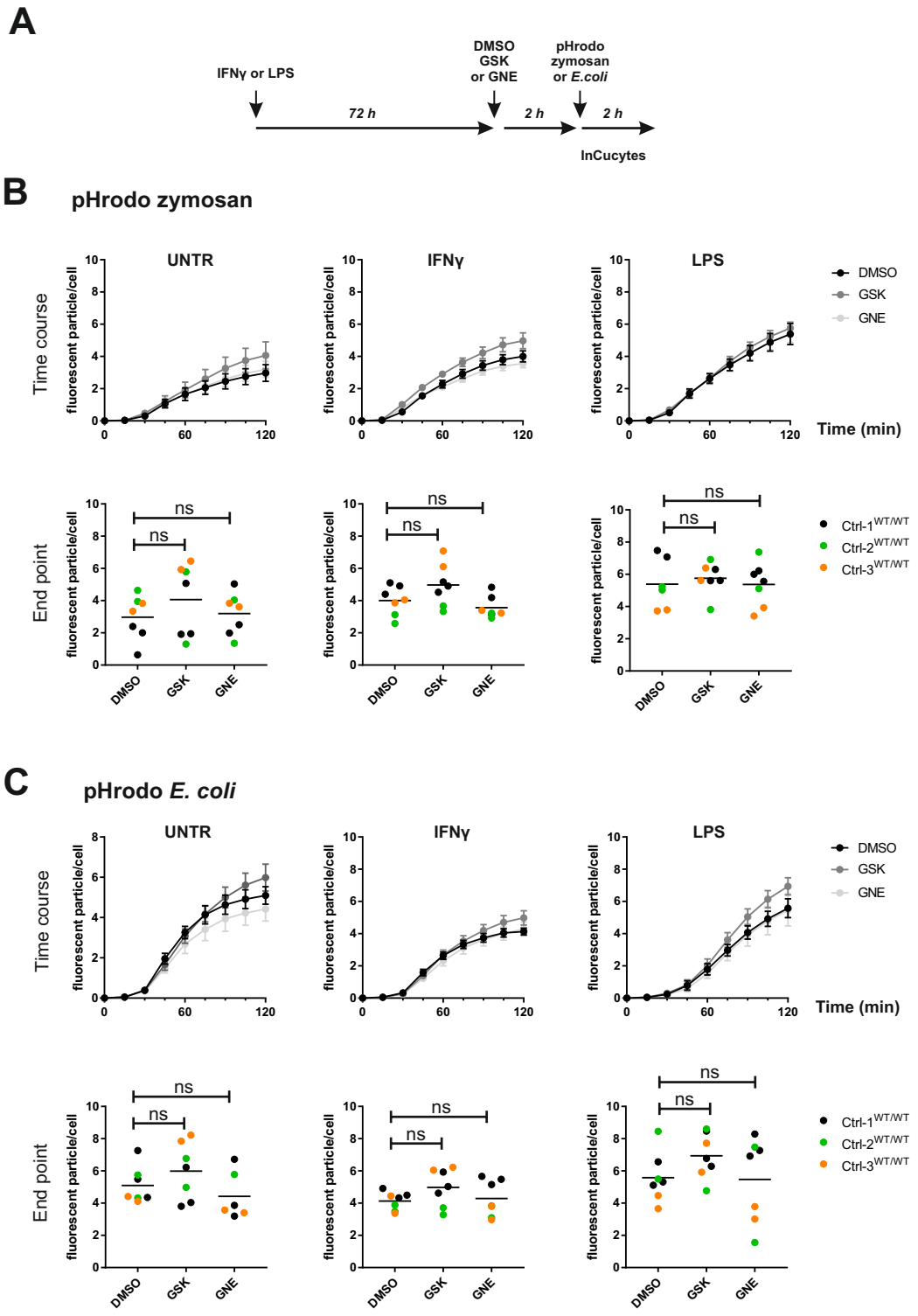

Figure 4.8 Application of LRRK2 kinase inhibitors does not affect the acidification of phagosomes in hiPSC-MΦs. (A) Outline of the experimental design. The number of acidified fluorescent zymosan **(B)** or *E. coli* **(C)** bioparticles was monitored for 2 h. Plot dot graphs represent quantification of end-point results in mean ± SEM from at least three independent experiments from three healthy control lines (Ctrl-1, -2, -3). Each dot represents data from each independent experiment. Two-way ANOVA with Dunnett multiple comparisons test against vehicle control (DMSO) was used for statistically analysis. ns denotes not significant

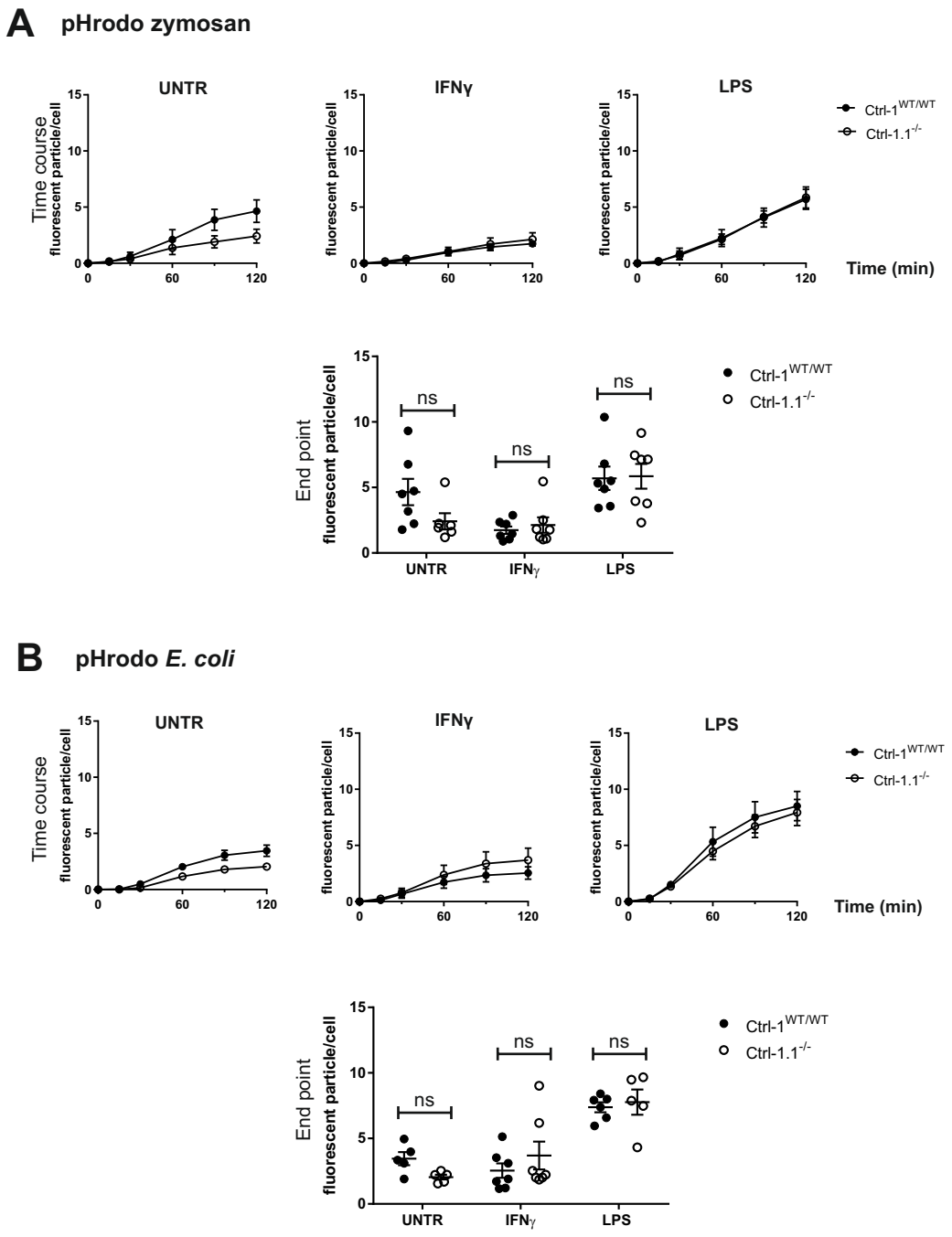

Figure 4.9 Complete absence of LRRK2 protein does not affect the acidification of phagosomes in hiPSC-MΦs. The number of acidified/fluorescent zymosan **(A)** or *E. coli* **(B)** bioparticles was monitored for 2 h in hiPSC-MΦs from LRRK2 KO (Ctril-1.1$^{-/-}$) and its parental control line (Ctrl-1$^{WT/WT}$). Plot-dot graphs represent quantification of end-point results in mean ± SEM from at least three independent experiments. Each dot represents data from each independent experiment. Two-way ANOVA with Dunnett multiple comparisons test was used for statistically analysis. ns denotes not significant.

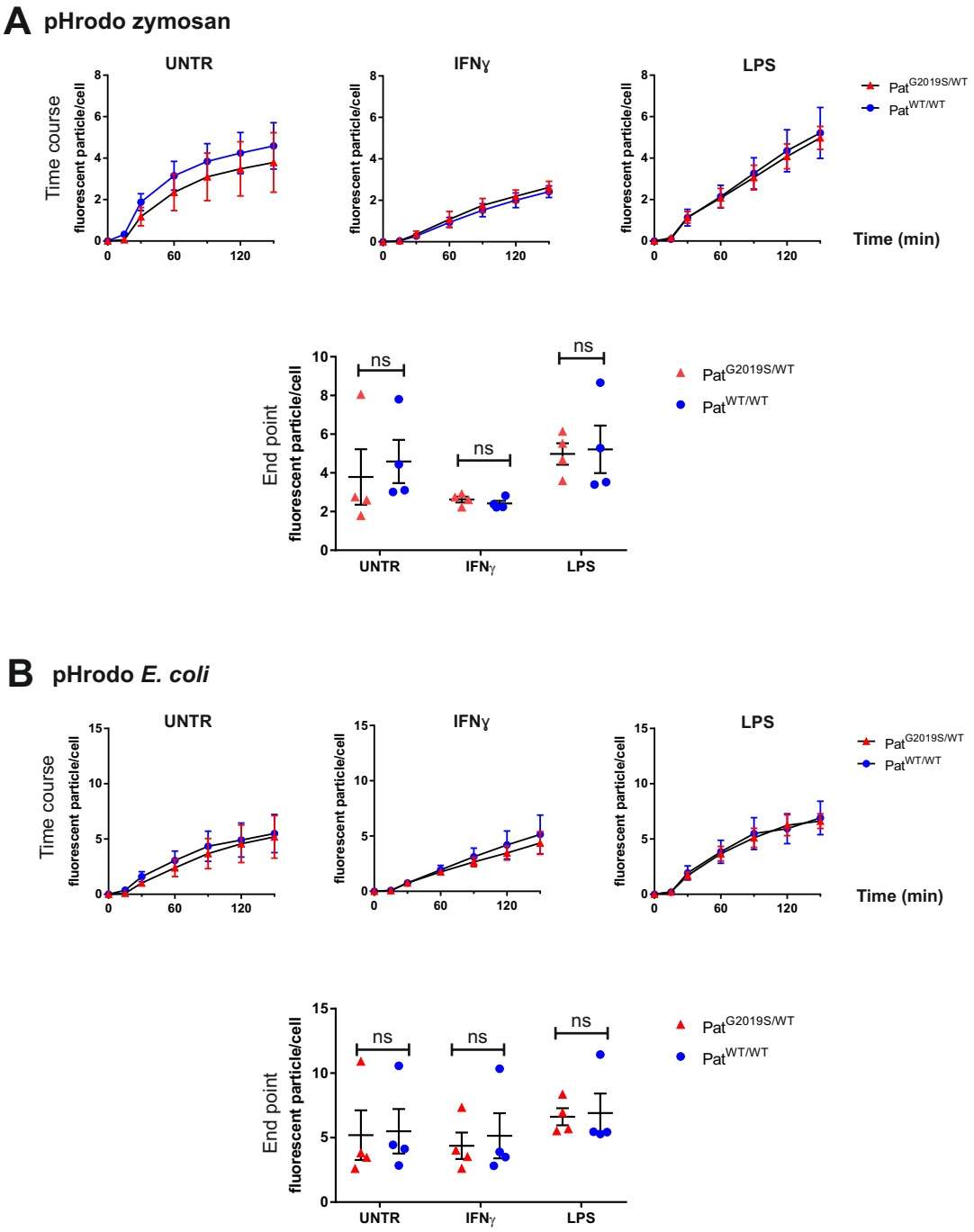

Figure 4.10 The presence of G2019S mutation does not affect the acidification of phagosomes in hiPSC-MΦs. The number of acidified fluorescent zymosan **(A)** or *E. coli* **(B)** bioparticles was monitored for 2 h in hiPSC- MΦs from LRRK2 G2019S patient line ($Pat^{G2019S/WT}$) and its CRISPR/Cas-9 edited isogenic control line ($Pat^{WT/WT}$). Plot-dot graphs represent quantification of end-point results in mean ± SEM from at least three independent experiments. Each dot represents data from each independent experiment. Two-way ANOVA with Dunnett multiple comparisons test was used for statistically analysis. ns denotes not significant.

4.2.4 Investigating the molecular interactors of LRRK2

So far, I have clearly shown that LRRK2 is recruited to the late phagosomes but it is functionally not involved in the acidification of phagosomes. Having ruled out these most obvious of roles, the question remains, what could be the role of LRRK2 at phagosomes?

Rab GTPases regulate various fission and fusion events during phagocytosis, and in LRRK2-overexpression system, LRRK2 associates physically with these proteins (Yun et al. 2015; Dodson et al. 2012; Gómez-Suaga et al. 2014; Steger et al. 2016; Waschbüsch et al. 2014). Recently, Rab8 and Rab10 have been identified as potential physiological substrates of LRRK2 in mouse fibroblasts (Steger et al. 2016). Knowing this, I stained hiPSC-MΦs undergoing phagocytosis with a panel of antibodies against Rab GTPases, Rab 4, 7, 8, and 10 (Figure 4.11). Unfortunately, LRRK2 did not show any co-localisation with these Rab GTPases although LRRK2 appears to be co-recruited with Rab8 (Figure 4.11) and Rab9 (Figure 4.3).

Next, I stained hiPSC-MΦs with markers of other cellular compartments involved in phagocytosis, notably ER (anti-calnexin) and peroxisomes (anti-catalase). ER plays an essential role during phagocytosis by providing necessary materials to phagosomes (e.g. intracellular membrane) (Desjardins 2003) while peroxisomes are important during phagosome maturation by sequestering and producing ROS, hydrogen peroxide (H_2O_2) and nitric oxide (NO) (Schrader and Fahimi 2006; Di Cara et al. 2017). Confocal images revealed that there was no colocalization of LRRK2 with any of these compartments (Figure 4.11).

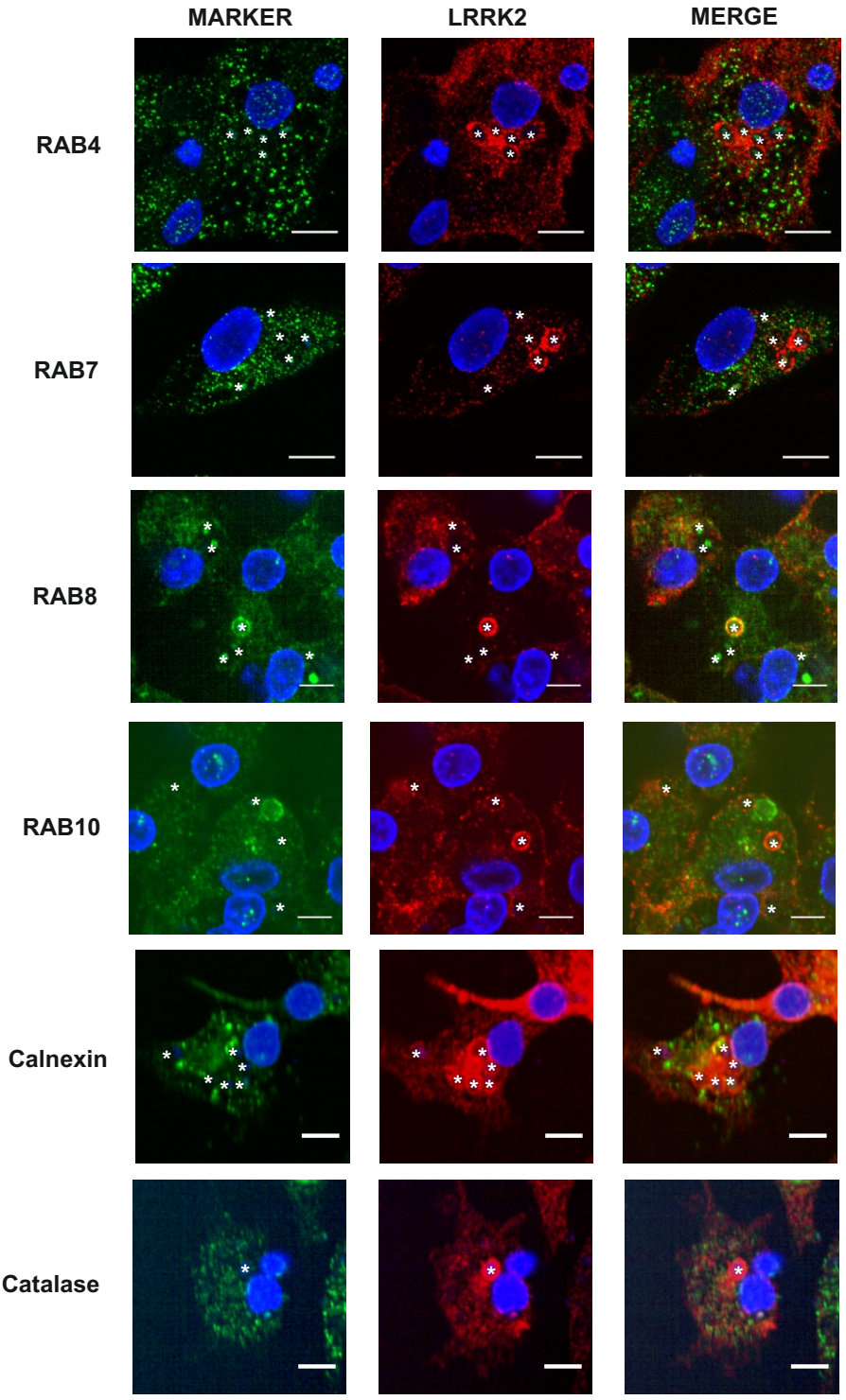

Figure 4.11 LRRK2 does not colocalise with Rab GTPases, ER, or peroxisomes. hiPSC- MΦs were fed with zymosan bioparticles for 120 min. Cells were fixed and stained with a panel of antibodies against Rab GTPases (Rab4, 7, 8, 10), calnexin (ER), and catalase (peroxisomes). All scale bar represents 10 µm. Internalised zymosan bioparticles are indicated in asterix.

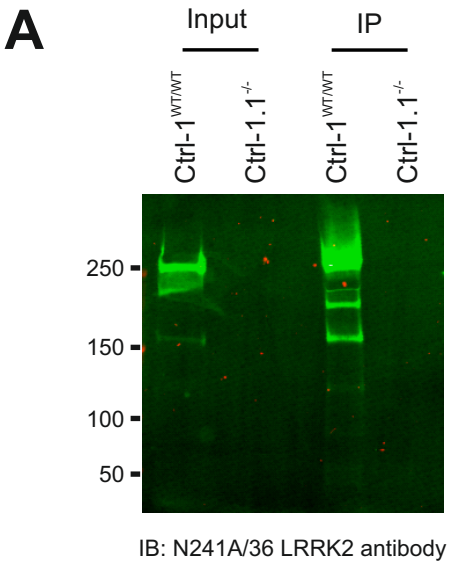

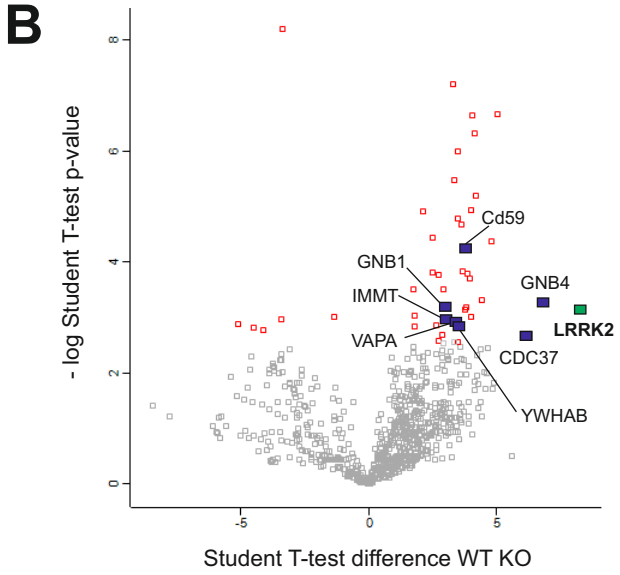

C

Protein names	Gene names	Student T-test difference WT KO	Peptide intensity						- log P-value
			KO 1	KO 2	KO 3	WT 1	WT 2	WT 3	
Leucine-rich repeat kinase 2	LRRK2	8.3	0.2	3.1	0.9	7.9	8.7	7.5	3.1
Guanine nucleotide-binding protein subunit beta-4	GNB4	6.8	-5.0	3.3	-5.0	2.8	2.1	0.5	3.3
Hsp90 co-chaperone Cdc37	CDC37	6.2	-5.0	2.7	-2.5	2.3	2.4	1.4	2.7
CD59 glycoprotein	CD59	3.8	-1.9	4.3	-2.4	1.9	1.7	1.5	4.3
14-3-3 protein beta/alpha	YWHAB	3.5	-3.2	2.9	-3.6	0.1	0.5	0.7	2.9
Mitochondrial inner membrane protein	IMMT	3.3	-2.4	2.9	-1.2	1.5	1.5	2.0	2.9
Vesicle-associated membrane protein-associated protein A	VAPA	3.0	-2.1	3.0	-2.4	0.6	0.1	0.7	3.0
Guanine nucleotide-binding protein subunit beta-1	GNB1	3.0	0.0	3.2	-0.2	3.4	2.7	3.1	3.2

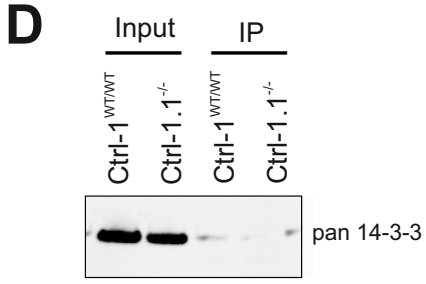

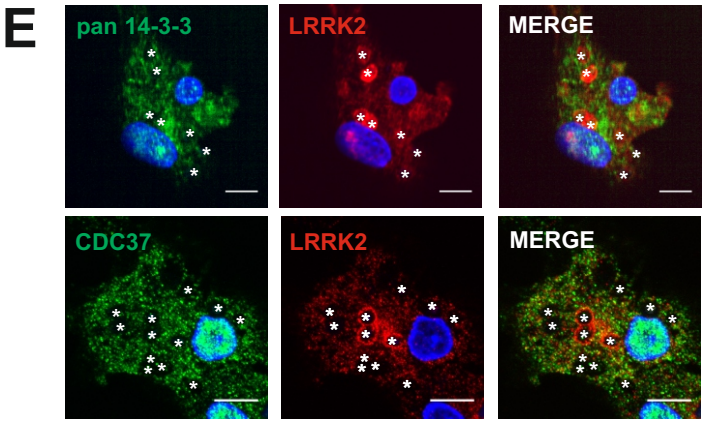

Figure 4.12 Interactome of LRRK2 in hiPSC-MΦs. (A) Endogenous LRRK2 protein was pulled down using antibody against LRRK2 (NeuroMAB, N241A/36). Ctrl1.1$^{-/-}$ MΦs were used to rule out any nonspecific proteins during IP. **(B-C)** Volcano plot and a table of potential interactors of LRRK2 identified by mass spectrometry. Candidates that display -log p value > 2.5 are labelled in red. And then candidates with peptide intensity value > 0 in WT samples and < 0 in KO samples were selected and labelled in blue and LRRK2 in green. The table shows the list of these candidates in the order of highest to lowest statistical value of the mean difference between WT and KO samples **(D)** Western blot was probed with the antibody against pan 14-3-3. **(E)** Immunostaining of hiPSC-MΦs with LRRK2 and 14-3-3, and CDC37. All scale bar represents 10 µm.

Lastly, to identify physiological interactors of LRRK2 in iPSC-MΦs, I used a proteomics approach. Endogenous LRRK2 protein, expressed at a physiological level was immunoprecipitated and *LRRK2* KO hiPSC-MΦs (Ctrl-1.1$^{-/-}$) was used as a negative control to exclude any non-specific proteins identified by mass spectrometry (Figure 4.12). Using this approach, I have identified numerous potential interactors of LRRK2. In the volcano plot, proteins with a -log P-value > 2.5 (student t-test; P<0.001) were first selected (indicated in red dots). These candidates represent proteins that have been reproducibly identified across three replicates. Most of these candidates, however, displayed peptide intensity level below 0. Therefore, only those that show the peptide intensity > 0 in WT samples and < 0 in KO samples were labelled and highlighted in blue (Figure 4.12B).

Mass spectrometry identified 14-3-3 protein, which has been repeatedly shown by other research groups to be an interactor of LRRK2 (Dzamko et al. 2010; Li et al. 2011; Nichols et al. 2010). However, although 14-3-3 protein was readily detectable in the input whole cell lysate by western blot analysis, it was barely detectable in the IP by Western blot, so failed validation of its interaction with LRRK2 in hiPSC-MΦs (Figure 4.12D). This is perhaps due to the amount of protein present in the final immunoprecipitated eluate being too low, making it difficult to judge whether my list of other interactors represent true interacting partners or random false positives.

Therefore, instead of validating these hits by western blot, I decided to stain hiPSC-MΦs undergoing phagocytosis to identify whether the listed candidates colocalised with LRRK2. From the list, hsp90 co-chaperone cdc37 (CDC37) was chosen because it displayed third highest difference between WT and KO samples after LRRK2 and GNB4 (Figure 4.12C) and it has been reported to interact with LRRK2 in HEK 293T cell overexpressing LRRK2 (Wang et al. 2008). However, immunostaining of hiPSC-MΦs

with either 14-3-3 or CDC37 showed no convincing co-localisation with LRRK2 (Figure 4.12E).

4.3 Summary and discussion

Results from this chapter provide new insight to LRRK2 involvement in phagocytosis. Using human MΦs differentiated from hiPSCs, I have shown that LRRK2 is recruited to the phagosomes during the late stages of phagocytosis, and that LRRK2 kinase inhibitors promote the formation of LRRK2 super-coated phagosomes. However, LRRK2 is not functionally involved in the initial internalisation of bioparticles or the acidification process during phagocytosis.

Knocking down LRRK2 protein expression using siRNA has been variously reported to reduce phagocytic uptake of latex beads in Tat-protein activated BV-2 cells (Marker et al. 2012), and, conversely, to have no effect on the uptake of FITC-conjugated beads in both LPS activated RAW264.7 and BV-2 cells (Schapansky et al. 2014). Similarly, Maekawa et al., reported no difference in the uptake of fluorescent latex beads in primary mouse *LRRK2* KO microglia compared to WT (Maekawa et al. 2016). By using human MΦs, my results are consistent with the findings that LRRK2 has no role in the initial stage of phagocytosis by showing that CRISPR/Cas-9 KO of *LRRK2* has no significant effect on the uptake of fluorescent zymosan bioparticles in LPS or IFNγ activated hiPSC-MΦs (Figure 4.6). *LRRK2* G2019S PD patient-derived hiPSC-MΦs ($Pat^{G2019S/WT}$) did not show any significant difference compared to CRISPR/Cas-9 edited isogenic control hiPSC-hiPSC-MΦs ($Pat^{WT/WT}$) (Figure 4.7). This is consistent with mice data, which showed that thioglycollate-elicited peritoneal MΦs (TEPMs) from *LRRK2* G2019S transgenic mice had no significant difference in the uptake of fluorescent zymosan bioparticles compared

to its WT (Moehle et al. 2015). Together, the results presented here suggest that LRRK2 is dispensable during the initial stage of phagocytosis.

Extending the observation made by Gardet et al., who reported the recruitment of LRRK2 to *S. typhimurium* containing phagosomes in murine MΦ-like RAW 264.7 cells (Gardet et al. 2010), I demonstrated that in hiPSC-MΦs, recruitment of LRRK2 to the phagolysosomes was observed in zymosan, *E. coli*, *S.typhimurium*, and IgG-opsonized zymosan and *E.coli* bioparticles but not in latex beads or αsyn fibrils (Figure 4.2). Zymosan bioparticles activate TLR2 and dectin-1 receptors, *E. coli* bioparticles activate TLR4, *S.typhimurium* activate TLR2 and TLR4, IgG-opsonized bioparticles activate FcRs. Latex beads used in this study was not conjugated with any specific antigens, therefore, are taken up by multiple scavenger receptors. It has been shown that oligomeric αsyn stimulates signalling through TLR1/2 while a high amount of monomeric αsyn stimulates TLR4 (Kim et al. 2013; Fellner et al. 2013; Stefanova et al. 2011). However, exactly which receptors αsyn fibrils activate is currently unclear. Recruitment of LRRK2 does not appear to be target size dependent because both IgG-opsonized *E.coli* bioparticles (0.5 – 1 μm) and zymosan (~3 μm) containing phagosomes displayed LRRK2 positivity (Figure 4.2A). Similarly, LRRK2 protein was not observed on the phagosomes containing latex beads (2.5 μm) with similar size as zymosan (Figure 4.2B). In this study, therefore, all TLRs and FcR-activating phagocytic substrates led to recruitment of LRRK2 to the late phagosomes.

Therefore, the absence of LRRK2 recruitment to αsyn is perplexing. One of the limitations of my immunostaining approach is that I only captured phagocytosis events at 2 h. It is possible that phagocytosis of αsyn fibrils has different kinetics compared to other TLR or FcR mediated phagocytosis. Maekawa et al., recently has shown that *LRRK2* KO mouse primary microglia had a significant defect in phagocytosis of

recombinant αsyn peptides, suggesting a relationship between LRRK2 and αsyn clearance (Maekawa et al. 2016). In their study, they allowed phagocytosis to occur for 24 – 48 h. Future experiments, therefore, could investigate different time points to critically assess whether LRRK2 is recruited to αsyn fibril containing phagosomes at later timepoints.

My results demonstrate that LRRK2 is recruited during the late stages of phagocytosis (Figure 4.3). LRRK2 is present on Rab9 and LAMP-1(+) phagosomes but not on Rab7(+) phagosomes. While Figure 4.11 also shows Rab8 co-existence with LRRK2 this should be confirmed with more experimental replicates. It is also interesting that LRRK2 does not co-exist with a classical late phagosome marker, Rab7 (Figure 4.11). Rab9 facilitates the recycling of mannose 6-phosphate receptors (M6PRs) between the phagosomes and the TGN. M6PRs are important in delivery newly synthesized lysosomal enzymes from the TGN to phagosomes (Riederer et al. 1994). LAMP-1 and LAMP-2 are transmembrane proteins, found abundantly on lysosomal components (Eskelinen, Tanaka, and Saftig 2003). LAMPs recruitment to phagosomes occurs prior to Rab7 recruitment which is required for the formation of phagolysosomes (K. Huynh et al. 2007). Therefore, it is conceivable that LRRK2 is recruited prior to the recruitment of Rab7.

LRRK2 kinase inhibitors increased the number of LRRK2 super-coated phagosomes by two to fourfold (Figure 4.4). The number of total LRRK2(+) phagosomes did not change, suggesting that recruitment of LRRK2 to the phagosomes is not altered by LRRK2 kinase inhibitors but the dissociation from phagosome process may be affected, leading to the accumulation of LRRK2 protein on the phagosomes. This means that under normal condition, presence of LRRK2 on the phagosomes is transient and LRRK2 must escape from phagosomes. Despite the presence of super-coated LRRK2 phagosomes, no profound defect in the overall phagocytosis, particularly acidification of phagosomes, was

observed (Figure 4.8). Therefore, it can be speculated that recruitment of LRRK2 is not a necessity for the acidification process but may serve in different role.

Lastly, in this chapter, I attempted to identify physiological interactors of LRRK2 in hiPSC-MΦs. Although mass spectrometry analysis identified several potential candidates, notably the supposedly LRRK2 interacting 14-3-3 protein and CDC37, none of these could be validated using either western blot analysis or immunostaining (Figure 4.12). Additionally, mass spectrometry did not identify any Rab GTPases. This could be due to the sub-optimal buffer conditions used for IP. For example, Rab GTPases quickly lose interaction with their interactors upon hydrolysis of GTP. To prevent this, future experiments can add GTPγS, a non-hydrolysable analog of GTP, in the IP buffer to prevent the formation of GDP-bound Rab GTPases. This way, if LRRK2 were to interact with a Rab GTPase, IP can pull down its interactors more efficiently. In this chapter, I used a commercially available antibody to pull down LRRK2, which required a minimum of 16 h incubation at 4ºC to pull down a substantial amount of LRRK2. It is not surprising that during this long incubation most of interactors would have been lost, making it difficult to validate the potential candidates via western blot analysis. One possible way of overcoming this problem is to generate a reporter-tagged endogenous LRRK2 (such as mCherry). This way, incubation time could be shortened to 1 – 2 h, allowing capture of more transient interactors of LRRK2.

5

LRRK2 in hiPSC-derived microglia and cortical neuron co-culture

5.1 Introduction

5.1.1 hiPSC-microglia and cortical neuron co-culture

Tissue-resident MΦs acquire tissue-specific properties according to the niche in which they differentiate. They display tissue-specific gene expression profiles and distinct developmental origins. Lineage-tracing studies in mice have uncovered that before birth, *MYB*-independent, yolk-sac MΦs migrate to the brain before the closure of the BBB and these MΦs mature together with neurons to fully functional microglia. Because of the establishment of the BBB, yolk-sac MΦs are the sole source of microglia. Fetal liver MΦs are responsible for generating MΦs in liver (Kupffer cells), lung (alveolar MΦs) and heart (cardiac MΦs). At birth and throughout the adulthood, bone-marrow derived MΦs constantly replace tissue-resident MΦs in the gut and dermis (Bain et al. 2013; Sieweke and Allen 2013; Gentek, Molawi, and Sieweke 2014; Ginhoux and Guilliams 2016).(Russo, Bubacco, and Greggio 2012)(Russo, Bubacco, and Greggio 2012)

Using this tissue-specific development of MΦs, Dr. Haenseler in our lab has developed a protocol to differentiate human microglia. This protocol mimics microglia ontogenesis by co-culturing *MYB*-independent MΦ precursors (Buchrieser, James, and Moore 2017) (recapitulating primitive, yolk-sac-derived MΦs), with hiPSC-derived cortical neurons

(recapitulating microglia differentiation in the neuronal environment) (Haenseler et al. 2017b) (Figure 5.1).

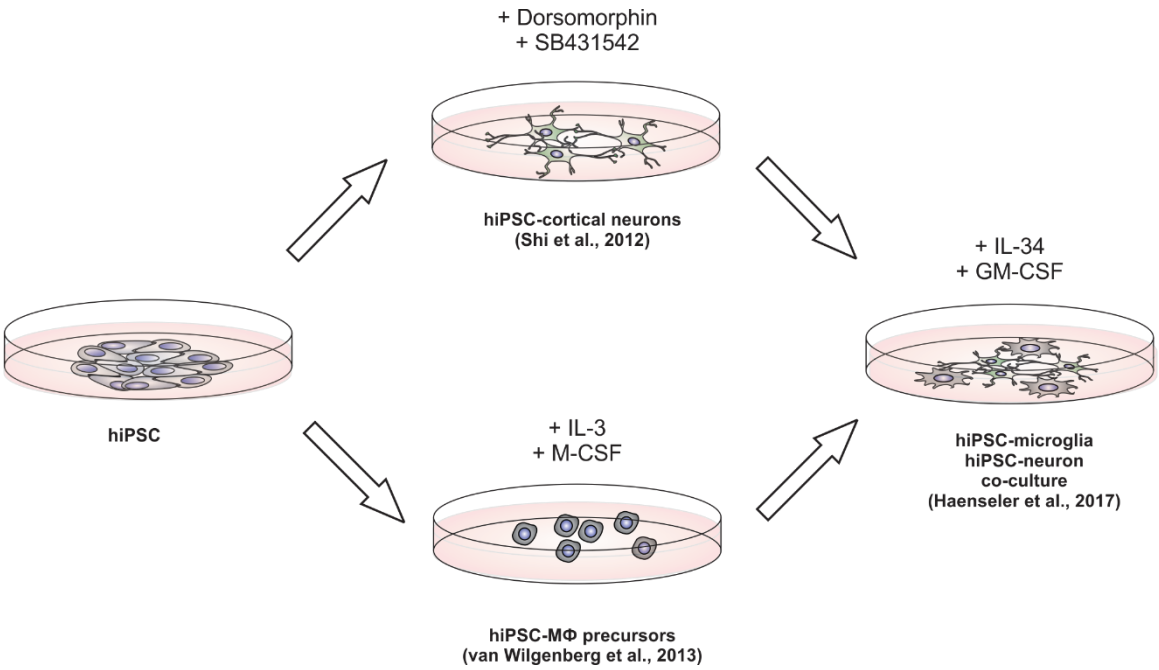

Figure 5.1 Differentiation of hiPSC-microglia. hiPSC cultures were differentiated into cortical neurons via dual SMAD inhibition using the protocol established by Shi et al. (Shi, Kirwan, and Livesey 2012). Differentiation of MΦ precursors in IL-3 and MCSF was carried out according to the protocol established by van Wilgenberg et al. (van Wilgenburg et al. 2013). Microglia differentiation was carried out according to the protocol established by Haenseler et al. (Haenseler et al. 2017b). hiPSC-cortical neurons were cultured for two weeks before the addition of MΦ precursors. MΦ precursors in co-culture with cortical neurons were differentiated to microglia in the media containing GM-CSF and IL-34 for two weeks.

5.1.2 LRRK2 in the regulation of cytokine release

Microglia play a crucial role in the initiation and resolution of neuro-inflammation by producing cytokines and chemokines. Microglia isolated from *LRRK2* R1441G mutant mice release higher levels of TNFα upon LPS stimulation. Conversely, KD of LRRK2 protein or pharmacological inhibition of LRRK2 kinase activity reduces LPS-induced

expression of TNFα, IL-6, and IL-1β in mouse primary microglia and BV-2 cells (Moehle et al. 2012; Kim et al. 2012; Russo et al. 2015).

However, results from MΦs contradict the observations seen in microglia. BMDMs isolated from *LRRK2* R1441G or G2019S mutant mice show no significant difference in TNFα or IL-6 secretion upon LPS stimulation compared to *LRRK2* WT BMDMs (Moehle et al. 2015; Hakimi et al. 2011). BMDMs from *LRRK2* KO mice show no change in LPS-driven release of cytokines, notably TNFα, IL-6, IL-1β, IL-10, IL-12, and IL-1α (Dzamko and Halliday 2012; Hakimi et al. 2011; Wandu et al. 2015; Yan and Liu 2017). Yet, other groups have reported LRRK2-dependent effects using stimulation other than by LPS. Liu et al., have shown that *LRRK2* KO mouse BMDMs produced significantly higher levels of IL-2 and IL-6 upon TLR2/Dectin-1 stimulation by zymosan but not upon TLR2 stimulation by Pam_3CSK_4 (Liu et al. 2011). Yan et al., stimulated *LRRK2* KO mouse BMDMs with a Nod2 activator, muramyl dipeptide (MDP), in the presence of low amount of LPS (10 ng/mL), and observed a significant reduction in the levels of TNFα, IL-6, and IL-1β release (Yan and Liu 2017). These observations suggest that LRRK2 function may be different in microglia and MΦs. However, the literature is missing studies which directly compare LRRK2 function in microglia and MΦs using the same experimental conditions. A recent study has reported high levels of inflammatory cytokines, notably IL-1β, TNFα, IL-6 and IL-12, in the sera of both asymptomatic *LRRK2* G2019S carriers and *LRRK2* G2019S PD patients (Dzamko, Rowe, and Halliday 2016). This suggests a link between pathological LRRK2 protein and elevated pro-inflammatory cytokines in humans, therefore, more rigorous experiments are merited to fully understand the involvement of LRRK2 mutations in this process.

5.1.3 Aim

Using hiPSC-microglia and cortical neuron co-culture, the aims for this chapter are to dissect the role of LRRK2 in hiPSC-microglia function, particularly assessing its ability to produce cytokines and chemokines. Furthermore, by directly comparing microglia and MΦs differentiated from the same MΦ precursor sources, the co-culture model offers a powerful experimental tool to test my hypothesis that LRRK2 has a differential role in MΦs and microglia.

5.2 Results

5.2.1 LRRK2 is expressed in hiPSC-microglia but not detectable in hiPSC-cortical neurons

To confirm LRRK2 protein expression in human microglia, hiPSC-microglia (Ctrl-$1^{WT/WT}$) co-cultured with hiPSC-cortical neurons (Ctrl-$1^{WT/WT}$) were fixed and stained with antibody against LRRK2, a microglia-specific marker (Ionized calcium Binding Adaptor molecule 1; IBA1), and a neuron-specific marker (Microtubule-Associated Protein 2; MAP2). LRRK2 protein was clearly expressed in hiPSC-microglia, while its expression level was not detectable in hiPSC-cortical neurons (Figure 5.2A). The specificity of LRRK2 staining in microglia but not neurons was confirmed by co-culturing microglia differentiated from *LRRK2* KO hiPSC (Ctrl-$1.1^{-/-}$) with cortical neurons differentiated from *LRRK2* WT hiPSCs (Ctrl-$1^{WT/WT}$) (Figure 5.2B).

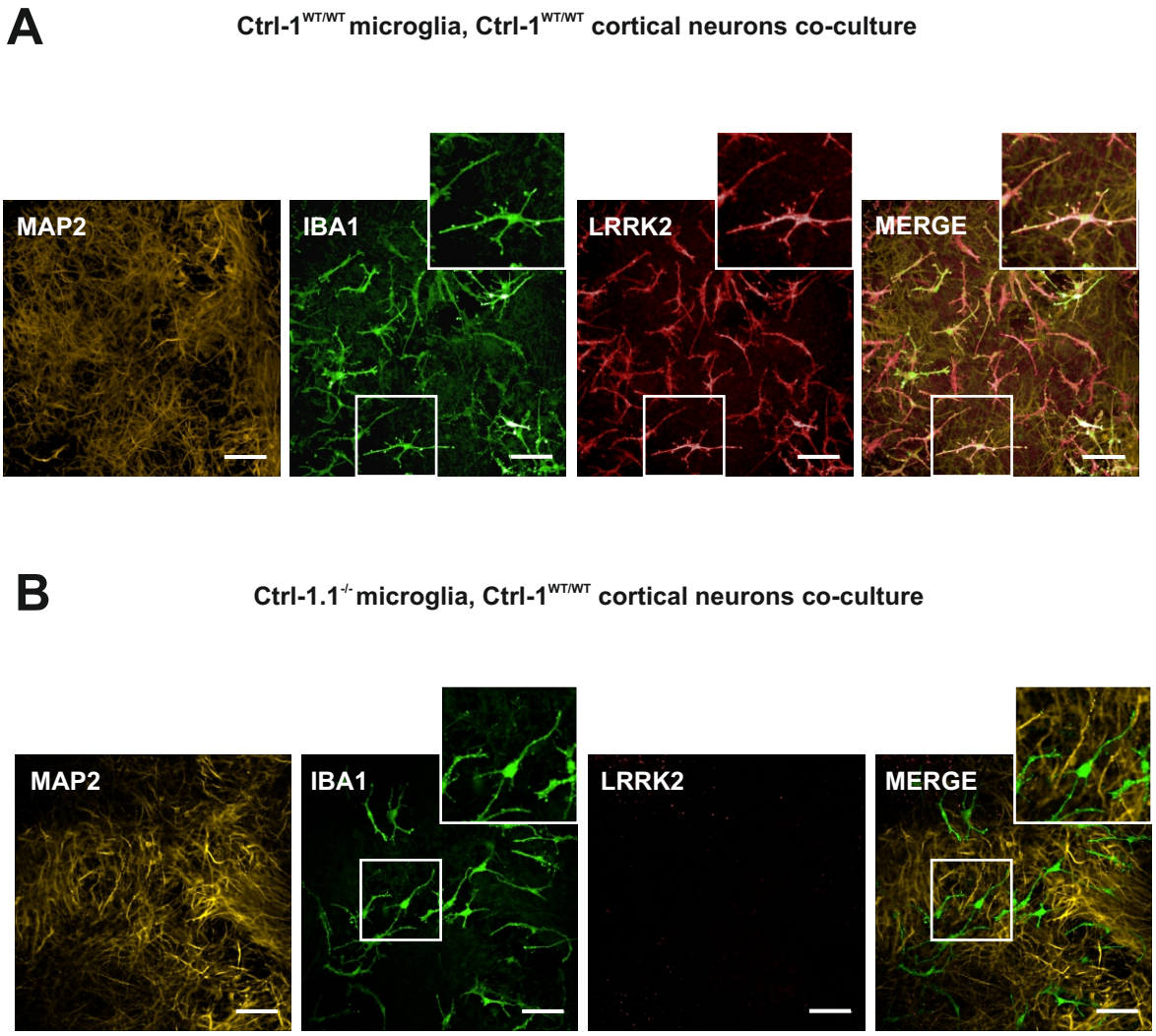

Figure 5.2 LRRK2 protein is expressed in hiPSC-microglia but not in hiPSC-cortical neurons. (A) Microglia differentiated from *LRRK2* WT hiPSC line (Ctrl-$1^{WT/WT}$) were co-cultured with hiPSC-cortical neurons from the same hiPSC line (Ctrl-$1^{WT/WT}$). After two weeks of differentiation, cells were treated with IFNγ (100 ng/mL) for 48 h to enhance LRRK2 protein expression to detectable level. Cells were fixed and stained with antibodies against a neuronal marker (MAP2), a microglia marker (IBA1), and LRRK2 (N241A/36). **(B)** Microglia differentiated from *LRRK2* KO hiPSC line (Ctrl-$1.1^{-/-}$) were co-cultured with cortical neurons differentiated from its parental hiPSC line (Ctrl-$1^{WT/WT}$). All scale bars represent 100 µm.

5.2.2 IFNγ upregulates LRRK2 protein expression in hiPSC-microglia

In chapter 3, I have shown that IFNγ significantly upregulates LRRK2 protein expression in hiPSC-MΦs. To test whether hiPSC-microglia have a similar response to IFNγ, hiPSC-microglia were treated with IFNγ for 16 h, 48 h, or 72 h. Z-stacked confocal images were acquired randomly using an Opera Phenix High-Content Screening system (PerkinElmer). The number of hiPSC-microglia showing LRRK2 protein signal was quantified by Columbus data storage and analysis system (PerkinElmer). IFNγ treatment significantly upregulated the percent of LRRK2 expressing hiPSC-microglia and its expression level plateaued by 48 h post IFNγ treatment (Figure 5.3).

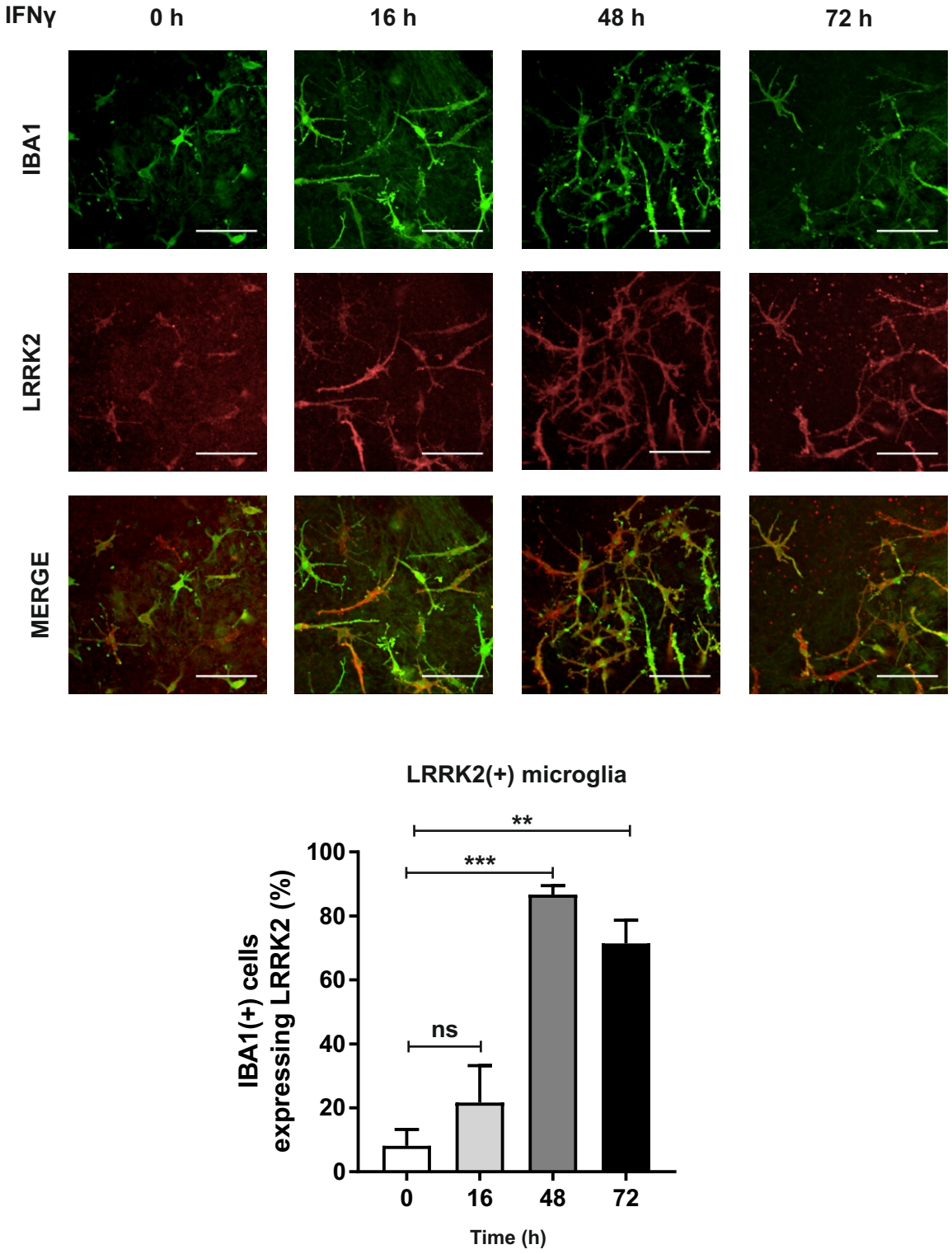

Figure 5.3 IFNγ upregulates LRRK2 protein expression in hiPSC-microglia. hiPSC-microglia, cortical neuron co-culture was treated with IFNγ (100 ng/ml) for 16 h, 48 h, or 72 h. The number of hiPSC-microglia (IBA1-positive cells) expressing LRRK2 signal was quantified using Columbus data storage and analysis system (PerkmanElmer). The bar graph shows the percent of LRRK2 expressing hiPSC-microglia in mean ± SEM of at least three independent experiments. Statistical significance was tested using one-way ANOVA against UNTR control. *$P < 0.05$, **$P < 0.01$, ***$P < 0.001$, ns denotes not significant.

5.2.3 TNFα release by hiPSC-microglia with *LRRK2* G2019S mutation

I next investigated whether LRRK2 has any role in pro-inflammatory cytokine release, and whether it has a distinct role in hiPSC-MΦs and in hiPSC-microglia. MΦ precursors from Ctrl-$1^{WT/WT}$, Ctrl-$1.1^{-/-}$, $Pat^{G2019S/WT}$, and $Pat^{WT/WT}$ hiPSC lines were co-cultured with cortical neurons differentiated from Ctrl-$1^{WT/WT}$ hiPSC line (referred as co-hiPSC-microglia) (Figure 5.4A). To control for any variability triggered by the presence of GM-CSF in the microglia differentiation media, MΦ precursors were also cultured in microglia differentiation media in the absence of hiPSC-cortical neurons (referred as hiPSC-microglia-like). Lastly, MΦ precursors were differentiated into hiPSC-MΦ to directly compare the role of LRRK2 in microglia and MΦs. Cells were either primed with IFNγ (100 ng/mL) for 72 h or kept in their own media before LPS (100 ng/mL) stimulation. Supernatants were collected and the levels of TNFα were quantified by TNFα ELISA (Figure 5.4B). The contribution of neurons to the level of TNFα in the supernatants collected from co-culture is minimal and this has been already assessed robustly by Dr. Haenseler (Haenseler et al. 2017a).

Upon stimulation, hiPSC-MΦs released around 100-fold more TNFα compared to hiPSC-microglia-like or co-hiPSC-microglia (Figure 5.4C). hiPSC-MΦs, hiPSC-microglia-like and co-hiPSC-microglia all showed no significant difference in the level of TNFα among four hiPSC lines (Ctrl-$1^{WT/WT}$, Ctrl-$1.1^{-/-}$, $Pat^{G2019S/WT}$, and $Pat^{WT/WT}$), under basal conditions or with LPS stimulation.

When cells were primed with IFNγ before LPS stimulation, Ctrl-$1.1^{-/-}$ hiPSC-MΦs released significantly higher level of TNFα compared to Ctrl-$1^{WT/WT}$ hiPSC-MΦs. The presence of G2019S mutation, however, did not cause any significant changes in hiPSC-MΦs. In hiPSC-microglia-like cells, the difference was more pronouncedly detected between the two hiPSC lines of same genomic background. G2019S patient hiPSC lines

(Pat$^{G2019S/WT}$ and Pat$^{WT/WT}$) showed significantly higher level of TNFα compared to healthy control hiPSC lines (Ctrl-1$^{WT/WT}$ and Ctrl-1.1$^{-/-}$). However, neither the presence of G2019S mutation nor the complete absence of LRRK2 protein had any effect on TNFα release in hiPSC-microglia-like cells. In co-hiPSC-microglia, while the absence of LRRK2 protein did not show any significant difference compared to its parental hiPSC-microglia, *LRRK2* G2019S mutation (Pat$^{G2019S/WT}$) significantly enhanced the release of TNFα compared to its isogenic control (Pat$^{WT/WT}$) (Figure 5.4C).

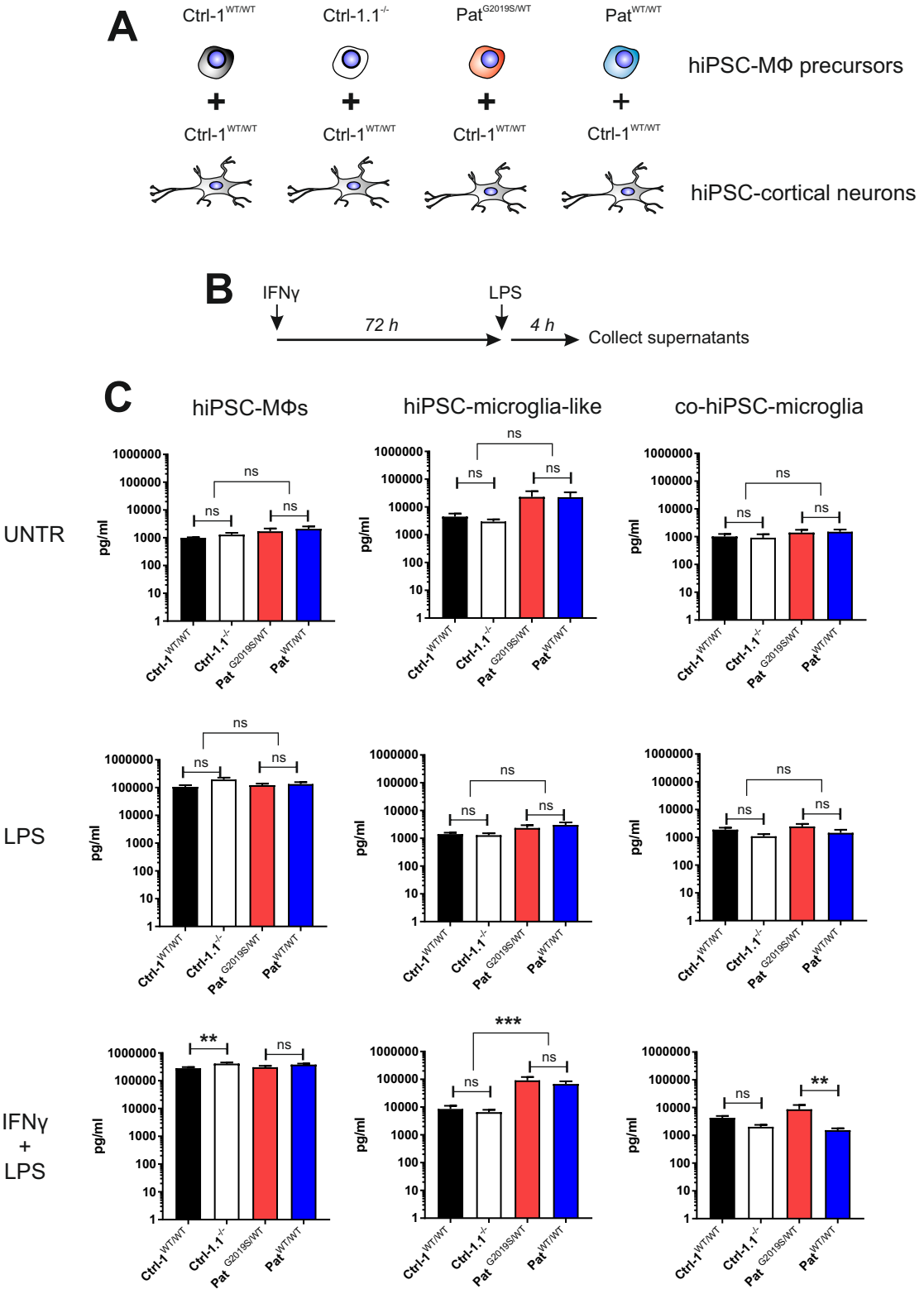

Figure 5.4 *LRRK2* G2019S mutation in co-hiPSC-microglia enhances TNFα release upon IFNγ priming and LPS stimulation. (A) MΦs precursors differentiated from four hiPSC lines (Ctrl-$1^{WT/WT}$, Ctrl-$1.1^{-/-}$, $Pat^{G2019S/WT}$, and $Pat^{WT/WT}$) were co-cultured with cortical neurons differentiated from Ctrl-$1^{WT/WT}$ hiPSC line. **(B)** Cells were primed with IFNγ (100 ng/ml) for 72h prior to LPS (100 ng/ml) stimulation for 4 h **(C)** Bar graphs show TNFα (pg/ml) level in mean ± SEM of three independent experiments. Statistical significance was tested using Two-way ANOVA with Tukey multiple comparison test. $*P < 0.05$, $**P < 0.01$, $***P < 0.001$, ns denotes not significant.

5.2.4 Multiplex cytokine and chemokine profiling in hiPSC-MΦs and hiPSC-microglia

To explore the role of LRRK2 in cytokine/chemokine release, the same supernatants used for TNFα ELISA were analysed using Luminex multiplex array. Five cytokines gave readings below detection limit (IFNα, IL-15, IL-13, IL-31, and TNFβ) and were not considered further for the statistical analysis. Out of 29 remaining cytokines, statistical differences among four *LRRK2* genotypes were detected in the following six cytokines or chemokines; IL1-ra, IL-6, CXCL10 (IP-10), CCL2 (MCP-1), CCL4 (MIP-1β). Interestingly, Luminex multiplex array did not detect any significant difference in the level of TNFα. However, TNFα was included in the final graph so that reference can be made with results acquired by TNFα ELISA.

When no stimulation was given, Pat hiPSC-MΦs ($Pat^{G2019S/WT}$, $Pat^{WT/WT}$) released significantly less IL1-ra than Ctrl hiPSC-MΦs ($Ctrl\text{-}1^{WT/WT}$, $Ctrl\text{-}1.1^{-/-}$). Conversely, Pat hiPSC-MΦs produced significantly less CXCL10 than Ctrl hiPSC-MΦs. However, neither KO of *LRRK2* nor the presence of G2019S mutation contributed to the change in IL1-ra and CXCL10 levels (Figure 5.5B). In hiPSC-microglia-like cells, *LRRK2* G2019S mutation significantly increased IL1-ra but KO of *LRRK2* had no effect (Figure 5.5C). In co-hiPSC-microglia, Pat hiPSC lines significantly increased IL1-ra and IL-6 compared to Ctrl hiPSC lines. *LRRK2* KO significantly lowered CCL2 and CCL4 while *LRRK2* G2019S mutation had no effect (Figure 5.5D).

When LPS stimulation was given for 4 h, *LRRK2* KO hiPSC-MΦs released significantly less CCL4 while the presence of *LRRK2* G2019S mutation had no significant effect (Figure 5.6B). In hiPSC-microglia-like cells, *LRRK2* G2019S mutation significantly increased IL1-ra, while *LRRK2* KO significantly decreased IL1-ra. and CXCL10 (Figure

5.6C). In co-hiPSC-microglia, *LRRK2* KO significantly decreased IL1-ra while *LRRK2* G2019S significantly increased IL1-ra compared to its isogenic pair (Figure 5.6D).

When cells were primed with IFNγ before LPS stimulation, *LRRK2* KO hiPSC-MΦs and *LRRK2* G2019S hiPSC-MΦs released significantly more CCL4 compared to their isogenic pairs (Figure 5.7B). *LRRK2* KO significantly decreased CXCL10 in both hiPSC-microglia-like cells and co-hiPSC-microglia. LRRK2 G2019S mutation had no effect on CXCL10 level. (Figure 5.7 C-D). Results of multiplex cytokine and chemokine profiling are summarised in (Table 5.1).

	Figure 5	Figure 6	Figure 7
	No stimulation	LPS	IFNγ + LPS
hiPSC-MΦs		**CCL4**: KO, ↓ G2019s, ns	**CCL4**: KO, ↑ G2019s, ↑
hiPSC-microglia-like		**IL1-ra**: KO, ↓ G2019s, ↑	**CXCL10**: KO, ↓ G2019s, ns
hiPSC-microglia	**CCL2**: KO, ↓ G2019s, ns **CCL4**: KO, ↓ G2019s, ns	**IL1-ra**: KO, ↓ G2019s, ↑	**CXCL10**: KO, ↓ G2019s, ns

Table 1. Summary of the results from multiplex cytokine and chemokine profiling. Only cytokine or chemokine that displayed significant difference by the effect of LRRK2 KO or the G2019S mutation are shown. Ns, not significant.

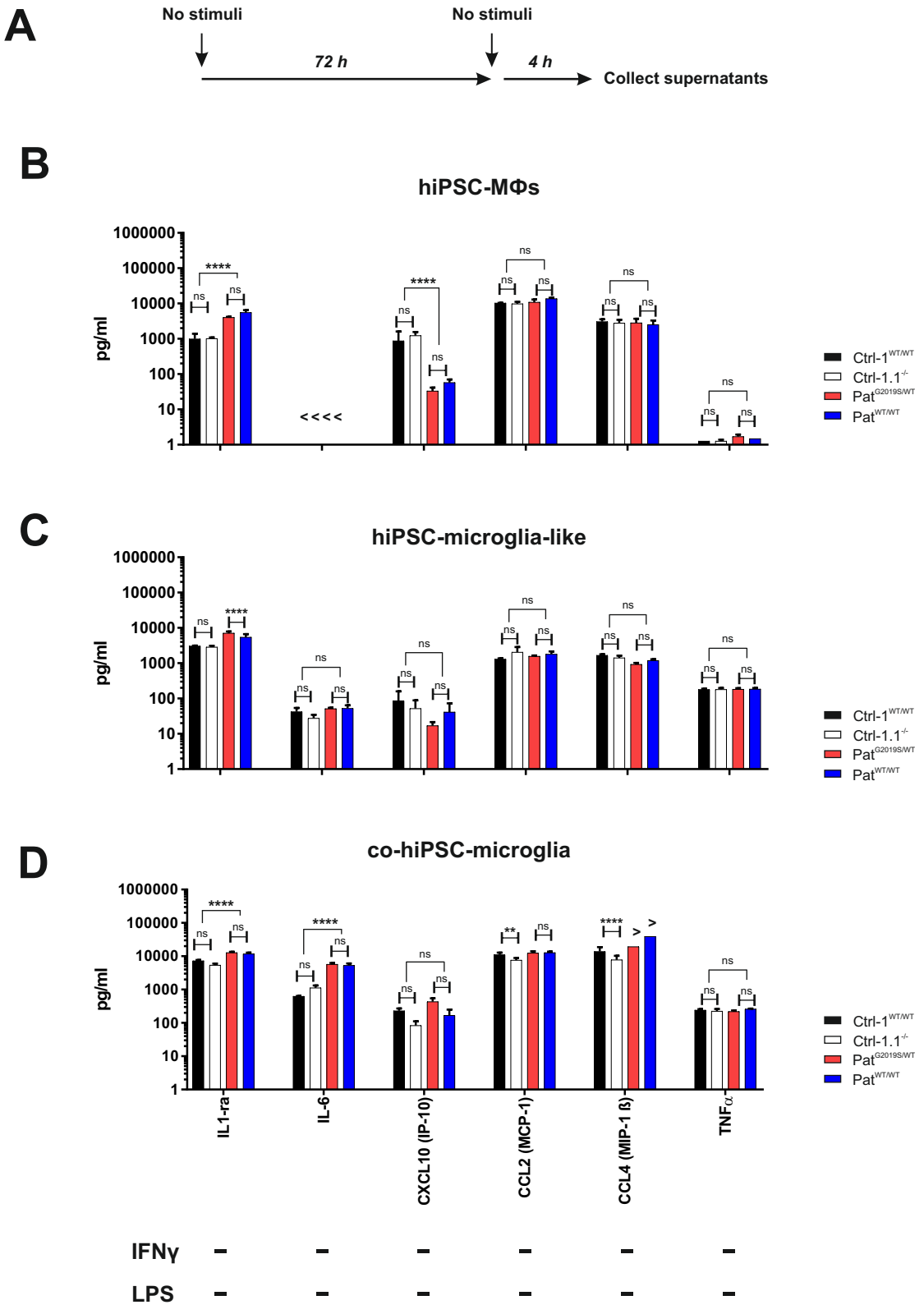

Figure 5.5 *LRRK2* KO co-hiPSC-microglia display low levels of CCL2 and CCL4. **(A)** Experimental design. Bar graphs show cytokine/chemokine level (pg/ml) in **(B)** hiPSC-MΦs, **(C)** hiPSC-microglia-like cells and **(D)** co-hiPSC-microglia. Data represent mean ± SEM of three independent experiments. Statistical significance was tested using Two-way ANOVA with Tukey multiple comparison test. $*P < 0.05$, $**P < 0.01$, $***P < 0.001$, ns denotes not significant, <, reading below detection range, >, reading above detection range.

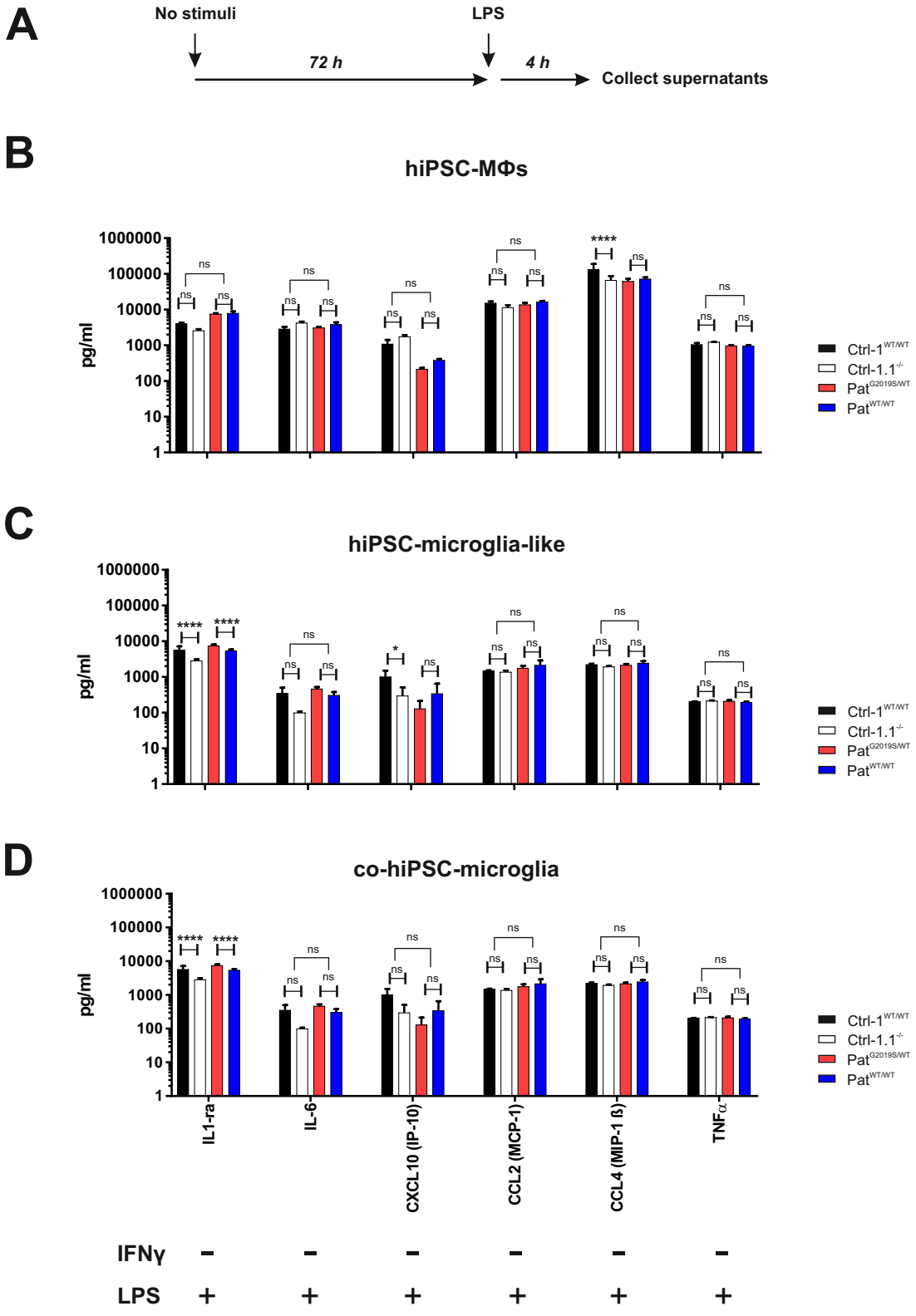

Figure 5.6 LPS stimulation decreases the level of CCL4 in *LRRK2* KO hiPSC-MΦs **(A)** Experimental design. Bar graphs show cytokine/chemokine level (pg/ml) in **(B)** hiPSC-MΦs, **(C)** hiPSC-microglia-ike cells and **(D)** co-hiPSC-microglia. Data represent mean ± SEM of three independent experiments. Statistical significance was tested using Two-way ANOVA with Tukey multiple comparison test. $*P < 0.05$, $**P < 0.01$, $***P < 0.001$, ns denotes not significant.

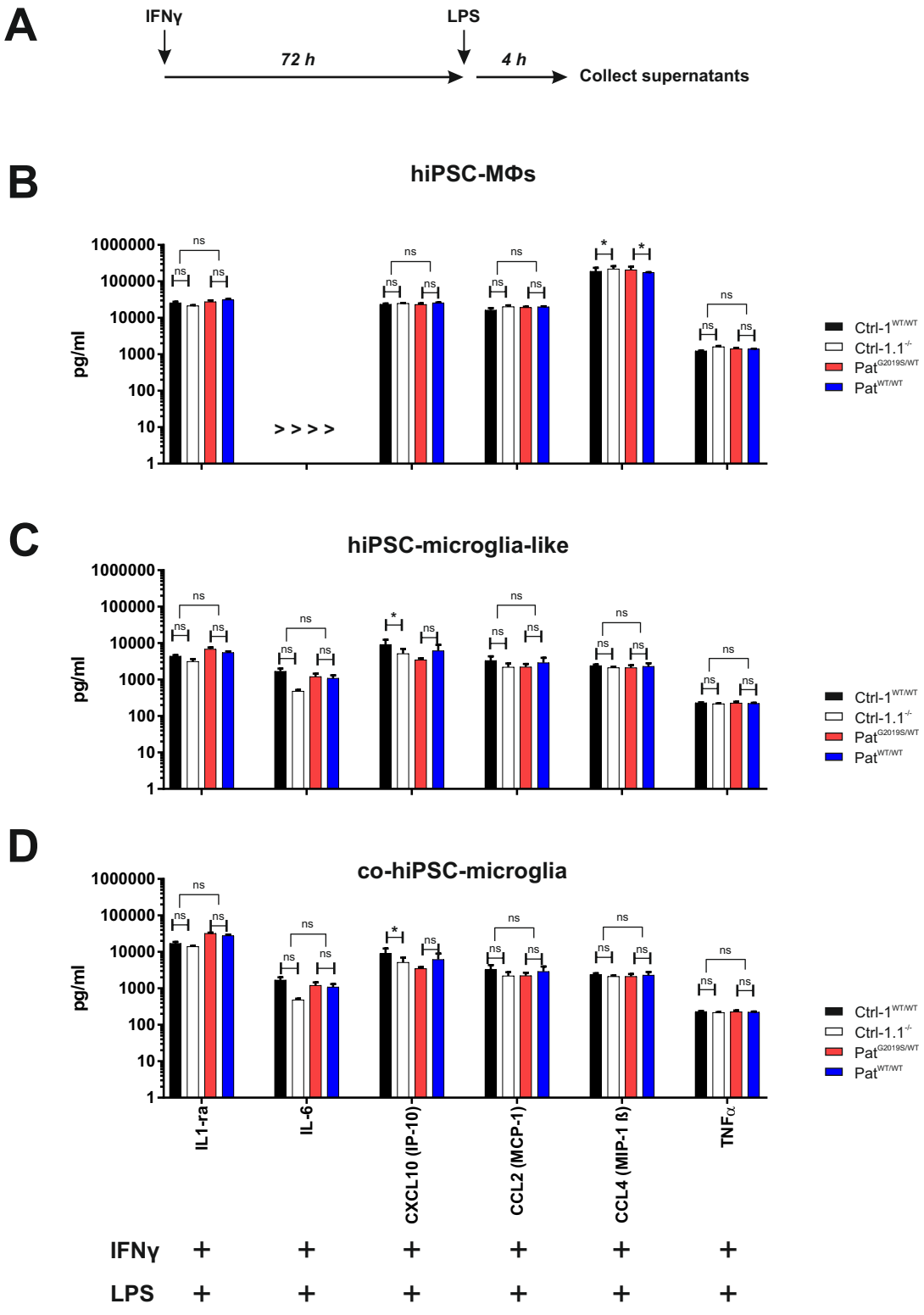

Figure 5.7 *LRRK2* KO and *LRRK2* G2019S hiPSC-MΦs display and an elevated level of CCL4. (A) Experimental design. Bar graphs show cytokine/chemokine level (pg/ml) in **(B)** hiPSC-MΦs, **(C)** hiPSC-microglia-ike cells and **(D)** co-hiPSC-microglia. Data represent mean ± SEM of three independent experiments. Statistical significance was tested using Two-way ANOVA with Tukey multiple comparison test. *$P < 0.05$, **$P < 0.01$, ***$P < 0.001$, ns denotes not significant, <, reading below detection range, >, reading above detection range.

5.3 Summary and Discussion

In this chapter, I have shown that LRRK2 protein is abundantly expressed in co-hiPSC-microglia, while its expression is not detected in hiPSC-cortical neurons. Similar to hiPSC-MΦs, IFNγ significantly induces LRRK2 expression in co-hiPSC-microglia. In the past, the expression of LRRK2 protein has been shown mainly in mouse microglia (Moehle et al. 2012; Gillardon, Schmid, and Draheim 2012; Schapansky et al. 2014). Immunostaining of mouse brain sections revealed an upregulation of LRRK2 protein expression in microglia after the intracranial injection of LPS (Moehle et al. 2012). Likewise, similar observation has been made by western blot analysis of cell lysates collected from LPS or IFNγ stimulated primary microglia isolated from adult mice (Gillardon, Schmid, and Draheim 2012) or LPS stimulated murine BV-2 microglia like cells (Schapansky et al. 2014).

Currently there is limited evidence showing LRRK2 expression in human microglia. Previous immunostaining studies using post-mortem human brains reported exclusive labelling of LRRK2 in neurons (Giasson et al. 2006; Greggio et al. 2006; Biskup et al. 2006; Higashi et al. 2007), except for one study by Miklossy et al., which reported that LRRK2 expression is found not only in neurons but also in microglia (Miklossy et al. 2006). However, the specificity of the LRRK2 antibodies used in these early studies is poorly validated due to lack of *LRRK2* KO cell lines. NB300-207 and NB300-268 antibodies (Novus Biologicals) used by Miklossy et al., and Greggio et al., were raised against human-specific epitopes therefore its specificity could not be validated in mouse *LRRK2* KO animals (Higashi et al. 2007).

Using hiPSC-microglia and hiPSC-cortical neuron co-culture, my results clearly demonstrate that endogenous LRRK2 expression is robust in human microglia and much

higher than in neurons. The specificity of LRRK2 immunostaining was validated by microglia differentiated from *LRRK2* KO hiPSCs (Figure 5.2B). Although my results showed no LRRK2 expression in hiPSC-cortical neurons, other research groups have shown the expression of LRRK2 in hiPSC-dopaminergic neurons (Nguyen et al. 2011; López de Maturana et al. 2016). However, the cross-reactivity of the LRRK2 antibody (Millipore) used by Nguyen et al., has not been tested, and NB110-58771 LRRK2 antibody (Novus Biologicals) was validated by only western blot analysis using shRNA *LRRK2* KD neuron lysates (López de Maturana et al. 2016). In conclusion, no really convincing evidence has been supplied by others to demonstrate the presence of LRRK2 protein expression in neurons. The co-culture model provides an ideal platform to evaluate LRRK2 expression in human microglia and neurons, therefore, the next step would be to co-culture microglia with other neuronal types, particularly dopaminergic neurons, to clearly verify the expression of LRRK2 in these cell types.

By directly comparing MΦs and microglia differentiated from the same batch of MΦ precursors, the aim for this chapter was to investigate whether genetic manipulation of LRRK2 function has a differential effect in human MΦs and microglia. TNFα ELISA results showed that *LRRK2* G2019S mutation significantly enhances TNFα release in co-hiPSC-microglia but not in hiPSC-MΦs (Figure 5.4C). This result is consistent with previous observations in mouse primary microglia and MΦs (Lee, James, and Cowley 2017; Moehle et al. 2012; Kim et al. 2012; Russo et al. 2015; Moehle et al. 2015; Hakimi et al. 2011).

Extending this observation, I investigated whether other cytokines or chemokines are also differentially affected by *LRRK2* G2019S mutation in MΦs and microglia. Luminex multiplex array screened a panel of 34 cytokines and chemokines, including TNFα, in the same supernatants used for TNFα ELISA experiments.

Perplexingly, the effect of *LRRK2* G2019S mutation on TNFα level in co-hiPSC-microglia was no longer observed. Additionally, TNFα ELISA detected almost 1000-fold more TNFα than Luminex multiplex array. The manufacturer has confirmed that TNFα ELISA kit and Luminex kit use different antibody to detect TNFα but further information about the antibody was available. Without knowing exact details of the antibodies used to detect TNFα in each kit, it is hard to explain why the results obtained by two kits are so different. This clearly merits further investigation, because if the difference seen by ELISA is a real effect of the *LRRK2* G2019S mutation, it would be an important finding that could contribute to the progression of disease in these patients. Alternatively, mRNA expression of TNFα can be assessed to examine the effect of *LRRK2* G2019S mutation observed in co-hiPSC-microglia.

Results from Luminex array show significant changes in the levels of IL-1ra, CXCL10, CCL2 and CCL4 by *LRRK2* KO or G2019S mutation. Upon LPS stimulation, *LRRK2* KO significantly reduced IL1-ra and CXCL10 while G2019S mutation increased IL1-ra in both hiPSC-microglia-like and co-hiPSC-microglia but not in hiPSC-MΦs. Because the changes in the level of IL1-ra and CXCL10 were detected in in both hiPSC-microglia-like and co-hiPSC-microglia, it is likely that this effect may be due to the presence of GM-CSF in the differentiation media. GM-CSF promote ramification of microglia and has been shown to be important in microglia differentiation (Etemad et al. 2012).

On the other hand, a significant difference in the levels of CCL2 and CCL4 levels was detected between hiPSC-MΦs and co-hiPSC-microglia with *LRRK2* KO or *LRRK2* G2019S mutation. CCL2 and CCL4 are inflammatory chemokines, responsible for recruitment of monocytes or microglia to the site of inflammation. The level of CCL2 has been shown to be enhanced in PD patients and in MPTP-treated mice (Lindqvist et al. 2013; Kalkonde et al. 2007). My results show that *LRRK2* KO reduced levels of CCL2

and CCL4 in co-hiPSC-microglia while no significant difference in CCL2 or CCL4 was observed in hiPSC-MΦs under basal condition (Table 5.1). Conversely, *LRRK2* KO reduced the level of CCL4 with LPS stimulation in hiPSC-MΦs, but no significant difference was observed in co-hiPSC-microglia. G2019S mutation increased the level of CCL4 in hiPSC-MΦs with IFNγ priming while no difference was detected in co-hiPSC-microglia (Table 5.1). Taken together, results obtained by Luminex multiplex array suggest that LRRK2 is important in the release of CCL2 and CCL4 in microglia under basal condition but not in MΦs. Conversely, LRRK2 is required for the LPS-mediated release of CCL4 in MΦs but not in microglia. This observation is somewhat different from mouse studies. *LRRK2* KO mouse TEPMs treated with LPS did not show any change in the level of CCL2 (Wandu et al. 2015). In murine BV-2 microglia-like cells, KD of LRRK2 protein reduced release of CCL2 after tat-protein stimulation (Marker et al. 2012).

Additionally, no significant change in the levels of pro-inflammatory cytokine was observed using Luminex multiplex array. The levels of IL-1β, TNFα, and IL-6, were not changed either in hiPSC-MΦs or in co-hiPSC-microglia with *LRRK2* KO or *LRRK2* G2019S mutation. LPS treatment elevates these cytokines in mouse primary microglia with *LRRK2* R1441G mutation (Gillardon, Schmid, and Draheim 2012) or decreases with shRNA *LRRK2* KD (Marker et al. 2012; Moehle et al. 2012; Russo et al. 2015). Both asymptomatic *LRRK2* G2019S carriers and PD patients display elevated levels of IL-6, TNFα, and IL-10, compare to the age-matched healthy individuals (Dzamko, Rowe, and Halliday 2016). Therefore, no significant detection in the changes of these cytokines was unexpected. It is possible that physiological levels of *LRRK2* G2019S mutants only result in subtle changes in the levels of these pro-inflammatory cytokines. Future experiments

may also include stimulations that are directly relevant in PD, notably αsyn fibrils, to better understand LRRK2 disease mechanisms in PD.

While this highly authentic co-culture model did not reveal any changes in the inflammatory cytokine production between genetically modified *LRRK2* and its isogenic pairs, the immunostaining results provide an important evidence that LRRK2 function may be more significant in microglia rather than in neurons. Thus, the co-culture model can be used as an ideal platform to examine the role of LRRK2 in other aspects of microglial function, notably phagocytosis of dying neurons or αsyn aggregates. Since LRRK2 has been reported to play a role in neurite length (Chapter 1.2), investigating how *LRRK2* PD-causing mutations affect microglia ramification would be an interesting investigation.

6

General discussion

6.1 General discussion and future perspectives

The aim of this thesis was to investigate the role of LRRK2 in MΦs and microglia and its implications in inflammation-mediated PD pathology. Using hiPSC-MΦs and microglia, this thesis has clarified some of the findings from LRRK2 overexpression systems and has presented several novel findings about LRRK2 biology.

6.1.1 LRRK2 has diverse regulatory mechanisms

Protein kinases are important regulators of diverse intracellular signal pathways and their activity is tightly regulated. For example, kinases can be activated or inactivated by phosphorylation, dephosphorylation, protein cleavage, translocation, dimerization, and interactions with other proteins, and their activity can be terminated by protein degradation (Zhimin Lu and Hunter 2009). Accordingly, several observations imply the existence of multiple regulatory mechanisms for LRRK2: 1) LRRK2 is phosphorylated at multiple Ser residues which can be dephosphorylated by PP1 (Lobbestael et al. 2013) and LRRK2 kinase inhibitors, 2) LRRK2 protein expression is upregulated in a subset of immune cells by inflammatory stimuli, and 3) dimerization and membrane cellular localisation are required for activation of LRRK2 enzymatic activity (Berger, Smith, and Lavoie 2010; James et al. 2012; Schapansky et al. 2014). Since MΦs are a major LRRK2-expressing cell type, and most of above observations have been made in

LRRK2-overexpressing transformed cell lines, chapter 3 explored some of the key aspects of LRRK2 regulation in hiPSC-MΦs.

First, I have shown that LRRK2 is upregulated by IFNγ and LPS in hiPSC-MΦs. This observation was in accordance with multiple published studies which have consistently reported IFNγ-mediated upregulation of LRRK2 in human PBMC-derived CD11b(+) monocytes, CD3(+) T lymphocytes, CD19(+) B lymphocytes (Gardet et al. 2010), human blood monocyte-derived MΦs, mouse primary microglia (Gillardon, Schmid, and Draheim 2012), and in transformed cell lines, including human THP-1 monocytic leukaemia cells (Gardet et al. 2010; Kuss, Adamopoulou, and Kahle 2014). While the effect of LPS has been inconsistent in the literature (Gillardon, Schmid, and Draheim 2012; Moehle et al. 2012; Russo et al. 2015; Dzamko and Halliday 2012), my results clearly show that LPS significantly upregulates LRRK2 but not to the same extent as IFNγ. While IFNγ resulted in tenfold increase, LPS resulted in two – threefold increase (Figure 3.4). The LRRK2 promoter region contains IRF binding sites and it has been shown that IFNγ mediates LRRK2 expression via JAK/STAT and ERK5 mediated pathways (Gardet et al. 2010; Kuss, Adamopoulou, and Kahle 2014). TLR4 activation by LPS leads to activation of several transcription factors in MΦs, namely NF-kB, IRFs, PU.1, and runt-related transcription factor 1 (RUNX1) (Medzhitov and Horng 2009). Some of these transcription factors, particularly PU.1 and RUNX1, are MΦ specific. Therefore, it can be speculated that the inconsistency in LPS-mediated LRRK2 regulation by others could be due to different cell types used.

In accordance with the literature, LRRK2 kinase inhibitors significantly reduced the phosphorylation level of LRRK2 at S935 in hiPSC-MΦs (Figure 3.5) (Kamikawaji, Ito, and Iwatsubo 2009; Doggett et al. 2012; Nichols et al. 2010). Exactly how LRRK2 kinase inhibitors lead to reduced phosphorylation level of LRRK2 is uncertain. A simple, logical

explanation would be that these phosphorylation sites are phosphorylated by LRRK2 or by an unknown substrate of LRRK2 kinase. However, evidence refutes this idea because *LRRK2* G2019S mutation, which enhances LRRK2 kinase activity, displays similar phosphorylation levels to WT *LRRK2*, demonstrated by my results in hiPSC-MΦs (Figure 3.5) and by others in LRRK2-overexpression system (Doggett et al. 2012; Nichols et al. 2010; Li et al. 2011). Additionally, homozygous LRRK2 kinase-dead mutants are still phosphorylated at these Ser sites (Kamikawaji, Ito, and Iwatsubo 2009; Doggett et al. 2012; Nichols et al. 2010). Despite lack of a clear connection with LRRK2 kinase activity, S910, S935 phosphosites have been used as a surrogate to measure the effectiveness of these inhibitors in the cells. This is because the physiological substrates of LRRK2 are still uncertain and the autophosphorylation sites are hardly detectable in the cell. Recently Steger et al., have identified Rab10 as a physiological substrate of LRRK2, validated in mouse fibroblasts (Steger et al. 2016). Therefore, Rab10 could potentially be used for validating the efficacy of LRRK2 kinase inhibitors, although this finding requires further confirmation in other cell types, notably MΦs.

Although the mechanism by which LRRK2 kinase inhibitors lead to lower levels of phosphorylation of LRRK2 S935 is unclear, the consequences of treatment with LRRK2 kinase inhibitors appear to be clear. Combined treatment with GNE and CX significantly reduced the total LRRK2 protein in hiPSC-MΦs (Figure 3.6). This has also been shown in SH-SY5Y and HEK 293T cells overexpressing LRRK2 using a wide variety of LRRK2 kinase inhibitors (Zhao et al. 2015; E Lobbestael et al. 2016). Zhao et al., have reported that LRRK2 becomes degraded via the UPS in LRRK2-overexpressing HEK 293T cells. But caution should be taken interpreting that system, as the artificially higher level of LRRK2 may trigger the degradation pathway anyway, which may not necessarily reflect how LRRK2 is processed under physiological conditions. Regardless, Zhao et al.

have demonstrated that inhibitor-induced lower phosphorylation at Ser residues is responsible for degradation of LRRK2. PP1 has been reported to dephosphorylate LRRK2 at S910 and S935, therefore, application of the PP1 inhibitor, CalyculinA, has been shown to maintain S910/S935 phosphorylation upon LRRK2 kinase inhibitor treatment. In other words, combined treatment of CalyculinA and LRRK2 kinase inhibitors generate a phosphor-positive (at S910, 935) but kinase-inactive form of LRRK2. Using this approach, Zhao et al., have demonstrated that CalyculinA prevents inhibitor-induced degradation of LRRK2 (Zhao et al. 2015).

In hiPSC-MΦs, however, inhibition of the proteasome pathway by MG-132 and lactacystin or the lysosomal pathway by leupeptin did not result in an increase in LRRK2 protein level (Figure 3.6), but MG-132 significantly reduced the level of cleaved product (Figure 3.6). Using mass spectrometry, I have confirmed that this cleaved product is derived from LRRK2 missing the N-terminus. The cleavage site is mapped to be within ANK-LRR interdomain region, where Ser910/S935 phosphorylation sites are located (Figure3.7). While previous studies have noted the existence of this cleaved form of LRRK2 in mouse kidney (E Lobbestael et al. 2016; Herzig et al. 2011; Dächsel et al. 2007), the position of the cleavage site by mass spectrometry has never been reported. Analysing peptide distribution, I have mapped the cleavage site to be between aa901 and aa910, where a chymotrypsin target site is located (Figure 3.7). Since mass spectrometry analysed trypsin digested peptides, using other proteases (e.g. chymotrypsin) would narrow down more accurate cleavage site. The cleavage site then can be genetically modified to create non-cleavable LRRK2. Whether this will affect phosphorylation at S910, S935, formation of LRRK2 dimers, and its enzymatic activity can be explored to gain better understanding of biological implications of LRRK2 cleaving.

Interestingly, this cleaved product is missing phosphorylation at S935 (Figure 3.7), implying a potential link between phosphor-regulation of Ser residues and cleavage. Furthermore, my results show that full-length LRRK2 and cleaved LRRK2 form a heterodimer complex (Figure 3.7). When I used the antibody recognizing the N-terminus of LRRK2 (N138/6) to pull down LRRK2 and the antibody recognizing C-terminus of LRRK2 to perform western blot, the western blot clearly indicated the presence of cleaved LRRK2 in the final eluate (Figure 3.7). Guaitoli et al. recently described a low-resolution 3D structural model of LRRK2 dimer. Based on the interactions of each domain of LRRK2, Guaitoli et al. suggests that the N-terminus of LRRK2 may be important in regulating LRRK2 kinase and GTPase activity by either exposing the substrate biding site or alleviating an auto-inhibition site (Guaitoli et al. 2016). The proteolytic cleavage that I have described here, of LRRK2 at the ANK-LRR inter-domain region, could therefore play a role in LRRK2 enzymatic activity and is an intriguing research question to follow-up. Protein kinase C (PKC), for example, undergoes activity-dependent degradation by UPS, causing downregulation of its own activity (Z Lu et al. 1998; Kang et al. 2000; Basu, Sridharan, and Persaud 2009; Zhimin Lu and Hunter 2009). Conversely, NF-κB precursor p105 is processed by proteasome to acquire the active subunit, p50. While the long loop of carboxy-terminal domain enters the proteasome activity and becomes degraded, the amino-acid terminal transcription factor domain, p50, remains outside (Ciechanover et al. 2001). Whether similar mechanisms apply to LRRK2 must be determined.

Another important aspect of this thesis is the contribution of PD-causing mutations on the regulation of LRRK2 within ANK-LRR interdomain region. So far, this thesis explored the effect of the most common mutation, G2019S mutation. By comparing MΦs differentiated from heterozygous *LRRK2* G2019S mutation to its CRISPR/Cas9 corrected

isogenic line, the results from chapter 3 showed that *LRRK2* G2019S hiPSC-MΦs undergoes inhibitor-induced dephosphorylation and degradation to a similar extent to its isogenic pair. All of the pathogenic PD mutations (R1441C, R144G, R1441H, Y1699C and I2020T) except G2019S display reduced phosphorylation level at S910, S935 in LRRK2-overexpressing HEK 293T cells (Nichols et al. 2010; Doggett et al. 2012). Therefore, the next step would be to use hiPSC-MΦs with other pathogenic mutations. In collaboration with Dr. Rowan Flynn and Mr. Jesus Madero-Perez, I was involved in generating hiPSCs lines with CRISPR/Cas9-corrected R1441C mutation and introduction of R1441C mutation into the control hiPSC line. As R1441C mutation is found within the GTPase domain of LRRK2, comparing how these two PD-causing mutations affect phosphorylation at S910, S935 and cleavage would be an interesting project. More importantly, by examining phosphorylation level of endogenous LRRK2 protein, it is important to confirm data generated by LRRK2-overexpressing HEK 293T cells to understand how the level of phosphorylation at S910, S935 is connected with LRRK2 PD-mutations.

6.1.2 LRRK2 is recruited to phagosomes during late stages of phagocytosis

What could possibly be the reason for upregulating LRRK2 in response to immune stimuli? To investigate this question, in chapter 4, I explored the role of LRRK2 in one of the main functions of macrophages, phagocytosis.

Along with other professional phagocytes, MΦs are equipped with special machineries that recognize and distinguish the identity of target and process these according to the context of the target. For example, Blander et al. showed that phagosomes containing *E.coli* showed faster maturation than phagosomes containing apoptotic cells (Blander and Medzhitov 2004). This induced-phagosome maturation was mediated not by simply

activating TLR4 at the plasma membrane but by TLR4-engaged cargoes present on the phagosomes containing bacteria; activation of TLR4 by LPS during apoptotic cell phagocytosis did not result in faster maturation of phagosome containing apoptotic cells. In other words, phagosomes carrying different targets can be distinguished inside the cell, triggering different maturation machineries. What is even more remarkable is that this was only observed in MΦs but not in dendritic cells, which showed equal kinetics of phagosome maturation regardless bacteria or dead cells (Blander and Medzhitov 2004). This is a stunning example of how phagocytosis pathways are coordinated in a highly sophisticated way.

In hiPSC-MΦs, particles that activate TLRs, notably zymosan (Dectin-1, TLR2), *E.coli* (TLR4) and *S.typhimurium* (TLR2, TRL4), all showed strong positivity for LRRK2 on the phagosomes. LRRK2 was also recruited to both small (*E.coli*) and relatively larger (zymosan) targets that were opsonized with IgG, i.e. FcR-mediated uptake. By using targets with similar size but activating different receptors (zymosan and latex beads), I showed that recruitment of LRRK2 depends on the receptors and not the size of phagocytic targets. To further examine the selectivity of LRRK2 recruitment, future experiments could provide both zymosan and latex beads at the same to examine whether the recruitment of LRRK2 is only observed in zymosan containing phagosomes.

Although all TLR or FcR activating targets showed LRRK2 positive phagosomes, αsyn fibril-containing phagosomes were negative for LRRK2. It has been reported that misfolded αsyn binds to TRL1,2 and 4 (C. Kim et al. 2013; Fellner et al. 2013; Stefanova et al. 2011). One possible explanation would be that the downstream signalling of protein aggregates (e.g. αsyn fibrils)-mediated TLR activation may be different from pathogenic materials (e.g. zymosan, *E.coli* bioparticles, *S.Typhimurium*). In my experiments, I only allowed 2 h to phagocytose and digest αsyn-fibrils so it is possible that recruitment of

LRRK2 to αsyn fibrils containing phagosomes may occur at a later time point. The outcome of this investigation may provide an intriguing insight to the functional link between these two PD-related proteins.

Another novel finding of this chapter is the presence of super-coated LRRK2 upon treatment with LRRK2 kinase inhibitors. Since the total number of LRRK2(+) phagosomes did not change but the number of LRRK2 super-coated phagosomes were significantly increased, LRRK2 appears to be 'locked' onto the phagosomes in the presence of LRRK2 kinase inhibitors (Figure 4.4). This suggests that LRRK2 may need to phosphorylate a substrate to be able to be released from the phagosomal surfaces. Since LRRK2 kinase inhibitors lead to reduced phosphorylation level of LRRK2 at S910/S935, future experiments can investigate whether LRRK2 phospho-dead (S910A/S935A) or phospho-mimetic (S910D/S935D) mutants would change the turnover of LRRK2 on phoagosomes.

Since LRRK2 was found within late phagosomes, I hypothesized that LRRK2 may play a role during late stages of phagocytosis. First, in agreement with the literature (Maekawa et al. 2016; Schapansky et al. 2014; Moehle et al. 2015), LRRK2 was not involved in the initial internalisation of bioparticles in hiPSC-MΦs. This experiment was performed so that the quantification of acidified phagosomes is not affected by the rate of internalisation. Bioparticles (zymosan and *E.coli*) conjugated with an acid sensitive dye were used to quantify acidification of phagosomes. My results show that LRRK2 does not affect the acidification of phagosomes.

To gain better understanding of its possible role on the phagosomes, I performed immunostaining of various Rab GTPases and cellular organelles but none of these co-localized with LRRK2 (Figure 4.11). Although mass spectrometry following IP of

endogenous LRRK2 in hiPSC-MΦs identified several interesting potential interactors of LRRK2, including those that have been published in the past (14-3-3 and CDC37), when I followed these up by Western Blot of IPed samples, the interaction with LRRK2 was not detectable.

However, LRRK2 clearly co-exists on the phagosomes at the same time point that LAMP-1 and Rab9 are recruited (Figure 4.3). Since LRRK2 does not co-exist with Rab7 but does with LAMP-1, it can be speculated that LRRK2 recruitment happens prior to Rab7 and is removed before the arrival of Rab7. Experiments to follow this up would be to examine whether the inability of LRRK2 retrieval from the phagosomes by LRRK2 kinase inhibitors impacts recruitment of other phagosome machineries, including Rab7. However, since LRRK2 kinase inhibitors did not impact the overall acidification process, it can be inferred that Rab7 recruitment may not be impaired. One ambitious investigation to undertake would be to examine the proteome profiles of LRRK2(+) phagosomes and LRRK2(-) phagosomes and compare the profiles in the presence and the absence of LRRK2 kinase inhibitors. This way, the exact stage of phagosomes in which LRRK2 is present can be identified, which would provide a better understanding of its role on phagosomes.

6.1.3 LRRK2 is highly expressed in microglia but not in neurons

Higher levels of inflammatory cytokines, notably IL-1β, TNFα, IL-6 and IL-12, were detected in the sera of asymptomatic *LRRK2* G2019S carriers and *LRRK2* G2019S carriers with parkinsonism compared to age-matched *LRRK2* WT carriers (Dzamko, Rowe, and Halliday 2016). This suggests a strong link between LRRK2 and inflammatory cytokine release. In the literature, LRRK2-mediated inflammatory cytokine release has been observed in microglia (mouse primary microglia, murine BV-2

microglia-like cells) but not in MΦs (mouse primary MΦs, murine macrophage-like RAW 264.7 cells) (Lee, James, and Cowley 2017; Moehle et al. 2012; B. Kim et al. 2012; Russo et al. 2015; Moehle et al. 2015; Hakimi et al. 2011). None of these studies, however, has directly compared microglia and MΦs under the same experimental conditions, so direct evidence for opposing role of LRRK2 is still lacking. The aim for chapter 5 was to explore the role of LRRK2 in inflammatory cytokine release by comparing MΦs and microglia differentiated from hiPSCs.

First, the expression level of LRRK2 was compared between hiPSC-microglia and hiPSC-cortical neurons. While past studies have investigated the expression level of LRRK2 in human *post mortem* brains, which reported exclusive labelling of LRRK2 in neurons (Giasson et al. 2006; Greggio et al. 2006; Biskup et al. 2006), the specificity of antibodies used in these early studies has been questionable. By using CRISPR/Cas9 and hiPSC technologies, my results convincingly demonstrate a robust and exclusive expression of LRRK2 in hiPSC-microglia but not in hiPSC-cortical neurons (Figure 5.2). While this observation does not exclude the possibility of LRRK2 expression in other neuronal cell types, notably dopaminergic neurons, recent RNA-seq data have also revealed that hiPSC-dopaminergic neurons display relatively low level of LRRK2 expression (Sandor et al. 2017).

In chapter 5, MΦs and microglia differentiated from the same MΦ precursors were used to perform TNFα ELISA in parallel. Results showed that *LRRK2* G2019S mutation increased TNFα only in hiPSC-microglia but not in hiPSC-MΦs, supporting my original hypothesis that microglia are more affected by *LRRK2* PD mutation than MΦs (Figure 5.4). Interestingly, this was observed only after the cells were primed with IFNγ prior to the LPS stimulation. It has been shown that microglial activation can be amplified by systemic inflammation. For example, exposure to *Salmonella* prior to the injection of LPS

to the brain triggers exaggerated and prolonged microglial activation (Püntener et al. 2012). This concept of microglial priming has been tested experimentally in the context of PD, where prenatal exposure to LPS in rats triggered stronger inflammatory responses upon subsequent LPS injection in midlife, leading to progressive loss of nigral dopaminergic neurons (Ling et al. 2006). This could help explain the age-dependence of LRRK2 pathology. Throughout life, constant exposure to inflammatory stimuli (e.g. environmental toxins, infections) together with *LRRK2* mutation may accelerate reaching a critical threshold of neuroinflammation, triggering a self-perpetuating cycle of microglial activation and neurodegeneration.

Unfortunately, this observation was not replicated by Luminex multiplex array. This kit analysed 34 chemokines and cytokines present in the same supernatants used in TNFα ELISA. Not only the difference in the level of TNFα by *LRRK2* G2019S mutation was no longer present, none of other inflammatory cytokines implicated in PD showed any changes in their levels in *LRRK2* KO or *LRRK2* G2019S mutation. Only CCL2 and CCL4 levels showed significant changes by different genotypes of *LRRK2* (Figure 5.5-7), but this time, changes were observed in hiPSC-MΦs not in hiPSC-microglia. Since the TNFα kit and Luminex detect TNFα using two different antibodies, a multiplex kit using same antibody as the TNFα ELISA kit would need to be used to clarify discordant results obtained by Luminex and TNFα ELISA.

6.2 Concluding remarks

This thesis has presented novel observations on LRRK2 using new and highly authentic models, hiPSC-MΦs and microglia. I have identified the cleavage site of LRRK2 to be within ANK-LRR, which may potentially be a novel mechanism in which LRRK2 activity is regulated. Another important finding of this thesis is the recruitment of LRRK2

on late phagosomes and inhibitor-induced formation of super-coated LRRK2 phagosomes. This thesis has shown recruitment of LRRK2 to phagosomes containing pathogen-derivatives (zysmoan, *E.coli, S.typhimurium*). Lastly, by using hiPSC-microglia, cortical neuron co-culture, this thesis clearly demonstrates the robust expression of LRRK2 in hiPSC-microglia and not in hiPSC-cortical neurons. While MΦs and microglia derived from hiPSCs are powerful physiologically-relevant cell models to investigate LRRK2 biology, there were only limited set of lines used in this thesis. Given the high variability between hiPSC lines, the incorporation of more hiPSC lines and generation of more comprehensive panels of isogenic pairs would strengthen the observations made in this thesis. Furthermore, more optimisation of co-culture model should be undertaken. While hiPSC-microglia and hiPSC-cortical neurons co-culture offers valuable insight, microglia co-culture using dopaminergic neurons would be more relevant PD model. Finally, all my results demonstrate that LRRK2 expression in MΦs and microglia are likely contributing factors in PD progression, possibly through its association in phagocytosis.

A

Appendix

A1. Proteasome activity

Dr. Walther Haenseler performed the chymotrypsin-like activity inhibitor assay. hiPSC-MΦs were treated with lactacystin or MG-132 overnight in 37ºC. Proteasome-Glo Chymotrypsin-Like Assay kit was used according to the manufacturer's instructions. The data are plotted fold change against no inhibitor control in mean ± S.D of three technical replicates.

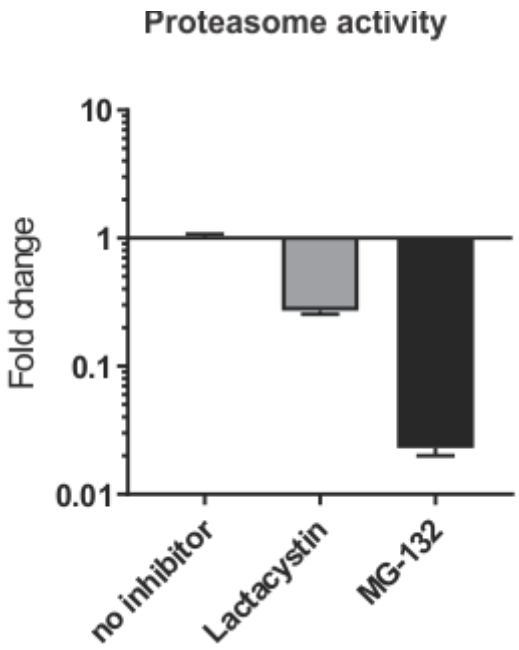

A2. List of LRRK2 peptide sequences analysed by mass spectrometry

Trypsin-digested peptides identified by mass spectrometry are listed below. They are ordered from N-terminus to C-terminus of LRRK2.

PEPTIDE ID	PEPTIDE SEQUENCE
1	ASGSCQGCEEDEETLK
2	ASGSCQGCEEDEETLKK
3	NIHVPLLIVLDSYMR
4	VASVQQVGWSLLCK
5	LIEVCPGTMQSLMGPQDVGNDWEVLGVHQLILK
6	MLTVHNASVNLSVIGLK
7	TLDLLLTSGK
8	ALHVLFER
9	VSEEQLTEFVENK
10	CYNIVVEAMK
11	AFPMSER
12	IQEVSCCLLHR
13	NKHVQEAACWALNNLLMYQNSLHEK
14	HVQEAACWALNNLLMYQNSLHEK
15	IGDEDGHFPAHR
16	EVMLSMLMHSSSK
17	EVFQASANALSTLLEQNVNFR
18	GIHLNVLELMQK
19	HIHSPEVAESGCK
20	MLNHLFEGSNTSLDIMAAVVPK
21	RHETSLPVQLEALR
22	HETSLPVQLEALR
23	AILHFIVPGMPEESR

24 AILHFIVPGMPEESREDTEFHHK

25 LVLAALNR

26 FIGNPGIQK

27 KNVFIGTGHLLAK

28 NVFIGTGHLLAK

29 ILVSSLYR

30 FKDVAEIQTK

31 DVAEIQTK

32 GFQTILAILK

33 LSASFSK

34 DQQFLNLCCK

35 VAMDDYLK

36 EGSSLICQVCEK

37 LVELLLNSGSR

38 KALTISIGK

39 ALTISIGK

40 GDSQIISLLLR

41 LALDVANNSICLGGFCIGK

42 VEPSWLGPLFPDK

43 KQTNIASTLAR

44 QTNIASTLAR

45 SAVEEGTASGSDGNFSEDVLSK

46 KSNSISVGEFYR

47 SNSISVGEFYR

48 HSNSLGPIFDHEDLLK

49 HSNSLGPIFDHEDLLKR

50 KILSSDDSLR

51 ILSSDDSLR

52 HSDSISSLASER

53 HSDSISSLASEREYITSLDLSANELR

54 EYITSLDLSANELR

55 DIDALSQK

56 CCISVHLEHLEK

57 LELHQNALTSFPQQLCETLK

58 SLTHLDLHSNK

59 SLTHLDLHSNKFTSFPSYLLK

60 FTSFPSYLLK

61 MSCIANLDVSR

62 NDIGPSVVLDPTVK

63 QFNLSYNQLSFVPENLTDVVEK

64 QFNLSYNQLSFVPENLTDVVEKLEQLILEGNK

65 LEQLILEGNK

66 ISGICSPLR

67 NHISSLSENFLEACPK

68 VESFSAR

69 MNFLAAMPFLPPSMTILK

70 LSQNKFSCIPEAILNLPHLR

71 FSCIPEAILNLPHLR

72 SLDMSSNDIQYLPGPAHWK

73 ELLFSHNQISILDLSEK

74 LKEIPPEIGCLENLTSLDVSYNLELR

75 EIPPEIGCLENLTSLDVSYNLELR

76 SFPNEMGK

77 IWDLPLDELHLNFDFK

78 MKLMIVGNTGSGK

79 LMIVGNTGSGK

80 TTLLQQLMK

81 KSDLGMQSATVGIDVK

82 KSDLGMQSATVGIDVKDWPIQIR

83 SDLGMQSATVGIDVK

84 SDLGMQSATVGIDVKDWPIQIR

85 DWPIQIR

86 DLVLNVWDFAGR

87 DLVLNVWDFAGREEFYSTHPHFMTQR

88 EEFYSTHPHFMTQR

89 ALYLAVYDLSK

90 GQAEVDAMKPWLFNIK

91 ASSSPVILVGTHLDVSDEK

92 ASSSPVILVGTHLDVSDEKQR

93 RGFPAIR

94 DYHFVNATEESDALAK

95 KTIINESLNFK

96 TIINESLNFK

97 IRDQLVVGQLIPDCYVELEK

98 DQLVVGQLIPDCYVELEK

99 KNVPIEFPVIDR

100 KNVPIEFPVIDRK

101 NVPIEFPVIDR

102 NVPIEFPVIDRK

103 RLLQLVR

104 IMAQILTVK

105 NYMSQYFK

106 FQIALPIGEEYLLVPSSLSDHR

107 FQIALPIGEEYLLVPSSLSDHRPVIELPHCENSEIIIR

108 LYEMPYFPMGFWSR

109 LLEISPYMLSGR

110 QGIYLNWSPEAYCLVGSEVLDNHPESFLK

111 ITVPSCR

112 KWALYSFNDGEEHQK

113 WALYSFNDGEEHQK

114 ILLDDLMK

115 ILLDDLMKK

116 KAEEGDLLVNPDQPR

117 AEEGDLLVNPDQPR

118 LTIPISQIAPDLILADLPR

119 NIMLNNDELEFEQAPEFLLGDGSFGSVYR

120 AAYEGEEVAVK

121 QELVVLCHLHHPSLISLLAAGIR

122 MLVMELASK

123 IALHVADGLR

124 YLHSAMIIYR

125 DLKPHNVLLFTLYPNAAIIAK

126 IADYGIAQYCCR

127 TSEGTPGFR

128 GNVIYNQQADVYSFGLLLYDILTTGGR

129 IVEGLKFPNEFDELEIQGK

130 FPNEFDELEIQGK

131 LPDPVKEYGCAPWPMVEK

132 EYGCAPWPMVEK

133 QCLKENPQERPTSAQVFDILNSAELVCLTR

134 ENPQERPTSAQVFDILNSAELVCLTR

135 NVIVECMVATHHNSR

136 NASIWLGCGHTDR

137 GQLSFLDLNTEGYTSEEVADSR

138 ILCLALVHLPVEK

139 ESWIVSGTQSGTLLVINTEDGK

140 ESWIVSGTQSGTLLVINTEDGKK

141 MTDSVTCLYCNSFSK

142 QKNFLLVGTADGK

143 NFLLVGTADGK

144 LAIFEDK

145 ILNIGNVSTPLMCLSESTNSTER

146 NVMWGGCGTK

147 IFSFSNDFTIQK

148 TSQLFSYAAFSDSNIITVVVDTALYIAK

149 QNSPVVEVWDK

150 QNSPVVEVWDKK

151 LCGLIDCVHFLR

152 NTALWIGTGGGHILLLDLSTR

153 VIYNFCNSVR

154 VMMTAQLGSLK

155 NVMLVLGYNR

156 NVMLVLGYNRK

157 QKEIQSCLTVWDINLPHEVQNLEK

158 EIQSCLTVWDINLPHEVQNLEK

A3. SNP analysis results

SNP analysis results of CRISPR/Cas-9 edited hiPSC lines along with the parental lines are attached below.

Ctrl-1 (SFC840-03-03)

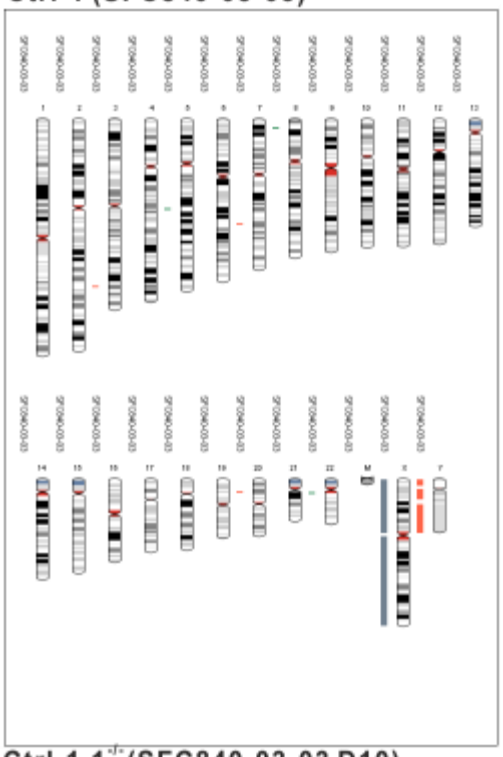

Ctrl-1.1$^{-/-}$(SFC840-03-03 D10)

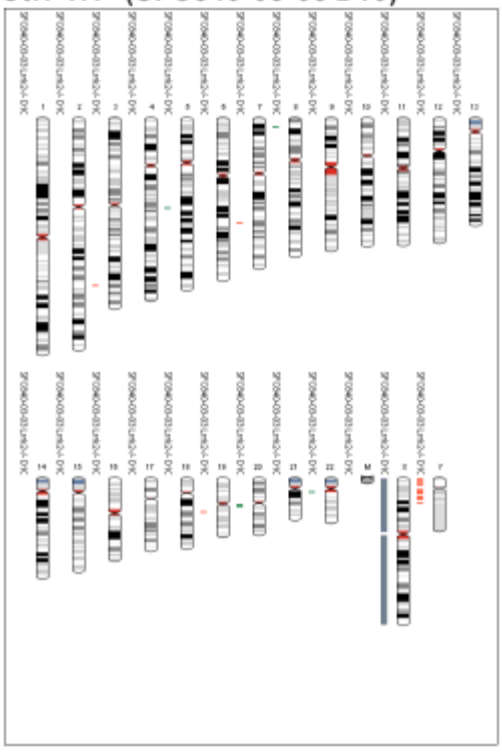

Ctrl-1.1$^{-/-}$(SFC840-03-03 C11)

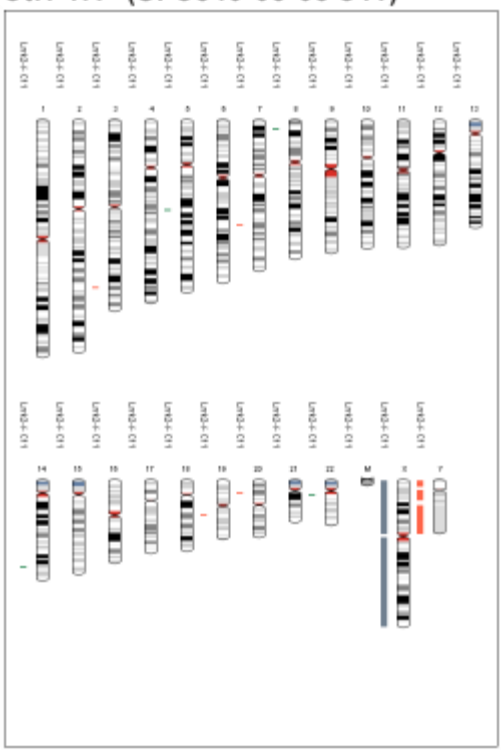

Pat$^{G2019S/WT}$ (SFC832-03-06)

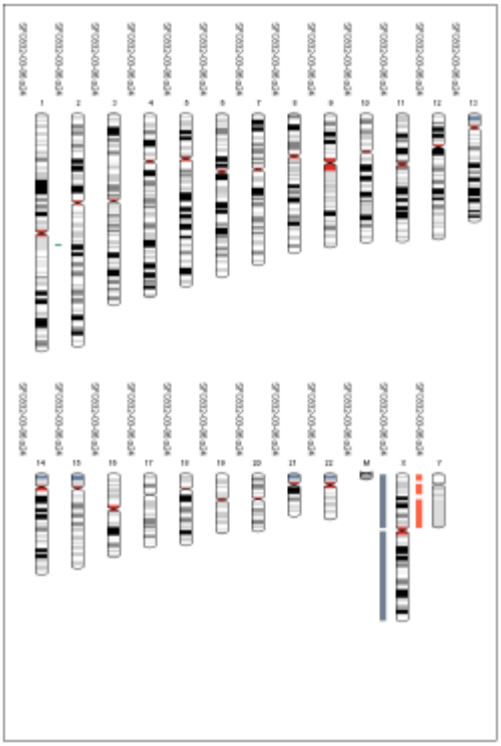

Pat$^{WT/WT}$ (SFC832-03-06 RFC47)

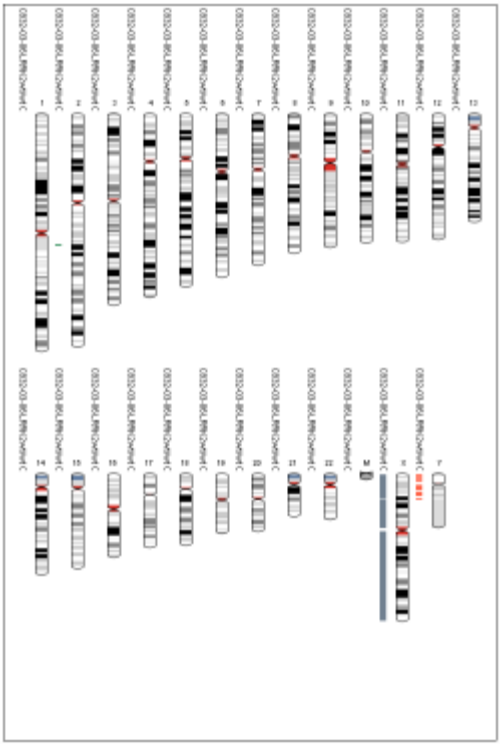

A4. Quantification of LRRK2(+) phagosomes

Data from Figure 4.4C are presented here in percent of zymosan containing phagosomes displaying LRRK2 positivity (A) or in the percent of LRRK2(+) phagosomes displaying super-coated LRRK2 (B).

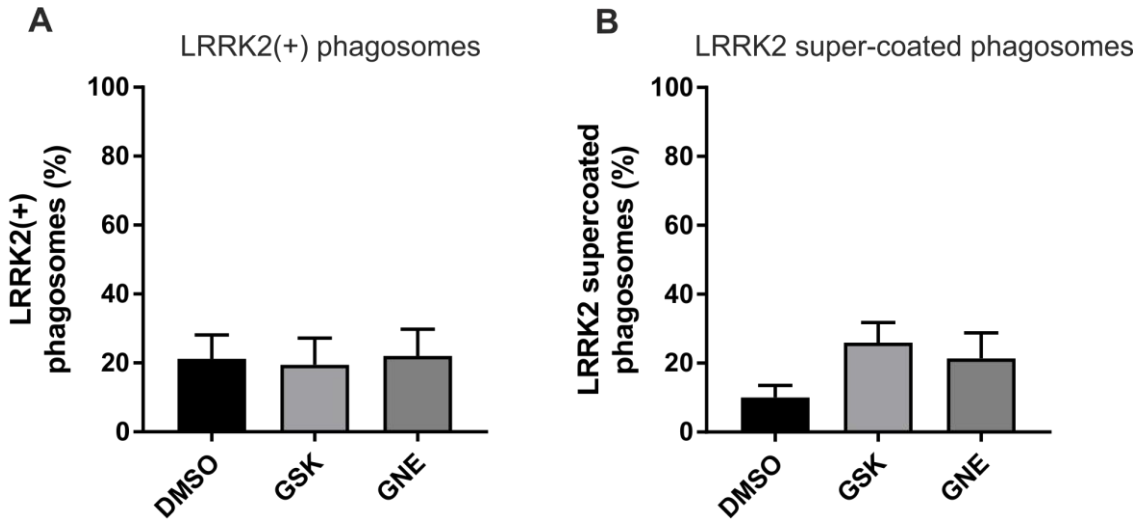

Bibliography

Abbas, N, C B Lücking, S Ricard, A Dürr, V Bonifati, G De Michele, S Bouley, et al. 1999. "A Wide Variety of Mutations in the Parkin Gene Are Responsible for Autosomal Recessive Parkinsonism in Europe. French Parkinson's Disease Genetics Study Group and the European Consortium on Genetic Susceptibility in Parkinson's Disease." *Human Molecular Genetics* 8 (4): 567–74. http://www.ncbi.nlm.nih.gov/pubmed/10072423.

Aflaki, Elma, Barbara K. Stubblefield, Emerson Maniwang, Grisel Lopez, Nima Moaven, Ehud Goldin, Juan Marugan, et al. 2014. "Macrophage Models of Gaucher Disease for Evaluating Disease Pathogenesis and Candidate Drugs." *Science Translational Medicine* 6 (240): 240ra73. doi:10.1126/scitranslmed.3008659.

Aharon-Peretz, Judith, Hanna Rosenbaum, and Ruth Gershoni-Baruch. 2004. "Mutations in the Glucocerebrosidase Gene and Parkinson's Disease in Ashkenazi Jews." *The New England Journal of Medicine* 351 (19): 1972–77. doi:10.1056/NEJMoa033277.

Alcalay, Roy N., Anat Mirelman, Rachel Saunders-Pullman, Ming X. Tang, Helen Mejia Santana, Deborah Raymond, Ernest Roos, et al. 2013. "Parkinson Disease Phenotype in Ashkenazi Jews with and without LRRK2 G2019S Mutations." *Movement Disorders* 28 (14): 1966–71. doi:10.1002/mds.25647.

Alegre-Abarrategui, Javier, Helen Christian, Michele M P Lufino, Ruxandra Mutihac, Lara Lourenço Venda, Olaf Ansorge, and Richard Wade-Martins. 2009. "LRRK2 Regulates Autophagic Activity and Localizes to Specific Membrane Microdomains in a Novel Human Genomic Reporter Cellular Model." *Human Molecular Genetics* 18 (21): 4022–34. doi:10.1093/hmg/ddp346.

Anand, Vasanti S., Laurie J. Reichling, Kerri Lipinski, Wayne Stochaj, Weili Duan, Kerry Kelleher, Pooja Pungaliya, et al. 2009. "Investigation of Leucine-Rich Repeat Kinase 2." *FEBS Journal* 276 (2): 466–78. doi:10.1111/j.1742-4658.2008.06789.x.

Anderson, Peter C., and Valerie Daggett. 2008. "Molecular Basis for the Structural Instability of Human DJ-1 Induced by the L166P Mutation Associated with Parkinson's Disease †." *Biochemistry* 47 (36): 9380–93. doi:10.1021/bi800677k.

Ard, M D, G M Cole, J Wei, A P Mehrle, and J D Fratkin. 1996. "Scavenging of Alzheimer's Amyloid Beta-Protein by Microglia in Culture." *Journal of Neuroscience Research* 43 (2): 190–202. doi:10.1002/(SICI)1097-4547(19960115)43:2<190::AID-JNR7>3.0.CO;2-B.

Arranz, A. M., L. Delbroek, K. Van Kolen, M. R. Guimaraes, W. Mandemakers, G. Daneels, S. Matta, et al. 2015. "LRRK2 Functions in Synaptic Vesicle Endocytosis through a Kinase-Dependent Mechanism." *Journal of Cell Science* 128 (3): 541–52. doi:10.1242/jcs.158196.

Bader, Verian, Xin Ran Zhu, Hermann Lübbert, and Christine C Stichel. 2005. "Expression

of DJ-1 in the Adult Mouse CNS." *Brain Research* 1041 (1): 102–11. doi:10.1016/j.brainres.2005.02.006.

Bain, C C, C L Scott, H Uronen-Hansson, S Gudjonsson, O Jansson, O Grip, M Guilliams, B Malissen, W W Agace, and A McI Mowat. 2013. "Resident and pro-Inflammatory Macrophages in the Colon Represent Alternative Context-Dependent Fates of the Same Ly6Chi Monocyte Precursors." *Mucosal Immunology* 6 (3): 498–510. doi:10.1038/mi.2012.89.

Bains, Mona, Vincent Zaegel, Janna Mize-Berge, and Kim A. Heidenreich. 2011. "IGF-I Stimulates Rab7-RILP Interaction during Neuronal Autophagy." *Neuroscience Letters* 488 (2): 112–17. doi:10.1016/j.neulet.2010.09.018.

Banerjee, Rebecca, M. Flint Beal, and Bobby Thomas. 2010. "Autophagy in Neurodegenerative Disorders: Pathogenic Roles and Therapeutic Implications." *Trends in Neurosciences* 33 (12): 541–49. doi:10.1016/j.tins.2010.09.001.

Baptista, Marco A. S., Kuldip D. Dave, Mark A. Frasier, Todd B. Sherer, Melanie Greeley, Melissa J. Beck, Julie S. Varsho, et al. 2013. "Loss of Leucine-Rich Repeat Kinase 2 (LRRK2) in Rats Leads to Progressive Abnormal Phenotypes in Peripheral Organs." Edited by Darren J Moore. *PLoS ONE* 8 (11). Public Library of Science: e80705. doi:10.1371/journal.pone.0080705.

Bar-Nur, Ori, Holger A. Russ, Shimon Efrat, and Nissim Benvenisty. 2011. "Epigenetic Memory and Preferential Lineage-Specific Differentiation in Induced Pluripotent Stem Cells Derived from Human Pancreatic Islet Beta Cells." *Cell Stem Cell* 9 (1): 17–23. doi:10.1016/j.stem.2011.06.007.

Barbero, Pierre, Lenka Bittova, and Suzanne R Pfeffer. 2002. "Visualization of Rab9-Mediated Vesicle Transport from Endosomes to the Trans-Golgi in Living Cells." *The Journal of Cell Biology* 156 (3). The Rockefeller University Press: 511–18. doi:10.1083/jcb.200109030.

Barcia, Carlos, Carmen Ros, Francisco Ros-Bernal, Aurora Gómez, Valentina Annese, María Carrillo-de Sauvage, José Yuste, et al. 2013. "Persistent Phagocytic Characteristics of Microglia in the Substantia Nigra of Long-Term Parkinsonian Macaques." *Journal of Neuroimmunology* 261 (1–2): 60–66. doi:doi: 10.1016/j.jneuroim.2013.05.001.

Barrangou, R., C. Fremaux, H. Deveau, M. Richards, P. Boyaval, S. Moineau, D. A. Romero, and P. Horvath. 2007. "CRISPR Provides Acquired Resistance Against Viruses in Prokaryotes." *Science* 315 (5819): 1709–12. doi:10.1126/science.1138140.

Barrett, Jeffrey C, Sarah Hansoul, Dan L Nicolae, Judy H Cho, Richard H Duerr, John D Rioux, Steven R Brant, et al. 2008. "Genome-Wide Association Defines More than 30 Distinct Susceptibility Loci for Crohn's Disease." *Nature Genetics* 40 (8): 955–62. doi:10.1038/ng.175.

Basu, Alakananda, Savitha Sridharan, and Shalini Persaud. 2009. "Regulation of Protein Kinase Cδ Downregulation by Protein Kinase Cε and Mammalian Target of Rapamycin Complex 2." *Cellular Signalling* 21 (11): 1680–85. doi:10.1016/j.cellsig.2009.07.006.

Beevers, Joel E., Mang Ching Lai, Emma Collins, Heather D.E. Booth, Federico Zambon, Laura Parkkinen, Jane Vowles, Sally A. Cowley, Richard Wade-Martins, and Tara M. Caffrey. 2017. "MAPT Genetic Variation and Neuronal Maturity Alter Isoform

Expression Affecting Axonal Transport in iPSC-Derived Dopamine Neurons." *Stem Cell Reports* 9 (2): 587–99. doi:10.1016/j.stemcr.2017.06.005.

Beilina, Alexandria, Iakov N Rudenko, Alice Kaganovich, Laura Civiero, Hien Chau, Suneil K Kalia, Lorraine V Kalia, et al. 2014. "Unbiased Screen for Interactors of Leucine-Rich Repeat Kinase 2 Supports a Common Pathway for Sporadic and Familial Parkinson Disease." *Proceedings of the National Academy of Sciences of the United States of America* 111 (7). National Academy of Sciences: 2626–31. doi:10.1073/pnas.1318306111.

Belluzzi, Elisa, Adriano Gonnelli, Maria-Daniela Cirnaru, Antonella Marte, Nicoletta Plotegher, Isabella Russo, Laura Civiero, et al. 2016. "LRRK2 Phosphorylates Pre-Synaptic N-Ethylmaleimide Sensitive Fusion (NSF) Protein Enhancing Its ATPase Activity and SNARE Complex Disassembling Rate." *Molecular Neurodegeneration* 11 (1): 1. doi:10.1186/s13024-015-0066-z.

Beningo, Karen A, and Yu-li Wang. 2002. "Fc-Receptor-Mediated Phagocytosis Is Regulated by Mechanical Properties of the Target." *Journal of Cell Science* 115 (Pt 4): 849–56. http://www.ncbi.nlm.nih.gov/pubmed/11865040.

Berger, Zdenek, Kelsey Smith, and Matthew Lavoie. 2010. "Membrane Localization of LRRK2 Is Associated with Increased Formation of the Highly Active LRRK2 Dimer and Changes in Its Phosphorylation." *Biochemistry* 49 (26): 5511–23. doi:doi: 10.1021/bi100157u.

Bibikova, M., Kelly Beumer, Jonathan K Trautman, and Dana Carroll. 2003. "Enhancing Gene Targeting with Designed Zinc Finger Nucleases." *Science* 300 (5620): 764–764. doi:10.1126/science.1079512.

Bichler, Zoë, Han Chi Lim, Li Zeng, and Eng King Tan. 2013. "Non-Motor and Motor Features in LRRK2 Transgenic Mice." Edited by Huaibin Cai. *PLoS ONE* 8 (7): e70249. doi:10.1371/journal.pone.0070249.

Biskup, Saskia, Darren J. Moore, Fulvio Celsi, Shinji Higashi, Andrew B. West, Shaida A. Andrabi, Kaisa Kurkinen, et al. 2006. "Localization of LRRK2 to Membranous and Vesicular Structures in Mammalian Brain." *Annals of Neurology* 60 (5). Wiley Subscription Services, Inc., A Wiley Company: 557–69. doi:10.1002/ana.21019.

Blander, J. M., and Ruslan Medzhitov. 2004. "Regulation of Phagosome Maturation by Signals from Toll-Like Receptors." *Science* 304 (5673): 1014–18. doi:10.1126/science.1096158.

Blesa, Javier, and Serge Przedborski. 2014. "Parkinsonâ€™s Disease: Animal Models and Dopaminergic Cell Vulnerability." *Frontiers in Neuroanatomy* 8 (December): 155. doi:10.3389/fnana.2014.00155.

Boch, J., H. Scholze, S. Schornack, A. Landgraf, S. Hahn, S. Kay, T. Lahaye, A. Nickstadt, and U. Bonas. 2009. "Breaking the Code of DNA Binding Specificity of TAL-Type III Effectors." *Science* 326 (5959): 1509–12. doi:10.1126/science.1178811.

Bolotin, Alexander, Benoit Quinquis, Alexei Sorokin, and S Dusko Ehrlich. 2005. "Clustered Regularly Interspaced Short Palindrome Repeats (CRISPRs) Have Spacers of Extrachromosomal Origin." *Microbiology* 151 (8): 2551–61. doi:10.1099/mic.0.28048-0.

Bonifati, V., Patrizia Rizzu, Marijke J van Baren, Onno Schaap, Guido J Breedveld, Elmar Krieger, Marieke C J Dekker, et al. 2003. “Mutations in the DJ-1 Gene Associated with Autosomal Recessive Early-Onset Parkinsonism.” *Science* 299 (5604): 256–59. doi:10.1126/science.1077209.

Bosgraaf, Leonard, and Peter J.M. Van Haastert. 2003. “Roc, a Ras/GTPase Domain in Complex Proteins.” *Biochimica et Biophysica Acta (BBA) - Molecular Cell Research* 1643 (1–3): 5–10. doi:10.1016/j.bbamcr.2003.08.008.

Bouhouche, Ahmed, Houyam Tibar, Rafiqua Ben El Haj, Khalil El Bayad, Rachid Razine, Sanaa Tazrout, Asmae Skalli, et al. 2017. “LRRK2 G2019S Mutation: Prevalence and Clinical Features in Moroccans with Parkinson’s Disease.” *Parkinson’s Disease* 2017 (March). Hindawi: 1–7. doi:10.1155/2017/2412486.

Bras, Jose, Rita Guerreiro, Maria Ribeiro, Ana Morgadinho, Cristina Januario, Margarida Dias, Ana Calado, et al. 2008. “Analysis of Parkinson Disease Patients from Portugal for Mutations in SNCA, PRKN, PINK1 and LRRK2.” *BMC Neurology* 8 (1): 1. doi:10.1186/1471-2377-8-1.

Bravo-San Pedro, José M., Mireia Niso-Santano, Rubén Gómez-Sánchez, Elisa Pizarro-Estrella, Ana Aiastui-Pujana, Ana Gorostidi, Vicente Climent, et al. 2013. “The LRRK2 G2019S Mutant Exacerbates Basal Autophagy through Activation of the MEK/ERK Pathway.” *Cellular and Molecular Life Sciences* 70 (1): 121–36. doi:10.1007/s00018-012-1061-y.

Brochard, Vanessa, Béhazine Combadière, Annick Prigent, Yasmina Laouar, Aline Perrin, Virginie Beray-Berthat, Olivia Bonduelle, et al. 2009. “Infiltration of CD4+ Lymphocytes into the Brain Contributes to Neurodegeneration in a Mouse Model of Parkinson Disease.” *The Journal of Clinical Investigation* 119 (1): 182–92. doi:doi: 10.1172/jci36470.

Buchman, Aron S., Joshua M. Shulman, Sukriti Nag, Sue E. Leurgans, Steven E. Arnold, Martha C. Morris, Julie A. Schneider, and David A. Bennett. 2012. “Nigral Pathology and Parkinsonian Signs in Elders without Parkinson Disease.” *Annals of Neurology* 71 (2): 258–66. doi:10.1002/ana.22588.

Buchrieser, Julian, William James, and Michael D. Moore. 2017. “Human Induced Pluripotent Stem Cell-Derived Macrophages Share Ontogeny with MYB-Independent Tissue-Resident Macrophages.” *Stem Cell Reports* 8 (2): 334–45. doi:10.1016/j.stemcr.2016.12.020.

Bus, J S, S D Aust, and J E Gibson. 1976. “Paraquat Toxicity: Proposed Mechanism of Action Involving Lipid Peroxidation.” *Environmental Health Perspectives* 16 (August): 139–46. http://www.ncbi.nlm.nih.gov/pubmed/1017417.

Cabin, Deborah E, Kazuhiro Shimazu, Diane Murphy, Nelson B Cole, Wolfram Gottschalk, Kellie L McIlwain, Bonnie Orrison, et al. 2002. “Synaptic Vesicle Depletion Correlates with Attenuated Synaptic Responses to Prolonged Repetitive Stimulation in Mice Lacking Alpha-Synuclein.” *The Journal of Neuroscience : The Official Journal of the Society for Neuroscience* 22 (20): 8797–8807. http://www.ncbi.nlm.nih.gov/pubmed/12388586.

Campenhausen, Sonja von, Bernhard Bornschein, Regina Wick, Kai Bötzel, Cristina Sampaio, Werner Poewe, Wolfgang Oertel, Uwe Siebert, Karin Berger, and Richard

Dodel. 2005. “Prevalence and Incidence of Parkinson’s Disease in Europe.” *European Neuropsychopharmacology* 15 (4): 473–90. doi:10.1016/j.euroneuro.2005.04.007.

Cara, Francesca Di, Avinash Sheshachalam, Nancy E. Braverman, Richard A. Rachubinski, and Andrew J. Simmonds. 2017. “Peroxisome-Mediated Metabolism Is Required for Immune Response to Microbial Infection.” *Immunity* 47 (1): 93–106.e7. doi:10.1016/j.immuni.2017.06.016.

Chan, C. Savio, Jaime N. Guzman, Ema Ilijic, Jeff N. Mercer, Caroline Rick, Tatiana Tkatch, Gloria E. Meredith, and D. James Surmeier. 2007. “‘Rejuvenation’ Protects Neurons in Mouse Models of Parkinson’s Disease.” *Nature* 447 (7148): 1081–86. doi:10.1038/nature05865.

Chartier-Harlin, Marie-Christine, Jennifer Kachergus, Christophe Roumier, Vincent Mouroux, Xavier Douay, Sarah Lincoln, Clotilde Levecque, et al. 2004. “α-Synuclein Locus Duplication as a Cause of Familial Parkinson’s Disease.” *The Lancet* 364 (9440): 1167–69. doi:10.1016/S0140-6736(04)17103-1.

Chen, C-Y, Y-H Weng, K-Y Chien, K-J Lin, T-H Yeh, Y-P Cheng, C-S Lu, and H-L Wang. 2012. “(G2019S) LRRK2 Activates MKK4-JNK Pathway and Causes Degeneration of SN Dopaminergic Neurons in a Transgenic Mouse Model of PD.” *Cell Death and Differentiation* 19 (10): 1623–33. doi:10.1038/cdd.2012.42.

Cheng, Hsiao-Chun, Christina M. Ulane, and Robert E. Burke. 2010. “Clinical Progression in Parkinson Disease and the Neurobiology of Axons.” *Annals of Neurology* 67 (6): 715–25. doi:10.1002/ana.21995.

Chia, Ruth, Sara Haddock, Alexandra Beilina, Iakov N Rudenko, Adamantios Mamais, Alice Kaganovich, Yan Li, Ravindran Kumaran, Michael A Nalls, and Mark R Cookson. 2014. “Phosphorylation of LRRK2 by Casein Kinase 1α Regulates Trans-Golgi Clustering via Differential Interaction with ARHGEF7.” *Nature Communications* 5: 5827. doi:10.1038/ncomms6827.

Cho, H. J., J. Yu, C. Xie, P. Rudrabhatla, X. Chen, J. Wu, L. Parisiadou, et al. 2014. “Leucine-Rich Repeat Kinase 2 Regulates Sec16A at ER Exit Sites to Allow ER-Golgi Export.” *The EMBO Journal* 33 (20): 2314–31. doi:10.15252/embj.201487807.

Choi, Hwan Geun, Jinwei Zhang, Xianming Deng, John M. Hatcher, Matthew P. Patricelli, Zheng Zhao, Dario R. Alessi, and Nathanael S. Gray. 2012. “Brain Penetrant LRRK2 Inhibitor.” *ACS Medicinal Chemistry Letters* 3 (8): 658–62. doi:10.1021/ml300123a.

Choulika, A, A Perrin, B Dujon, and J F Nicolas. 1995. “Induction of Homologous Recombination in Mammalian Chromosomes by Using the I-SceI System of Saccharomyces Cerevisiae.” *Molecular and Cellular Biology* 15 (4): 1968–73. http://www.ncbi.nlm.nih.gov/pubmed/7891691.

Christensen, Kaare, Gabriele Doblhammer, Roland Rau, and James W Vaupel. 2009. “Ageing Populations: The Challenges Ahead.” *The Lancet*. doi:10.1016/S0140-6736(09)61460-4.

Christian, M., T. Cermak, E. L. Doyle, C. Schmidt, F. Zhang, A. Hummel, A. J. Bogdanove, and D. F. Voytas. 2010. “Targeting DNA Double-Strand Breaks with TAL Effector Nucleases.” *Genetics* 186 (2): 757–61. doi:10.1534/genetics.110.120717.

Chung, Ji-Yun, Hee Ra Park, Su-Jin Lee, Sun-Hye Lee, Jin Sik Kim, Youn-Sang Jung, Sang

Hyun Hwang, et al. 2013. “Elevated TRAF2/6 Expression in Parkinson’s Disease Is Caused by the Loss of Parkin E3 Ligase Activity.” *Laboratory Investigation* 93 (6): 663–76. doi:10.1038/labinvest.2013.60.

Chung, Kenny K.K., Yi Zhang, Kah Leong Lim, Yuji Tanaka, Hui Huang, Jun Gao, Christopher A. Ross, Valina L. Dawson, and Ted M. Dawson. 2001. “Parkin Ubiquitinates the Alpha-Synuclein-Interacting Protein, Synphilin-1: Implications for Lewy-Body Formation in Parkinson Disease.” *Nature Medicine* 7 (10): 1144–50. doi:10.1038/nm1001-1144.

Ciechanover, Aaron, Hedva Gonen, Beatrice Bercovich, Shai Cohen, Ifat Fajerman, Alain Israël, Frank Mercurio, et al. 2001. “Mechanisms of Ubiquitin-Mediated, Limited Processing of the NF-κB1 Precursor Protein p105.” In *Biochimie*, 83:341–49. doi:10.1016/S0300-9084(01)01239-1.

Cilia, Roberto, Chiara Siri, Damiana Rusconi, Roberta Allegra, Andrea Ghiglietti, Giorgio Sacilotto, Michela Zini, et al. 2014. “LRRK2 Mutations in Parkinson’s Disease: Confirmation of a Gender Effect in the Italian Population.” *Parkinsonism & Related Disorders* 20 (8): 911–14. doi:10.1016/j.parkreldis.2014.04.016.

Clarkson, E D, F G Rosa, J Edwards-Prasad, D A Weiland, S E Witta, C R Freed, and K N Prasad. 1998. “Improvement of Neurological Deficits in 6-Hydroxydopamine-Lesioned Rats after Transplantation with Allogeneic Simian Virus 40 Large Tumor Antigen Gene-Induced Immortalized Dopamine Cells.” *Proceedings of the National Academy of Sciences of the United States of America* 95 (3): 1265–70. http://www.ncbi.nlm.nih.gov/pubmed/9448320.

Collier, Timothy J., Nicholas M. Kanaan, and Jeffrey H. Kordower. 2011. “Ageing as a Primary Risk Factor for Parkinson’s Disease: Evidence from Studies of Non-Human Primates.” *Nature Reviews Neuroscience* 12 (6): 359–66. doi:10.1038/nrn3039.

Cong, L., F. A. Ran, D. Cox, S. Lin, R. Barretto, N. Habib, P. D. Hsu, et al. 2013. “Multiplex Genome Engineering Using CRISPR/Cas Systems.” *Science* 339 (6121): 819–23. doi:10.1126/science.1231143.

Conway, Kelly A., James D. Harper, and Peter T. Lansbury. 1998. “Accelerated in Vitro Fibril Formation by a Mutant α-Synuclein Linked to Early-Onset Parkinson Disease.” *Nature Medicine* 4 (11). Nature Publishing Group: 1318–20. doi:10.1038/3311.

Corti, Olga, Cornelia Hampe, Hana Koutnikova, Frédéric Darios, Sandrine Jacquier, Annick Prigent, Jean-Charles Robinson, et al. 2003. “The p38 Subunit of the Aminoacyl-tRNA Synthetase Complex Is a Parkin Substrate: Linking Protein Biosynthesis and Neurodegeneration.” *Human Molecular Genetics* 12 (12): 1427–37. http://www.ncbi.nlm.nih.gov/pubmed/12783850.

Dächsel, Justus C., Bahareh Behrouz, Mei Yue, Joel E. Beevers, Heather L. Melrose, and Matthew J. Farrer. 2010. “A Comparative Study of Lrrk2 Function in Primary Neuronal Cultures.” *Parkinsonism & Related Disorders* 16 (10): 650–55. doi:10.1016/j.parkreldis.2010.08.018.

Dächsel, Justus C, Julie P Taylor, Su San Mok, Owen A Ross, Kelly M Hinkle, Rachel M Bailey, Jacob H Hines, et al. 2007. “Identification of Potential Protein Interactors of Lrrk2.” *Parkinsonism & Related Disorders* 13 (7). NIH Public Access: 382–85. doi:10.1016/j.parkreldis.2007.01.008.

Damiani, María T., Martín Pavarotti, Natalia Leiva, Andrew J. Lindsay, Mary W. McCaffrey, and Maria I. Colombo. 2004. “Rab Coupling Protein Associates with Phagosomes and Regulates Recycling from the Phagosomal Compartment.” *Traffic* 5 (10). Blackwell Publishing Ltd: 785–97. doi:10.1111/j.1600-0854.2004.00220.x.

Damier, P, E C Hirsch, Y Agid, and A M Graybiel. 1999. “The Substantia Nigra of the Human Brain. II. Patterns of Loss of Dopamine-Containing Neurons in Parkinson’s Disease.” *Brain : A Journal of Neurology* 122 (Pt 8 (August): 1437–48. http://www.ncbi.nlm.nih.gov/pubmed/10430830.

Dauer, William, and Serge Przedborski. 2003. “Parkinson’s Disease: Mechanisms and Models.” *Neuron* 39 (6): 889–909. http://www.ncbi.nlm.nih.gov/pubmed/12971891.

Davis, G C, A C Williams, S P Markey, M H Ebert, E D Caine, C M Reichert, and I J Kopin. 1979. “Chronic Parkinsonism Secondary to Intravenous Injection of Meperidine Analogues.” *Psychiatry Research* 1 (3): 249–54. http://www.ncbi.nlm.nih.gov/pubmed/298352.

Dawson, Ted M., Han Seok Ko, and Valina L. Dawson. 2010. “Genetic Animal Models of Parkinson’s Disease.” *Neuron* 66 (5): 646–61. doi:10.1016/j.neuron.2010.04.034.

Day, B J, M Patel, L Calavetta, L Y Chang, and J S Stamler. 1999. “A Mechanism of Paraquat Toxicity Involving Nitric Oxide Synthase.” *Proceedings of the National Academy of Sciences of the United States of America* 96 (22). National Academy of Sciences: 12760–65. http://www.ncbi.nlm.nih.gov/pubmed/10535996.

Delbroek, Lore, Kristof Van Kolen, Liesbeth Steegmans, Raquel da Cunha, Wim Mandemakers, Guy Daneels, Pieter-Jan De Bock, et al. 2013. “Development of an Enzyme-Linked Immunosorbent Assay for Detection of Cellular and in Vivo LRRK2 S935 Phosphorylation.” *Journal of Pharmaceutical and Biomedical Analysis* 76 (March): 49–58. doi:10.1016/j.jpba.2012.12.002.

Deng, Xianming, Nicolas Dzamko, Alan Prescott, Paul Davies, Qingsong Liu, Qingkai Yang, Jiing-Dwan Lee, et al. 2011. “Characterization of a Selective Inhibitor of the Parkinson’s Disease Kinase LRRK2.” *Nature Chemical Biology* 7 (4): 203–5. doi:10.1038/nchembio.538.

Desjardins, Michel. 2003. “ER-Mediated Phagocytosis: A New Membrane for New Functions.” *Nature Reviews. Immunology* 3 (4): 280–91. doi:10.1038/nri1053.

Ding, Xiaodong, and Matthew Goldberg. 2009. “Regulation of LRRK2 Stability by the E3 Ubiquitin Ligase CHIP.” *PLoS ONE* 4 (6). Public Library of Science: e5949. doi:doi: 10.1371/journal.pone.0005949.

Dobbs, R J, A Charlett, A G Purkiss, S M Dobbs, C Weller, and D W Peterson. 1999. “Association of Circulating TNF-Alpha and IL-6 with Ageing and Parkinsonism.” *Acta Neurologica Scandinavica* 100 (1): 34–41. http://www.ncbi.nlm.nih.gov/pubmed/10416510.

Dodson, M. W., T. Zhang, C. Jiang, S. Chen, and M. Guo. 2012. “Roles of the Drosophila LRRK2 Homolog in Rab7-Dependent Lysosomal Positioning.” *Human Molecular Genetics* 21 (6): 1350–63. doi:10.1093/hmg/ddr573.

Doggett, Elizabeth A., Jing Zhao, Christina N. Mork, Dongmei Hu, R. Jeremy Nichols, Ana Gorostidi, Julio Águila, et al. 2012. “Phosphorylation of LRRK2 Serines 955 and 973

Is Disrupted by Parkinson?s Disease Mutations and LRRK2 Pharmacological Inhibition." *Journal of Neurochemistry* 120 (1). BioMed Central: 37–45. doi:10.1111/j.1471-4159.2011.07537.x.

Dorsey, E. R., R. Constantinescu, J. P. Thompson, K. M. Biglan, R. G. Holloway, K. Kieburtz, F. J. Marshall, et al. 2007. "Projected Number of People with Parkinson Disease in the Most Populous Nations, 2005 through 2030." *Neurology* 68 (5): 384–86. doi:10.1212/01.wnl.0000247740.47667.03.

Dupont, Nicolas, Shanya Jiang, Manohar Pilli, Wojciech Ornatowski, Dhruva Bhattacharya, and Vojo Deretic. 2011. "Autophagy-Based Unconventional Secretory Pathway for Extracellular Delivery of IL-1β." *The EMBO Journal* 30 (23): 4701–11. doi:10.1038/emboj.2011.398.

Dzamko, Nicolas, Germaine Chua, Madelaine Ranola, Dominic Rowe, and Glenda Halliday. 2013. "Measurement of LRRK2 and Ser910/935 Phosphorylated LRRK2 in Peripheral Blood Mononuclear Cells from Idiopathic Parkinson's Disease Patients." *Journal of Parkinson's Disease* 3 (2): 145–52. doi:doi: 10.3233/jpd-130174.

Dzamko, Nicolas, Maria Deak, Faycal Hentati, Alastair D. Reith, Alan R. Prescott, Dario R. Alessi, and R. Jeremy Nichols. 2010. "Inhibition of LRRK2 Kinase Activity Leads to Dephosphorylation of Ser ^{910} /Ser ^{935} , Disruption of 14-3-3 Binding and Altered Cytoplasmic Localization." *Biochemical Journal* 430 (3): 405–13. doi:10.1042/BJ20100784.

Dzamko, Nicolas, and Glenda M Halliday. 2012. "An Emerging Role for LRRK2 in the Immune System." *Biochemical Society Transactions* 40 (5): 1134–39. http://www.ncbi.nlm.nih.gov/pubmed/22988878.

Dzamko, Nicolas, Dominic B Rowe, and Glenda M Halliday. 2016. "Increased Peripheral Inflammation in Asymptomatic Leucine-Rich Repeat Kinase 2 Mutation Carriers." *Movement Disorders : Official Journal of the Movement Disorder Society* 31 (6): 889–97. doi:10.1002/mds.26529.

Ellson, C.D., K.E. Anderson, G. Morgan, E.R. Chilvers, P. Lipp, L.R. Stephens, and P.T. Hawkins. 2001. "Phosphatidylinositol 3-Phosphate Is Generated in Phagosomal Membranes." *Current Biology*. Vol. 11. doi:10.1016/S0960-9822(01)00447-X.

Eskelinen, Eeva-Liisa, Yoshitaka Tanaka, and Paul Saftig. 2003. "At the Acidic Edge: Emerging Functions for Lysosomal Membrane Proteins." *Trends in Cell Biology* 13 (3): 137–45. http://www.ncbi.nlm.nih.gov/pubmed/12628346.

Estrada, Anthony A., Xingrong Liu, Charles Baker-Glenn, Alan Beresford, Daniel J. Burdick, Mark Chambers, Bryan K. Chan, et al. 2012. "Discovery of Highly Potent, Selective, and Brain-Penetrable Leucine-Rich Repeat Kinase 2 (LRRK2) Small Molecule Inhibitors." *Journal of Medicinal Chemistry* 55 (22). American Chemical Society: 9416–33. doi:10.1021/jm301020q.

Etemad, Samar, Rasheeda Mohd Zamin, Marc J. Ruitenberg, and Luis Filgueira. 2012. "A Novel in Vitro Human Microglia Model: Characterization of Human Monocyte-Derived Microglia." *Journal of Neuroscience Methods* 209 (1): 79–89. doi:10.1016/j.jneumeth.2012.05.025.

Fadok, V A, D L Bratton, A Konowal, P W Freed, J Y Westcott, and P M Henson. 1998. "Macrophages That Have Ingested Apoptotic Cells in Vitro Inhibit Proinflammatory

Cytokine Production through Autocrine/paracrine Mechanisms Involving TGF-Beta, PGE2, and PAF." *Journal of Clinical Investigation* 101 (4): 890–98. doi:10.1172/JCI1112.

Farrer, M, D M Maraganore, P Lockhart, A Singleton, T G Lesnick, M de Andrade, A West, R de Silva, J Hardy, and D Hernandez. 2001. "Alpha-Synuclein Gene Haplotypes Are Associated with Parkinson's Disease." *Human Molecular Genetics* 10 (17): 1847–51. http://www.ncbi.nlm.nih.gov/pubmed/11532993.

Farrer, Matt, Jennifer Kachergus, Lysia Forno, Sarah Lincoln, Deng-Shun Wang, Mary Hulihan, Demetrius Maraganore, et al. 2004. "Comparison of Kindreds with Parkinsonism and ?-Synuclein Genomic Multiplications." *Annals of Neurology* 55 (2): 174–79. doi:10.1002/ana.10846.

Fearnley, J M, and A J Lees. 1991. "Ageing and Parkinson's Disease: Substantia Nigra Regional Selectivity." *Brain : A Journal of Neurology* 114 (Pt 5 (October): 2283–2301. http://www.ncbi.nlm.nih.gov/pubmed/1933245.

Fell, Matthew, Christian Mirescu, Kallol Basu, Boonlert Cheewatrakoolpong, Duane DeMong, Michael Ellis, Lynn Hyde, et al. 2015. "MLi-2, a Potent, Selective, and Centrally Active Compound for Exploring the Therapeutic Potential and Safety of LRRK2 Kinase Inhibition." *Journal of Pharmacology and Experimental Therapeutics* 355 (3). American Society for Pharmacology and Experimental Therapeutics: 397–409. doi:doi: 10.1124/jpet.115.227587.

Fellner, Lisa, Regina Irschick, Kathrin Schanda, Markus Reindl, Lars Klimaschewski, Werner Poewe, Gregor K. Wenning, and Nadia Stefanova. 2013. "Toll-like Receptor 4 Is Required for ?-Synuclein Dependent Activation of Microglia and Astroglia." *Glia* 61 (3): 349–60. doi:10.1002/glia.22437.

Fenteany, G, and S L Schreiber. 1998. "Lactacystin, Proteasome Function, and Cell Fate." *The Journal of Biological Chemistry* 273 (15). American Society for Biochemistry and Molecular Biology: 8545–48. doi:10.1074/JBC.273.15.8545.

Fernandes, Hugo J.R., Elizabeth M. Hartfield, Helen C. Christian, Evangelia Emmanoulidou, Ying Zheng, Heather Booth, Helle Bogetofte, et al. 2016. "ER Stress and Autophagic Perturbations Lead to Elevated Extracellular α-Synuclein in GBA-N370S Parkinson's iPSC-Derived Dopamine Neurons." *Stem Cell Reports* 6 (3): 342–56. doi:10.1016/j.stemcr.2016.01.013.

Ferreira, Joaquim J., Leonor Correia Guedes, Mário Miguel Rosa, Miguel Coelho, Marina van Doeselaar, Dorothea Schweiger, Alessio Di Fonzo, Ben A. Oostra, Cristina Sampaio, and Vincenzo Bonifati. 2007. "High Prevalence ofLRRK2 Mutations in Familial and Sporadic Parkinson's Disease in Portugal." *Movement Disorders* 22 (8): 1194–1201. doi:10.1002/mds.21525.

Fischer von Mollard, G, B Stahl, C Walch-Solimena, K Takei, L Daniels, A Khoklatchev, P De Camilli, T C Südhof, and R Jahn. 1994. "Localization of Rab5 to Synaptic Vesicles Identifies Endosomal Intermediate in Synaptic Vesicle Recycling Pathway." *European Journal of Cell Biology* 65 (2): 319–26. http://www.ncbi.nlm.nih.gov/pubmed/7720727.

Franke, Andre, Dermot P B McGovern, Jeffrey C Barrett, Kai Wang, Graham L Radford-Smith, Tariq Ahmad, Charlie W Lees, et al. 2010. "Genome-Wide Meta-Analysis

Increases to 71 the Number of Confirmed Crohn's Disease Susceptibility Loci." *Nature Genetics* 42 (12): 1118–25. doi:10.1038/ng.717.

Fraser, Deborah A., Karntipa Pisalyaput, and Andrea J. Tenner. 2010. "C1q Enhances Microglial Clearance of Apoptotic Neurons and Neuronal Blebs, and Modulates Subsequent Inflammatory Cytokine Production." *Journal of Neurochemistry* 112 (3): 733–43. doi:10.1111/j.1471-4159.2009.06494.x.

Fu, Yanfang, Jennifer A Foden, Cyd Khayter, Morgan L Maeder, Deepak Reyon, J Keith Joung, and Jeffry D Sander. 2013. "High-Frequency off-Target Mutagenesis Induced by CRISPR-Cas Nucleases in Human Cells." *Nature Biotechnology* 31 (9): 822–26. doi:10.1038/nbt.2623.

Funayama, Manabu, Kazuko Hasegawa, Hisayuki Kowa, Masaaki Saito, Shoji Tsuji, and Fumiya Obata. 2002. "A New Locus for Parkinson's Disease (PARK8) Maps to Chromosome 12p11.2-q13.1." *Annals of Neurology* 51 (3): 296–301. http://www.ncbi.nlm.nih.gov/pubmed/11891824.

Funayama, Manabu, Kazuko Hasegawa, Etsuro Ohta, Noriko Kawashima, Masaru Komiyama, Hisayuki Kowa, Shoji Tsuji, and Fumiya Obata. 2005. "AnLRRK2 Mutation as a Cause for the Parkinsonism in the originalPARK8 Family." *Annals of Neurology* 57 (6): 918–21. doi:10.1002/ana.20484.

Gaig, Carles, María José Martí, Mario Ezquerra, Maria Jesús Rey, Adriana Cardozo, and Eduardo Tolosa. 2007. "G2019S LRRK2 Mutation Causing Parkinson's Disease without Lewy Bodies." *Journal of Neurology, Neurosurgery, and Psychiatry* 78 (6). BMJ Publishing Group: 626–28. doi:10.1136/jnnp.2006.107904.

Gantner, Benjamin N., Randi M. Simmons, Scott J. Canavera, Shizuo Akira, and David M. Underhill. 2003. "Collaborative Induction of Inflammatory Responses by Dectin-1 and Toll-like Receptor 2." *The Journal of Experimental Medicine* 197 (9): 1107–17. doi:10.1084/jem.20021787.

Gardai, Shyra J., Wenxian Mao, Birgitt Schüle, Michael Babcock, Sue Schoebel, Carlos Lorenzana, Jeff Alexander, et al. 2013. "Elevated Alpha-Synuclein Impairs Innate Immune Cell Function and Provides a Potential Peripheral Biomarker for Parkinson's Disease." Edited by Kostas Vekrellis. *PLoS ONE* 8 (8): e71634. doi:10.1371/journal.pone.0071634.

Gardet, Agnès, Yair Benita, Chun Li, Bruce Sands, Isabel Ballester, Christine Stevens, Joshua Korzenik, et al. 2010. "LRRK2 Is Involved in the IFN-Gamma Response and Host Response to Pathogens." *Journal of Immunology (Baltimore, Md. : 1950)* 185 (9). American Association of Immunologists: 5577–85. doi:doi: 10.4049/jimmunol.1000548.

Garneau, Josiane E., Marie-Ève Dupuis, Manuela Villion, Dennis A. Romero, Rodolphe Barrangou, Patrick Boyaval, Christophe Fremaux, Philippe Horvath, Alfonso H. Magadán, and Sylvain Moineau. 2010. "The CRISPR/Cas Bacterial Immune System Cleaves Bacteriophage and Plasmid DNA." *Nature* 468 (7320): 67–71. doi:10.1038/nature09523.

Gasper, Raphael, Simon Meyer, Katja Gotthardt, Minhajuddin Sirajuddin, and Alfred Wittinghofer. 2009. "It Takes Two to Tango: Regulation of G Proteins by Dimerization." *Nature Reviews Molecular Cell Biology* 10 (6): 423–29.

doi:10.1038/nrm2689.

Geisler, Sven, Kira M. Holmström, Diana Skujat, Fabienne C. Fiesel, Oliver C. Rothfuss, Philipp J. Kahle, and Wolfdieter Springer. 2010. “PINK1/Parkin-Mediated Mitophagy Is Dependent on VDAC1 and p62/SQSTM1.” *Nature Cell Biology* 12 (2): 119–31. doi:10.1038/ncb2012.

Gelb, D J, E Oliver, and S Gilman. 1999. “Diagnostic Criteria for Parkinson Disease.” *Archives of Neurology* 56 (1): 33–39. http://www.ncbi.nlm.nih.gov/pubmed/9923759.

Gentek, Rebecca, Kaaweh Molawi, and Michael H. Sieweke. 2014. “Tissue Macrophage Identity and Self-Renewal.” *Immunological Reviews* 262 (1): 56–73. doi:10.1111/imr.12224.

Giasson, Benoit I., Jason P. Covy, Nancy M. Bonini, Howard I. Hurtig, Matthew J. Farrer, John Q. Trojanowski, and Vivianna M. Van Deerlin. 2006a. “Biochemical and Pathological Characterization of Lrrk2.” *Annals of Neurology* 59 (2): 315–22. doi:10.1002/ana.20791.

Gillardon, F., R. Schmid, and H. Draheim. 2012. “Parkinson’s Disease-Linked Leucine-Rich Repeat Kinase 2(R1441G) Mutation Increases Proinflammatory Cytokine Release from Activated Primary Microglial Cells and Resultant Neurotoxicity.” *Neuroscience*. doi:10.1016/j.neuroscience.2012.02.001.

Ginhoux, Florent, and Martin Guilliams. 2016. “Tissue-Resident Macrophage Ontogeny and Homeostasis.” *Immunity* 44 (3): 439–49. doi:10.1016/j.immuni.2016.02.024.

Gloeckner, C. J., Norbert Kinkl, Annette Schumacher, Ralf J Braun, Eric O’Neill, Thomas Meitinger, Walter Kolch, Holger Prokisch, and Marius Ueffing. 2005. “The Parkinson Disease Causing LRRK2 Mutation I2020T Is Associated with Increased Kinase Activity.” *Human Molecular Genetics* 15 (2): 223–32. doi:10.1093/hmg/ddi439.

Gloeckner, Christian Johannes, Karsten Boldt, Felix von Zweydorf, Sandra Helm, Ludwig Wiesent, Hakan Sarioglu, and Marius Ueffing. 2010. “Phosphopeptide Analysis Reveals Two Discrete Clusters of Phosphorylation in the N-Terminus and the Roc Domain of the Parkinson-Disease Associated Protein Kinase LRRK2.” *Journal of Proteome Research* 9 (4). American Chemical Society: 1738–45. doi:10.1021/pr9008578.

Goetz, Christopher G. 2011. “The History of Parkinson’s Disease: Early Clinical Descriptions and Neurological Therapies.” *Cold Spring Harbor Perspectives in Medicine* 1 (1). Cold Spring Harbor Laboratory Press: a008862. doi:10.1101/cshperspect.a008862.

Goetz, Christopher G. 1986. “Charcot on Parkinson’s Disease.” *Movement Disorders* 1 (1): 27–32. doi:10.1002/mds.870010104.

Goker-Alpan, Ozlem, Barbara K. Stubblefield, Benoit I. Giasson, and Ellen Sidransky. 2010. “Glucocerebrosidase Is Present in α-Synuclein Inclusions in Lewy Body Disorders.” *Acta Neuropathologica* 120 (5): 641–49. doi:10.1007/s00401-010-0741-7.

Goldberg, Alfred L. 2012. “Development of Proteasome Inhibitors as Research Tools and Cancer Drugs.” *The Journal of Cell Biology* 199 (4). http://jcb.rupress.org/content/199/4/583.figures-only.

Gómez-Suaga, P, E Fdez, B Fernández, M Martínez-Salvador, M Blanca Ramírez, J

Madero-Pérez, P Rivero-Ríos, J M Fuentes, and S Hilfiker. 2014. “Novel Insights into the Neurobiology Underlying LRRK2-Linked Parkinson’s Disease.” *Neuropharmacology* 85 (October): 45–56. citeulike-article-id:13203222.

Gómez-Suaga, Patricia, Berta Luzón-Toro, Dev Churamani, Ling Zhang, Duncan Bloor-Young, Sandip Patel, Philip G. Woodman, Grant C. Churchill, and Sabine Hilfiker. 2012. “Leucine-Rich Repeat Kinase 2 Regulates Autophagy through a Calcium-Dependent Pathway Involving NAADP.” *Human Molecular Genetics* 21 (3): 511–25. doi:10.1093/hmg/ddr481.

González-Hernández, Tomás. 2010. “Vulnerability of Mesostriatal Dopaminergic Neurons in Parkinson’s Disease.” *Frontiers in Neuroanatomy* 4 (October). Frontiers Media SA: 14. doi:10.3389/fnana.2010.00140.

Gorostidi, A., J. Ruiz-Martínez, A. Lopez de Munain, A. Alzualde, and J. F. Martí Massó. 2009. “LRRK2 G2019S and R1441G Mutations Associated with Parkinson’s Disease Are Common in the Basque Country, but Relative Prevalence Is Determined by Ethnicity.” *Neurogenetics* 10 (2): 157–59. doi:10.1007/s10048-008-0162-0.

Gotthardt, Katja, Michael Weyand, Arjan Kortholt, Peter J M Van Haastert, and Alfred Wittinghofer. 2008. “Structure of the Roc–COR Domain Tandem of C. Tepidum, a Prokaryotic Homologue of the Human LRRK2 Parkinson Kinase.” *The EMBO Journal* 27 (16): 2239–49. doi:10.1038/emboj.2008.150.

Greenfield, J G, and Frances D Bosanquet. 1953. “The Brain-Stem Lesions in Parkinsonism.” *Journal of Neurology, Neurosurgery, and Psychiatry* 16 (4): 213–26. doi:10.1136/jnnp.16.4.213.

Greggio, Elisa, Shushant Jain, Ann Kingsbury, Rina Bandopadhyay, Patrick Lewis, Alice Kaganovich, Marcel P. van der Brug, et al. 2006. “Kinase Activity Is Required for the Toxic Effects of Mutant LRRK2/dardarin.” *Neurobiology of Disease* 23 (2): 329–41. doi:10.1016/j.nbd.2006.04.001.

Greggio, Elisa, Jean-Marc Taymans, Eugene Yuejun Zhen, John Ryder, Renée Vancraenenbroeck, Alexandra Beilina, Peng Sun, et al. 2009. “The Parkinson’s Disease Kinase LRRK2 Autophosphorylates Its GTPase Domain at Multiple Sites.” *Biochemical and Biophysical Research Communications* 389 (3): 449–54. doi:10.1016/j.bbrc.2009.08.163.

Griciuc, Ana, Alberto Serrano-Pozo, Antonio R. Parrado, Andrea N. Lesinski, Caroline N. Asselin, Kristina Mullin, Basavaraj Hooli, Se Hoon Choi, Bradley T. Hyman, and Rudolph E. Tanzi. 2013. “Alzheimer’s Disease Risk Gene cd33 Inhibits Microglial Uptake of Amyloid Beta.” *Neuron* 78 (4). Elsevier: 631–43. doi:10.1016/j.neuron.2013.04.014.

Guaitoli, Giambattista, Francesco Raimondi, Bernd K Gilsbach, Yacob Gómez-Llorente, Egon Deyaert, Fabiana Renzi, Xianting Li, et al. 2016. “Structural Model of the Dimeric Parkinson’s Protein LRRK2 Reveals a Compact Architecture Involving Distant Interdomain Contacts.” *Proceedings of the National Academy of Sciences of the United States of America*, June. doi:10.1073/pnas.1523708113.

Guo, Luxuan, Payal N. Gandhi, Wen Wang, Robert B. Petersen, Amy L. Wilson-Delfosse, and Shu G. Chen. 2007. “The Parkinson’s Disease-Associated Protein, Leucine-Rich Repeat Kinase 2 (LRRK2), Is an Authentic GTPase Thatstimulates Kinase Activity.”

Experimental Cell Research 313 (16): 3658–70. doi:10.1016/j.yexcr.2007.07.007.

Gurdon, J B, T R Elsdale, and M Fischberg. 1958. "Sexually Mature Individuals of Xenopus Laevis from the Transplantation of Single Somatic Nuclei." *Nature* 182 (4627): 64–65. doi:10.1038/182064a0.

Gutierrez, Maximiliano Gabriel. 2013. "Functional Role(s) of Phagosomal Rab GTPases." *Small GTPases* 4 (3): 148–58. doi:10.4161/sgtp.25604.

Guzman, Jaime N., Javier Sanchez-Padilla, David Wokosin, Jyothisri Kondapalli, Ema Ilijic, Paul T. Schumacker, and D. James Surmeier. 2010. "Oxidant Stress Evoked by Pacemaking in Dopaminergic Neurons Is Attenuated by DJ-1." *Nature* 468 (7324): 696–700. doi:10.1038/nature09536.

Häbig, Karina, Sandra Gellhaar, Birgit Heim, Verena Djuric, Florian Giesert, Wolfgang Wurst, Carolin Walter, Thomas Hentrich, Olaf Riess, and Michael Bonin. 2013. "LRRK2 Guides the Actin Cytoskeleton at Growth Cones Together with ARHGEF7 and Tropomyosin 4." *Biochimica et Biophysica Acta (BBA) - Molecular Basis of Disease* 1832 (12): 2352–67. doi:10.1016/j.bbadis.2013.09.009.

Haenseler, W; Zambon, F; Lee, H; Vowles, Jane; Rinaldi, F; Duggal, G; Houlden, H; Gwinn, K; Wray, S; Luk, K; Wade-Martins, R; James, W; Cowley, SA. 2017. "Excess α-Synuclein Compromises Phagocytosis in iPSC-Derived Macrophage." *Scientific Reports* Manuscript.

Haenseler, Walther, Stephen N. Sansom, Julian Buchrieser, Sarah E. Newey, Craig S. Moore, Francesca J. Nicholls, Satyan Chintawar, et al. 2017. "A Highly Efficient Human Pluripotent Stem Cell Microglia Model Displays a Neuronal-Co-Culture-Specific Expression Profile and Inflammatory Response." *Stem Cell Reports* 8 (6): 1727–42. doi:10.1016/j.stemcr.2017.05.017.

Hakimi, Mansoureh, Thirumahal Selvanantham, Erika Swinton, Ruth F Padmore, Youren Tong, Ghassan Kabbach, Katerina Venderova, et al. 2011. "Parkinson's Disease-Linked LRRK2 Is Expressed in Circulating and Tissue Immune Cells and Upregulated Following Recognition of Microbial Structures." *Journal of Neural Transmission (Vienna, Austria : 1996)* 118 (5): 795–808. doi:10.1007/s00702-011-0653-2.

Hatcher, John M., Hwan Geun Choi, Dario R. Alessi, and Nathanael S. Gray. 2017. "Small-Molecule Inhibitors of LRRK2." In *Advances in Neurobiology*, 14:241–64. doi:10.1007/978-3-319-49969-7_13.

Hayashi, Fumitaka, Kelly D. Smith, Adrian Ozinsky, Thomas R. Hawn, Eugene C. Yi, David R. Goodlett, Jimmy K. Eng, Shizuo Akira, David M. Underhill, and Alan Aderem. 2001. "The Innate Immune Response to Bacterial Flagellin Is Mediated by Toll-like Receptor 5." *Nature* 410 (6832): 1099–1103. doi:10.1038/35074106.

Healy, Daniel G, Mario Falchi, Sean S O'Sullivan, Vincenzo Bonifati, Alexandra Durr, Susan Bressman, Alexis Brice, et al. 2008. "Phenotype, Genotype, and Worldwide Genetic Penetrance of LRRK2-Associated Parkinson's Disease: A Case-Control Study." *The Lancet Neurology* 7 (7): 583–90. doi:10.1016/S1474-4422(08)70117-0.

Henn, Anja, Søren Lund, Maj Hedtjärn, Andreé Schrattenholz, Peter Pörzgen, and Marcel Leist. 2009. "The Suitability of BV2 Cells as Alternative Model System for Primary Microglia Cultures or for Animal Experiments Examining Brain Inflammation." *ALTEX* 26 (2): 83–94. http://www.ncbi.nlm.nih.gov/pubmed/19565166.

Hentze, M W, and A E Kulozik. 1999. “A Perfect Message: RNA Surveillance and Nonsense-Mediated Decay.” *Cell* 96 (3): 307–10. http://www.ncbi.nlm.nih.gov/pubmed/10025395.

Heo, Hye Young, Kwang-Soo Kim, Wongi Seol, P Lichtner, M Farrer, S Lincoln, J Kachergus, et al. 2010. “Coordinate Regulation of Neurite Outgrowth by LRRK2 and Its Interactor, Rab5.” *Experimental Neurobiology* 19 (2): 97. doi:10.5607/en.2010.19.2.97.

Herzig, Martin C, Carine Kolly, Elke Persohn, Diethilde Theil, Tatjana Schweizer, Thomas Hafner, Christine Stemmelen, et al. 2011. “LRRK2 Protein Levels Are Determined by Kinase Function and Are Crucial for Kidney and Lung Homeostasis in Mice.” *Human Molecular Genetics* 20 (21). Oxford University Press: 4209–23. doi:10.1093/hmg/ddr348.

Higashi, Shinji, Saskia Biskup, Andrew B. West, Daniel Trinkaus, Valina L. Dawson, Richard L.M. Faull, Henry J. Waldvogel, et al. 2007. “Localization of Parkinson?s Disease-Associated LRRK2 in Normal and Pathological Human Brain.” *Brain Research* 1155 (June): 208–19. doi:10.1016/j.brainres.2007.04.034.

Hirota, Yuko, and Yoshitaka Tanaka. 2009. “A Small GTPase, Human Rab32, Is Required for the Formation of Autophagic Vacuoles under Basal Conditions.” *Cellular and Molecular Life Sciences* 66 (17): 2913–32. doi:10.1007/s00018-009-0080-9.

Hirsch, Etienne, Ann M. Graybiel, and Yves A. Agid. 1988. “Melanized Dopaminergic Neurons Are Differentially Susceptible to Degeneration in Parkinson’s Disease.” *Nature* 334 (6180): 345–48. doi:10.1038/334345a0.

Hoenen, Claire, Audrey Gustin, Cindy Birck, Mélanie Kirchmeyer, Nicolas Beaume, Paul Felten, Luc Grandbarbe, Paul Heuschling, and Tony Heurtaux. 2016. “Alpha-Synuclein Proteins Promote Pro-Inflammatory Cascades in Microglia: Stronger Effects of the A53T Mutant.” Edited by Serge Nataf. *PLOS ONE* 11 (9): e0162717. doi:10.1371/journal.pone.0162717.

Hong, S., V. F. Beja-Glasser, B. M. Nfonoyim, A. Frouin, S. Li, S. Ramakrishnan, K. M. Merry, et al. 2016. “Complement and Microglia Mediate Early Synapse Loss in Alzheimer Mouse Models.” *Science* 352 (6286): 712–16. doi:10.1126/science.aad8373.

Hoop, M J de, L A Huber, H Stenmark, E Williamson, M Zerial, R G Parton, and C G Dotti. 1994. “The Involvement of the Small GTP-Binding Protein Rab5a in Neuronal Endocytosis.” *Neuron* 13 (1): 11–22. http://www.ncbi.nlm.nih.gov/pubmed/8043272.

Hruska, Kathleen S., Mary E. LaMarca, C. Ronald Scott, and Ellen Sidransky. 2008. “Gaucher Disease: Mutation and Polymorphism Spectrum in the Glucocerebrosidase Gene (GBA).” *Human Mutation* 29 (5): 567–83. doi:10.1002/humu.20676.

Huang, Jinsha, Lijun Hao, Nian Xiong, Xuebin Cao, Zhihou Liang, Shenggang Sun, and Tao Wang. 2009. “Involvement of Glyceraldehyde-3-Phosphate Dehydrogenase in Rotenone-Induced Cell Apoptosis: Relevance to Protein Misfolding and Aggregation.” *Brain Research* 1279 (July): 1–8. doi:10.1016/j.brainres.2009.05.011.

Hughes, A J, S E Daniel, L Kilford, and A J Lees. 1992. “Accuracy of Clinical Diagnosis of Idiopathic Parkinson’s Disease: A Clinico-Pathological Study of 100 Cases.” *Journal of Neurology, Neurosurgery, and Psychiatry* 55 (3): 181–84. http://www.ncbi.nlm.nih.gov/pubmed/1564476.

Hulihan, Mary M, Lianna Ishihara-Paul, Jennifer Kachergus, Liling Warren, Rim Amouri, Ramu Elango, Rab K Prinjha, et al. 2008. “LRRK2 Gly2019Ser Penetrance in Arab–Berber Patients from Tunisia: A Case-Control Genetic Study.” *The Lancet Neurology* 7 (7): 591–94. doi:10.1016/S1474-4422(08)70116-9.

Huynh, Kassidy, Eeva-Liisa Eskelinen, Cameron Scott, Anatoly Malevanets, Paul Saftig, and Sergio Grinstein. 2007. “LAMP Proteins Are Required for Fusion of Lysosomes with Phagosomes.” *The EMBO Journal* 26 (2). Nature Publishing Group: 313–24. doi:doi: 10.1038/sj.emboj.7601511.

Huynh, Mai-Lan N, Valerie A Fadok, and Peter M Henson. 2002. “Phosphatidylserine-Dependent Ingestion of Apoptotic Cells Promotes TGF-beta1 Secretion and the Resolution of Inflammation.” *The Journal of Clinical Investigation* 109 (1). American Society for Clinical Investigation: 41–50. doi:10.1172/JCI11638.

Ibáñez, P, A-M Bonnet, B Débarges, E Lohmann, F Tison, Y Agid, A Dürr, A Brice, and P Pollak. 2004. “Causal Relation between α-Synuclein Locus Duplication as a Cause of Familial Parkinson’s Disease.” *The Lancet* 364 (9440): 1169–71. doi:10.1016/S0140-6736(04)17104-3.

Imai, Yuzuru, Stephan Gehrke, Hua-Qin Wang, Ryosuke Takahashi, Kazuko Hasegawa, Etsuro Oota, and Bingwei Lu. 2008. “Phosphorylation of 4E-BP by LRRK2 Affects the Maintenance of Dopaminergic Neurons in Drosophila.” *The EMBO Journal* 27 (18): 2432–43. doi:10.1038/emboj.2008.163.

Ishihara, Lianna, Rachel A. Gibson, Liling Warren, Rim Amouri, Kelly Lyons, Catherine Wielinski, Christine Hunter, et al. 2007. “Screening for Lrrk2 G2019S and Clinical Comparison of Tunisian and North American Caucasian Parkinson’s Disease Families.” *Movement Disorders* 22 (1): 55–61. doi:10.1002/mds.21180.

Ishihara, Lianna, Liling Warren, Rachel Gibson, Rim Amouri, Suzanne Lesage, Alexandra Dürr, Meriem Tazir, et al. 2006. “Clinical Features of Parkinson Disease Patients With Homozygous Leucine-Rich Repeat Kinase 2 G2019S Mutations.” *Archives of Neurology* 63 (9): 1250. doi:10.1001/archneur.63.9.1250.

Islam, Shariful, Hendrik Nolte, Wright Jacob, Anna B. Ziegler, Stefanie Pütz, Yael Grosjean, Karolina Szczepanowska, et al. 2016. “Human R1441C LRRK2 Regulates the Synaptic Vesicle Proteome and Phosphoproteome in a *Drosophila* Model of Parkinson’s Disease.” *Human Molecular Genetics*, October, ddw352. doi:10.1093/hmg/ddw352.

Ito, Genta, Takeshi Iwatsubo, T. M. Dawson, V. L. Dawson, J. Q. Trojanowski, V. M. Lee, M. G. Spillantini, et al. 2012. “Re-Examination of the Dimerization State of Leucine-Rich Repeat Kinase 2: Predominance of the Monomeric Form.” *The Biochemical Journal* 441 (3). Portland Press Limited: 987–94. doi:10.1042/BJ20111215.

Iwai, A, E Masliah, M Yoshimoto, N Ge, L Flanagan, H A de Silva, A Kittel, and T Saitoh. 1995. “The Precursor Protein of Non-A Beta Component of Alzheimer’s Disease Amyloid Is a Presynaptic Protein of the Central Nervous System.” *Neuron* 14 (2): 467–75. http://www.ncbi.nlm.nih.gov/pubmed/7857654.

Jaleel, Mahaboobi, Jeremy Nichols, Maria Deak, David Campbell, Frank Gillardon, Axel Knebel, and Dario Alessi. 2007. “LRRK2 Phosphorylates Moesin at Threonine-558: Characterization of How Parkinson’s Disease Mutants Affect Kinase Activity.” *The Biochemical Journal* 405 (2): 307–17. doi:doi: 10.1042/bj20070209.

James, Nicholas G., Michelle A. Digman, Enrico Gratton, Barbara Barylko, Xiaodong Ding, Joseph P. Albanesi, Matthew S. Goldberg, and David M. Jameson. 2012. “Number and Brightness Analysis of LRRK2 Oligomerization in Live Cells.” *Biophysical Journal* 102 (11): L41–43. doi:10.1016/j.bpj.2012.04.046.

Jin, Seok Min, Michael Lazarou, Chunxin Wang, Lesley A. Kane, Derek P. Narendra, and Richard J. Youle. 2010. “Mitochondrial Membrane Potential Regulates PINK1 Import and Proteolytic Destabilization by PARL.” *The Journal of Cell Biology* 191 (5): 933–42. doi:10.1083/jcb.201008084.

Jinek, M., K. Chylinski, I. Fonfara, M. Hauer, J. A. Doudna, and E. Charpentier. 2012. “A Programmable Dual-RNA-Guided DNA Endonuclease in Adaptive Bacterial Immunity.” *Science* 337 (6096): 816–21. doi:10.1126/science.1225829.

Johnson, Janel, Coro Paisán-Ruíz, Grisel Lopez, Cynthia Crews, Angela Britton, Roniel Malkani, E.Whitney Evans, et al. 2007. “Comprehensive Screening of a North American Parkinson’s Disease Cohort for <i>LRRK2</i> Mutation.” *Neurodegenerative Diseases* 4 (5): 386–91. doi:10.1159/000105160.

Kabadi, A. M., D. G. Ousterout, I. B. Hilton, and C. A. Gersbach. 2014. “Multiplex CRISPR/Cas9-Based Genome Engineering from a Single Lentiviral Vector.” *Nucleic Acids Research* 42 (19): e147–e147. doi:10.1093/nar/gku749.

Kabeya, Y, N Mizushima, T Ueno, A Yamamoto, T Kirisako, T Noda, E Kominami, Y Ohsumi, and T Yoshimori. 2000. “LC3, a Mammalian Homologue of Yeast Apg8p, Is Localized in Autophagosome Membranes after Processing.” *The EMBO Journal* 19 (21). European Molecular Biology Organization: 5720–28. doi:10.1093/emboj/19.21.5720.

Kahle, P J, M Neumann, L Ozmen, V Muller, H Jacobsen, A Schindzielorz, M Okochi, et al. 2000. “Subcellular Localization of Wild-Type and Parkinson’s Disease-Associated Mutant Alpha -Synuclein in Human and Transgenic Mouse Brain.” *The Journal of Neuroscience : The Official Journal of the Society for Neuroscience* 20 (17): 6365–73. http://www.ncbi.nlm.nih.gov/pubmed/10964942.

Kalia, Lorraine V, and Anthony E Lang. 2015. “Parkinson’s Disease.” *The Lancet* 386 (9996): 896–912. doi:10.1016/S0140-6736(14)61393-3.

Kalkonde, Yogeshwar V., William W. Morgan, Jose Sigala, Shivani K. Maffi, Carlo Condello, William Kuziel, Seema S. Ahuja, and Sunil K. Ahuja. 2007. “Chemokines in the MPTP Model of Parkinson’s Disease: Absence of CCL2 and Its Receptor CCR2 Does Not Protect against Striatal Neurodegeneration.” *Brain Research* 1128 (1): 1–11. doi:10.1016/j.brainres.2006.08.041.

Kamikawaji, Shogo, Genta Ito, and Takeshi Iwatsubo. 2009. “Identification of the Autophosphorylation Sites of LRRK2.” *Biochemistry* 48 (46). American Chemical Society: 10963–75. doi:10.1021/bi9011379.

Kampen, J.M. Van, E.G. McGeer, and A. Jon Stoessl. 2000. “Dopamine Transporter Function Assessed by Antisense Knockdown in the Rat: Protection from Dopamine Neurotoxicity.” *Synapse* 37 (3). John Wiley & Sons, Inc.: 171–78. doi:10.1002/1098-2396(20000901)37:3<171::AID-SYN1>3.0.CO;2-R.

Kang, Beom-Sik, Olivia G French, Julianne J Sando, and Chang S Hahn. 2000. “Activation-Dependent Degradation of Protein Kinase Cη.” *Oncogene* 19 (37): 4263–72.

doi:10.1038/sj.onc.1203779.

Kapellos, Theodore S., Lewis Taylor, Heyne Lee, Sally A. Cowley, William S. James, Asif J. Iqbal, and David R. Greaves. 2016. “A Novel Real Time Imaging Platform to Quantify Macrophage Phagocytosis.” *Biochemical Pharmacology* 116 (September): 107–19. doi:10.1016/j.bcp.2016.07.011.

Kay, Denise M., Cyrus P. Zabetian, Stewart A. Factor, John G. Nutt, Ali Samii, Alida Griffith, Tom D. Bird, Patricia Kramer, Donald S. Higgins, and Haydeh Payami. 2006. “Parkinson’s Disease and *LRRK2* : Frequency of a Common Mutation in U.S. Movement Disorder Clinics.” *Movement Disorders* 21 (4): 519–23. doi:10.1002/mds.20751.

Khan, N. L., Shushant Jain, John M Lynch, Nicola Pavese, Patrick Abou-Sleiman, Janice L Holton, Daniel G Healy, et al. 2005. “Mutations in the Gene LRRK2 Encoding Dardarin (PARK8) Cause Familial Parkinson’s Disease: Clinical, Pathological, Olfactory and Functional Imaging and Genetic Data.” *Brain* 128 (12): 2786–96. doi:10.1093/brain/awh667.

Khvotchev, Mikhail V, Mindong Ren, Shigeo Takamori, Reinhard Jahn, and Thomas C Südhof. 2003. “Divergent Functions of Neuronal Rab11b in Ca2+-Regulated versus Constitutive Exocytosis.” *The Journal of Neuroscience : The Official Journal of the Society for Neuroscience* 23 (33): 10531–39. http://www.ncbi.nlm.nih.gov/pubmed/14627637.

Kim, Beomsue, Myung-Soon Yang, Dongjoo Choi, Jong-Hyeon Kim, Hye-Sun Kim, Wongi Seol, Sangdun Choi, Ilo Jou, Eun-Young Kim, and Eun-Hye Joe. 2012. “Impaired Inflammatory Responses in Murine Lrrk2-Knockdown Brain Microglia.” *PloS One* 7 (4). Public Library of Science: e34693. doi:doi: 10.1371/journal.pone.0034693.

Kim, Changyoun, Dong-Hwan Ho, Ji-Eun Suk, Sungyong You, Sarah Michael, Junghee Kang, Sung Joong Lee, et al. 2013. “Neuron-Released Oligomeric α-Synuclein Is an Endogenous Agonist of TLR2 for Paracrine Activation of Microglia.” *Nature Communications* 4. NIH Public Access: 1562. doi:10.1038/ncomms2534.

Kim, Jun, Ji-Won Byun, Insup Choi, Beomsue Kim, Hey-Kyeong Jeong, Ilo Jou, and Eunhye Joe. 2013. “PINK1 Deficiency Enhances Inflammatory Cytokine Release from Acutely Prepared Brain Slices.” *Experimental Neurobiology* 22 (1): 38. doi:10.5607/en.2013.22.1.38.

Kim, Kitai, Rui Zhao, Akiko Doi, Kitwa Ng, Juli Unternaehrer, Patrick Cahan, Huo Hongguang, et al. 2011. “Donor Cell Type Can Influence the Epigenome and Differentiation Potential of Human Induced Pluripotent Stem Cells.” *Nature Biotechnology* 29 (12): 1117–19. doi:10.1038/nbt.2052.

Kim, S, Beom S Jeon, Chaejeong Heo, Pil Seon Im, T B Ahn, J H Seo, H S Kim, et al. 2004. “Alpha-Synuclein Induces Apoptosis by Altered Expression in Human Peripheral Lymphocyte in Parkinson’s Disease.” *Faseb J* 18 (13): 1615–17. doi:10.1096/fj.04-1917fje.

Kim, Y G, J Cha, and S Chandrasegaran. 1996. “Hybrid Restriction Enzymes: Zinc Finger Fusions to Fok I Cleavage Domain.” *Proceedings of the National Academy of Sciences of the United States of America* 93 (3): 1156–60. http://www.ncbi.nlm.nih.gov/pubmed/8577732.

Kinchen, Jason, and Kodi Ravichandran. 2008. “Phagosome Maturation: Going through the Acid Test.” *Nat Rev Mol Cell Biol* 9 (10). Nature Publishing Group: 781–95. doi:doi: 10.1038/nrm2515.

Kisselev, A F, T N Akopian, V Castillo, and A L Goldberg. 1999. “Proteasome Active Sites Allosterically Regulate Each Other, Suggesting a Cyclical Bite-Chew Mechanism for Protein Breakdown.” *Molecular Cell* 4 (3): 395–402. http://www.ncbi.nlm.nih.gov/pubmed/10518220.

Kleinberger, G., Y. Yamanishi, M. Suarez-Calvet, E. Czirr, E. Lohmann, E. Cuyvers, H. Struyfs, et al. 2014. “TREM2 Mutations Implicated in Neurodegeneration Impair Cell Surface Transport and Phagocytosis.” *Science Translational Medicine* 6 (243): 243ra86-243ra86. doi:10.1126/scitranslmed.3009093.

Kleine, T O, R Hackler, and P Zöfel. 2017. “Age-Related Alterations of the Blood-Brain-Barrier (Bbb) Permeability to Protein Molecules of Different Size.” *Zeitschrift Fur Gerontologie* 26 (4): 256–59. Accessed July 29. http://www.ncbi.nlm.nih.gov/pubmed/7692679.

Ko, Han Seok, Rachel Bailey, Wanli Smith, Zhaohui Liu, Joo-Ho Shin, Yun-Il Lee, Yong-Jie Zhang, et al. 2009. “CHIP Regulates Leucine-Rich Repeat Kinase-2 Ubiquitination, Degradation, and Toxicity.” *Proceedings of the National Academy of Sciences of the United States of America* 106 (8): 2897–2902. doi:doi: 10.1073/pnas.0810123106.

Kobayashi, Norimoto, Piia Karisola, Victor Peña-Cruz, David M. Dorfman, Masahisa Jinushi, Sarah E. Umetsu, Manish J. Butte, et al. 2007. “TIM-1 and TIM-4 Glycoproteins Bind Phosphatidylserine and Mediate Uptake of Apoptotic Cells.” *Immunity* 27 (6): 927–40. doi:10.1016/j.immuni.2007.11.011.

Koenigsknecht, J., and Gary Landreth. 2004. “Microglial Phagocytosis of Fibrillar - Amyloid through a 1 Integrin-Dependent Mechanism.” *Journal of Neuroscience* 24 (44): 9838–46. doi:10.1523/JNEUROSCI.2557-04.2004.

Koziorowski, Dariusz, Ryszard Tomasiuk, Stanisław Szlufik, and Andrzej Friedman. 2012. “Inflammatory Cytokines and NT-proCNP in Parkinson’s Disease Patients.” *Cytokine* 60 (3): 762–66. doi:10.1016/j.cyto.2012.07.030.

Krejci, L., V. Altmannova, M. Spirek, and X. Zhao. 2012. “Homologous Recombination and Its Regulation.” *Nucleic Acids Research* 40 (13): 5795–5818. doi:10.1093/nar/gks270.

Kriks, Sonja, Jae-Won Shim, Jinghua Piao, Yosif M. Ganat, Dustin R. Wakeman, Zhong Xie, Luis Carrillo-Reid, et al. 2011. “Dopamine Neurons Derived from Human ES Cells Efficiently Engraft in Animal Models of Parkinson’s Disease.” *Nature* 480 (7378): 547–51. doi:10.1038/nature10648.

Krüger, Rejko, Wilfried Kuhn, Thomas Müller, Dirk Woitalla, Manuel Graeber, Sigfried Kösel, Horst Przuntek, Jörg T. Epplen, Ludger Schols, and Olaf Riess. 1998. “AlaSOPro Mutation in the Gene Encoding α-Synuclein in Parkinson’s Disease.” *Nature Genetics* 18 (2): 106–8. doi:10.1038/ng0298-106.

Kurkowska-Jastrzębska, Iwona, Aneta Wrońska, Małgorzata Kohutnicka, Andrzej Członkowski, and Anna Członkowska. 1999. “The Inflammatory Reaction Following 1-Methyl-4-Phenyl-1,2,3,6-Tetrahydropyridine Intoxication in Mouse.” *Experimental Neurology* 156 (1): 50–61. doi:10.1006/exnr.1998.6993.

Kuss, Martin, Eleni Adamopoulou, and Philipp Kahle. 2014. “Interferon-γ Induces Leucine-Rich Repeat Kinase LRRK2 via Extracellular Signal-Regulated Kinase ERK5 in Macrophages.” *Journal of Neurochemistry* 129 (6): 980–87. doi:doi: 10.1111/jnc.12668.

Langston, J W, P Ballard, J W Tetrud, and I Irwin. 1983. “Chronic Parkinsonism in Humans due to a Product of Meperidine-Analog Synthesis.” *Science (New York, N.Y.)* 219 (4587): 979–80. http://www.ncbi.nlm.nih.gov/pubmed/6823561.

Langston, J W, L S Forno, J Tetrud, A G Reeves, J A Kaplan, and D Karluk. 1999. “Evidence of Active Nerve Cell Degeneration in the Substantia Nigra of Humans Years after 1-Methyl-4-Phenyl-1,2,3,6-Tetrahydropyridine Exposure.” *Annals of Neurology* 46 (4): 598–605. http://www.ncbi.nlm.nih.gov/pubmed/10514096.

Larsen, K. E., Y. Schmitz, M. D. Troyer, E. Mosharov, P. Dietrich, A. Z. Quazi, M. Savalle, et al. 2006. “-Synuclein Overexpression in PC12 and Chromaffin Cells Impairs Catecholamine Release by Interfering with a Late Step in Exocytosis.” *Journal of Neuroscience* 26 (46): 11915–22. doi:10.1523/JNEUROSCI.3821-06.2006.

Larsen, N.J., G. Ambrosi, S.J. Mullett, S.B. Berman, and D.A. Hinkle. 2011. “DJ-1 Knock-down Impairs Astrocyte Mitochondrial Function.” *Neuroscience* 196 (November): 251–64. doi:10.1016/j.neuroscience.2011.08.016.

Latourelle, Jeanne C, Mei Sun, Mark F Lew, Oksana Suchowersky, Christine Klein, Lawrence I Golbe, Margery H Mark, et al. 2008a. “The Gly2019Ser Mutation in LRRK2is Not Fully Penetrant in Familial Parkinson’s Disease: The GenePD Study.” *BMC Medicine* 6 (1): 32. doi:10.1186/1741-7015-6-32.

Lau, Lonneke M L de, Monique M B Breteler, JT Greenamyre, and Hastings. 2006. “Epidemiology of Parkinson’s Disease.” *The Lancet. Neurology* 5 (6): 525–35. doi:10.1016/S1474-4422(06)70471-9.

Lawe, D. C., A. Chawla, E. Merithew, J. Dumas, W. Carrington, K. Fogarty, L. Lifshitz, R. Tuft, D. Lambright, and S. Corvera. 2002. “Sequential Roles for Phosphatidylinositol 3-Phosphate and Rab5 in Tethering and Fusion of Early Endosomes via Their Interaction with EEA1.” *Journal of Biological Chemistry* 277 (10): 8611–17. doi:10.1074/jbc.M109239200.

Lee, He-Jin, Ji-Eun Suk, Eun-Jin Bae, Jung-Ho Lee, Seung R. Paik, and Seung-Jae Lee. 2008. “Assembly-Dependent Endocytosis and Clearance of Extracellular a-Synuclein.” *The International Journal of Biochemistry & Cell Biology* 40 (9): 1835–49. doi:10.1016/j.biocel.2008.01.017.

Lee, Heyne, William S. James, and Sally A. Cowley. 2017. “LRRK2 in Peripheral and Central Nervous System Innate Immunity: Its Link to Parkinson’s Disease.” *Biochemical Society Transactions* 45 (1): 131–39. doi:10.1042/BST20160262.

Lee, Hyun Jung, Sung Hee Jang, Hyeyoung Kim, Joo Heon Yoon, and Kwang Chul Chung. 2012. “PINK1 Stimulates Interleukin-1β-Mediated Inflammatory Signaling via the Positive Regulation of TRAF6 and TAK1.” *Cellular and Molecular Life Sciences* 69 (19): 3301–15. doi:10.1007/s00018-012-1004-7.

Lesage, Suzanne, Pablo Ibanez, Ebba Lohmann, Pierre Pollak, François Tison, Myriem Tazir, Anne-Louise Leutenegger, et al. 2005. “G2019S LRRK2 Mutation in French and North African Families with Parkinson’s Disease.” *Annals of Neurology* 58 (5): 784–

87. doi:10.1002/ana.20636.

Lewis, Patrick A, Elisa Greggio, Alexandra Beilina, Shushant Jain, Acacia Baker, and Mark R Cookson. 2007. “The R1441C Mutation of LRRK2 Disrupts GTP Hydrolysis.” *Biochemical and Biophysical Research Communications* 357 (3). NIH Public Access: 668–71. doi:10.1016/j.bbrc.2007.04.006.

Li, X., J. C. Patel, J. Wang, M. V. Avshalumov, C. Nicholson, J. D. Buxbaum, G. A. Elder, M. E. Rice, and Z. Yue. 2010. “Enhanced Striatal Dopamine Transmission and Motor Performance with LRRK2 Overexpression in Mice Is Eliminated by Familial Parkinson’s Disease Mutation G2019S.” *Journal of Neuroscience* 30 (5): 1788–97. doi:10.1523/JNEUROSCI.5604-09.2010.

Li, Xianting, Yin-Cai Tan, Shibu Poulose, C. Warren Olanow, Xin-Yun Huang, and Zhenyu Yue. 2007. “Leucine-Rich Repeat Kinase 2 (LRRK2)/PARK8 Possesses GTPase Activity That Is Altered in Familial Parkinson?s Disease R1441C/G Mutants.” *Journal of Neurochemistry* 0 (0): 070710052154004–??? doi:10.1111/j.1471-4159.2007.04743.x.

Li, Xianting, Qing Jun Wang, Nina Pan, Sangkyu Lee, Yingming Zhao, Brian T. Chait, and Zhenyu Yue. 2011. “Phosphorylation-Dependent 14-3-3 Binding to LRRK2 Is Impaired by Common Mutations of Familial Parkinson’s Disease.” Edited by Tsuneya Ikezu. *PLoS ONE* 6 (3): e17153. doi:10.1371/journal.pone.0017153.

Liang, Gaoyang, and Yi Zhang. 2013. “Genetic and Epigenetic Variations in iPSCs: Potential Causes and Implications for Application.” *Cell Stem Cell* 13 (2). NIH Public Access: 149–59. doi:10.1016/j.stem.2013.07.001.

Liao, J., C.-X. Wu, C. Burlak, S. Zhang, H. Sahm, M. Wang, Z.-Y. Zhang, et al. 2014. “Parkinson Disease-Associated Mutation R1441H in LRRK2 Prolongs the "active State" of Its GTPase Domain.” *Proceedings of the National Academy of Sciences* 111 (11): 4055–60. doi:10.1073/pnas.1323285111.

Lill, Christina M. 2016. “Genetics of Parkinson’s Disease.” *Molecular and Cellular Probes* 30 (6): 386–96. doi:10.1016/j.mcp.2016.11.001.

Lin, Xian, Loukia Parisiadou, Xing-Long Gu, Lizhen Wang, Hoon Shim, Lixin Sun, Chengsong Xie, et al. 2009. “Leucine-Rich Repeat Kinase 2 Regulates the Progression of Neuropathology Induced by Parkinson’s-Disease-Related Mutant α-Synuclein.” *Neuron* 64 (6): 807–27. doi:10.1016/j.neuron.2009.11.006.

Lindqvist, Daniel, Sara Hall, Yulia Surova, Henrietta M. Nielsen, Shorena Janelidze, Lena Brundin, and Oskar Hansson. 2013. “Cerebrospinal Fluid Inflammatory Markers in Parkinson’s Disease – Associations with Depression, Fatigue, and Cognitive Impairment.” *Brain, Behavior, and Immunity* 33 (October): 183–89. doi:10.1016/j.bbi.2013.07.007.

Ling, Zaodung, Yuangui Zhu, Chong wai Tong, Joshua Snyder, Jack Lipton, and Paul Carvey. 2006. “Progressive Dopamine Neuron Loss Following Supra-Nigral Lipopolysaccharide (LPS) Infusion into Rats Exposed to LPS Prenatally.” *Experimental Neurology* 199 (2): 499–512. doi:doi: 10.1016/j.expneurol.2006.01.010.

Liu, J., D. Lamb, M. M. Chou, Y.-J. Liu, and G. Li. 2007. “Nerve Growth Factor-Mediated Neurite Outgrowth via Regulation of Rab5.” *Molecular Biology of the Cell* 18 (4): 1375–84. doi:10.1091/mbc.E06-08-0725.

Liu, Min, Stephanie Kang, Soumya Ray, Justin Jackson, Alexandra D Zaitsev, Scott A Gerber, Gregory D Cuny, and Marcie A Glicksman. 2011. “Kinetic, Mechanistic, and Structural Modeling Studies of Truncated Wild-Type Leucine-Rich Repeat Kinase 2 and the G2019S Mutant.” *Biochemistry* 50 (43). NIH Public Access: 9399–9408. doi:10.1021/bi201173d.

Lobbestael, E, L Civiero, T De Wit, J-M Taymans, E Greggio, and V Baekelandt. 2016. “Pharmacological LRRK2 Kinase Inhibition Induces LRRK2 Protein Destabilization and Proteasomal Degradation.” *Scientific Reports* 6 (September). Nature Publishing Group: 33897. doi:10.1038/srep33897.

Lobbestael, Evy, Jing Zhao, Iakov N. Rudenko, Aleksandra Beylina, Fangye Gao, Justin Wetter, Monique Beullens, et al. 2013. “Identification of Protein Phosphatase 1 as a Regulator of the LRRK2 Phosphorylation Cycle.” *The Biochemical Journal* 456 (1): 119–28. doi:10.1042/BJ20121772.

Lombardi, D, T Soldati, M A Riederer, Y Goda, M Zerial, and S R Pfeffer. 1993. “Rab9 Functions in Transport between Late Endosomes and the Trans Golgi Network.” *The EMBO Journal* 12 (2). European Molecular Biology Organization: 677–82. http://www.ncbi.nlm.nih.gov/pubmed/8440258.

Longatti, Andrea, Christopher A. Lamb, Minoo Razi, Shin-ichiro Yoshimura, Francis A. Barr, and Sharon A. Tooze. 2012. “TBC1D14 Regulates Autophagosome Formation via Rab11- and ULK1-Positive Recycling Endosomes.” *The Journal of Cell Biology* 197 (5): 659–75. doi:10.1083/jcb.201111079.

Loos, Ben, André du Toit, and Jan-Hendrik S Hofmeyr. 2014. “Defining and Measuring Autophagosome Flux—concept and Reality.” *Autophagy* 10 (11). Taylor & Francis: 2087–96. doi:10.4161/15548627.2014.973338.

Lopes, Fernanda Martins, Rafael Schröder, Mário Luiz Conte da Frota Júnior, Alfeu Zanotto-Filho, Carolina Beatriz Müller, André Simões Pires, Rosalva Thereza Meurer, et al. 2010. “Comparison between Proliferative and Neuron-like SH-SY5Y Cells as an in Vitro Model for Parkinson Disease Studies.” *Brain Research* 1337 (June): 85–94. doi:10.1016/j.brainres.2010.03.102.

López de Maturana, Rakel, Valérie Lang, Amaia Zubiarrain, Amaya Sousa, Nerea Vázquez, Ana Gorostidi, Julio Águila, et al. 2016. “Mutations in LRRK2 Impair NF-κB Pathway in iPSC-Derived Neurons.” *Journal of Neuroinflammation* 13 (1): 295. doi:10.1186/s12974-016-0761-x.

Lu, Z, D Liu, A Hornia, W Devonish, M Pagano, and D A Foster. 1998. “Activation of Protein Kinase C Triggers Its Ubiquitination and Degradation.” *Molecular and Cellular Biology* 18 (2). American Society for Microbiology (ASM): 839–45. http://www.ncbi.nlm.nih.gov/pubmed/9447980.

Lu, Zhimin, and Tony Hunter. 2009. “Degradation of Activated Protein Kinases by Ubiquitination.” *Annual Review of Biochemistry* 78: 435–75. doi:10.1146/annurev.biochem.013008.092711.

Lücking, Christoph B., Alexandra Dürr, Vincenzo Bonifati, Jenny Vaughan, Giuseppe De Michele, Thomas Gasser, Biswadjiet S. Harhangi, et al. 2000. “Association between Early-Onset Parkinson’s Disease and Mutations in the *Parkin* Gene.” *New England Journal of Medicine* 342 (21): 1560–67. doi:10.1056/NEJM200005253422103.

Luerman, Gregory C., Chuong Nguyen, Harry Samaroo, Paula Loos, Hualin Xi, Andres Hurtado-Lorenzo, Elie Needle, et al. 2014. “Phosphoproteomic Evaluation of Pharmacological Inhibition of Leucine-Rich Repeat Kinase 2 Reveals Significant off-Target Effects of LRRK-2-IN-1.” *Journal of Neurochemistry* 128 (4): 561–76. doi:10.1111/jnc.12483.

Luzon-Toro, B., E. R. de la Torre, A. Delgado, J. Perez-Tur, and S. Hilfiker. 2007. “Mechanistic Insight into the Dominant Mode of the Parkinson’s Disease-Associated G2019S LRRK2 Mutation.” *Human Molecular Genetics* 16 (17): 2031–39. doi:10.1093/hmg/ddm151.

MacLeod, David, Julia Dowman, Rachel Hammond, Thomas Leete, Keiichi Inoue, and Asa Abeliovich. 2006. “The Familial Parkinsonism Gene LRRK2 Regulates Neurite Process Morphology.” *Neuron* 52 (4): 587–93. doi:10.1016/j.neuron.2006.10.008.

Maekawa, Tatsunori, Toshikuni Sasaoka, Sadahiro Azuma, Takafumi Ichikawa, Heather L. Melrose, Matthew J. Farrer, Fumiya Obata, et al. 2016. “Leucine-Rich Repeat Kinase 2 (LRRK2) Regulates α-Synuclein Clearance in Microglia.” *BMC Neuroscience* 17 (1). BioMed Central: 77. doi:10.1186/s12868-016-0315-2.

Maio, R. Di, P. J. Barrett, E. K. Hoffman, C. W. Barrett, A. Zharikov, A. Borah, X. Hu, et al. 2016. “-Synuclein Binds to TOM20 and Inhibits Mitochondrial Protein Import in Parkinsons Disease.” *Science Translational Medicine* 8 (342): 342ra78-342ra78. doi:10.1126/scitranslmed.aaf3634.

Malgieri, Gaetano, and David Eliezer. 2008. “Structural Effects of Parkinson’s Disease Linked DJ-1 Mutations.” *Protein Science* 17 (5): 855–68. doi:10.1110/ps.073411608.

Mali, P., L. Yang, K. M. Esvelt, J. Aach, M. Guell, J. E. DiCarlo, J. E. Norville, and G. M. Church. 2013. “RNA-Guided Human Genome Engineering via Cas9.” *Science* 339 (6121): 823–26. doi:10.1126/science.1232033.

Manzanillo, Paolo S., Janelle S. Ayres, Robert O. Watson, Angela C. Collins, Gianne Souza, Chris S. Rae, David S. Schneider, Ken Nakamura, Michael U. Shiloh, and Jeffery S. Cox. 2013. “The Ubiquitin Ligase Parkin Mediates Resistance to Intracellular Pathogens.” *Nature* 501 (7468): 512–16. doi:10.1038/nature12566.

Maraganore, Demetrius M., Mariza de Andrade, Alexis Elbaz, Matthew J Farrer, John P Ioannidis, Rejko Krüger, Walter A Rocca, et al. 2006. “Collaborative Analysis of α-Synuclein Gene Promoter Variability and Parkinson Disease.” *JAMA* 296 (6): 661. doi:10.1001/jama.296.6.661.

Marder, Karen, Yuanjia Wang, Roy N Alcalay, Helen Mejia-Santana, Ming-Xin Tang, Annie Lee, Deborah Raymond, et al. 2015. “Age-Specific Penetrance of LRRK2 G2019S in the Michael J. Fox Ashkenazi Jewish LRRK2 Consortium.” *Neurology* 85 (1). American Academy of Neurology: 89–95. doi:10.1212/WNL.0000000000001708.

Marey-Semper, I, M Gelman, and M Lévi-Strauss. 1995. “A Selective Toxicity toward Cultured Mesencephalic Dopaminergic Neurons Is Induced by the Synergistic Effects of Energetic Metabolism Impairment and NMDA Receptor Activation.” *The Journal of Neuroscience : The Official Journal of the Society for Neuroscience* 15 (9): 5912–18. http://www.ncbi.nlm.nih.gov/pubmed/7666176.

Marín, Ignacio, Wouter N van Egmond, and Peter J M van Haastert. 2008. “The Roco Protein Family: A Functional Perspective.” *FASEB Journal : Official Publication of*

the Federation of American Societies for Experimental Biology 22 (9): 3103–10. doi:10.1096/fj.08-111310.

Marker, Daniel, Jenna Puccini, Taryn Mockus, Justin Barbieri, Shao-Ming Lu, and Harris Gelbard. 2012. "LRRK2 Kinase Inhibition Prevents Pathological Microglial Phagocytosis in Response to HIV-1 Tat Protein." *Journal of Neuroinflammation* 9 (1): 261. doi:doi: 10.1186/1742-2094-9-261.

Marongiu, Roberta, Daniele Ghezzi, Tamara Ialongo, Francesco Soleti, Antonio Elia, Stefania Cavone, Alberto Albanese, et al. 2006. "Frequency and Phenotypes of LRRK2 G2019S Mutation in Italian Patients with Parkinson's Disease." *Movement Disorders* 21 (8): 1232–35. doi:10.1002/mds.20890.

Mata, Ignacio F., Julie P. Taylor, Jennifer Kachergus, Mary Hulihan, Cecilia Huerta, Carlos Lahoz, Marta Blazquez, et al. 2005. "LRRK2 R1441G in Spanish Patients with Parkinson's Disease." *Neuroscience Letters* 382 (3): 309–11. doi:10.1016/j.neulet.2005.03.033.

Matsuda, Noriyuki, Shigeto Sato, Kahori Shiba, Kei Okatsu, Keiko Saisho, Clement A. Gautier, Yu-shin Sou, et al. 2010. "PINK1 Stabilized by Mitochondrial Depolarization Recruits Parkin to Damaged Mitochondria and Activates Latent Parkin for Mitophagy." *The Journal of Cell Biology* 189 (2): 211–21. doi:10.1083/jcb.200910140.

Matsuda, W., T. Furuta, K. C. Nakamura, H. Hioki, F. Fujiyama, R. Arai, and T. Kaneko. 2009. "Single Nigrostriatal Dopaminergic Neurons Form Widely Spread and Highly Dense Axonal Arborizations in the Neostriatum." *Journal of Neuroscience* 29 (2): 444–53. doi:10.1523/JNEUROSCI.4029-08.2009.

Matta, Samer, Kristof Van Kolen, Raquel da Cunha, Geert van den Bogaart, Wim Mandemakers, Katarzyna Miskiewicz, Pieter-Jan De Bock, et al. 2012. "LRRK2 Controls an EndoA Phosphorylation Cycle in Synaptic Endocytosis." *Neuron* 75 (6): 1008–21. doi:10.1016/j.neuron.2012.08.022.

Matthaei, Klaus I. 2007. "Genetically Manipulated Mice: A Powerful Tool with Unsuspected Caveats." *The Journal of Physiology* 582 (Pt 2). Wiley-Blackwell: 481–88. doi:10.1113/jphysiol.2007.134908.

McCormack, Alison L, and Donato A Di Monte. 2003. "Effects of L-Dopa and Other Amino Acids against Paraquat-Induced Nigrostriatal Degeneration." *Journal of Neurochemistry* 85 (1): 82–86. http://www.ncbi.nlm.nih.gov/pubmed/12641729.

McCormack, Alison L, Mona Thiruchelvam, Amy B Manning-Bog, Christine Thiffault, J William Langston, Deborah A Cory-Slechta, and Donato A Di Monte. 2002. "Environmental Risk Factors and Parkinson's Disease: Selective Degeneration of Nigral Dopaminergic Neurons Caused by the Herbicide Paraquat." *Neurobiology of Disease* 10 (2): 119–27. http://www.ncbi.nlm.nih.gov/pubmed/12127150.

McGeer, P L, S Itagaki, H Akiyama, and E G McGeer. 1988. "Rate of Cell Death in Parkinsonism Indicates Active Neuropathological Process." *Annals of Neurology* 24 (4): 574–76. citeulike-article-id:13448672.

Medzhitov, Ruslan, and Tiffany Horng. 2009. "Transcriptional Control of the Inflammatory Response." *Nature Reviews Immunology* 9 (10): 692–703. doi:10.1038/nri2634.

Meissner, Cathrin, Holger Lorenz, Andreas Weihofen, Dennis J. Selkoe, and Marius K.

Lemberg. 2011. “The Mitochondrial Intramembrane Protease PARL Cleaves Human Pink1 to Regulate Pink1 Trafficking.” *Journal of Neurochemistry* 117 (5): 856–67. doi:10.1111/j.1471-4159.2011.07253.x.

Melrose, H.L., J.C. Dächsel, B. Behrouz, S.J. Lincoln, M. Yue, K.M. Hinkle, C.B. Kent, et al. 2010. “Impaired Dopaminergic Neurotransmission and Microtubule-Associated Protein Tau Alterations in Human LRRK2 Transgenic Mice.” *Neurobiology of Disease* 40 (3): 503–17. doi:10.1016/j.nbd.2010.07.010.

Mertens, Jerome, Apua C.M. Paquola, Manching Ku, Emily Hatch, Lena Böhnke, Shauheen Ladjevardi, Sean McGrath, et al. 2015. “Directly Reprogrammed Human Neurons Retain Aging-Associated Transcriptomic Signatures and Reveal Age-Related Nucleocytoplasmic Defects.” *Cell Stem Cell* 17 (6): 705–18. doi:10.1016/j.stem.2015.09.001.

Miklossy, Judith, Tetsuaki Arai, Jian-Ping Guo, Andis Klegeris, Sheng Yu, Edith G. McGeer, and Patrick L. McGeer. 2006. “LRRK2 Expression in Normal and Pathologic Human Brain and in Human Cell Lines.” *Journal of Neuropathology & Experimental Neurology* 65 (10).

Miller, Jeffrey C, Michael C Holmes, Jianbin Wang, Dmitry Y Guschin, Ya-Li Lee, Igor Rupniewski, Christian M Beausejour, et al. 2007. “An Improved Zinc-Finger Nuclease Architecture for Highly Specific Genome Editing.” *Nature Biotechnology* 25 (7): 778–85. doi:10.1038/nbt1319.

Mizuno, Y, N Sone, and T Saitoh. 1987. “Effects of 1-Methyl-4-Phenyl-1,2,3,6-Tetrahydropyridine and 1-Methyl-4-Phenylpyridinium Ion on Activities of the Enzymes in the Electron Transport System in Mouse Brain.” *Journal of Neurochemistry* 48 (6): 1787–93. http://www.ncbi.nlm.nih.gov/pubmed/3106573.

Moehle, Mark, João Paulo Lima Daher, Travis Hull, Ravindra Boddu, Hisham Abdelmotilib, James Mobley, George Kannarkat, Malú Tansey, and Andrew West. 2015. “The G2019S LRRK2 Mutation Increases Myeloid Cell Chemotactic Responses and Enhances LRRK2 Binding to Actin-Regulatory Proteins.” *Human Molecular Genetics* 24 (15): 4250–67. citeulike-article-id:13600342.

Moehle, Mark, Philip Webber, Tonia Tse, Nour Sukar, David Standaert, Tara DeSilva, Rita Cowell, and Andrew West. 2012. “LRRK2 Inhibition Attenuates Microglial Inflammatory Responses.” *The Journal of Neuroscience* 32 (5). Society for Neuroscience: 1602–11. doi:doi: 10.1523/jneurosci.5601-11.2012.

Mogi, M., A. Togari, T. Kondo, Y. Mizuno, O. Komure, S. Kuno, H. Ichinose, and T. Nagatsu. 2000. “Caspase Activities and Tumor Necrosis Factor Receptor R1 (p55) Level Are Elevated in the Substantia Nigra from Parkinsonian Brain.” *Journal of Neural Transmission* 107 (3): 335–41. doi:10.1007/s007020050028.

Mouatt-Prigent, A., M.-P. Muriel, W.-J. Gu, K. H. El Hachimi, C. B. L[illegible]cking, A. Brice, and E. C. Hirsch. 2004. “Ultrastructural Localization of Parkin in the Rat Brainstem, Thalamus and Basal Ganglia.” *Journal of Neural Transmission* 111 (10–11): 1209–18. doi:10.1007/s00702-004-0144-9.

Muda, Kathrin, Daniela Bertinetti, Frank Gesellchen, Jennifer Sarah Hermann, Felix von Zweydorf, Arie Geerlof, Anette Jacob, Marius Ueffing, Christian Johannes Gloeckner, and Friedrich W Herberg. 2014. “Parkinson-Related LRRK2 Mutation R1441C/G/H

Impairs PKA Phosphorylation of LRRK2 and Disrupts Its Interaction with 14-3-3." *Proceedings of the National Academy of Sciences of the United States of America* 111 (1). National Academy of Sciences: E34-43. doi:10.1073/pnas.1312701111.

Mullett, Steven J., and David A. Hinkle. 2011. "DJ-1 Deficiency in Astrocytes Selectively Enhances Mitochondrial Complex I Inhibitor-Induced Neurotoxicity." *Journal of Neurochemistry* 117 (3): 375–87. doi:10.1111/j.1471-4159.2011.07175.x.

Munafó, Daniela B, and María I Colombo. 2002. "Induction of Autophagy Causes Dramatic Changes in the Subcellular Distribution of GFP-Rab24." *Traffic (Copenhagen, Denmark)* 3 (7): 472–82. http://www.ncbi.nlm.nih.gov/pubmed/12047555.

Munhoz, Renato P., Yosuke Wakutani, Connie Marras, Helio A. Teive, Salmo Raskin, Lineu C. Werneck, Danielle Moreno, Christine Sato, Anthony E. Lang, and Ekaterina Rogaeva. 2008. "The G2019S *LRRK2* Mutation in Brazilian Patients with Parkinson's Disease: Phenotype in Monozygotic Twins." *Movement Disorders* 23 (2): 290–94. doi:10.1002/mds.21832.

Murphy, D D, S M Rueter, J Q Trojanowski, and V M Lee. 2000. "Synucleins Are Developmentally Expressed, and Alpha-Synuclein Regulates the Size of the Presynaptic Vesicular Pool in Primary Hippocampal Neurons." *The Journal of Neuroscience : The Official Journal of the Society for Neuroscience* 20 (9): 3214–20. http://www.ncbi.nlm.nih.gov/pubmed/10777786.

Nakayama, M., H. Akiba, K. Takeda, Y. Kojima, M. Hashiguchi, M. Azuma, H. Yagita, and K. Okumura. 2009. "Tim-3 Mediates Phagocytosis of Apoptotic Cells and Cross-Presentation." *Blood* 113 (16): 3821–30. doi:10.1182/blood-2008-10-185884.

Narendra, Derek, Atsushi Tanaka, Der-Fen Suen, and Richard J. Youle. 2008. "Parkin Is Recruited Selectively to Impaired Mitochondria and Promotes Their Autophagy." *The Journal of Cell Biology* 183 (5): 795–803. doi:10.1083/jcb.200809125.

Nemani, Venu M., Wei Lu, Victoria Berge, Ken Nakamura, Bibiana Onoa, Michael K. Lee, Farrukh A. Chaudhry, Roger A. Nicoll, and Robert H. Edwards. 2010. "Increased Expression of α-Synuclein Reduces Neurotransmitter Release by Inhibiting Synaptic Vesicle Reclustering after Endocytosis." *Neuron* 65 (1): 66–79. doi:10.1016/j.neuron.2009.12.023.

Ness, Daniel, Zhao Ren, Shyra Gardai, Douglas Sharpnack, Victor J. Johnson, Richard J. Brennan, Elizabeth F. Brigham, and Andrew J. Olaharski. 2013. "Leucine-Rich Repeat Kinase 2 (LRRK2)-Deficient Rats Exhibit Renal Tubule Injury and Perturbations in Metabolic and Immunological Homeostasis." Edited by Shree Ram Singh. *PLoS ONE* 8 (6): e66164. doi:10.1371/journal.pone.0066164.

Nguyen, Ha Nam, Blake Byers, Branden Cord, Aleksandr Shcheglovitov, James Byrne, Prachi Gujar, Kehkooi Kee, et al. 2011. "LRRK2 Mutant iPSC-Derived DA Neurons Demonstrate Increased Susceptibility to Oxidative Stress." *Cell Stem Cell* 8 (3). NIH Public Access: 267–80. doi:10.1016/j.stem.2011.01.013.

Nichols, R Jeremy, Nicolas Dzamko, Nicholas a Morrice, David G Campbell, Maria Deak, Alban Ordureau, Thomas Macartney, et al. 2010. "14-3-3 Binding to LRRK2 Is Disrupted by Multiple Parkinson's Disease-Associated Mutations and Regulates Cytoplasmic Localization." *The Biochemical Journal* 430 (3): 393–404. doi:10.1042/BJ20100483.

Nicklas, W J, I Vyas, and R E Heikkila. 1985. “Inhibition of NADH-Linked Oxidation in Brain Mitochondria by 1-Methyl-4-Phenyl-Pyridine, a Metabolite of the Neurotoxin, 1-Methyl-4-Phenyl-1,2,5,6-Tetrahydropyridine.” *Life Sciences* 36 (26): 2503–8. http://www.ncbi.nlm.nih.gov/pubmed/2861548.

Nozawa, Takashi, Chihiro Aikawa, Akira Goda, Fumito Maruyama, Shigeyuki Hamada, and Ichiro Nakagawa. 2012. “The Small GTPases Rab9A and Rab23 Function at Distinct Steps in Autophagy during Group A Streptococcus Infection.” *Cellular Microbiology* 14 (8): 1149–65. doi:10.1111/j.1462-5822.2012.01792.x.

Ohi, Yuki, Han Qin, Chibo Hong, Laure Blouin, Jose M. Polo, Tingxia Guo, Zhongxia Qi, et al. 2011. “Incomplete DNA Methylation Underlies a Transcriptional Memory of Somatic Cells in Human iPS Cells.” *Nature Cell Biology* 13 (5): 541–49. doi:10.1038/ncb2239.

Orenstein, Samantha J, Sheng-Han Kuo, Inmaculada Tasset, Esperanza Arias, Hiroshi Koga, Irene Fernandez-Carasa, Etty Cortes, et al. 2013. “Interplay of LRRK2 with Chaperone-Mediated Autophagy.” *Nature Neuroscience* 16 (4): 394–406. doi:10.1038/nn.3350.

Orr, C. F., Dominic B Rowe, Yoshikuni Mizuno, Hideo Mori, and Glenda M Halliday. 2005. “A Possible Role for Humoral Immunity in the Pathogenesis of Parkinson’s Disease.” *Brain* 128 (11): 2665–74. doi:10.1093/brain/awh625.

Pagano, Gennaro, Nicola Ferrara, David J. Brooks, and Nicola Pavese. 2016. “Age at Onset and Parkinson Disease Phenotype.” *Neurology* 86 (15): 1400–1407. doi:10.1212/WNL.0000000000002461.

Paisán-Ruíz, C, S Jain, E W Evans, W P Gilks, J Simón, M van der Brug, A López de Munain, et al. 2004. “Cloning of the Gene Containing Mutations That Cause PARK8-Linked Parkinson's Disease.” *Neuron* 44 (4): 595–600. http://www.ncbi.nlm.nih.gov/pubmed/15541308.

Panicker, L. M., D. Miller, T. S. Park, B. Patel, J. L. Azevedo, O. Awad, M. A. Masood, et al. 2012. “Induced Pluripotent Stem Cell Model Recapitulates Pathologic Hallmarks of Gaucher Disease.” *Proceedings of the National Academy of Sciences* 109 (44): 18054–59. doi:10.1073/pnas.1207889109.

Papapetropoulos, Spiridon, Carlos Singer, Owen A. Ross, Mathias Toft, Joseph L. Johnson, Matthew J. Farrer, and Deborah C. Mash. 2006. “Clinical Heterogeneity of the LRRK2 G2019S Mutation.” *Archives of Neurology* 63 (9): 1242. doi:10.1001/archneur.63.9.1242.

Parisiadou, L., C. Xie, H. J. Cho, X. Lin, X.-L. Gu, C.-X. Long, E. Lobbestael, et al. 2009. “Phosphorylation of Ezrin/Radixin/Moesin Proteins by LRRK2 Promotes the Rearrangement of Actin Cytoskeleton in Neuronal Morphogenesis.” *Journal of Neuroscience* 29 (44): 13971–80. doi:10.1523/JNEUROSCI.3799-09.2009.

Parisiadou, Loukia, and Huaibin Cai. 2010. “LRRK2 Function on Actin and Microtubule Dynamics in Parkinson Disease.” *Communicative & Integrative Biology* 3 (5). Taylor & Francis: 396–400. doi:10.4161/cib.3.5.12286.

Park, Daeho, Annie-Carole Tosello-Trampont, Michael R. Elliott, Mingjian Lu, Lisa B. Haney, Zhong Ma, Alexander L. Klibanov, James W. Mandell, and Kodi S. Ravichandran. 2007. “BAI1 Is an Engulfment Receptor for Apoptotic Cells Upstream

of the ELMO/Dock180/Rac Module." *Nature* 450 (7168): 430–34. doi:10.1038/nature06329.

Park, Ji-Young, Seung R. Paik, Ilo Jou, and Sang Myun Park. 2008. "Microglial Phagocytosis Is Enhanced by Monomeric α-Synuclein, Not Aggregated α-Synuclein: Implications for Parkinson's Disease." *Glia* 56 (11): 1215–23. doi:10.1002/glia.20691.

Parkinson, James. 2002. "An Essay on the Shaking Palsy." *The Journal of Neuropsychiatry and Clinical Neurosciences* 14 (2): 223–36. doi:10.1176/jnp.14.2.223.

Pattanayak, Vikram, Steven Lin, John P Guilinger, Enbo Ma, Jennifer A Doudna, and David R Liu. 2013. "High-Throughput Profiling of off-Target DNA Cleavage Reveals RNA-Programmed Cas9 Nuclease Specificity." *Nature Biotechnology* 31 (9): 839–43. doi:10.1038/nbt.2673.

Pei, G., M. Bronietzki, and M. G. Gutierrez. 2012. "Immune Regulation of Rab Proteins Expression and Intracellular Transport." *Journal of Leukocyte Biology* 92 (1): 41–50. doi:10.1189/jlb.0212076.

Peplowska, Karolina, Daniel F. Markgraf, Clemens W. Ostrowicz, Gert Bange, and Christian Ungermann. 2007. "The CORVET Tethering Complex Interacts with the Yeast Rab5 Homolog Vps21 and Is Involved in Endo-Lysosomal Biogenesis." *Developmental Cell* 12 (5): 739–50. doi:10.1016/j.devcel.2007.03.006.

Perera, G., M. Ranola, D. B. Rowe, G. M. Halliday, and N. Dzamko. 2016. "Inhibitor Treatment of Peripheral Mononuclear Cells from Parkinson's Disease Patients Further Validates LRRK2 Dephosphorylation as a Pharmacodynamic Biomarker." *Scientific Reports* 6 (1): 31391. doi:10.1038/srep31391.

Piccoli, G., S. B. Condliffe, M. Bauer, F. Giesert, K. Boldt, S. De Astis, A. Meixner, et al. 2011. "LRRK2 Controls Synaptic Vesicle Storage and Mobilization within the Recycling Pool." *Journal of Neuroscience* 31 (6): 2225–37. doi:10.1523/JNEUROSCI.3730-10.2011.

Pickrell, Alicia M., and Richard J. Youle. 2015. "The Roles of PINK1, Parkin, and Mitochondrial Fidelity in Parkinson's Disease." *Neuron* 85 (2): 257–73. doi:10.1016/j.neuron.2014.12.007.

Plessis, A, A Perrin, J E Haber, and B Dujon. 1992. "Site-Specific Recombination Determined by I-SceI, a Mitochondrial Group I Intron-Encoded Endonuclease Expressed in the Yeast Nucleus." *Genetics* 130 (3): 451–60. http://www.ncbi.nlm.nih.gov/pubmed/1551570.

Plowey, Edward D., Salvatore J. Cherra, Yong-Jian Liu, and Charleen T. Chu. 2008. "Role of Autophagy in G2019S-LRRK2-Associated Neurite Shortening in Differentiated SH-SY5Y Cells." *Journal of Neurochemistry* 105 (3): 1048–56. doi:10.1111/j.1471-4159.2008.05217.x.

Polymeropoulos, M H, J J Higgins, L I Golbe, W G Johnson, S E Ide, G Di Iorio, G Sanges, et al. 1996. "Mapping of a Gene for Parkinson's Disease to Chromosome 4q21-q23." *Science (New York, N.Y.)* 274 (5290): 1197–99. http://www.ncbi.nlm.nih.gov/pubmed/8895469.

Polymeropoulos, M H, C Lavedan, E Leroy, S E Ide, A Dehejia, A Dutra, B Pike, et al. 1997. "Mutation in the Alpha-Synuclein Gene Identified in Families with Parkinson's

Disease." *Science (New York, N.Y.)* 276 (5321): 2045–47. http://www.ncbi.nlm.nih.gov/pubmed/9197268.

Püntener, Ursula, Steven G Booth, V Hugh Perry, and Jessica L Teeling. 2012. "Long-Term Impact of Systemic Bacterial Infection on the Cerebral Vasculature and Microglia." *Journal of Neuroinflammation* 9 (June). BioMed Central: 146. doi:10.1186/1742-2094-9-146.

Puopolo, M., E. Raviola, and B. P. Bean. 2007. "Roles of Subthreshold Calcium Current and Sodium Current in Spontaneous Firing of Mouse Midbrain Dopamine Neurons." *Journal of Neuroscience* 27 (3): 645–56. doi:10.1523/JNEUROSCI.4341-06.2007.

Rabinovitch, M. 1995. "Professional and Non-Professional Phagocytes: An Introduction." *Trends in Cell Biology* 5 (March): 85–87. doi:10.1016/S0962-8924(00)88955-2.

Rajkumar, S. Vincent, Paul G. Richardson, Teru Hideshima, and Kenneth C. Anderson. 2005. "Proteasome Inhibition As a Novel Therapeutic Target in Human Cancer." *Journal of Clinical Oncology* 23 (3): 630–39. doi:10.1200/JCO.2005.11.030.

Rajput, A., D. W. Dickson, C. A. Robinson, O. A. Ross, J. C. Dachsel, S. J. Lincoln, S. A. Cobb, M. L. Rajput, and M. J. Farrer. 2006. "Parkinsonism, Lrrk2 G2019S, and Tau Neuropathology." *Neurology* 67 (8): 1506–8. doi:10.1212/01.wnl.0000240220.33950.0c.

Ramonet, David, João Paulo L. Daher, Brian M. Lin, Klodjan Stafa, Jaekwang Kim, Rebecca Banerjee, Marie Westerlund, et al. 2011. "Dopaminergic Neuronal Loss, Reduced Neurite Complexity and Autophagic Abnormalities in Transgenic Mice Expressing G2019S Mutant LRRK2." Edited by Huaibin Cai. *PLoS ONE* 6 (4): e18568. doi:10.1371/journal.pone.0018568.

Ramsden, Nigel, Jessica Perrin, Zhao Ren, Byoung Dae Lee, Nico Zinn, Valina L. Dawson, Danny Tam, et al. 2011. "Chemoproteomics-Based Design of Potent LRRK2-Selective Lead Compounds That Attenuate Parkinson's Disease-Related Toxicity in Human Neurons." *ACS Chemical Biology* 6 (10): 1021–28. doi:10.1021/cb2002413.

Ran, F. Ann, Patrick D. Hsu, Chie-Yu Lin, Jonathan S. Gootenberg, Silvana Konermann, Alexandro E. Trevino, David A. Scott, et al. 2013. "Double Nicking by RNA-Guided CRISPR Cas9 for Enhanced Genome Editing Specificity." *Cell* 154 (6): 1380–89. doi:10.1016/j.cell.2013.08.021.

Ravikumar, B., S. Imarisio, S. Sarkar, C. J. O'Kane, and D. C. Rubinsztein. 2008. "Rab5 Modulates Aggregation and Toxicity of Mutant Huntingtin through Macroautophagy in Cell and Fly Models of Huntington Disease." *Journal of Cell Science* 121 (10): 1649–60. doi:10.1242/jcs.025726.

Reeve, Amy K., Tae-Kyung Park, Evelyn Jaros, Graham R Campbell, Nichola Z Lax, Philippa D Hepplewhite, Kim J Krishnan, et al. 2012. "Relationship Between Mitochondria and α-Synuclein." *Archives of Neurology* 69 (3): 385. doi:10.1001/archneurol.2011.2675.

Reinhardt, Peter, Benjamin Schmid, Lena F. Burbulla, David C. Schöndorf, Lydia Wagner, Michael Glatza, Susanne Höing, et al. 2013. "Genetic Correction of a LRRK2 Mutation in Human iPSCs Links Parkinsonian Neurodegeneration to ERK-Dependent Changes in Gene Expression." *Cell Stem Cell* 12 (3): 354–67. doi:10.1016/j.stem.2013.01.008.

Reith, Alastair D., Paul Bamborough, Karamjit Jandu, Daniele Andreotti, Lucy Mensah, Pamela Dossang, Hwan Geun Choi, et al. 2012. “GSK2578215A; A Potent and Highly Selective 2-Arylmethyloxy-5-Substitutent-N-Arylbenzamide LRRK2 Kinase Inhibitor.” *Bioorganic & Medicinal Chemistry Letters* 22 (17): 5625–29. doi:10.1016/j.bmcl.2012.06.104.

Rettig, L., S. P. Haen, A. G. Bittermann, L. von Boehmer, A. Curioni, S. D. Kramer, A. Knuth, and S. Pascolo. 2010. “Particle Size and Activation Threshold: A New Dimension of Danger Signaling.” *Blood* 115 (22): 4533–41. doi:10.1182/blood-2009-11-247817.

Riederer, M A, T Soldati, A D Shapiro, J Lin, and S R Pfeffer. 1994. “Lysosome Biogenesis Requires Rab9 Function and Receptor Recycling from Endosomes to the Trans-Golgi Network.” *The Journal of Cell Biology* 125 (3): 573–82. http://www.ncbi.nlm.nih.gov/pubmed/7909812.

Rink, Jochen, Eric Ghigo, Yannis Kalaidzidis, and Marino Zerial. 2005. “Rab Conversion as a Mechanism of Progression from Early to Late Endosomes.” *Cell* 122 (5): 735–49. doi:10.1016/j.cell.2005.06.043.

Rizzu, Patrizia, David A. Hinkle, Victoria Zhukareva, Vincenzo Bonifati, Lies-Anne Severijnen, Daniel Martinez, Rivka Ravid, et al. 2004. “DJ-1 Colocalizes with Tau Inclusions: A Link between Parkinsonism and Dementia.” *Annals of Neurology* 55 (1): 113–18. doi:10.1002/ana.10782.

Robertson, Claire, David D. Tran, and Steven C. George. 2013. “Concise Review: Maturation Phases of Human Pluripotent Stem Cell-Derived Cardiomyocytes.” *STEM CELLS* 31 (5): 829–37. doi:10.1002/stem.1331.

Rodriguez, Manuel, Clara Rodriguez-Sabate, Ingrid Morales, Alberto Sanchez, and Magdalena Sabate. 2015. “Parkinson’s Disease as a Result of Aging.” *Aging Cell*. doi:10.1111/acel.12312.

Rosenbloom, Barry, Manisha Balwani, Jeff M. Bronstein, Edwin Kolodny, Swati Sathe, Andrea R. Gwosdow, John S. Taylor, J. Alexander Cole, Ari Zimran, and Neal J. Weinreb. 2011. “The Incidence of Parkinsonism in Patients with Type 1 Gaucher Disease: Data from the ICGG Gaucher Registry.” *Blood Cells, Molecules, and Diseases* 46 (1): 95–102. doi:10.1016/j.bcmd.2010.10.006.

Ross, Owen A., Mathias Toft, Andrew J. Whittle, Joseph L. Johnson, Spiridon Papapetropoulos, Deborah C. Mash, Irene Litvan, et al. 2006. “Lrrk2 and Lewy Body Disease.” *Annals of Neurology* 59 (2): 388–93. doi:10.1002/ana.20731.

Rudi, K., F. Y. Ho, B. K. Gilsbach, H. Pots, A. Wittinghofer, A. Kortholt, and J. P. Klare. 2015. “Conformational Heterogeneity of the Roc Domains in C. Tepidum Roc-COR and Implications for Human LRRK2 Parkinson Mutations.” *Bioscience Reports* 35 (5): e00254–e00254. doi:10.1042/BSR20150128.

Ruiz-Martínez, Javier, Ana Gorostidi, Berta Ibañez, Ainhoa Alzualde, David Otaegui, Fermin Moreno, Adolfo López de Munain, Alberto Bergareche, Juan Carlos Gómez-Esteban, and José F. Martí Massó. 2010. “Penetrance in Parkinson’s Disease Related to the LRRK2 R1441G Mutation in the Basque Country (Spain).” *Movement Disorders* 25 (14): 2340–45. doi:10.1002/mds.23278.

Russo, Isabella, Giulia Berti, Nicoletta Plotegher, Greta Bernardo, Roberta Filograna, Luigi

Bubacco, and Elisa Greggio. 2015. “Leucine-Rich Repeat Kinase 2 Positively Regulates Inflammation and down-Regulates NF-κB p50 Signaling in Cultured Microglia Cells.” *Journal of Neuroinflammation* 12: 230. doi:10.1186/s12974-015-0449-7.

Russo, Isabella, Luigi Bubacco, and Elisa Greggio. 2012. “Exosomes-Associated Neurodegeneration and Progression of Parkinson’s Disease.” *American Journal of Neurodegenerative Disease* 1 (3): 217–25. citeulike-article-id:13121833.

Saha, Shamol, Maria D Guillily, Andrew Ferree, Joel Lanceta, Diane Chan, Joy Ghosh, Cindy H Hsu, et al. 2009. “LRRK2 Modulates Vulnerability to Mitochondrial Dysfunction in Caenorhabditis Elegans.” *The Journal of Neuroscience : The Official Journal of the Society for Neuroscience* 29 (29). NIH Public Access: 9210–18. doi:10.1523/JNEUROSCI.2281-09.2009.

Sakurai, Chiye, Hitoshi Hashimoto, Hideki Nakanishi, Seisuke Arai, Yoh Wada, Ge-Hong Sun-Wada, Ikuo Wada, and Kiyotaka Hatsuzawa. 2012. “SNAP-23 Regulates Phagosome Formation and Maturation in Macrophages.” *Molecular Biology of the Cell* 23 (24): 4849–63. doi:doi: 10.1091/mbc.e12-01-0069.

Salao, Kanin, Lele Jiang, Hui Li, Vicky W.-W. Tsai, Yasmin Husaini, Paul M. G. Curmi, Louise J. Brown, David A. Brown, and Samuel N. Breit. 2016. “CLIC1 Regulates Dendritic Cell Antigen Processing and Presentation by Modulating Phagosome Acidification and Proteolysis.” *Biology Open* 5 (5): 620–30. doi:10.1242/bio.018119.

Sandor, Cynthia, Paul Robertson, Charmaine Lang, Andreas Heger, Heather Booth, Jane Vowles, Lorna Witty, et al. 2017. “Transcriptomic Profiling of Purified Patient-Derived Dopamine Neurons Identifies Convergent Perturbations and Therapeutics for Parkinson’s Disease.” *Human Molecular Genetics* 26 (3). Oxford University Press: 552–66. doi:10.1093/hmg/ddw412.

Saner, A, and H Thoenen. 1971. “Model Experiments on the Molecular Mechanism of Action of 6-Hydroxydopamine.” *Molecular Pharmacology* 7 (2): 147–54. http://www.ncbi.nlm.nih.gov/pubmed/5125851.

Satake, Wataru, Yuko Nakabayashi, Ikuko Mizuta, Yushi Hirota, Chiyomi Ito, Michiaki Kubo, Takahisa Kawaguchi, et al. 2009. “Genome-Wide Association Study Identifies Common Variants at Four Loci as Genetic Risk Factors for Parkinson’s Disease.” *Nature Genetics* 41 (12): 1303–7. doi:10.1038/ng.485.

Saunders-Pullman, Rachel, Jose Cabassa, Marta San Luciano, Kaili Stanley, Deborah Raymond, Laurie J Ozelius, and Susan B Bressman. 2011. “LRRK2 G2019S Mutations May Be Increased in Puerto Ricans.” *Movement Disorders : Official Journal of the Movement Disorder Society* 26 (9). NIH Public Access: 1772–73. doi:10.1002/mds.23632.

Savina, Ariel, Carolina Jancic, Stephanie Hugues, Pierre Guermonprez, Pablo Vargas, Ivan Cruz Moura, Ana-Maria Lennon-Duménil, Miguel C. Seabra, Graça Raposo, and Sebastian Amigorena. 2006. “NOX2 Controls Phagosomal pH to Regulate Antigen Processing during Crosspresentation by Dendritic Cells.” *Cell* 126 (1): 205–18. doi:10.1016/j.cell.2006.05.035.

Schafer, Dorothy P, Emily K Lehrman, Amanda G Kautzman, Ryuta Koyama, Alan R Mardinly, Ryo Yamasaki, Richard M Ransohoff, Michael E Greenberg, Ben A Barres,

and Beth Stevens. 2012. “Microglia Sculpt Postnatal Neural Circuits in an Activity and Complement-Dependent Manner.” *Neuron* 74 (4): 691–705. doi:10.1016/j.neuron.2012.03.026.

Schapansky, J., J. D. Nardozzi, F. Felizia, and M. J. LaVoie. 2014. “Membrane Recruitment of Endogenous LRRK2 Precedes Its Potent Regulation of Autophagy.” *Human Molecular Genetics* 23 (16): 4201–14. doi:10.1093/hmg/ddu138.

Schapira, Anthony H. V., and Matthew E. Gegg. 2013. “Glucocerebrosidase in the Pathogenesis and Treatment of Parkinson Disease: Fig. 1.” *Proceedings of the National Academy of Sciences* 110 (9): 3214–15. doi:10.1073/pnas.1300822110.

Schlüter, Oliver M., Mikhail Khvotchev, Reinhard Jahn, and Thomas C. Südhof. 2002. “Localization *Versus* Function of Rab3 Proteins.” *Journal of Biological Chemistry* 277 (43): 40919–29. doi:10.1074/jbc.M203704200.

Schrader, Michael, and H.Dariush Fahimi. 2006. “Peroxisomes and Oxidative Stress.” *Biochimica et Biophysica Acta (BBA) - Molecular Cell Research* 1763 (12): 1755–66. doi:10.1016/j.bbamcr.2006.09.006.

Schrag, Anette, Laura Horsfall, Kate Walters, Alastair Noyce, and Irene Petersen. 2015. “Prediagnostic Presentations of Parkinson’s Disease in Primary Care: A Case-Control Study.” *The Lancet Neurology* 14 (1): 57–64. doi:10.1016/S1474-4422(14)70287-X.

Scott, D., and S. Roy. 2012. “-Synuclein Inhibits Intersynaptic Vesicle Mobility and Maintains Recycling-Pool Homeostasis.” *Journal of Neuroscience* 32 (30): 10129–35. doi:10.1523/JNEUROSCI.0535-12.2012.

Sen, Saurabh, Philip J Webber, and Andrew B West. 2009. “Dependence of Leucine-Rich Repeat Kinase 2 (LRRK2) Kinase Activity on Dimerization.” *The Journal of Biological Chemistry* 284 (52). American Society for Biochemistry and Molecular Biology: 36346–56. doi:10.1074/jbc.M109.025437.

Sherer, Todd B., Jason R. Richardson, Claudia M. Testa, Byoung Boo Seo, Alexander V. Panov, Takao Yagi, Akemi Matsuno-Yagi, Gary W. Miller, and J. Timothy Greenamyre. 2007. “Mechanism of Toxicity of Pesticides Acting at Complex I: Relevance to Environmental Etiologies of Parkinson’s Disease.” *Journal of Neurochemistry* 0 (0): 070214184024016–??? doi:10.1111/j.1471-4159.2006.04333.x.

Shi, Yichen, Peter Kirwan, and Frederick J Livesey. 2012. “Directed Differentiation of Human Pluripotent Stem Cells to Cerebral Cortex Neurons and Neural Networks.” *Nature Protocols* 7 (10): 1836–46. doi:10.1038/nprot.2012.116.

Shimizu, K, K Ohtaki, K Matsubara, K Aoyama, T Uezono, O Saito, M Suno, et al. 2001. “Carrier-Mediated Processes in Blood--Brain Barrier Penetration and Neural Uptake of Paraquat.” *Brain Research* 906 (1–2): 135–42. http://www.ncbi.nlm.nih.gov/pubmed/11430870.

Shin, Narae, Hyerhan Jeong, Jungsun Kwon, Hye Young Heo, Jung June Kwon, Hye Jin Yun, Cy-Hyun Kim, et al. 2008. “LRRK2 Regulates Synaptic Vesicle Endocytosis.” *Experimental Cell Research* 314 (10): 2055–65. doi:10.1016/j.yexcr.2008.02.015.

Sidransky, E., M.A. Nalls, J.O. Aasly, J. Aharon-Peretz, G. Annesi, E.R. Barbosa, A. Bar-Shira, et al. 2009. “Multicenter Analysis of Glucocerebrosidase Mutations in Parkinson’s Disease.” *New England Journal of Medicine* 361 (17): 1651–61.

doi:10.1056/NEJMoa0901281.

Sidransky, Ellen, and Grisel Lopez. 2012. “The Link between the GBA Gene and Parkinsonism.” *The Lancet. Neurology* 11 (11). NIH Public Access: 986–98. doi:10.1016/S1474-4422(12)70190-4.

Sierra, María, Isabel González-Aramburu, Pascual Sánchez-Juan, Coro Sánchez-Quintana, José Miguel Polo, José Berciano, Onofre Combarros, and Jon Infante. 2011. “High Frequency and Reduced Penetrance of LRRK2 G2019S Mutation among Parkinson’s Disease Patients in Cantabria (Spain).” *Movement Disorders : Official Journal of the Movement Disorder Society* 26 (13): 2343–46. doi:10.1002/mds.23965.

Sieweke, M. H., and J. E. Allen. 2013. “Beyond Stem Cells: Self-Renewal of Differentiated Macrophages.” *Science* 342 (6161): 1242974–1242974. doi:10.1126/science.1242974.

Simón-Sánchez, Javier, Claudia Schulte, Jose M Bras, Manu Sharma, J Raphael Gibbs, Daniela Berg, Coro Paisan-Ruiz, et al. 2009a. “Genome-Wide Association Study Reveals Genetic Risk Underlying Parkinson’s Disease.” *Nature Genetics* 41 (12). NIH Public Access: 1308–12. doi:10.1038/ng.487.

Singleton, A. B., M Farrer, J Johnson, A Singleton, S Hague, J Kachergus, M Hulihan, et al. 2003. “-Synuclein Locus Triplication Causes Parkinson’s Disease.” *Science* 302 (5646): 841–841. doi:10.1126/science.1090278.

Sloan, Max, Javier Alegre-Abarrategui, Dawid Potgieter, Anna-Kristin Kaufmann, Richard Exley, Thierry Deltheil, Sarah Threlfell, et al. 2016. “LRRK2 BAC Transgenic Rats Develop Progressive, L-DOPA-Responsive Motor Impairment, and Deficits in Dopamine Circuit Function.” *Human Molecular Genetics* 25 (5). Oxford University Press: 951–63. doi:10.1093/hmg/ddv628.

Smith, Y, and J Z Kieval. 2000. “Anatomy of the Dopamine System in the Basal Ganglia.” *Trends in Neurosciences* 23 (10 Suppl): S28-33. http://www.ncbi.nlm.nih.gov/pubmed/11052217.

Snyder, Heather, Kwame Mensah, Catherine Theisler, Jack Lee, Andreas Matouschek, and Benjamin Wolozin. 2003. “Aggregated and Monomeric α-Synuclein Bind to the S6′ Proteasomal Protein and Inhibit Proteasomal Function.” *Journal of Biological Chemistry* 278 (14): 11753–59. doi:10.1074/jbc.M208641200.

Spanaki, C., H. Latsoudis, and A. Plaitakis. 2006. “LRRK2 Mutations on Crete: R1441H Associated with PD Evolving to PSP.” *Neurology* 67 (8): 1518–19. doi:10.1212/01.wnl.0000239829.33936.73.

Spillantini, Maria Grazia, Marie Luise Schmidt, Virginia M.-Y. Lee, John Q. Trojanowski, Ross Jakes, and Michel Goedert. 1997. “Alpha-Synuclein in Lewy Bodies.” *Nature* 388 (6645): 839–40. doi:10.1038/42166.

Stafa, Klodjan, Alzbeta Trancikova, Philip J. Webber, Liliane Glauser, Andrew B. West, and Darren J. Moore. 2012. “GTPase Activity and Neuronal Toxicity of Parkinson’s Disease–Associated LRRK2 Is Regulated by ArfGAP1.” Edited by Harry T. Orr. *PLoS Genetics* 8 (2): e1002526. doi:10.1371/journal.pgen.1002526.

Stefanova, Nadia, Lisa Fellner, Markus Reindl, Eliezer Masliah, Werner Poewe, and Gregor K. Wenning. 2011. “Toll-Like Receptor 4 Promotes α-Synuclein Clearance and Survival of Nigral Dopaminergic Neurons.” *The American Journal of Pathology* 179

(2): 954–63. doi:10.1016/j.ajpath.2011.04.013.

Steger, Martin, Francesca Tonelli, Genta Ito, Paul Davies, Matthias Trost, Melanie Vetter, Stefanie Wachter, et al. 2016. “Phosphoproteomics Reveals That Parkinson’s Disease Kinase LRRK2 Regulates a Subset of Rab GTPases.” *eLife* 5 (January). doi:10.7554/eLife.12813.

Studer, Lorenz, Elsa Vera, and Daniela Cornacchia. 2015. “Programming and Reprogramming Cellular Age in the Era of Induced Pluripotency.” *Cell Stem Cell*. Elsevier. doi:10.1016/j.stem.2015.05.004.

Su, Xiaomin, Howard Federoff, and Kathleen Maguire-Zeiss. 2009. “Mutant Alpha-Synuclein Overexpression Mediates Early Proinflammatory Activity.” *Neurotoxicity Research* 16 (3): 238–54. doi:doi: 10.1007/s12640-009-9053-x.

Surmeier, D J, J N Guzman, J Sanchez-Padilla, and P T Schumacker. 2011. “The Role of Calcium and Mitochondrial Oxidant Stress in the Loss of Substantia Nigra Pars Compacta Dopaminergic Neurons in Parkinson’s Disease.” *Neuroscience* 198 (December). NIH Public Access: 221–31. doi:10.1016/j.neuroscience.2011.08.045.

Takahashi, Kazutoshi, Koji Tanabe, Mari Ohnuki, Megumi Narita, Tomoko Ichisaka, Kiichiro Tomoda, and Shinya Yamanaka. 2007. “Induction of Pluripotent Stem Cells from Adult Human Fibroblasts by Defined Factors.” *Cell* 131 (5): 861–72. doi:10.1016/j.cell.2007.11.019.

Takahashi, Kazutoshi, and Shinya Yamanaka. 2006. “Induction of Pluripotent Stem Cells from Mouse Embryonic and Adult Fibroblast Cultures by Defined Factors.” *Cell* 126 (4): 663–76. doi:10.1016/j.cell.2006.07.024.

Takahashi, N, L L Miner, I Sora, H Ujike, R S Revay, V Kostic, V Jackson-Lewis, S Przedborski, and G R Uhl. 1997. “VMAT2 Knockout Mice: Heterozygotes Display Reduced Amphetamine-Conditioned Reward, Enhanced Amphetamine Locomotion, and Enhanced MPTP Toxicity.” *Proceedings of the National Academy of Sciences of the United States of America* 94 (18): 9938–43. http://www.ncbi.nlm.nih.gov/pubmed/9275230.

Takeuchi, O, K Takeda, K Hoshino, O Adachi, T Ogawa, and S Akira. 2000. “Cellular Responses to Bacterial Cell Wall Components Are Mediated through MyD88-Dependent Signaling Cascades.” *International Immunology* 12 (1): 113–17. http://www.ncbi.nlm.nih.gov/pubmed/10607756.

Talaber, Gergely, Gabriella Miklossy, Zachary Oaks, Yuxin Liu, Sharon A. Tooze, Dmitriy M. Chudakov, Katalin Banki, and Andras Perl. 2014. “HRES-1/Rab4 Promotes the Formation of LC3+ Autophagosomes and the Accumulation of Mitochondria during Autophagy.” Edited by Amr H. Sawalha. *PLoS ONE* 9 (1): e84392. doi:10.1371/journal.pone.0084392.

Tanaka, Keiji, Hideki Shimura, Nobutaka Hattori, Shin-ichiro Kubo, Yoshikuni Mizuno, Shuichi Asakawa, Shinsei Minoshima, et al. 2000. “Familial Parkinson Disease Gene Product, Parkin, Is a Ubiquitin-Protein Ligase.” *Nature Genetics* 25 (3): 302–5. doi:10.1038/77060.

Tanner, Caroline M, Freya Kamel, G Webster Ross, Jane A Hoppin, Samuel M Goldman, Monica Korell, Connie Marras, et al. 2011. “Rotenone, Paraquat, and Parkinson’s Disease.” *Environmental Health Perspectives* 119 (6). National Institute of

Environmental Health Science: 866–72. doi:10.1289/ehp.1002839.

Tauber, Alfred I. 2003. “Metchnikoff and the Phagocytosis Theory.” *Nature Reviews. Molecular Cell Biology* 4 (11). Nature Publishing Group: 897–901. doi:10.1038/nrm1244.

Taymans, Jean-Marc, Renée Vancraenenbroeck, Petri Ollikainen, Alexandra Beilina, Evy Lobbestael, Marc De Maeyer, Veerle Baekelandt, and Mark R. Cookson. 2011. “LRRK2 Kinase Activity Is Dependent on LRRK2 GTP Binding Capacity but Independent of LRRK2 GTP Binding.” Edited by Philipp J. Kahle. *PLoS ONE* 6 (8): e23207. doi:10.1371/journal.pone.0023207.

TCW, Julia, Minghui Wang, A.A. Pimenova, K.R. Bowles, B.J. Hartley, Emre Lacin, S.I. Machlovi, et al. 2017. “An Efficient Platform for Astrocyte Differentiation from Human Induced Pluripotent Stem Cells.” *Stem Cell Reports* 9 (2). Elsevier: 600–614. doi:10.1016/j.stemcr.2017.06.018.

Tepper, J M, S F Sawyer, and P M Groves. 1987. “Electrophysiologically Identified Nigral Dopaminergic Neurons Intracellularly Labeled with HRP: Light-Microscopic Analysis.” *The Journal of Neuroscience : The Official Journal of the Society for Neuroscience* 7 (9): 2794–2806. http://www.ncbi.nlm.nih.gov/pubmed/3625274.

Thanvi, Bhomraj, Nelson Lo, and Tom Robinson. 2007. “Levodopa-Induced Dyskinesia in Parkinson’s Disease: Clinical Features, Pathogenesis, Prevention and Treatment.” *Postgraduate Medical Journal* 83 (980). BMJ Publishing Group: 384–88. doi:10.1136/pgmj.2006.054759.

Thévenet, Jonathan, Rosanna Pescini Gobert, Robertus Hooft van Huijsduijnen, Christoph Wiessner, and Yves Jean Sagot. 2011. “Regulation of LRRK2 Expression Points to a Functional Role in Human Monocyte Maturation.” *PloS One* 6 (6). doi:doi: 10.1371/journal.pone.0021519.

Thomas, B., and M. F. Beal. 2007. “Parkinson’s Disease.” *Human Molecular Genetics* 16 (R2): R183–94. doi:10.1093/hmg/ddm159.

Thomas, M G, M Saldanha, R J Mistry, D T Dexter, D B Ramsden, and R B Parsons. 2013. “Nicotinamide N-Methyltransferase Expression in SH-SY5Y Neuroblastoma and N27 Mesencephalic Neurones Induces Changes in Cell Morphology via Ephrin-B2 and Akt Signalling.” *Cell Death and Disease* 4 (6): e669. doi:10.1038/cddis.2013.200.

Tian, E, Guoqiang Sun, Guihua Sun, Jianfei Chao, Peng Ye, Charles Warden, Arthur D. Riggs, and Yanhong Shi. 2016. “Small-Molecule-Based Lineage Reprogramming Creates Functional Astrocytes.” *Cell Reports* 16 (3): 781–92. doi:10.1016/j.celrep.2016.06.042.

Toft, M., L. Pielsticker, O. A. Ross, J. O. Aasly, and M. J. Farrer. 2006. “Glucocerebrosidase Gene Mutations and Parkinson Disease in the Norwegian Population.” *Neurology* 66 (3): 415–17. doi:10.1212/01.wnl.0000196492.80676.7c.

Tong, Y., H. Yamaguchi, E. Giaime, S. Boyle, R. Kopan, R. J. Kelleher, and J. Shen. 2010. “Loss of Leucine-Rich Repeat Kinase 2 Causes Impairment of Protein Degradation Pathways, Accumulation of -Synuclein, and Apoptotic Cell Death in Aged Mice.” *Proceedings of the National Academy of Sciences* 107 (21): 9879–84. doi:10.1073/pnas.1004676107.

Tong, Youren, Emilie Giaime, Hiroo Yamaguchi, Takaharu Ichimura, Yumin Liu, Huiqing Si, Huaibin Cai, Joseph V Bonventre, and Jie Shen. 2012. “Loss of Leucine-Rich Repeat Kinase 2 Causes Age-Dependent Bi-Phasic Alterations of the Autophagy Pathway.” *Molecular Neurodegeneration* 7 (1): 2. doi:10.1186/1750-1326-7-2.

Tran, Thi A, Andrew D Nguyen, Jianjun Chang, Matthew S Goldberg, Jae-Kyung Lee, and Malú G Tansey. 2011. “Lipopolysaccharide and Tumor Necrosis Factor Regulate Parkin Expression via Nuclear Factor-Kappa B.” *PloS One* 6 (8). Public Library of Science: e23660. doi:10.1371/journal.pone.0023660.

Trinh, Joanne, Ilaria Guella, and Matthew James Farrer. 2014. “Disease Penetrance of Late-Onset Parkinsonism.” *JAMA Neurology* 71 (12): 1535. doi:10.1001/jamaneurol.2014.1909.

Trudler, Dorit, Orly Weinreb, Silvia A. Mandel, Moussa B. H. Youdim, and Dan Frenkel. 2014. “DJ-1 Deficiency Triggers Microglia Sensitivity to Dopamine toward a pro-Inflammatory Phenotype That Is Attenuated by Rasagiline.” *Journal of Neurochemistry* 129 (3): 434–47. doi:10.1111/jnc.12633.

Ujiie, Sachiko, Taku Hatano, Shin-Ichiro Kubo, Satoshi Imai, Shigeto Sato, Toshiki Uchihara, Saburo Yagishita, et al. 2012. “LRRK2 I2020T Mutation Is Associated with Tau Pathology.” *Parkinsonism & Related Disorders* 18 (7): 819–23. doi:10.1016/j.parkreldis.2012.03.024.

Ullrich, O, S Reinsch, S Urbé, M Zerial, and R G Parton. 1996. “Rab11 Regulates Recycling through the Pericentriolar Recycling Endosome.” *The Journal of Cell Biology* 135 (4): 913–24. http://www.ncbi.nlm.nih.gov/pubmed/8922376.

Umeno, Junji, Kouichi Asano, Tomonaga Matsushita, Takayuki Matsumoto, Yutaka Kiyohara, Mitsuo Iida, Yusuke Nakamura, Naoyuki Kamatani, and Michiaki Kubo. 2011. “Meta-Analysis of Published Studies Identified Eight Additional Common Susceptibility Loci for Crohn’s Disease and Ulcerative Colitis.” *Inflammatory Bowel Diseases* 17 (12): 2407–15. doi:10.1002/ibd.21651.

Ungerstedt, U. 1968. “6-Hydroxy-Dopamine Induced Degeneration of Central Monoamine Neurons.” *European Journal of Pharmacology* 5 (1): 107–10. http://www.ncbi.nlm.nih.gov/pubmed/5718510.

Valente, E M, A R Bentivoglio, P H Dixon, A Ferraris, T Ialongo, M Frontali, A Albanese, and N W Wood. 2001. “Localization of a Novel Locus for Autosomal Recessive Early-Onset Parkinsonism, PARK6, on Human Chromosome 1p35-p36.” *American Journal of Human Genetics* 68 (4): 895–900. http://www.ncbi.nlm.nih.gov/pubmed/11254447.

Villarroel-Campos, David, Francisca C Bronfman, and Christian Gonzalez-Billault. 2016. “Rab GTPase Signaling in Neurite Outgrowth and Axon Specification.” *Cytoskeleton (Hoboken, N.J.)* 73 (9): 498–507. doi:10.1002/cm.21303.

Vives-Bauza, C., C. Zhou, Y. Huang, M. Cui, R. L. A. de Vries, J. Kim, J. May, et al. 2010. “PINK1-Dependent Recruitment of Parkin to Mitochondria in Mitophagy.” *Proceedings of the National Academy of Sciences* 107 (1): 378–83. doi:10.1073/pnas.0911187107.

Waak, J., S. S. Weber, A. Waldenmaier, K. Gorner, M. Alunni-Fabbroni, H. Schell, D. Vogt-Weisenhorn, et al. 2009. “Regulation of Astrocyte Inflammatory Responses by the Parkinson’s Disease-Associated Gene DJ-1.” *The FASEB Journal* 23 (8): 2478–89.

doi:10.1096/fj.08-125153.

Wandu, Wambui S, Cuiyan Tan, Osato Ogbeifun, Barbara P Vistica, Guangpu Shi, Samuel J.H. Hinshaw, Chengsong Xie, et al. 2015. “Leucine-Rich Repeat Kinase 2 (Lrrk2) Deficiency Diminishes the Development of Experimental Autoimmune Uveitis (EAU) and the Adaptive Immune Response.” *PLoS ONE* 10 (6): e0128906. doi:10.1371/journal.pone.0128906.

Wang, Lizhen, Chengsong Xie, Elisa Greggio, Loukia Parisiadou, Hoon Shim, Lixin Sun, Jayanth Chandran, et al. 2008. “The Chaperone Activity of Heat Shock Protein 90 Is Critical for Maintaining the Stability of Leucine-Rich Repeat Kinase 2.” *Journal of Neuroscience* 28 (13). http://www.jneurosci.org/content/28/13/3384.long.

Wang, Xinglong, Timothy G. Petrie, Yingchao Liu, Jun Liu, Hisashi Fujioka, and Xiongwei Zhu. 2012. “Parkinson’s Disease-Associated DJ-1 Mutations Impair Mitochondrial Dynamics and Cause Mitochondrial Dysfunction.” *Journal of Neurochemistry* 121 (5): 830–39. doi:10.1111/j.1471-4159.2012.07734.x.

Waragai, Masaaki, Masaaki Nakai, Jianshe Wei, Masayo Fujita, Hideya Mizuno, Gilbert Ho, Eliezer Masliah, Hiroyasu Akatsu, Fusako Yokochi, and Makoto Hashimoto. 2007. “Plasma Levels of DJ-1 as a Possible Marker for Progression of Sporadic Parkinson’s Disease.” *Neuroscience Letters* 425 (1): 18–22. doi:10.1016/j.neulet.2007.08.010.

Waschbüsch, Dieter, Helen Michels, Swantje Strassheim, Edith Ossendorf, Daniel Kessler, Christian Johannes Gloeckner, and Angelika Barnekow. 2014. “LRRK2 Transport Is Regulated by Its Novel Interacting Partner Rab32.” *PloS One* 9 (10). Public Library of Science: e111632. doi:10.1371/journal.pone.0111632.

Webster, Scott D., Austin J. Yang, Larry Margol, William Garzon-Rodriguez, Charles G. Glabe, and Andrea J. Tenner. 2000. “Complement Component C1q Modulates the Phagocytosis of Aβ by Microglia.” *Experimental Neurology* 161 (1): 127–38. doi:10.1006/exnr.1999.7260.

West, Andrew, Darren Moore, Saskia Biskup, Artem Bugayenko, Wanli Smith, Christopher Ross, Valina Dawson, and Ted Dawson. 2005. “Parkinson’s Disease-Associated Mutations in Leucine-Rich Repeat Kinase 2 Augment Kinase Activity.” *Proceedings of the National Academy of Sciences of the United States of America* 102 (46). Institute for Cell Engineering, Department of Neurology, The Johns Hopkins University School of Medicine, Baltimore, MD 21205, USA.: 16842–47. doi:doi: 10.1073/pnas.0507360102.

West, Andrew, Darren Moore, Catherine Choi, Shaida Andrabi, Xiaojie Li, Dustin Dikeman, Saskia Biskup, et al. 2007. “Parkinson’s Disease-Associated Mutations in LRRK2 Link Enhanced GTP-Binding and Kinase Activities to Neuronal Toxicity.” *Human Molecular Genetics* 16 (2). Oxford University Press: 223–32. doi:doi: 10.1093/hmg/ddl471.

Westerink, R H S, and A G Ewing. 2008. “The PC12 Cell as Model for Neurosecretion.” *Acta Physiologica (Oxford, England)* 192 (2). NIH Public Access: 273–85. doi:10.1111/j.1748-1716.2007.01805.x.

Widdowson, PS, MJ Farnworth, MG Simpson, and EA Lock. 1996. “Influence of Age on the Passage of Paraquat through the Blood-Brain Barrier in Rats: A Distribution and Pathological Examination.” *Human & Experimental Toxicology* 15 (3): 231–36.

doi:10.1177/096032719601500308.

Wilgenburg, Bonnie van, Cathy Browne, Jane Vowles, and Sally A. Cowley. 2013. "Efficient, Long Term Production of Monocyte-Derived Macrophages from Human Pluripotent Stem Cells under Partly-Defined and Fully-Defined Conditions." Edited by Dimas Tadeu Covas. *PLoS ONE* 8 (8). Public Library of Science: e71098. doi:10.1371/journal.pone.0071098.

Wilhelmus, Micha M.M., Susanne M.A. van der Pol, Quentin Jansen, Maarten E. Witte, Paul van der Valk, Annemieke J.M. Rozemuller, Benjamin Drukarch, Helga E. de Vries, and Jack Van Horssen. 2011. "Association of Parkinson Disease-Related Protein PINK1 with Alzheimer Disease and Multiple Sclerosis Brain Lesions." *Free Radical Biology and Medicine* 50 (3): 469–76. doi:10.1016/j.freeradbiomed.2010.11.033.

Winner, B., H.L. Melrose, C. Zhao, K.M. Hinkle, M. Yue, C. Kent, A.T. Braithwaite, et al. 2011. "Adult Neurogenesis and Neurite Outgrowth Are Impaired in LRRK2 G2019S Mice." *Neurobiology of Disease* 41 (3): 706–16. doi:10.1016/j.nbd.2010.12.008.

Wu, Hao, Eric V. Brown, Nimish K. Acharya, Denah M. Appelt, Alexander Marks, Robert G. Nagele, and Venkat Venkataraman. 2016. "Age-Dependent Increase of Blood–brain Barrier Permeability and Neuron-Binding Autoantibodies in S100B Knockout Mice." *Brain Research* 1637 (April): 154–67. doi:10.1016/j.brainres.2016.02.026.

Xiong, Yulan, Valina L Dawson, and Ted M Dawson. 2012. "LRRK2 GTPase Dysfunction in the Pathogenesis of Parkinson's Disease." *Biochemical Society Transactions* 40 (5). NIH Public Access: 1074–79. doi:10.1042/BST20120093.

Yan, Ruiqing, and Zhihua Liu. 2017. "LRRK2 Enhances Nod1/2-Mediated Inflammatory Cytokine Production by Promoting Rip2 Phosphorylation." *Protein & Cell* 8 (1). Higher Education Press: 55–66. doi:10.1007/s13238-016-0326-x.

Yanagida, Takashi, Kazuyuki Takata, Masatoshi Inden, Yoshihisa Kitamura, Takashi Taniguchi, Kanji Yoshimoto, Takahiro Taira, and Hiroyoshi Ariga. 2006. "Distribution of DJ-1, Parkinson's Disease-Related Protein PARK7, and Its Alteration in 6-Hydroxydopamine-Treated Hemiparkinsonian Rat Brain." *Journal of Pharmacological Sciences* 102 (2): 243–47. http://www.ncbi.nlm.nih.gov/pubmed/17038803.

Yates, Robin M., Albin Hermetter, and David G. Russell. 2009. "Recording Phagosome Maturation Through the Real-Time, Spectrofluorometric Measurement of Hydrolytic Activities." In *Methods in Molecular Biology (Clifton, N.J.)*, 531:157–71. doi:10.1007/978-1-59745-396-7_11.

Yates, Robin M, Albin Hermetter, Gregory A Taylor, and David G Russell. 2007. "Macrophage Activation Downregulates the Degradative Capacity of the Phagosome." *Traffic (Copenhagen, Denmark)* 8 (3): 241–50. doi:10.1111/j.1600-0854.2006.00528.x.

Yescas, Petra, Marisol López, Nancy Monroy, Marie-Catherine Boll, Mayela Rodríguez-Violante, Ulises Rodríguez, Adriana Ochoa, and María Elisa Alonso. 2010. "Low Frequency of Common LRRK2 Mutations in Mexican Patients with Parkinson's Disease." *Neuroscience Letters* 485 (2): 79–82. doi:10.1016/j.neulet.2010.08.029.

Yun, Hye Jin, Hyejung Kim, Inhwa Ga, Hakjin Oh, Dong Hwan Ho, Jiyoung Kim, Hyemyung Seo, Ilhong Son, and Wongi Seol. 2015a. "An Early Endosome Regulator, Rab5b, Is an LRRK2 Kinase Substrate." *The Journal of Biochemistry* 157 (6): 485–95.

doi:10.1093/jb/mvv005.

Zabetian, C P, A Samii, A D Mosley, J W Roberts, B C Leis, D Yearout, W H Raskind, and A Griffith. 2005. “A Clinic-Based Study of the LRRK2 Gene in Parkinson Disease Yields New Mutations.” *Neurology* 65 (5): 741–44. doi:10.1212/01.wnl.0000172630.22804.73.

Zarranz, Juan J., Javier Alegre, Juan C. Gómez-Esteban, Elena Lezcano, Raquel Ros, Israel Ampuero, Lídice Vidal, et al. 2004. “The New Mutation, E46K, of α-Synuclein Causes Parkinson and Lewy Body Dementia.” *Annals of Neurology* 55 (2): 164–73. doi:10.1002/ana.10795.

Zhang, Fu-Ren, Wei Huang, Shu-Min Chen, Liang-Dan Sun, Hong Liu, Yi Li, Yong Cui, et al. 2009. “Genomewide Association Study of Leprosy.” *New England Journal of Medicine* 361 (27): 2609–18. doi:10.1056/NEJMoa0903753.

Zhang, Y., J. Gao, K. K. K. Chung, H. Huang, V. L. Dawson, and T. M. Dawson. 2000. “Parkin Functions as an E2-Dependent Ubiquitin- Protein Ligase and Promotes the Degradation of the Synaptic Vesicle-Associated Protein, CDCrel-1.” *Proceedings of the National Academy of Sciences* 97 (24): 13354–59. doi:10.1073/pnas.240347797.

Zhao, Jing, Tyler Molitor, William Langston, and Jeremy Nichols. 2015. “LRRK2 Dephosphorylation Increases Its Ubiquitination.” *The Biochemical Journal* 469 (1): 107–20. citeulike-article-id:13604065.

Zhou, Hongxia, Cao Huang, Jianbin Tong, Weimin C Hong, Yong-Jian Liu, and Xu-Gang Xia. 2011. “Temporal Expression of Mutant LRRK2 in Adult Rats Impairs Dopamine Reuptake.” *International Journal of Biological Sciences* 7 (6): 753–61. http://www.ncbi.nlm.nih.gov/pubmed/21698001.

Zimprich, Alexander, Saskia Biskup, Petra Leitner, Peter Lichtner, Matthew Farrer, Sarah Lincoln, Jennifer Kachergus, et al. 2004. “Mutations in LRRK2 Cause Autosomal-Dominant Parkinsonism with Pleomorphic Pathology.” *Neuron* 44 (4): 601–7. doi:10.1016/j.neuron.2004.11.005.